

AD 668871

FTD-MT-65-161

# FOREIGN TECHNOLOGY DIVISION



JOURNAL OF APPLIED MECHANICS AND TECHNICAL PHYSICS  
(COLLECTION OF ARTICLES)

D D C  
RECEIVED  
MAY 17 1968  
B.



Distribution of this document  
is unlimited. It may be  
released to the Clearinghouse,  
Department of Commerce, for  
sale to the general public.

Reproduced by the  
CLEARINGHOUSE  
for Federal Scientific & Technical  
Information Springfield Va. 22151

324

# EDITED MACHINE TRANSLATION

JOURNAL OF APPLIED MECHANICS AND TECHNICAL PHYSICS  
(COLLECTION OF ARTICLES)

English Pages: 293

UR/0207-064-000-005

TP7500526-555

THIS TRANSLATION IS A RENDITION OF THE ORIGINAL FOREIGN TEXT WITHOUT ANY ANALYTICAL OR EDITORIAL COMMENT. STATEMENTS OR THEORIES ADVOCATED OR IMPLIED ARE THOSE OF THE SOURCE AND DO NOT NECESSARILY REFLECT THE POSITION OR OPINION OF THE FOREIGN TECHNOLOGY DIVISION.

PREPARED BY:

TRANSLATION DIVISION  
FOREIGN TECHNOLOGY DIVISION  
WP-APB, OHIO.

Akademiya Nauk SSSR - Sibirskoye Otdeleniye

PMTF

No. 5

Sentyabr' - Oktyabr'

ZHURNAL PRIKLADNOY MEKHANIKI I TEKHNICHESKOY FIZIKI

Izdatel'stva "Nauka"

1964

Pages 1-168

# ITIS INDEX CONTROL FORM

01 Acc Nr TP7500526		68 Translation Nr MT6500161		65 X Ref Acc Nr AP5002858		76 Reel/F ame Nr 1654 1031	
97 Header Clas UNCL		63 Clas UNCL, 0		64 Control Markings 0		94 Expansion UR	
02 Ctry UR	03 Ref 0207	04 Yr 64	05 Vol 000	06 Iss 005	07 B. Pg. 0003	45 E. Pg. 0010	10 Date NONE

Transliterated Title OB OBTEKANII TELA POTOKOM SIL'NO  
RAZREZHENNOY PLAZMY

09 English Title FLOW AROUND A BODY BY A FLUX OF STRONGLY  
RAREFIED PLASMA

43 Source  
ZHURNAL PRIKLADNOY MEKHANIKI I TEKHNIЧЕСКОY FIZIKI (RUSSIAN)

42 Author  
PASHCHENKO, N. T.

98 Document Location

16 Co-Author  
NONE

47 Subject Codes  
20

16 Co-Author  
NONE

39 Topic Tags: plasma flow, rarefied gas-  
dynamics, rarefied gas, distribution  
function, electron, electric field, Laplace  
equation

16 Co-Author  
NONE

16 Co-Author  
NONE

**ABSTRACT:** The author considers the high velocity flow of a highly rarefied plasma around a stationary charged body. Assuming that the perturbations produced by the body are small and that the Debye sphere is small in comparison to the dimensions of the body, the field potential and the parameters of flow are calculated. In a system of coordinates rigidly attached to the body, the system of equations for the self-consistent field is given by

$$c^{\alpha} \frac{\partial f_{\alpha}}{\partial x^{\alpha}} + \frac{e}{m_{\alpha}} \frac{\partial \varphi}{\partial x^{\alpha}} \frac{\partial f_{\alpha}}{\partial c^{\alpha}} g^{\alpha\beta} = 0, \quad c^{\alpha} \frac{\partial f_1}{\partial x^{\alpha}} - \frac{e}{m_1} \frac{\partial \varphi}{\partial x^{\alpha}} \frac{\partial f_1}{\partial c^{\alpha}} g^{\alpha\beta} = 0$$

$$c^{\alpha} \frac{\partial f}{\partial x^{\alpha}} = 0, \quad \varphi_{,\alpha\beta} g^{\alpha\beta} = 4\pi e \left\{ \int_{\Omega} f_{\alpha} d\Omega - \int_{\Omega} f_1 d\Omega \right\}$$

Here  $f_e$ ,  $f_1$ , and  $f$  are the distribution functions of the electrons, ions, and the neutral particles respectively. Also,  $c$  is the velocity of random motion,  $e$  is the electronic charge,  $\varphi$  is the potential of the electric field,  $g^{\alpha\beta}$  is the basic metric tensor for the considered coordinate system and  $\varphi_{,\alpha\beta} g^{\alpha\beta}$  is the Laplacian operator on the function  $\varphi$ . The boundary conditions are given by

$$f_1^{+}(c, x_s) = \int_{(c' \cdot n) < 0} K(c, c', x_s) f_1^{-}(c', x_s) dc'$$

$$f_1^{-}(c, x_s) = f_1(c, x_s) \quad \text{при } (c, n) < 0, \quad f_1^{+}(c, x_s) = f_1(c, x_s) \quad \text{при } (c, n) > 0,$$

where  $x_s$  is the radius vector at any point on the surface,  $n$  is the normal to the surface at this point, and  $K(c, c', x_s)$  is a kernel function of interaction. After nondimensionalizing all quantities in the following manner:

$$\bar{y}^1 = \frac{x^1}{R_0}, \quad \Phi = \frac{e\varphi}{kT}, \quad F_j = \frac{I_j (c_j \pi)^{1/2}}{n_0}, \quad v_j^2 = \frac{c_j^2}{c_j^1}$$

the small parameters in the problem were found to be

$$S_0 = \frac{V}{c_0}, \quad \frac{1}{S_1} = \frac{c_1}{V}, \quad \mu = \max \left| \frac{e\varphi}{kT} \right|, \quad \mu_0 = \frac{e\varphi_0}{kT}, \quad s = \frac{R_0}{R_D}$$

The solution for the potential was obtained in the form

$$e^{\Phi} \Phi_{, \alpha \beta} = \frac{1}{(\pi)^{1/2}} (n_0 (1 + \Phi) - n_1) \quad \left( n_1 = \int_0^r F_1 dv_1, \quad n_0 = \int_0^r F_0 dv_0 \right)$$

As an illustration, a specific example was worked out for the case of flow around a cylinder. The potential at any radius  $r$  and distance  $x$  is given by

$$\Phi = \left[ \mu_0 + \frac{1}{2s} \int_1^{\infty} n_0 \exp\left(-\frac{z-1}{s}\right) dz - \frac{1}{2s} \int_1^r n_0 \exp\left(\frac{z-1}{s}\right) dz \right] \exp\left(-\frac{r-1}{s}\right) - \frac{1}{2s} \int_1^{\infty} n_0 \exp\left(-\frac{z-1}{s}\right) dz \exp\left(\frac{r-1}{s}\right)$$

Original article has: 5 figures and 37 formulas. English translation: 14 pages.

01 Acc Nr TP7500527		68 Translation Nr MT6500161		65 X Ref Acc Nr AP5002859		76 Reel/Frame Nr 1654 1033	
97 Header Clas UNCL		63 Clas UNCL; 0	64 Control Markings 0			94 Expansion	40 Ctry Info UR
02 Ctry UR	03 Ref 0207	04 Yr 64	05 Vol 000	06 Iss 005	07 B. Pg. 0011	45 B. Pg. 0017	10 Date NONE

Transliterated Title DIFFUZIYA I PROVODIMOST' V CHASTICHNO IONIZOVANNOY MNOGOTEMPERATURNNOY GAZOVOY SMESI

09 English Title DIFFUSION AND CONDUCTIVITY IN A PARTIALLY IONIZED MULTITEMPERATURE GAS MIXTURE

43 Source

ZHURNAL PRIKLADNOY MEKHANIKI I TEKHNIЧЕСKOY FIZIKI (RUSSIAN)

42 Author

POLYANSKIY, V. A.

98 Document Location

16 Co-Author

NONE

47 Subject Codes

20

16 Co-Author

NONE

39 Topic Tags: gas diffusion, thermal diffusion, ionized gas, electro magnetic field, Boltzmann constant, Maxwell equation

16 Co-Author

NONE

16 Co-Author

NONE

**ABSTRACT:** The author presents the expressions for the diffusion current and generalized coefficients of diffusion in a partially ionized gas mixture with different component temperatures sustained by an electromagnetic field. For the starting point in this analysis, he takes the set of transport equations obtained from the kinetic equations with the 13-moment method by M. Ya. Aliyevskiy and V. M. Zhdanov (Uravneniya perenosa dlya neizotermicheskoy mnogosortnoy plazmy. PMTF 1963, No. 5). The Landau type collision integrals were used for particles interacting through Coulomb forces, and Boltzmann type integrals were used for neutral particles. Starting from the macroscopic equations and Maxwell's equations, expressions were derived for the generalized Ohm's law, for the mobility coefficients, and for the conductivity. The following expression was derived for the mass flow current

$$J_{\alpha}^{\alpha} = \sum_{\beta} \frac{m_{\alpha}}{kT_{\alpha}} \left\{ \left[ G_{\alpha\beta}^{\perp} + \frac{0.4}{kn_{\beta}} \sum_{\gamma} b_{\gamma\beta} (\lambda_{\beta\gamma}^{\perp} D_{\alpha\gamma}^{\perp} - \lambda_{\beta\gamma}^{\wedge} D_{\alpha\gamma}^{\wedge}) \right] \text{div } \pi^{\beta} + \right. \\ \left. + \left[ G_{\alpha\beta}^{\parallel} - G_{\alpha\beta}^{\perp} + \frac{0.4}{kn_{\beta}} \sum_{\gamma} b_{\gamma\beta} (\lambda_{\beta\gamma}^{\parallel} D_{\alpha\gamma}^{\parallel} - \lambda_{\beta\gamma}^{\perp} D_{\alpha\gamma}^{\perp} + \right. \right. \\ \left. \left. + \lambda_{\beta\gamma}^{\wedge} D_{\alpha\gamma}^{\wedge}) \right] (\text{div } \pi^{\beta} \cdot \kappa) \kappa + \left[ G_{\alpha\beta}^{\wedge} + \frac{0.4}{kn_{\beta}} \sum_{\gamma} b_{\gamma\beta} (\lambda_{\beta\gamma}^{\wedge} D_{\alpha\gamma}^{\perp} + \right. \right. \\ \left. \left. + \lambda_{\beta\gamma}^{\perp} D_{\alpha\gamma}^{\wedge}) \right] (\text{div } \pi^{\beta} \times \kappa) \right\} \cdot$$

Here  $\alpha$  refers to the species,  $n$  is the partial pressure,  $k$  is the Boltzmann constant,  $T$  is the temperature,  $\parallel$  and  $\perp$  refer to the directions parallel and perpendicular to the magnetic field, (symbol missing in document) and  $\chi$  is a unit vector in the direction of the magnetic field. The diffusion

TP7500527

MT6500161

coefficients and the coefficients  $G$  are related by

$$D_{\alpha\beta}^{\parallel} = \frac{kT_{\alpha}}{m_{\alpha}} \frac{|a^{(0)}|_{\beta\alpha} - |a^{(0)}|_{\alpha\alpha}}{|a^{(0)}|}, \quad D_{\alpha\beta}^{\perp} = \frac{kT_{\alpha}}{m_{\alpha}} \frac{|a^{(2)}|_{\beta\alpha} - |a^{(2)}|_{\alpha\alpha}}{|a^{(2)}|},$$

$$D_{\alpha\beta}^{\wedge} = -\frac{kT_{\alpha}}{m_{\alpha}} \sum_{\gamma, \delta} a_{\gamma\delta}^{(2)} \frac{(|a^{(1)}|_{\beta\delta} - |a^{(1)}|_{\alpha\delta}) |a^{(2)}|_{\gamma\alpha}}{|a^{(1)}| |a^{(2)}|}, \quad G_{\alpha\beta}^{\parallel} = D_{\alpha\beta}^{\parallel} - \sum_{\gamma} c_{\gamma} D_{\alpha\gamma}^{\parallel}.$$

The conductivity along the magnetic field is given by

$$\sigma^{\parallel} = -\sum_{\alpha} c_{\alpha} n_{\alpha} K_{\alpha}^{\parallel},$$

where

$$K_{\alpha}^{\parallel} = \sum_{\beta} \frac{n_{\beta}}{n_{\alpha} kT_{\alpha}} \left( c_{\beta} - \sum_{\gamma} \frac{m_{\beta}}{m_{\gamma}} c_{\gamma} c_{\gamma} \right) D_{\alpha\beta}^{\parallel}.$$

Here  $a_{\alpha\beta}$  and  $b_{\alpha\gamma}$  are Chapman-Cowling coefficients. The various coefficients are computed for the case when the anisotropies appearing in the transport can be considered small. The coefficient of ambipolar diffusion for such a gas is obtained in the form

$$D_{\alpha}^{\parallel} = \frac{20^{-1} G_{\alpha}^{\parallel} K_{\alpha}^{\parallel} + 2^{-1} G_{\alpha}^{\parallel} K_{\alpha}^{\parallel}}{K_{\alpha}^{\parallel} + K_{\alpha}^{\parallel}}.$$

Original article has: 35 formulas. English translation: 13 pages.

# ITIS INDEX CONTROL FORM

01 Acc Nr TP7500528	68 Translation Nr MT6500161	65 X Ref Acc Nr AP5002860	76 Reel/Frame Nr 1654 1035
97 Header Clas UNCL	63 Clas UNCL 0	64 Control Markings 0	94 Expansion UR
02 Ctry UR	03 Ref 0207	04 Yr 64	05 Vol 000
06 Iss 005	07 B. Pg. 0018	45 B. Pg. 0029	10 Date NONE

Transliterated Title RAZLET PODOGREVAYEMOY MASSY GAZA V  
REGULYARNOM REZHIME

09 English Title  
DISPERSION OF A HEATED MASS OF GAS IN REGULAR CONDITIONS

43 Source  
ZHURNAL PRIKLADNOY MEKHANIKI I TEKHNICHESKOY FIZIKI (RUSSIAN)

42 Author  
NEMCHINOV, I. V.

16 Co-Author  
NONE

16 Co-Author  
NONE

16 Co-Author  
NONE

16 Co-Author  
NONE

16 Co-Author  
NONE

98 Document Location

47 Subject Codes  
20

39 Topic Tags: gas flow, nonadiabatic process, kinetic energy, equation of state

**ABSTRACT:** The author investigated the problem of the nonadiabatic flow of a gas with the intensity of energy liberation from the molecules depending on the thermodynamic parameters characterizing the state, such as temperature and density. The analysis for deriving the solutions is analogous to that presented by L. I. Sedov (Metody podobiya i razmernosti v mekhanike. Izd. 3-e. Gostekhdat. 1954, 242-248) for the problem of adiabatic dispersion of a gas. The equations of energy and momentum are given by

$$\frac{\partial e}{\partial t} + p \frac{\partial v}{\partial t} = Q = Q_0 \left( \frac{e}{e_0} \right)^{-\alpha} \left( \frac{v}{v_0} \right)^{-\beta} \varphi \left( \frac{t}{t_0} \right) / \left( \frac{m}{m_0} \right)$$

$$\left( \dot{e} = \frac{pv}{\kappa - 1}, \quad \dot{v} = \frac{1}{\rho} \right)$$

$$\frac{\partial u}{\partial t} + \frac{\partial p}{\partial m} r^{\nu-1} = 0, \quad \frac{\partial r}{\partial t} = u, \quad \frac{1}{v} \frac{\partial r^{\nu}}{\partial m} = v$$

where  $e$  is the energy per unit mass of the gas,  $\kappa$  is the adiabatic index,  $v$  is the specific volume,  $\rho$  is the density,  $t$  is the time,  $m$  is the Lagrangian coordinate of the particle,  $u$  is the velocity of the gas,  $r$  is the Eulerian coordinate, and  $\nu = 1, 2, 3$  for the plane, cylindrical, and spherical geometries, respectively. In the regular regime, solutions of the following form were sought:

$$p = P(m) p^0(t), \quad v = V(m) v^0(t)$$

$$u = U(m) u^0(t), \quad r = R(m) r^0(t)$$

A function  $f$ , characterizing the energy distribution in the molecules, is defined by

$$|PV^{\kappa}/(m) = \text{const.}$$

TP7500528

MT6500161

The following boundary conditions were considered

$$\begin{aligned} P=0, \quad U=1, \quad R=1, \quad m\zeta(\nu) &= M \\ P=1, \quad V=1, \quad R=0, \quad U=0, \quad m &= 0 \end{aligned}$$

Here  $\zeta(\nu) = 2, 2\pi$  and  $4\pi$  when  $\nu = 1, 2$  and  $3$ , respectively. When  $f$  is a constant, the kinetic energy  $E_k$ , the thermal energy  $E_t$ , and the total mass  $M$  are given by the expression

$$E_k = \frac{1}{2} \zeta(\nu) \rho^* (u^*)^2 (r^*)^\nu J_k$$

$$E_t = \frac{1}{2} \zeta(\nu) \rho^* (r^*)^\nu J_T / (\kappa - 1)$$

$$M = \zeta(\nu) \rho^* (r^*)^\nu J_M$$

where

$$J_M = \frac{r \left(\frac{\nu}{2}\right) \Gamma\left(\frac{\nu}{\nu-1}\right)}{2\Gamma\left(\frac{\nu}{2} + \frac{\nu}{\nu-1}\right)}, \quad J_k = \frac{r \left(\frac{\nu}{2} + 1\right) \Gamma\left(\frac{\nu}{\nu-1}\right)}{2\Gamma\left(\frac{\nu}{2} + \frac{\nu}{\nu-1} + 1\right)}$$

The time dependence of the various parameters is also discussed. The following expression was derived for the pressure at the center at any time  $t^*$ :

$$p^* = \frac{3^{1/2}(\kappa-1)^{1/2} \pi^{1/2}}{(3\kappa-1)^{1/2} \pi^{1/2}} \left(\frac{E}{\tau}\right)^{1/2} \left(\frac{M}{L}\right)^{1/2}$$

Original article has: 2 figures and 66 formulas. English translation: 19 pages.

# ITIS INDEX CONTROL FORM

01 Acc Nr TP7500529		68 Translation Nr MT6500161		65 X Ref Acc Nr AP5002861		76 Reel/Frame Nr 1654 1037	
97 Header Clas UNCL		63 Clas UNCL, 0		64 Control Markings 0		94 Expansion UR	
02 Ctry UR	03 Ref 0207	04 Yr 64	05 Vol 000	06 Iss 005	07 B. Pg. 0030	45 E. Pg. 0037	10 Date NONE

## Transliterated Title

O NELINEYNOY GEOMETRICHESKOY AKUSTIKE. SLABYYE UDARNYYE VOLNY

## 09 English Title

NONLINEAR GEOMETRIC ACOUSTICS. WEAK SHOCK WAVES

## 43 Source

ZHURNAL PRIKLADNOY MEKHANIKI I TEKHNICHESKOY FIZIKI (RUSSIAN)

## 42 Author

KOROTKOV, P. F.

## 98 Document Location

## 16 Co-Author

NONE

## 47 Subject Codes

20

## 16 Co-Author

NONE

39 Topic Tags: shock wave front, shock wave velocity, acoustic propagation, acoustic wave, weak shock wave

## 16 Co-Author

NONE

## 16 Co-Author

NONE

**ABSTRACT:** Two nonlinear effects of weak shock waves are considered: 1) the dissipation effect; 2) the effect of supplementary path curvature. Both phenomena are studied in propagation through a nonhomogeneous medium. The derivations of the weak wave effects are developed first for the general case. In final form the nonlinear geometrical acoustics equations are the closed system

$$\begin{aligned} \left(n_k + \frac{w_k}{c}\right) \frac{\partial n_i}{\partial x_k} - (n_i n_k - \delta_{ik}) \frac{\partial m}{\partial x_k} &= \\ &= (n_i n_k - \delta_{ik}) \left(\frac{1}{c} \frac{\partial c}{\partial x_k} + \frac{n_i}{c} \frac{\partial w_i}{\partial x_k}\right) \quad (n_i^2 = 1) \\ 2 \left(n_k + \frac{w_k}{c}\right) \frac{\partial m}{\partial x_k} + m \frac{\partial}{\partial x_k} \left(n_k + \frac{w_k}{c}\right) &= \\ &= -m \left(n_k + \frac{w_k}{c}\right) \left[\frac{1}{\rho} \frac{\partial \rho}{\partial x_k} + \frac{3}{c} \frac{\partial c}{\partial x_k} + \frac{c}{c + w_i n_i} \frac{\partial}{\partial x_k} \left(\frac{w_i n_i}{c}\right)\right] - \frac{2m^2}{\lambda} \\ \left(n_k + \frac{w_k}{c}\right) \frac{\partial \lambda}{\partial x_k} &= \frac{c n_k + w_k}{c + w_i n_i} \frac{\lambda}{c} \frac{\partial}{\partial x_k} (c + w_i n_i) + m \end{aligned}$$

in which i, l, and k are unit coordinate vector subscripts, n - a unit vector in the direction denoted by its subscript, c - the speed of sound in the medium,  $\rho$  - the density of the medium, p' - the difference between the pressure at the shock wave front and the internal pressure,  $\lambda$  - the length of the positive phase of the wave along the normal to the wave

TP7500529

MT6500161

front, and  $\omega$  is a velocity vector. The remaining sections deal with particular cases, the first of which is the case of small variations in the speed of sound. Other solutions are offered for a variety of limiting conditions and combining of variables. Certain combinations of factors lend themselves to a graphical solution. The author expresses gratitude to O. S. Ryzhov for his useful comments and to V. I. Kozhevnikov for his assistance in performing the computations. Orig. art. has: 42 equations and 1 figure. English translation: 8 pages.

# ITIS INDEX CONTROL FORM

01 Acc Nr TP7500530		68 Translation Nr MT6500161		65 X Ref Acc Nr AP5002862		76 Reel/Frame Nr 1654 1059	
97 Header Clas UNCL		63 Clas UNCL, 0		64 Control Markings 0		94 Expansion 40 Ctry Info UR	
02 Ctry UR	03 Ref 0207	04 Yr 64	05 Vol 000	06 Iss 005	07 B. Pg. 0038	45 E. Pg. 0043	10 Date NONE

## Transliterated Title

OB USTOYCHIVOSTI GORENIYA POROKHA

## 09 English Title

BURNING STABILITY OF POWDER

## 43 Source

ZHURNAL PRIKLADNOY MEKHANIKI I TEKHNICHESKOY FIZIKI (RUSSIAN)

## 42 Author

ISTRATOV, A. G.

## 98 Document Location

## 16 Co-Author

LIBROVICH, V. B.

## 47 Subject Codes

20, 21

## 16 Co-Author

NONE

39 Topic Tags: combustion, combustion temperature, solid fuel, explosive, propellant

## 16 Co-Author

NONE

## 16 Co-Author

NONE

**ABSTRACT:** The steady-state combustion of powder was investigated and corresponding stability criteria were established. It is assumed that in the combustion model chemical reactions are concentrated in a zone which is negligibly thin in comparison to the region of preheating. The temperature distribution and concentration during combustion are divided into three regions (see Fig. 1 of the Enclosure). In region 1 heating starts at  $T_0$  in solid powder and increases to  $T_s$  at interface 1-2. Chemical reaction takes place between zones 1 and 2, changing the powder into gas. These gaseous products diffuse through region 2 to the interface of combustion, attain the combustion temperature  $T_b$ , and undergo the reaction in zone 2-3. Zone 3 represents the combustion products. The heat conduction equations for each zone are written under the assumption that the Lewis number is unity and the heat capacity and the transfer coefficients are constant. A set of eight boundary conditions is given at the powder surface  $\xi = 0$  and in the gas, at the reaction zone  $\xi = \xi_0$ , satisfying temperature continuity flow and mass conservation, and complete consumption of reacting substances. The solution of the heat conduction equation yields

$$\begin{aligned} 0_1' &= a \exp(r\xi + \omega\tau) \quad (r = 1/2(1 + \sqrt{1 + 4\omega})) \\ 0_2' &= b e^{\omega\tau} + c \exp\left(\frac{c_p}{\lambda} \xi + \omega\tau\right) - \frac{\Delta_1}{\lambda} \omega \xi \exp\left[\frac{c_p}{\lambda} (\xi - \xi_0) + \omega\tau\right] \\ s_2' &= k e^{\omega\tau} + l \exp\left(\frac{c_p}{\lambda} \xi + \omega\tau\right) + \frac{c_p}{\lambda} \omega \xi \exp\left[\frac{c_p}{\lambda} (\xi - \xi_0) + \omega\tau\right] \\ 0_3' &= d e^{\omega\tau}, \quad \xi_1' = f e^{\omega\tau}, \quad \xi_2' = g e^{\omega\tau} \end{aligned}$$

# ITIS INDEX CONTROL FORM

01 Acc Nr TP7500531		68 Translation Nr MT6500161		65 X Ref Acc Nr AP5002863		76 Reel/Frame Nr 1654 1041	
97 Header Clas UNCL		63 Clas UNCL, 0		64 Control Markings 0		94 Expansion 40 Ctry Info UR	
02 Ctry UR	03 Ref 0207	04 Yr 64	05 Vol 000	06 Iss 005	07 B. Pg. 0044	45 E. Pg. 0055	10 Date NONE

## Transliterated Title

ASIMPTOTICHESKIYE METODY GIDRODINAMICHESKOY TEORII USTOYCHIVOSTI

## 09 English Title

ASYMPTOTIC METHODS OF HYDRODYNAMIC THEORY OF STABILITY

## 43 Source

ZHURNAL PRIKLADNOY MEKHANIKI I TEKHNICHESKOY FIZIKI (RUSSIAN)

## 42 Author

ZASLAVSKIY, G. M.

## 16 Co-Author

MOISEYEV, S. S.

## 16 Co-Author

SAGDEYEV, R. Z.

## 16 Co-Author

NONE

## 16 Co-Author

NONE

## 98 Document Location

## 47 Subject Codes

20, 12

39 Topic Tags: asymptotic property, hydrodynamic theory, differential equation, plasma physics

**ABSTRACT:** The authors present an asymptotic method for solving a differential equation of the fourth order. Several problems in the hydrodynamic theory of stability and problems of frequency transformation in magnetic hydrodynamics and plasma physics can be described by the fourth order equation of this type. The differential equation is given as  $\alpha \frac{d^4 \varphi}{d\xi^4} - U_2(\xi, k, \omega) \frac{d^2 \varphi}{d\xi^2} + U_1(\xi, k, \omega) \varphi = 0$ , where  $\alpha$  is a minor parameter,  $\xi$  - a coordinate variable, and  $\omega$  is a frequency variable. Expressed in terms of an additional minor parameter, the problem becomes one of solving the equation  $\alpha \beta^2 \frac{d^4 \varphi}{dx^4} - \beta U_2(x, k, \omega) \frac{d^2 \varphi}{dx^2} + U_1(x, k, \omega) \varphi = 0$  ( $\alpha, \beta \ll 1$ ), in which  $x$  is a dimensionless coordinate,  $k, \omega$  - are problem parameters,  $\alpha$  and  $\beta$  are minor parameters, and  $U_1$  and  $U_2$  are dimensionless funtions. The general solution of this equation is given as  $\varphi(x) = C \exp \left\{ \frac{1}{\sqrt{\beta}} \int q(x) dx \right\}$ ,  $q(x) = q^{(0)}(x) + \sqrt{\beta} q^{(1)}(x) + \dots$  and it is shown that the solution can also be written

$$\varphi_i = \frac{C}{\sqrt{\beta}} \exp \int p_i dx \quad (i = 1, 2)$$

$$\varphi_i = \frac{C}{\sqrt{\beta}} \exp \int p_i dx \quad (i = 3, 4)$$

The solution by asymptotic method is demonstrated for the weak case where  $U_2 = Ux$ ,  $x < 1$ ,  $U \sim 1$ , and for the strong case wherein complex variables are introduced. The author demonstrated that the classification of solution cases can be related to certain inequality relationships between  $\alpha$  and  $\beta$ . A discussion is given concerning plasma instability in gravitational field. The author thanks I. B. Khriplovich, A. A. Galeev, V. N. Orayevskiy for their valued discussions. Original article has: 61 equations and 4 figures. English translation: 12 pages.

# ITIS INDEX CONTROL FORM

01 Acc Nr TP7500532	68 Translation Nr MT6500161	65 X Ref Acc Nr AP5002864	76 Reel, Frame Nr 1654 1042
97 Header Clas UNCL	63 Clas UNCL, 0	64 Control Markings 0	94 Expansion UR
02 Ctry UR	03 Ref 0207	04 Yr 64	05 Vol 000
06 Iss 005	07 B. Pg. 0056	45 B. Pg. 0058	10 Date NONE

Transliterated Title OB ODNOM SLUCHAYE SVOBODNOY KONVEKTSII ZHIDKOSTI PRI NALICHII RASTVORYAYUSHCHIKHSYA I POGLOSHCHAYUSHCHIKH STENOK

09 English Title ONE CASE OF FREE CONVECTION OF A LIQUID IN THE PRESENCE OF DISSOLVING AND ABSORBING WALLS

## 43 Source

ZHURNAL PRIKLADNOY MEKHANIKI I TEKHNICHESKOY FIZIKI (RUSSIAN)

## 42 Author

BUGAYENKO, G. A.

## 98 Document Location

## 16 Co-Author

NONE

## 47 Subject Codes

20

## 16 Co-Author

NONE

39 Topic Tags: heat diffusion, thermal diffusion, heat convection

## 16 Co-Author

NONE

## 16 Co-Author

NONE

**ABSTRACT:** The exact solution is found for the problem of the convection of a liquid enclosed between two vertical coaxial cylinders heated to different temperatures. The outer cylinder (radius  $R_2$ , temperature  $T_1$ ) is soluble so that at its surface the concentration  $C$  is that of the saturated solution  $C_*$ . The inner cylinder (radius  $R_1$ , temperature  $T_0$ ) absorbs all the diffusing material on its surface so that  $C(R_1) = 0$ . The temperature and concentration between the cylinders is then given by  $T = \frac{T_1 - T_0}{\ln(R_2/R_1)} \ln \frac{r}{R_1} + T_0$ ,  $C = \frac{C_*}{\ln(R_2/R_1)} \ln \frac{r}{R_1}$ .

The hydrodynamic velocity  $v_z = v(r)$  ( $z$  is directed vertically upwards and  $v_r = v_\theta = 0$ ), is given by  $v = \frac{1}{4} r^2 [a(1 - \ln \frac{r}{R_1}) - b] + k \ln \frac{r}{R_1} + k_1$ ,

$$a = \left( \beta_1 \frac{T_1 - T_0}{\ln(R_2/R_1)} + \beta_2 \frac{C_*}{\ln(R_2/R_1)} \right) \frac{\kappa}{\nu}, \quad b = \beta_1 T_0 \frac{\kappa}{\nu} - A_2$$

$$k_1 = \frac{R_1^2}{4\Delta} \left( P \ln \frac{R_2}{R_1} - MQ \right), \quad k = \frac{1}{\ln(R_2/R_1)} \left[ M + k_1 \left( \frac{R_2^2}{R_1^2} - 1 \right) \right]$$

$$4\Delta = \frac{1}{2} (R_2^2 - R_1^2) \ln \frac{R_1}{R_2} + \frac{1}{2} (R_2^2 - R_1^2) R_1^2 \ln \frac{R_2}{R_1} + Q(R_2^2 - R_1^2)$$

$$M = \frac{1}{2} a R_2^2 \ln \frac{R_2}{R_1}$$

$$P = a/16 [R_2^2 \ln \frac{R_2}{R_1} - \frac{1}{2} (R_2^2 - R_1^2)]$$

$$Q = \frac{1}{2} [R_2^2 \ln \frac{R_2}{R_1} - \frac{1}{2} (R_2^2 - R_1^2)]$$

$$A = \frac{\rho_1 T_0}{\nu} - a + \frac{1}{\Delta} \left\{ P \ln \frac{R_1}{R_2} + MQ \right\}$$

TP7500532

MT6500161

The coefficients of expansion  $\beta_1$  and  $\beta_2$  and of the kinematic viscosity  $\nu$  are taken at the mean values of  $T$  and  $C$ , and  $g$  is the gravitational potential. The diffusion flux of the dissolved material is given by  $J_n = - \frac{\rho_0 D}{\ln(\kappa_2/\kappa_1)} [(T_1 - T_0)\lambda + C_0]$ ,

where  $D$  and  $\lambda$  are the coefficients of diffusion and thermal diffusion respectively (also at the mean values of  $T$  and  $C$ ). Original article has: 47 equations. English translation: 3 pages.

# ITIS INDEX CONTROL FORM

01 Acc Nr TP7500533		68 Translation Nr MT6500161		65 X Ref Acc Nr AP5002865		76 Reel . . . . . Nr 1654 1044	
97 Header Clas UNCL		63 Clas UNCL, 0		64 Control Markings 0		94 Expansion 40 Ctry Int UR	
02 Ctry UR	03 Ref 0207	04 Yr 64	05 Vol 000	06 Iss 005	07 B. Pg. 0059	45 E. Pg. 0065	10 Date NONE

## Transliterated Title

0 DROBLEMII STRUI ZHIDKOSTI, OBTEKAYEMOY GAZOVYM POTOKOM

09 English Title  
SPLITTING A STREAM OF LIQUID, STREAMLINED BY A GAS FLOW

## 43 Source

ZHURNAL PRIKLADNOY MEKHANIKI I TEKHNIЧЕСКОY FIZIKI (RUSSIAN)

42 Author  
BORODIN, V. A.

98 Document Location

16 Co-Author  
BRITNEVA, L. N.

47 Subject Codes  
20

16 Co-Author  
DITYAKIN, YU. F.

39 Topic Tags: jet stream, transverse flow, fuel injection, jet breakup, Laplace equation

16 Co-Author  
YAGODKIN, V. I.

16 Co-Author  
NONE

**ABSTRACT:** The breakup of a cylindrical ideal liquid jet (radius  $a$ , density  $\rho_1$ ) by the transverse flow of another ideal fluid (density  $\rho_2$ , velocity  $U_0$ ) was studied analytically. Two types of waves propagating along the jet surface were considered: 1) tangential waves deforming the jet in the plane of its cross section; 2) longitudinal waves. Time-dependent potential functions are introduced for the jet and the fluid in cylindrical coordinates, and the following solution is assumed  $\Phi(r, \varphi, t) = u(r, \varphi)e^{-i\omega t}$ . The continuity of the

normal component of the velocity at the interface is used as a boundary condition. From Laplace's equation a generalized solution is obtained in the form

$$u_1 = \sum_{m=0}^{\infty} A_m R^m e^{im\varphi}, \quad u_2 = \sum_{m=0}^{\infty} B_m R^{-m} e^{im\varphi}.$$

For  $m = 0$  and  $R = 1$ , the velocity of surface rise of the jet is given by

$$v_r = \frac{1}{a} \sum_{m=0}^{\infty} m A_m R^{m-1} \cos m\varphi e^{-i\omega t}.$$

and the equations of nodal lines on the perturbed jet take the form of

$$\sum_{k=0}^{\infty} m A_m \cos m\varphi = 0$$

(for  $m = 2k$  and  $m = 2k + 1$ )

Numerical calculations show that at  $2 < W < 27.6$  ( $W$  = Weber number), four nodal lines appear on the jet surface and two nodal lines at  $0.656 < W < 1.24$ . To determine the wave propagation along the jet, the stream function is assumed to have the form

$$\Phi(r, \varphi, z, t) = u(r, \varphi)e^{-i\omega t + i\lambda z}.$$

1654 1045

TP7500533

MT6500161

Substituting in the cylindrical Laplace equation, the solution is obtained in a Bessel function of imaginary arguments. Numerical results are obtained for  $W = 5$  and  $10$ . Original article has: 4 figures and 46 formulas. English translation: 7 pages.

# ITIS INDEX CONTROL FORM

01 Acc Nr TP7500534	68 Translation Nr MT6500161	65 X Ref Acc Nr AP5002866	76 Reel, Frame Nr 1654 1046
97 Header Clas UNCL	63 Clas UNCL 0	64 Control Markings 0	94 Expansion UR
02 Ctry UR	03 Ref 0207	04 Yr 64	05 Vol 000
06 Iss 005	07 B. Pg. 0066	45 E. Pg. 0074	10 Date NONE

## Transliterated Title

REOLOGICHESKIYE SVOYSTVA POLIMEROV V TEKUCHEM SOSTOYANII

## 09 English Title

RHEOLOGICAL PROPERTIES OF POLYMERS IN THE FLUID STATE

## 43 Source

ZHURNAL PRIKLADNOY MEKHANIKI I TEKHNICHESKOY FIZIKI (RUSSIAN)

## 42 Author

VINOGRADOV, G. V.

## 16 Co-Author

MALKIN, A. YA.

## 16 Co-Author

NONE

## 16 Co-Author

NONE

## 16 Co-Author

NONE

## 98 Document Location

## 47 Subject Codes

20, 11

39 Topic Tags: polymer rheology, creep, viscosimeter, polypropylene, polyethylene

**ABSTRACT:** The rheological properties of polymers were investigated in an effort to obtain mathematical models of observed physical phenomena. Tests were performed upon the commercial polymers polybutylene P-20, polypropylene OP-30, certain polyethylenes, polystyroles, and others. Testing equipment included rotation viscosimeter REV-1 and a capillary constant pressure viscosimeter. Deforming stress was measured with respect to relative deformation at various temperatures and various constant speeds of deformation. Figure 1 on the Enclosure is a plot of stress  $\tau$  vs relative deformation  $\gamma$  (right side) and of stress vs time  $t$  during stress relaxation after flow has ceased. The authors developed a temperature invariant form of presenting polymer strength characteristics. A parameter  $\eta_0/\eta$  is defined which is related to strength

by the empirical equation  $\eta_0/\eta = 1 + 0.12 \cdot 10^{-3} (\gamma \eta_0)^{0.25} + 2.35 \cdot 10^{-4} (\gamma \eta_0)^{0.75}$

where  $\eta_0$  is a variable defining the strength as a function of molecular weight and temperature. The experimental data which led to the establishment of the empirical formula are given in a logarithmic graph of  $\eta/\eta_0$  vs  $\tau/\eta_0$ . Dynamic strength characteristics were also fitted to the empirical equations

$$\eta_0/\eta = 1 + 0.12 \cdot 10^{-3} (\omega \eta_0)^{0.25} + 2.35 \cdot 10^{-4} (\omega \eta_0)^{0.75}$$

$$N(\omega) = \eta_0 \left[ \sum_{k=1}^n L_k (\omega \eta_0)^{0.25k} \right] : \left[ \sum_{k=1}^n M_k (\omega \eta_0)^{0.75k} \right]$$

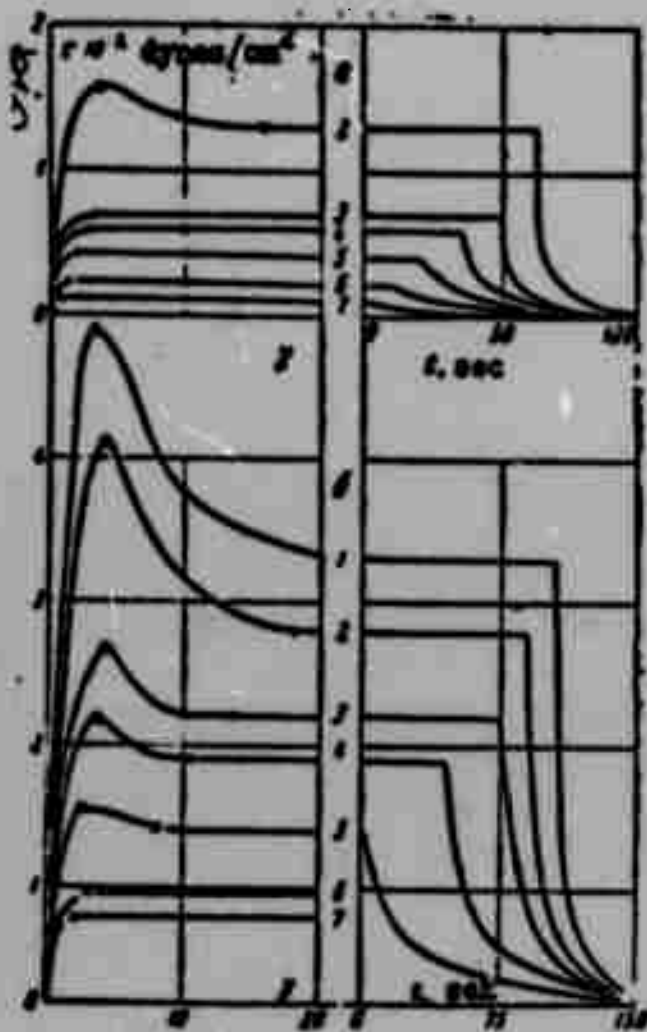
where  $\eta_d$  is the dynamic strength parameter,  $\omega$  is the dynamic frequency,  $N(\omega)$  is the Laplace function, and  $L_k$  and  $M_k$  are constants obtained from the equation for  $\eta_0/\eta_d$ . The temperature invariant stress vs time relationship is given in the form

$$\frac{\tau(t)}{\eta_0} = \int_0^t \frac{N(\omega)}{\eta_0} \omega d\omega$$

TP7500534

MT6500161

and experimental data are plotted to demonstrate this relationship. Original article has: 8 equations and 6 figures. English translation: 9 pages.



# ITIS INDEX CONTROL FORM

01 Acc Nr TP7500535		68 Translation Nr MT6500161		65 X Ref Acc Nr AP5002867		76 Reel/Frame Nr 1654 1048	
97 Header Clas UNCL		63 Clas UNCL, 0		64 Control Markings 0		94 Expansion 40 Ctry Info UR	
02 Ctry UR	03 Ref 0207	04 Yr 64	05 Vol 000	06 Iss 005	07 B. Pg. 0075	45 E. Pg. 0082	10 Date NONE

## Transliterated Title

0 POLZUCHESTI POLIMEROV V STEKLOOBRAZNOY SOSTOYANII

## 09 English Title

POLYMER CREEP IN THE VITREOUS STATE

## 43 Source

ZHURNAL PRIKLADNOY MEKHANIKI I TEKHNIЧЕСКОY FIZIKI (RUSSIAN)

## 42 Author

DOLGOV, A. V.

## 16 Co-Author

MALININ, N. I.

## 16 Co-Author

NONE

## 16 Co-Author

NONE

## 16 Co-Author

NONE

## 98 Document Location

## 47 Subject Codes

20, 11, 07

39 Topic Tags: fiberglass, Volterra equation, creep, deformation rate, amorphous polymer, elasticity, oscilloscope

**ABSTRACT:** The deformation properties of amorphous fiber glass polymers were studied analytically and experimentally, using the stress-strain integral equation

$$\epsilon = \frac{\sigma}{E} + \int_0^t (1 - \theta; \sigma) \sigma(0) d\theta$$

This equation is subsequently modified to yield a nonlinear Volterra equation of the type

$$\epsilon = \frac{\sigma}{E} + \int_0^t K(\sigma, t - \theta) d\theta$$

The material under study was unplasticized polyvinylchloride (PVC) at  $T = 19^\circ\text{C}$ , and the experiment was carried out on a programmed machine with magnetic loading. Three different methods were used to determine the "instantaneous" elasticity  $F(\sigma) = \sigma/E$ , and all three gave the same value for the modulus  $E$ . The creep deformation  $\epsilon^{[c]}$  versus  $t$  curves were plotted logarithmically with the empirical result  $\epsilon^{[c]} = A_1 t^n$ , where  $A_1$  and  $n$  are functions of the

stress  $\sigma$ . This leads to the following expression for the kernel in the integral equation  $\epsilon$ :

$$\epsilon = \frac{\sigma}{E} + \int_0^t \frac{f_1(\sigma)}{(t - \theta)^{1/2}} d\theta$$

Experimental determination of  $f_1(\sigma)$  leads to a value given by  $A_2 \ln \sigma/\sigma_0$ , where  $A_2 = 1.64 \times 10^5$  and  $\sigma_0 = 1.086 \text{ kg/mm}^2$ . Curves were also obtained depicting  $\epsilon$  versus  $t$  where the load was increased in steps. For this purpose, the integral equation is written as a summation, and the calculated results agreed with the data points very favorably. A cyclic load-unload type deformation-time curve showed that under load-on conditions the creep deformation increases, whereas, for no-load conditions, it decreases. Orig. art. has: 14 formulas

# ITIS INDEX CONTROL FORM

01 Acc Nr TP7500536		68 Translation Nr MT6500161		65 X Ref Acc Nr		76 Reel, Frame Nr 1654 1049	
97 Header Clas UNCL		63 Clas UNCL, 0		64 Control Markings 0		94 Expansion 40 Ctry Info UR	
02 Ctry UR	03 Ref 0207	04 Yr 64	05 Vol 000	06 Iss 005	07 B. Pg. 0083	45 B. Pg. 0090	10 Date NONE

## Transliterated Title

RAZRYV TELA S LINEYNOY DISLOKATSIYEV

09 English Title  
RUPTURE OF A BODY WITH LINEAR DISLOCATION

43 Source  
ZHURNAL PRIKLADNOY MEKhanIKI I TEKHNIChESKOY FIZIKI (RUSSIAN)

42 Author  
LEONOV, M. YA.

16 Co-Author  
RUSINKO, K. N.

16 Co-Author  
NONE

16 Co-Author  
NONE

16 Co-Author  
NONE

98 Document Location

47 Subject Codes  
20

39 Topic Tags: brittleness, rupture strength, crystal dislocation phenomenon, tensile stress

**ABSTRACT:** Brittle rupture of an unbounded body with introduced material half-plane is investigated (edge dislocation) during its uniform extension to infinity by forces perpendicular to the shown half-plane. The basic purpose of this work is clarification of the influence of different laws of interaction of opposite edges of cracks on conditions of brittle rupture. In this meaning it is the continuation and development of [1]. English translation: 13 pages.

# ITIS INDEX CONTROL FORM

01 Acc Nr JP7500537	68 Translation Nr MT6500161	65 X Ref Acc Nr AP5002868	76 Reel/Frame Nr 1654 1050
97 Header Clas UNCL	63 Clas UNCL, 0	64 Control Markings 0	94 Expansion 40 Ctry Info UR
02 Ctry UR	03 Ref 0207	04 Yr 64	05 Vol 000
06 Iss 005	07 B. Pg. 0091	45 E. Pg. 0101	10 Date NONE

## Transliterated Title

IZLUCHENIYE METODAMI TEORII TRESHCHIN RAZRUSHENIYA KHRUPKIKH SKLEYEK

## 09 English Title

STUDIES IN BREAKING OF BRITTLE SPLICES BY USING FRACTURE THEORY METHODS

## 43 Source

ZHURNAL PRIKLADNOY MEKhanIKI I TEKHNIChESKOY FIZIKI (RUSSIAN)

## 42 Author

MALYSHEV, B. M.

## 98 Document Location

## 16 Co-Author

SALGANIK, R. L.

## 47 Subject Codes

20, 11

## 16 Co-Author

NONE

39 Topic Tags: crack propagation, resin, elastic deformation, stress concentration, epoxy resin

## 16 Co-Author

NONE

## 16 Co-Author

NONE

**ABSTRACT:** Analytical and experimental investigations were carried out to determine the mechanism of fracture propagation in homogeneous as well as nonhomogeneous materials spliced together by resins. Equations are given describing the normal and tangential stresses ( $\sigma_y$ ,  $\tau_{xy}$ ) generated at the cut between two elastic bodies which, outside the cut, are in complete cohesion. These stresses are shown to be functions of  $\beta$ , which depends on the shear moduli and Poisson coefficients of the material, and  $s$ , the distance from the point in consideration on the cut to be end of the cut. From these two expressions, a functional equation is obtained for the fracture energy  $T$  of a cut or slit, given by  $T = T_0 / (A_0 / B_0) = T_0 / (\sigma_y / \tau_{xy})$

where  $A_0$  and  $B_0$  are "coefficients of stress intensity." To verify this result experimentally, three simplified fracture (or tear) schemes are introduced where  $A_0$  and  $B_0$  take on a geometric meaning,  $A_0 / B_0 = \tan \alpha$ . These three schemes are depicted in Figures 1, 2, and 3 on the Enclosures. For Figures 2 and 3, the fracture or tear energy takes on simplified forms given by

$$T = \frac{3Pw}{2bl} = \frac{P^2 l^3}{2bEI} = \frac{9EIw^3}{2bl^3} = \left( \frac{9P^2 w^3}{8bEI} \right)^{1/2} \quad T = \frac{P^2}{32\pi D^3} = \frac{Pw}{2\pi a^3} = \frac{8Dw^3}{a^3} \quad (2.6)$$

All three cases were tested experimentally by using plastic-on-plastic and plastic-on-steel splices with epoxy resin bonds. For case 1, it was assumed that  $E(\text{Plastic}) = 3 \times 10^4 \text{ kg/cm}^2$  and  $\nu = 0.4$ . Measurements showed that  $T$  remains approximately constant (at 0.06 kg/cm) under a tensile force  $P$  ranging from 45 to 85 kg. In case 2,  $T$  was found to oscillate around the value of 0.04 kg/cm. The only disagreements with theory were obtained at  $w = 1$  and 2.75-mm values where nonhomogeneities were found in the spliced joint. Finally, the case 3 results were plotted graphically as  $P$  versus deflection  $w$  and fracture radius "a" versus  $w$ . The fracture energy was estimated to be

TP7500537

MT6500161

0.017 kg/cm. "The authors are grateful to G. I. Barenblatt for his constant influence on the work and his illuminating discussions." Orig. art. has: 11 formulas and 8 figures.  
English translation: 11 pages.

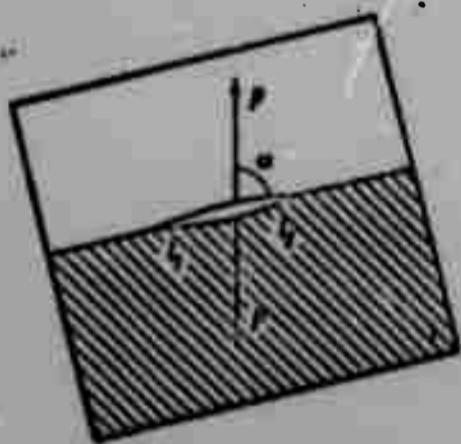


Fig. 1.

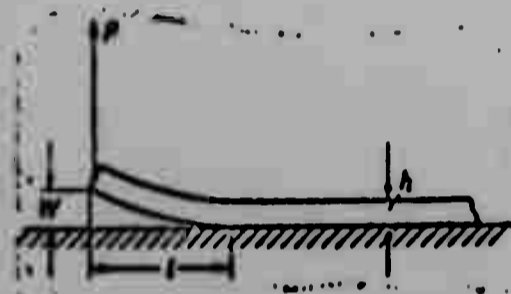


Fig. 2.

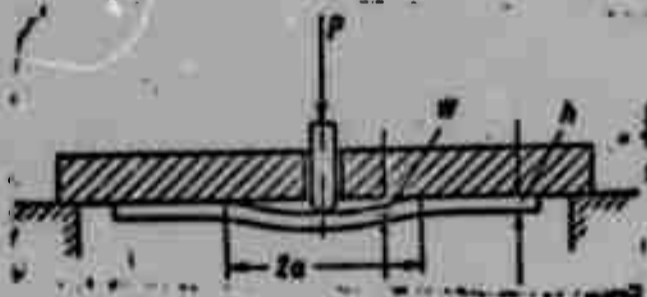


Fig. 3.

# ITIS INDEX CONTROL FORM

01 Acc Nr TP7500538		68 Translation Nr MT6500161		65 X Ref Acc Nr		76 Reel/Frame Nr 1654 1052	
97 Header Clas UNCL		63 Clas UNCL, 0		64 Control Markings 0		94 Expansion UR	
02 Ctry UR	03 Ref 0207	04 Yr 64	05 Vol 000	06 Iss 005	07 B. Pg. 0102	45 E. Pg. 0108	10 Date NONE
Transliterated Title K TEORII OSESIMMETRICHNOGO SOSTOYANIYA IDEAL'NO-PLASTICHESKOGO MATERIALA							
09 English Title THE THEORY OF THE AXIALLY SYMMETRIC STATE OF AN IDEAL PLASTIC MATERIAL							
43 Source ZHURNAL PRIKLADNOY MEKHANIKI I TEKHNICHESKOY FIZIKI (RUSSIAN)							
42 Author BYKOVTSSEV, G. I.				98 Document Location			
16 Co-Author IVLEV, D. D.				47 Subject Codes 20, 11			
16 Co-Author MARTYNOVA, T. N.				39 Topic Tags: plastic deformation, plastic strength, flow stress, plasticity			
16 Co-Author NONE							
16 Co-Author NONE							

**ABSTRACT :** Properties of equations of the axially symmetric state under the condition of plasticity of Tresca were considered in [1-3].

In [4] are considered equations of the axially symmetric problem of an ideal plastic material when the stressed and deformed state corresponds to the edge of an arbitrary piecewise-linear surface of fluidity, interpreting the condition of plasticity in the space of main stresses.

In this work are considered equations of the axially symmetric problem of an isotropic ideal plastic material when the stressed and deformed state corresponds to the edge of an arbitrary piecewise-linear surface of fluidity. It is shown that in this case the initial system of equations always has real characteristics, coinciding with trajectories of main stresses (isostatic curves). It is shown that there cannot exist a line of discontinuity of rates of displacements.

Let us note that if in the case of conformity of the stressed and deformed state to edge of surface of fluidity the problem is statically definable [4], then for the edge of the surface of fluidity there is always kinematic definability. The last for the condition of plasticity of Tresca was noted in [1, 3]. The work considers also self-simulating solutions, corresponding to conical and spherical flows of ideal plastic material.

Considerations are made that the stressed and deformed state, corresponding to an edge of a prism of fluidity, cannot correspond to basic types of axially symmetric flows of ideal plastic material.  
English translation: 13 pages.

# ITIS INDEX CONTROL FORM

01 Acc Nr TP7500539		68 Translation Nr MT6500161		65 X Ref Acc Nr AP5002869		76 Reel/.rame Nr 1654 1053	
97 Header Clas UNCL		63 Clas UNCL, 0		64 Control Markings 0		94 Expansion 40 Ctry Info UR	
02 Ctry UR	03 Ref 0207	04 Yr 64	05 Vol 000	06 Iss 005	07 B. Pg. 0109	45 E. Pg. 0117	10 Date NONE

Transliterated Title TEORIYA VYAZKO-UPRUGIKH MNOGOSLOYNYKH OBOLOCHEK S ZHESTIKIMI ZAPOLNITELYAMI PRI KONECHNYKH PROGIBAKH

09 English Title THEORY OF VISCOELASTIC MULTILAYERS OF SHELLS WITH RIGID FILLERS WITH THE EXISTENCE OF FINITE BENDING

43 Source

ZHURNAL PRIKLADNOY MEKHANIKI I TEKHNICHESKOY FIZIKI (RUSSIAN)

42 Author

GRIGOLYUK, E. I.

98 Document Location

16 Co-Author

CHULKOV, P. P.

47 Subject Codes

20

16 Co-Author

NONE

39 Topic Tags: shell structure, shallow shell, shell vibration, sandwich structure

16 Co-Author

NONE

16 Co-Author

NONE

**ABSTRACT:** The theory of finite deflection of multilayer sandwich snells is developed. The arbitrarily alternated load carrying layers and the filler layers are both made of different viscoelastic materials, and they are laterally incompressible and rigidly joined with each other. The theory is based on the equations for shallow shells, assuming a linear variation of displacements over the thickness of the whole pack. The accepted modified Kirchhoff-Love hypothesis (that the straight fibers originally normal to the surface of the shell remain straight under deformation, but not normal to the distorted surface) permits one to consider shifts in the material of the layers. Two solving differential equilibrium equations containing the displacement and force functions are set up; the systems of equations for various particular cases (rigid-core and light-core sandwich plates) are obtained from these equations. The application of these equations to investigating vibrations of thin, shallow, multilayer shells is indicated. The formulation of basic boundary conditions for simply supported and clamped shallow shells is given. Original article has: 28 formulas. English translation: 9 pages.

**ITIS INDEX CONTROL FORM**

01 Acc Nr TP7500540		68 Translation Nr MT6500161		65 X Ref Acc Nr AP5002870		76 Reel/frame Nr 1654 1054	
97 Header Clas UNCL		63 Clas UNCL, 0	64 Control Markings 0			94 Expansion	40 Ctry Info UR
02 Ctry UR	03 Ref 0207	04 Yr 64	05 Vol 000	06 Iss 005	07 B. Pg. 0118	45 E. Pg. 0119	10 Date NONE

**Transliterated Title**

ZAVISIMOST' RAZMEROV KRATERA OF TVERDOSTI MISHENI

**09 English Title**

DEPENDENCE OF DIMENSIONS OF CRATER ON HARDNESS OF TARGET

**43 Source**

ZHURNAL PRIKLADNOY MEKHANIKI I TEKHNICHESKOY FIZIKI (RUSSIAN)

**42 Author**

FADEYENKO, YU. I.

**16 Co-Author**

NONE

**16 Co-Author**

NONE

**16 Co-Author**

NONE

**16 Co-Author**

NONE

**98 Document Location**

**47 Subject Codes**

11, 20

**39 Topic Tags:** aluminum alloy, mechanical property, nickel alloy, alloy steel, steel, aluminum property

**ABSTRACT:** Several experiments were carried out in which Nichrome projectiles measuring  $160 \pm 5\mu$  in diameter were explosively accelerated into aluminum-alloy and steel plates. The experiments were conducted under vacuum in order to avoid air braking. Constant acceleration conditions were maintained throughout the tests so that impact velocity and the size of the particle did not change from test to test. A target area containing 20—25 craters was investigated so as to determine the depth and the diameter of the individual craters. The quantity of projectile material remaining in the target after impact could be disregarded because earlier experiments had shown that the amount of projectile left in the craters is only 3—8%. Test results obtained for various target materials are summarized and illustrated. Original article has: 3 figures, 3 formulas and 1 table. English translation: 2 pages.

ITIS INDEX CONTROL FORM

01 Acc Nr TP7500541		68 Translation Nr MT6500161		65 X Ref Acc Nr		76 Reel, Frame Nr 1654 1055	
97 Header Clas UNCL		63 Clas UNCL, 0		64 Control Markings 0		94 Expansion UR	
02 Ctry UR	03 Ref 0207	04 Yr 64	05 Vol 000	06 Iss 005	07 B. Pg. 0120	45 E. Pg. 0122	10 Date NONE

Transliterated Title

O PODOBII POVERKHNOSTNYKH VOLN PRI VZRYVAKH V GRUNTAKH

09 English Title

SIMILARITY OF SURFACE WAVES DURING EXPLOSIONS IN THE GROUND

43 Source

ZHURNAL PRIKLADNOY MEKHANIKI I TEKHNICHESKOY FIZIKI (RUSSIAN)

42 Author

GRIGORYAN, S. S.

98 Document Location

16 Co-Author

NONE

47 Subject Codes

20, 08

16 Co-Author

NONE

39 Topic Tags: seismic wave, seismic wave propagation, seismography, underground explosion, compression shock wave

16 Co-Author

NONE

16 Co-Author

NONE

**ABSTRACT:** In [1] are discussed results of experimental study of surface waves formed near the epicenter of shallow sunken explosion in clay ground, and an attempt is made to give with the help of analysis of experimental data generalized empirical relationships, founded on considerations of theory of dimension and similarity. The initial section of surface wave (environment of first entry of seismogram) is subjected to detailed consideration. English translation: 7 pages.

# ITIS INDEX CONTROL FORM

01 Acc Nr TP7500542		68 Translation Nr MT6500161		65 X Ref Acc Nr AP5002872		76 Reel/Frame Nr 1654 1056	
97 Header Clas UNCL		63 Clas UNCL 0		64 Control Markings 0		94 Expansion UR	
02 Ctry UR	03 Ref 0207	04 Yr 64	05 Vol 000	06 Iss 005	07 B. Pg. 0123	45 E. Pg. 0126	10 Date NONE

## Transliterated Title

PRIKLIZHENNOYE URAVNIENIYE SOSTOYANIYA TVERDYKH TEL

## 09 English Title

APPROXIMATE EQUATION OF STATE OF SOLID BODIES

## 43 Source

ZHURNAL PRIKLADNOY MEKHNAIKI I TEKHNIЧЕСКОY FIZIKI (RUSSIAN)

## 42 Author

KORYAVOV, V. P.

## 98 Document Location

## 16 Co-Author

NONE

## 47 Subject Codes

20

## 16 Co-Author

NONE

39 Topic Tags: adiabatic compression, compression shock wave, shock wave thermodynamics, thermodynamic equation of state

## 16 Co-Author

NONE

## 16 Co-Author

NONE

**ABSTRACT :** The description of the state of a substance compressed in strong shock waves is considered. For a wide variety of solids it is found experimentally that the velocity of the shock wave  $D$  and the velocity of the material behind the front  $u$  are related linearly;  $D = D_0 + su$ . The constant  $s$  does not differ much from 1.5, and  $D_0$  is close to the so-called Bridgeman velocity of sound  $C_B$ . With several additional assumptions, the complete thermodynamic description for the behavior of a substance with isotropic compression can be obtained. The energy and pressure are separated into a thermal and a so-called cold part ( $E_x, p_x$ ), which is connected with deformations of the crystal lattice and is independent of temperature. The relation between the thermal parts is given by the Mie-Grüneisen equation  $\frac{p - p_x}{E - E_x} = \gamma\sigma$ , where the density  $\sigma$  is in units of the initial density  $\rho_0$ , the pressure  $p$  is in units of  $\rho_0 D_0^2$ , the energy  $E$  is in units of  $D_0^2$ . Neglecting the initial pressure and initial internal energy of the undisturbed material, the following system of equations is obtained;  $\frac{p_H - p_x}{E_H - E_x} = \gamma\sigma, p_x' = \sigma^2 \frac{dE_x}{d\sigma}, p_H = \frac{\sigma(\sigma - 1)}{[s - (s - 1)\sigma]^2}, E_H = \frac{1}{2} \left[ \frac{\sigma - 1}{s - (s - 1)\sigma} \right]^2$ , where  $p_H$  and  $E_H$  are the pressure and energy at the shock wave front. The solution depends on the form of the Grüneisen coefficient  $\gamma$ . Solutions are indicated for  $\gamma$  - a constant equalling 1 or 2 and for  $\gamma$  - function of  $\sigma$   $\gamma = 2(4 - \sigma)/(5 - \sigma)$ . The author thanks S. S. Grigoryan and Yu. P. Rayzer for helpful discussion of the article. Orig. art. has: 36 equations, 2 diagrams, and 1 table. English translation: 4 pages.

# ITIS INDEX CONTROL FORM

01 Acc Nr TP7500543		68 Translation Nr MT6500161		65 X Ref Acc Nr AP5002873		76 Reel/Frame Nr 1654 1057	
97 Header Clas UNCL		63 Clas UNCL, 0		64 Control Markings 0		94 Expansion UR	
02 Ctry UR		03 Ref 0207		04 Yr 64		05 Vol 000	
06 Iss 005		07 B. Pg. 0127		45 E. Pg. 0131		10 Date NONE	

Transliterated Title EKSPERIMENTAL'NOYE ISSLEDOVANIYE OBTEKANIYA ZATUPLennyKH  
TEL PLOSKIM POTOKOM VYAZKO-PLASTICHESKOY SREDY

09 English Title EXPERIMENTAL INVESTIGATION OF FLOW AROUND BLUNTED BODIES  
BY A FLAT FLOW OF A PLASTIC MEDIUM

43 Source  
ZHURNAL PRIKLADNOY MEKHANIKI I TEKHNIChESKOY FIZIKI (RUSSIAN)

42 Author  
BULINA, I. G.

98 Document Location

16 Co-Author  
MYASNIKOV, V. P.

47 Subject Codes

20

16 Co-Author  
SAVIN, V. G.

39 Topic Tags: plane flow, drag coefficient,  
blunt body, wedge body

16 Co-Author  
NONE

16 Co-Author  
NONE

**ABSTRACT:** The problem of a plane stream of viscous-plastic medium flowing around a blunt body has been studied in great detail. The experiments, aimed at determining resistance, were carried out with a specially designed dynamometer. The results obtained agreed well with the theoretical data on the nature of the relationship between drag coefficient of the body and the controlling parameters of the problem. For geometrically shaped bodies (parallelepipeds, cylinders, and wedge-shaped bodies were tested), the  $\gamma C_a$  product is a universal function of  $S_1$ , which can be determined experimentally on one model and later used to compute the streamlining of bodies having different geometric parameters. The main geometric characteristics of a streamlined body are its maximum thickness and its length. It was found that the drag of wedge-shaped bodies moving in a viscous-plastic medium, unlike the drag of bodies streamlined by a viscous fluid under similar conditions, does not depend upon whether the body moves with its base or its nose forward. Orig. art. has: 7 figures, and 12 formulas, 1 table. English translation: 11 pages.

# ITIS INDEX CONTROL FORM

01 Acc Nr TP7500544		68 Translation Nr MT6500161		65 X Ref Acc Nr AP5002874		76 Reel/Frame Nr 1654 1058	
97 Header Clas UNCL		63 Clas UNCL, 0		64 Control Markings 0		94 Expansion 40 Ctry Info UR	
02 Ctry UR	03 Ref 0207	04 Yr 64	05 Vol 000	06 Iss 005	07 B. Pg. 0132	45 E. Pg. 0134	10 Date NONE

## Transliterated Title

K RASCHETU OBTEKANIYA PLASTINY KAPEL'NOY ZHIDKOST'YU S PEREMENNOY VYAZKOST'YU

09 English Title CALCULATION OF FLOW AROUND A PLATE BY A LIQUID-DROP  
LIQUID WITH VARIABLE VISCOSITY

## 43 Source

ZHURNAL PRIKLADNOY MEKHANIKI I TEKHNICHESKOY FIZIKI (RUSSIAN)

## 42 Author

KASHKAROV, V. P.

## 98 Document Location

## 16 Co-Author

LUK'YANOV, A. T.

## 47 Subject Codes

20

## 16 Co-Author

NONE

39 Topic Tags: liquid flow. flat plate.  
boundary layer flow.

## 16 Co-Author

NONE

## 16 Co-Author

NONE

**ABSTRACT:** The solution of the system of equations for the boundary layer of a liquid with variable viscosity flowing in a uniform current around a plate is considered. The system of equations in dimensionless variables is of the form

$$u \frac{\partial u}{\partial x} + v \frac{\partial u}{\partial y} = \frac{\partial}{\partial y} \left[ \nu \frac{\partial u}{\partial y} \right], \quad \frac{\partial u}{\partial x} + \frac{\partial v}{\partial y} = 0, \quad u \frac{\partial \theta}{\partial x} + v \frac{\partial \theta}{\partial y} = \frac{1}{Pr} \frac{\partial^2 \theta}{\partial y^2},$$

where P is the Prandtl number, with the boundary conditions

$$u = 0, v = 0, \theta = 0 \text{ for } y = 0; \quad u = 1, \theta = 1 \text{ for } y = \infty$$

$$\left( u = \frac{U}{U_\infty}, v = \frac{V}{U_\infty}, \theta = \frac{T - T_\infty}{T_\infty - T_w}, x = \frac{X}{L}, y = \frac{Y}{L}, L = \frac{v_\infty}{v_\infty}, v = \frac{v_\infty}{U_\infty}, Pr = \frac{v_\infty}{\alpha} \right).$$

The initial differential equations are converted to a system of nonlinear finite-difference equations. Their solution can be obtained with the use of static electric integrators whose construction and method of operation are discussed in detail. The solutions for the velocities in the boundary layer along the plate are shown graphically for several particular cases. Original article has: 42 equations and 5 diagrams. English translation: 3 pages.

# ITIS INDEX CONTROL FORM

01 Acc Nr TP7500545		68 Translation Nr MT6500161		65 X Ref Acc Nr		76 Reel/Frame Nr 1654 1059	
97 Header Clas UNCL		63 Clas UNCL. 0		64 Control Markings 0		94 Expansion UR	
02 Ctry UR		03 Ref 0207		04 Yr 64		05 Vol 000	
06 Iss 005		07 B. Pg. 0135		45 E. Pg. 0137		10 Date NONE	

## Transliterated Title

K TEORII NESTATSIONARNYKH POVERKHNOSTNYKH VOLN

## 09 English Title

THE THEORY OF NONSTATIONARY SURFACE WAVES

## 43 Source

ZHURNAL PRIKLADNOY MEKHANIKI I TEKHNICHESKOY FIZIKI (RUSSIAN)

## 42 Author

BEREZIN, YU. A.

## 98 Document Location

## 16 Co-Author

KARPMAN, V. I.

## 47 Subject Codes

20

## 16 Co-Author

NONE

39 Topic Tags: fluid surface, wave mechanics, wave propagation

## 16 Co-Author

NONE

## 16 Co-Author

NONE

**ABSTRACT:** A nonsteady-state solution is found for the Korteweg-de Vries equation [1], describing profile of surface wave of finite but small amplitude at large distances from initial perturbation.

# ITIS INDEX CONTROL FORM

01 Acc Nr TP7500546		68 Translation Nr MT6500161		65 X Ref Acc Nr AP5002875		76 Reel/Frame Nr 1654 1062	
97 Header Clas UNCL		63 Clas UNCL, 0		64 Control Markings 0		94 Expansion 40 Ctry Info UR	
02 Ctry UR	03 Ref 0207	04 Yr 64	05 Vol 000	06 Iss 005	07 B. Pg. 0138	45 E. Pg. 0140	10 Date NONE

Transliterated Title  
O STRUKTURE POTOKA V ELEKTORAZRYADNYKH UDARNYKH TRUBKAKH

09 English Title  
THE STRUCTURE OF FLOW IN ELECTRODISCHARGE SHOCK TUBES

43 Source  
ZHURNAL PRIKLADNOY MEKHANIKI I TEKHNIЧЕСKОY FIZIKI (RUSSIAN)

42 Author  
VOROTNIKOVA, M. I.

98 Document Location

16 Co-Author  
SOLOUKHIN; R. I.

47 Subject Codes  
20

16 Co-Author  
NONE

39 Topic Tags: shock tube, electric discharge, shock wave, nonequilibrium flow, photomultiplier

16 Co-Author

NONE

16 Co-Author  
NONE

**ABSTRACT :** Pressure measurement techniques, using piezoelectric counters and other probe methods, are compared with optical charts to determine the state of a gas behind shock waves generated in electric discharge shock tubes in order to determine more accurately departures from homogeneity. The discharge takes place in air at 0.2 mm Hg pressure. The results of pressure measurement and photomultiplier records on the oscillograph agree to within 0.1  $\mu$ sec. A plot of absolute pressure versus shock velocity behind the shock waves shows measured values to be 50% lower than calculated values. This discrepancy is attributed primarily to experimental errors and possible nonequilibrium effects in the nonthermal plasma. Furthermore, a plot of reflected shock wave speed  $D'$  versus incident wave speed  $D$  shows that experimental points are 1.2-1.5 times higher than the values obtained from one-dimensional equilibrium calculations. If, in the relationship  $D' = u/\beta - 1$ , the compressibility  $\beta_2' \approx 5.0$ , the experimental data will agree with calculated values. Measurements were made on shock stand-off distance over a cylindrical obstacle placed inside the shock tube. Once more a discrepancy was observed between calculated and measured Mach number values, indicating the absence of a clear demarcation between thermal and discharge plasmas in electromagnetic shock tubes at pressure levels below 1 mm mercury. "The authors are grateful to B. V. Boshenyatov for his help in the experiments." Original article has: 8 figures. English translation: 3 pages.

**BLANK PAGE**

# ITIS INDEX CONTROL FORM

01 Acc Nr TP7500547		68 Translation Nr MT6500161		65 X Ref Acc Nr AP5002876		76 Reel, Frame Nr 1654 1060	
97 Header Clas UNCL		63 Clas UNCL, 0		64 Control Markings 0		94 Expansion UR	
02 Ctry UR		03 Ref 0207		04 Yr 64		05 Vol 000	
06 Iss 005		07 B. Pg. 0140		45 E. Pg. 0141		10 Date NONE	

## Transliterated Title

O STRUKTURE UDARNYKH VOLN V SLUCHAYE FAZOVYKH PEREKHODOV PЕРVOGO RODA

## 09 English Title

THE STRUCTURE OF SHOCK WAVES IN THE CASE OF PHASE TRANSITIONS OF THE FIRST KIND

## 43 Source

ZHURNAL PRIKLADNOY MEKHANIKI I TEKHNICHESKOY FIZIKI (RUSSIAN)

## 42 Author

KUZNETSOV, N. M.

## 98 Document Location

## 16 Co-Author

NONE

## 47 Subject Codes

20

## 16 Co-Author

NONE

## 39 Topic Tags:

shock wave, phase transition, thermodynamic equilibrium, adiabatic process

## 16 Co-Author

NONE

## 16 Co-Author

NONE

**ABSTRACT:** The author examines the qualitative character of shock-wave structure in the case when  $\delta p < 0$ , where  $\delta p$  is the pressure difference between the "frozen" and equilibrium branches of the shock adiabatic curve. This examination applies only to strong shock waves, since  $\delta p$  is always positive for weak waves, and nothing new may be learned of the phase transition from it. As the gaseous medium approaches perfect thermodynamic equilibrium, the point defining the state of the medium on the  $pV$  plane shifts along a chord of the curve. The density and pressure decrease. Figure 1 shows this behavior, and Fig. 2 shows the dependence of both pressure and density on distance, up to the jump in condensation. The author also considers the case of two-wave configuration when  $\delta p > 0$ . Original article has: 4 figures. English translation: 5 pages.

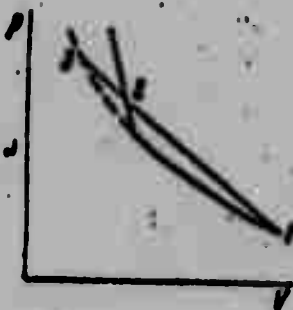


Fig. 1. Shock adiabatic curves of the "frozen" and equilibrium states in the case when  $\delta p < 0$ ;  $p$  is pressure,  $V$  is volume. As the substance approaches complete thermodynamic equilibrium, the point defining state shifts along chord from 3 to 2, from which point both pressure and density increase.

TP7500547

MT6500161

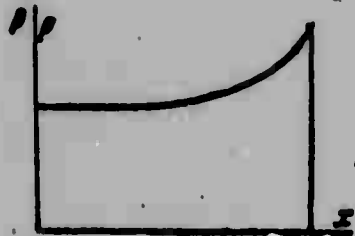


Fig. 2. Dependence of  $p$  (pressure) and  $\rho$  (density) on  $x$  (distance)

# ITIS INDEX CONTROL FORM

01 Acc Nr TP7500548		68 Translation Nr MT6500161		65 X Ref Acc Nr AP5002877		76 Reel/Frame Nr 1654 1063	
97 Header Clas UNCL		63 Clas UNCL, 0		64 Control Markings 0		94 Expansion 40 Ctry Info UR	
02 Ctry UR	03 Ref 0207	04 Yr 64	05 Vol 000	06 Iss 005	07 B. Pg. 0142	45 E. Pg. 0144	10 Date NONE

Transliterated Title OBTEKANIYE KRUGLOY PLASTINY V USLOVIYAKH MOLEKULYARNOGO POGRANICHNOGO SLOYA

09 English Title FLOW AROUND A CIRCULAR PLATE UNDER CONDITIONS OF A MOLECULAR BOUNDARY LAYER

## 43 Source

ZHURNAL PRIKLADNOY MEKHANIKI I TEKHNICHESKOY FIZIKI (RUSSIAN)

## 42 Author

PEREPUKHOV, V. A.

## 98 Document Location

## 16 Co-Author

NONE

## 47 Subject Codes

20

## 16 Co-Author

NONE

39 Topic Tags: boundary layer flow, supersonic flow, rarefied gas, boundary layer

## 16 Co-Author

NONE

## 16 Co-Author

NONE

**ABSTRACT:** The problem is considered of the flow of a very tenuous gas around a circular plate at a zero angle of attack. The gas molecules are considered as solid spheres of diameter  $\sigma$ . They are assumed to be reflected from the plate by diffusion with a Maxwellian distribution of velocities. The mean free paths for the collisions of various types are as follows. For incident molecules colliding with each other,  $\lambda_{11} \sim M_{\infty} \lambda_0$ ; for reflected molecules colliding with incident molecules,  $\lambda_{21} \sim \lambda_0 / M_{\infty}$ ; for incident molecules colliding with reflected molecules,  $\lambda_{12} \sim \lambda_0$ ; for reflected molecules colliding with each other,  $\lambda_{22} \sim \lambda_0$ . Here  $\lambda_0 = \frac{1}{\sqrt{2} \pi \sigma^2 n_{\infty}}$ ,  $M_{\infty} = \frac{U}{\sqrt{2KT_{\infty}}}$

where  $n_{\infty}$  and  $T_{\infty}$  are the density and temperature of the undisturbed gas and the macroscopic flow velocity  $U$  is much greater than the thermal velocity of the incident molecules and the velocity of the reflected molecules. Under these conditions, the number of molecules incident on the plate and reflected from it increases until the influx of molecules from infinity not suffering collisions equals the flow of reflected molecules escaping around the edges of the plate. This process is valid for the following relation between the Knudsen and Mach numbers  $K_{\infty}^2 > M_{\infty} > K_{\infty} > 1$ , and the problem can be solved with the theory of first collisions. An involved integral expression is found for the density of molecules at the surface of the plate. Expressions are also given for the momentum, energy, and aerodynamic coefficients. Numerical and graphical results are presented as an example for the particular case  $M_{\infty} = 30$ ,  $K_{\infty} = 12$ . The author thanks M. N. Kogan for discussion of the results and interest in the work. Original article has: 49 equations and 3 diagrams. English translation: 3 pages.

# ITIS INDEX CONTROL FORM

01 Acc Nr TP7500549		68 Translation Nr MT6500161		65 X Ref Acc Nr AP5002878		76 Reel/Frame Nr 1654 1064	
97 Header Clas UNCL		63 Clas UNCL, 0		64 Control Markings 0		94 Expansion 40 Ctry Info UR	
02 Ctry UR	03 Ref 0207	04 Yr 64	05 Vol 000	06 Iss 005	07 B. Pg. 0145	45 E. Pg. 0148	10 Date NONE

Transliterated Title GIPERZVUKOVOYE OBTEKANIYE TONKIKH PRITUPLENNYKH TEL S  
FIZIKO-KHIMICHESKIMI PREVRASHCHENIYAMI GAZA V VYSOKOENTROPIYNOM SLOYE

09 English Title HYPERSONIC FLOW AROUND THIN DULLED BODIES WITH  
PHYSICOCHEMICAL TRANSFORMATIONS OF GAS IN A HIGH-ENTROPY SHELL

43 Source

ZHURNAL PRIKLADNOY MEKHANIKI I TEKHNIЧЕСКОY FIZIKI (RUSSIAN)

42 Author

LUNEV, V. V.

98 Document Location

16 Co-Author

47 Subject Codes

NONE

20

16 Co-Author

39 Topic Tags: hypersonic flow, equilibrium  
flow, nonequilibrium flow, drag coefficient,  
similitude law

NONE

16 Co-Author

NONE

16 Co-Author

NONE

**ABSTRACT :** Hypersonic flows over slender, blunt-nosed bodies in the presence of physicochemical transformations in the high-entropy layer are investigated. Two-dimensional and axially symmetric flows are considered and the law of similitude based on the introduction of the effective drag coefficient  $c_x$  of the nose is established in order to take account of the effect of physicochemical reactions in the high-entropy layer on flow over bodies. The integral relations of energy and momentum are used to describe flows over slender, blunt-nosed bodies for dissociating air and nonequilibrium flow. The pressure distribution on the body surface, the shapes of shock waves and the distribution of gas parameters outside the high-entropy layer present a general-purpose form, which is independent of equilibrium and nonequilibrium processes taking place in the high-entropy layer. The effective drag coefficients for a sphere and the pressure distributions for a spherically blunted cylinder and a cone in perfect gas flow and in equilibrium dissociating air at  $M = 30$  and  $\infty$  are plotted in graphs. The extension of the law of similitude to a blast wave in the atmosphere is discussed. Original article has: 2 figures and 8 formulas. English translation: 4 pages.

# ITIS INDEX CONTROL FORM

01 Acc Nr TP7500550		68 Translation Nr MT6500161		65 X Ref Acc Nr AP5002879		76 Reel/Frame Nr 1654 1065	
97 Header Clas UNCL		63 Clas UNCL, 0		64 Control Markings 0		94 Expansion 40 Ctry Info UR	
02 Ctry UR	03 Ref 0207	04 Yr 64	05 Vol 000	06 Iss 005	07 B. Pg. 0149	45 E. Pg. 0151	10 Date NONE

Transliterated Title TORMOZNOYE IZLUCHENIYE ELEKTRONA PRI RASSEYANII  
NEYTRAL'NYMI ATOMAMI S UCHETOM KORRELYATSII STOLKNOVENIY

09 English Title RETARDATION RADIATION OF ELECTRONS DURING SCATTERING BY  
NEUTRAL ATOMS. TAKING INTO ACCOUNT THE COLLISIONAL CORRELATIONS

43 Source  
ZHURNAL PRIKLADNOY MEKHANIKI I TEKHNIЧЕСКОY FIZIKI (RUSSIAN)

42 Author  
RAYZER, YU. P.

98 Document Location

16 Co-Author  
NONE

47 Subject Codes  
20

16 Co-Author  
NONE

39 Topic Tags: radiation, electron,  
correlation, Fourier analysis

16 Co-Author  
NONE

16 Co-Author  
NONE

**ABSTRACT:** A formula for the radiation power, containing the frequency factor, is derived by the direct consideration of the retardation radiation of electrons during collisions with neutral atoms and by taking into account the correlations between the collisions. In classical electrodynamics an electron undergoing accelerated motion radiates an amount of energy in the interval  $\omega$  to  $\omega + d\omega$ , given by

$$dE_{\omega} = \frac{8\pi e^2}{3c^3} |w_{\omega}|^2 d\omega$$

where  $w_{\omega}$  is the Fourier component of acceleration. Using Kirchoff's law, G. Bekefi, I. L. Hirshfield, and S. C. Brown (Zakon Kirkhgofa dlya plazmy s nemaksvellovskim raspredeleniyem. Phys. Fluids, 1961, v. 4, No. 2, p. 173) obtained the following expression for the radiation power:

$$dQ_{\omega} = \frac{4}{3\pi} \frac{e^2 v_{eff}^2}{c^3} \frac{\omega^2}{\omega^2 + v_{eff}^2} d\omega$$

The present author expresses  $w(t)$  directly in the form

$$w(t) = \sum_{k=1}^N \Delta v_k \delta(t_k)$$

and derives an expression for  $\langle |w_{\omega}|^2 \rangle$ :  $\langle |w_{\omega}|^2 \rangle = \frac{1}{4\pi^2} N \left\{ 2v^2(1-\mu) - 2v^2(1-\mu) \frac{v_{eff}^2}{\omega^2 + v_{eff}^2} \right\}$

In these formulas  $t_k$  is the instant of the k-th collision, and  $\Delta v_k$  is the corresponding change in the velocity. Also  $v_{eff} = (1 - \mu)v$ . The author acknowledges his sincere appreciation to Ya. B. Zel'dovich for noticing the effect of the correlations. Orig. art. has: 12 formulas. English translation: 3 pages.

# ITIS INDEX CONTROL FORM

01 Acc Nr TP7500551	68 Translation Nr MT6500161	65 X Ref Acc Nr AP5002880	76 Reel/Frame Nr 1654 1066
97 Header Clas UNCL	63 Clas UNCL, 0	64 Control Markings 0	94 Expansion 40 Ctry Info UR
02 Ctry UR	03 Ref 0207	04 Yr 64	05 Vol 000
06 Iss 005	07 B. Pg. 0151	45 E. Pg. 0154	10 Date NONE

Transliterated Title IZMERENIYE RASKHODA ZHIDKOSTI V KRUGLOY TRUBE  
MAGNITOGIDRODINAMICHESKIM METODOM

09 English Title MEASURING THE FLOW OF A FLUID IN A CIRCULAR PIPE BY  
THE MAGNETOHYDRODYNAMIC METHOD

## 43 Source

ZHURNAL PRIKLADNOY MEKHANIKI I TEKHNIЧЕСКОY FIZIKI (RUSSIAN)

## 42 Author

YAKUBENKO, A. YE.

## 98 Document Location

## 16 Co-Author

NONE

## 47 Subject Codes

20

## 16 Co-Author

NONE

39 Topic Tags: fluid flow, magnetohydro-  
dynamics, analytic function, elliptic  
integral

## 16 Co-Author

NONE

## 16 Co-Author

NONE

**ABSTRACT :** The magnetohydrodynamic method for measuring the rate of flow of a fluid through a circular pipe is discussed. This method is based on the relationship between the flow rate and the potential difference between the electrodes. The relationship is theoretically derived in this paper; the equations governing the axisymmetric flow of a conducting fluid under a transverse magnetic field and the equation of Ohm's law are solved. The Ohm's law is reduced to the form

$$i_r = \sigma \left[ -\frac{\partial \Phi}{\partial r} - \frac{H_0}{c} \left( \frac{1}{R_0^3} \int_0^{R_0} rV(r) dr + \frac{1}{r^3} \int_r^{R_0} rV(r) dr \right) \cos \theta \right]$$

$$i_\theta = \sigma \left[ -\frac{1}{r} \frac{\partial \Phi}{\partial \theta} + \frac{H_0}{c} \left( V(r) + \frac{1}{R_0^3} \int_0^{R_0} rV(r) dr - \frac{1}{r^3} \int_r^{R_0} rV(r) dr \right) \sin \theta \right],$$

where

$$\Phi = \Phi(r, \theta) + \frac{H_0}{c} \left[ \frac{r}{R_0^3} \int_0^{R_0} rV(r) dr - \frac{1}{r} \int_r^{R_0} rV(r) dr \right] \cos \theta$$

Here  $H_0$  is the magnetic field,  $R_0$  is the radius of the pipe,  $V$  is the velocity of flow which is equal to 0 at  $R_0$ , and  $\Phi$  is the electric potential. The boundary conditions are:  $\Phi = -\Phi_e$ , at  $r = R_0$  for  $-\alpha < \theta < \alpha$ ;  $\Phi = \Phi_e$  at  $r = r_0$  for  $\Pi - \alpha < \theta < \Pi + \alpha$ . Using an analytic function defined by

$$w(z) = u + iv = r \frac{\partial \Phi}{\partial r} - i \frac{\partial \Phi}{\partial \theta} \quad (z = r + iy)$$

the relation obtained between the flow rate  $Q$  and the potential difference between the electrodes is defined as

$$2\Phi_e = \frac{QH_0}{cR_0} \frac{\sigma R}{K(\cos \alpha) + \sigma R K(\sin \alpha)}$$

Here  $K$  is a complete elliptic integral of the first kind. Orig. art. has: 1 figure and 20 formulas. English translation: 4 pages.

ITIS INDEX CONTROL FORM

01 Acc Nr TP7500552		68 Translation Nr MT6500161		65 X Ref Acc Nr AP5002881		76 Reel/Frame Nr 1654 1087	
97 Header Clas UNCL		63 Clas UNCL, 0		64 Control Markings 0		94 Expansion 40 Ctry Info UR	
02 Ctry UR	03 Ref 0107	04 Yr 64	05 Vol 000	06 Iss 005	07 B. Pg. 0154	45 E. Pg. 0159	10 Date NONE

Transliterated Title NEKOTORYYE METODY ISSLEDOVANIYA NESTATSIONARNYKH YAVLENIY V UDARNYKH TRUBAKH

09 English Title CERTAIN METHODS OF INVESTIGATION OF NONSTATIONARY PHENOMENA IN SHOCK TUBES

43 Source  
ZHURNAL PRIKLADNOY MEKHANIKI I TEKHNICHESKOY FIZIKI (RUSSIAN)

42 Author  
BEREZKINA, M. K.

98 Document Location

16 Co-Author  
SEMENOV, A. N.

47 Subject Codes  
20

16 Co-Author  
SYSHCHIKOVA, M. P.  
16 Co-Author  
NONE

39 Topic Tags: shock tube, shock wave, detached shock wave, boundary layer, reflected shock wave, shock wave diffraction

16 Co-Author  
NONE

**ABSTRACT :** An experimental investigation is presented of nonstationary phenomena in shock tubes, such as formation and development of flow near a model generated by a travelling shock wave. The process of flow formation consisting of the reflection and diffraction of shock waves, the formation of a bow shock wave ahead of a body, the generation and development of a boundary layer, and the formation of flow in the wake of a body are of particular interest to the theory of nonstationary gasdynamic processes and are of great practical value. A detailed description of the shock tube (with a 150 x 50 mm cross section and 8 m long) and a block diagram of the experimental setup are given and various photographic methods for data recording are outlined. The data obtained make it possible to determine the velocities of the incident shock wave, of the flow in heated and cold regions, and of the contact surface, and also to determine the duration of flow between a shock wave and contact surface, and the Mach number of the flow from the detachment distance of the shock in homogeneous regions of flow. It is also possible to determine the time necessary for a shock wave to reach a steady state, and the dependence of this time on the parameters of the shock wave. Original article has: 10 figures. English translation: 6 pages.

# ITIS INDEX CONTROL FORM

01 Acc Nr TP7500553		68 Translation Nr MT6500161		65 X Ref Acc Nr AP5002882		76 Reel/Frame Nr 1654 1068	
97 Header Clas UNCL		63 Clas UNCL, 0		64 Control Markings 0		94 Expansion UR	
02 Ctry UR		03 Ref 0207		04 Yr 64		05 Vol 000	
06 Iss 005		07 B. Pg. 0159		45 E. Pg. 0162		10 Date NONE	

Transliterated Title EKSPERIMENTAL'NOYE OPREDELENIYE SKOROSTI RASPROSTRANENIYA ZVUKOVYKH VOLN V NASYSHCHENNOM PARE VODY PRI VYSOKIKH DAVLENIYAKH

09 English Title EXPERIMENTAL DETERMINATION OF SPEED OF PROPAGATION OF SOUND WAVES IN SATURATED WATER VAPOR AT HIGH PRESSURES

43 Source

ZHURNAL PRIKLADNOY MEKHANIKI I TEKHNIЧЕСКОY FIZIKI (RUSSIAN)

42 Author

AVDONIN, V. I.

98 Document Location

16 Co-Author

47 Subject Codes

NOVIKOV, I. I.

20

16 Co-Author

SHELUDYAKOV, Ye. P.

39 Topic Tags: sound wave, high pressure, temperature dependence, stainless steel, potentiometer

16 Co-Author

NONE

16 Co-Author

NONE

**ABSTRACT:** A new experimental chamber has been devised for measuring sound velocity at temperatures up to 350°C. Results are compared with those from previous apparatus, where the temperatures overlap. Both techniques are based on the method of standing waves. In the new apparatus, a new acoustical resonator made of stainless steel is used. The chamber has a length of 803.75 mm, an inner diameter of 65 mm, and a wall thickness of 10 mm. This was used in a new autoclave made of 1Kh18N9T stainless steel with a length of 124.0 cm, an inner diameter of 12.0 cm, and a wall thickness of 1.5 cm. Temperature control was obtained by two heating elements, one principal, one auxiliary. Temperature was measured in the autoclave by a 100-ohm platinum thermometer and by four copper-constantan thermocouples on PMS-48 and PPTN-1 potentiometers, with an accuracy within 0.2°C. Results of measurements on sound velocity in saturated water vapor are shown graphically in Fig. 1 on the Enclosure in comparison with an empirical curve. It is seen that the experimental values between 150 and 350°C are in good agreement with the empirical curve, and are in good agreement up to 320°C with the theoretical values proposed by I. I. Novikov (Pokazatel' adiabaty\* nasyshchennogo vodyanogo para. Dokl. AN SSSR, 1948, t. 9, No. 8, str. 1425). At higher temperatures the difference becomes marked, and it is concluded that a factor for transition through the saturation curve must be added to the theoretical calculations. Orig. art. has: 3 figures and 2 tables. English translation: 4 pages.

TP7500553

MT6500161

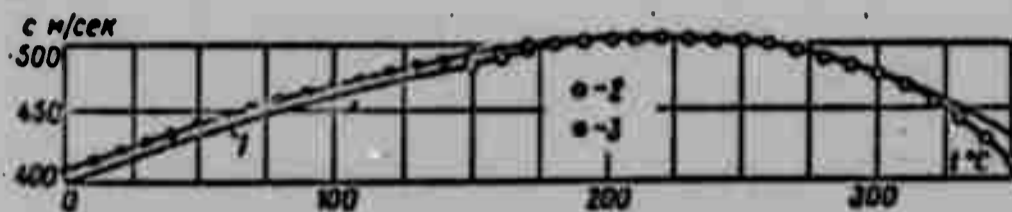


Fig. 1. Variation of sound velocity with temperature

- 1- empirical curve based on formula  $c = \sqrt{1.25gP_s v''}$ , where  $P_s$  is the water vapor pressure ( $\text{kg/m}^2$ ) and  $v''$  the specific volume of the water vapor ( $\text{m}^3/\text{kg}$ ),
- 2- observed values in new device;
- 3- observed values in old, reconstructed device.

# ITIS INDEX CONTROL FORM

01 Acc Nr TP7500554	68 Translation Nr MT6500161	65 X Ref Acc Nr	76 Reel/Frame Nr 1654 1070
97 Header Clas UNCL	63 Clas UNCL, 0	64 Control Markings 0	94 Expansion 40 Ctry Info UR
02 Ctry UR	03 Ref 0207	04 Yr 64	05 Vol 000
06 Iss 005	07 B. Pg. 0162	45 E. Pg. 0166	10 Date NONE

Transliterated Title NESTATIONARNYY LUCHISTO-KONVEKTIVNYY  
TEPLOOBMEN NA PRYAMOUGOL'NIKE

09 English Title  
NONSTATIONARY RADIANT-CONVECTION HEAT EXCHANGE ON RECTANGLE

43 Source

ZHURNAL PRIKLADNOY MEKHANIKI I TEKHNICHESKOY FIZIKI (RUSSIAN)

42 Author

BURKA, A. L.

16 Co-Author

NONE

16 Co-Author

NONE

16 Co-Author

NONE

16 Co-Author

NONE

98 Document Location

47 Subject Codes

20

39 Topic Tags: boundary value problem,  
mixed boundary value problem, heat convection  
heat radiation

**ABSTRACT:** We consider the boundary value problem for a right angle region  
[ $0 \leq x \leq L$ ;  $0 \leq y \leq l$ ] with mixed boundary conditions, including convection  
and radiant fluxes. (Ambient temperature is assumed equal to zero.)  
English translation: 9 pages.

ITIS INDEX CONTROL FORM

01 Acc Nr TP7500555		68 Translation Nr MT6500161		65 X Ref Acc Nr AP5002883		76 Reel/Frame Nr 1654 1071	
97 Header Clas UNCL		63 Clas UNCL, 0		64 Control Markings 0		94 Expansion UR	
02 Ctry UR	03 Ref 0207	04 Yr 64	05 Vol 000	06 Iss 005	07 B. Pg. 0167	45 E. Pg. 0168	10 Date NONE

Transliterated Title

O NESTATSIONARNOM GORENII TONKIKH PLASTIN POROKHA

09 English Title

NON STEADY-STATE BURNING OF THIN PLATES OF POWDER

43 Source

ZHURNAL PRIKLADNOY MEKhanIKI I TEKHNIChESKOY FIZIKI (RUSSIAN)

42 Author

GOSTINTSEV, YU. A.

98 Document Location

16 Co-Author

MARGOLIN, A. D.

47 Subject Codes

21, 20

16 Co-Author

NONE

39 Topic Tags: combustion, powder combustion rate, powder, porous medium

16 Co-Author

NONE

16 Co-Author

NONE

**ABSTRACT:** The equations governing the nonstationary combustion of a plate of powder are solved by the method of integral relations. A formula is obtained for the time of complete combustion,  $\tau_+$ , of a plate of thickness  $2\delta_0$ . The combustion was considered to take place along the two unbounded directions parallel to the plane of the plate. The system of equations governing the combustion of the plate is:

$$\omega = \eta - (\eta - 1) \left( \frac{\partial \theta(\xi, \tau)}{\partial \xi} \right)_{\xi=\delta}$$

$$\frac{\partial \theta(\xi, \tau)}{\partial \tau} = \frac{\partial^2 \theta(\xi, \tau)}{\partial \xi^2} \quad (\tau > 0, 0 \leq \xi \leq \delta(\tau))$$

$$\theta(\xi, \tau) = 1 \text{ at } \xi = \delta(\tau), \quad \frac{\partial \theta(\xi, \tau)}{\partial \xi} = 0 \text{ at } \xi = 0, \quad \theta = \frac{\text{ch } \xi}{\text{ch } \delta} \text{ at } \delta \rightarrow \infty.$$

All the quantities here are dimensionless;  $\omega$  is the stationary rate of combustion,  $\eta$  a parameter characterizing the porosity of the plate,  $\theta$  the temperature at any point,  $\tau$  the time, and  $\xi$  the distance along the thickness of the plate. The time for complete combustion was obtained in the form

$$\tau_+ = \frac{\eta - 1}{\eta} \left[ \frac{\delta_0}{\eta - 1} - \psi_0 (\text{th } \delta_0 - \delta_0) \right]$$

where  $\psi_0$  is the value at the center of the plate of the function  $\psi(\tau)$  given

$$\text{by } \theta = \psi(\tau) \frac{\text{ch } \xi}{\text{ch } \delta(\tau)} + 1 - \psi(\tau)$$

Orig. art. has: 2 figures and 11 formulas. English translation: 2 pages.

**BLANK PAGE**

# TABLE OF CONTENTS

U. S. Board on Geographic Names Transliteration System.....	111
Designations of the Trigonometric Functions.....	iv
N. T. Pashchenko. Flow Around a Body by a Flux of Strongly Rarefied Plasma:.....	1
V. A. Polyanskiy. Diffusion and Conductivity in a Partially Ionized Multitemperature Gas Mixture:.....	15
I. V. Nemchinov. Dispersion of a Heated Mass of Gas in Regular Conditions	27
F. F. Koromkov. Nonlinear Geometric Acoustics. Weak Shock Waves:.....	47
A. G. Istratov and V. B. Librovich. Burning Stability of Powder.....	61
G. M. Zaslavskiy, S. S. Molseyev and R. Z. Saldeyev. Asymptotic Methods of Hydrodynamic Theory of Stability.....	69
G. A. Bugayenko. One Case of Free Convection of a Liquid in the Presence of Dissolving and Absorbing Walls.....	87
V. A. Borodin, L. N. Britneva, Yu. F. Dityakin and V. I. Yagodkin. Splitting a Stream of Liquid, Streamlined by a Gas Flow:.....	91
G. V. Vinogradov and A. Ya. Malkin. Rheological Properties of Polymers in the Fluid State:.....	103
A. V. Dolgov and N. I. Malinin. Polymer Creep in the Vitreous State.....	115
M. Ya. Leonov and K. N. Rusinko. Rupture of a Body with Linear Dislocation:.....	129
B. M. Malyshev and R. L. Salganik. Study of Destruction of Brittle Bondings by Methods of the Theory of Cracks.....	141
G. I. Bykovtsev, D. D. Ivlev and T. N. Martynova. The Theory of the Axially Symmetric State of an Ideal Plastic Material.....	159
E. I. Grigolyuk and P. P. Chulkov. Theory of Viscoelastic Multilayers of Shells with Rigid Fillers with the Existence of Finite Bending:.....	171
Yu. I. Fadeyenko. Dependence of Dimensions of Crater on Hardness of Target.....	185
S. S. Grigoryan. Similarity of Surface Waves During Explosions in the Ground:.....	189
V. P. Koryavov. Approximate Equation of State of Solid Bodies.....	195
I. G. Bulina, V. P. Myasnikov and V. G. Savin. Experimental Investigation of Flow Around Blunted Bodies by a Flat Flow of a Plastic Medium:.....	203
V. P. Kashkarov and A. T. Luk'yanov (Alma Ata). Calculation of Flow Around a Plate by a Liquid-Drop Liquid with Variable Viscosity:.....	213

Yu. A. Berezin and V. I. Karpman. The Theory of Nonstationary Surface Waves:.....	219
M. I. Vorotnikova and R. I. Soloukhin. The Structure of Flow in Electrodischarge Shock Tubes:.....	225
N. M. Kuznetsov. The Structure of Shock Waves in the Case of Phase Transitions of the First Kind.....	233
V. A. Perepukhov. Flow Around a Round Plate in Conditions of Molecular Boundary Layer:.....	237
V. V. Lunev. Hypersonic Flow Around Thin Dulled Bodies with Physicochemical Transformations of Gas in a High-Entropy Shell:.....	243
Yu. P. Rayzer. Bremsstrahlung of an Electron During Scattering by Neutral Atoms Taking into Account Collision Correlation:.....	251
A. Ye. Yakubenko. Measurement of Flow Rate of Liquid in a Round Pipe by the Magnetohydrodynamic Method:.....	257
M. K. Berezkina, A. N. Semenov and M. P. Syshchikova. Certain Methods of Investigation of Nonstationary Phenomena in Shock Tubes.....	263
V. I. Avdonin, I. I. Novikov and Ye. P. Sheludyakov. Experimental Determination of Speed of Propagation of Sound Waves in Saturated Water Vapor at High Pressures.....	275
A. L. Burka. Nonstationary Radiant-Convection Heat Exchange on Rectangle:.....	281
Yu. A. Gostintsev and A. D. Margolin. Non Steady-State Burning of Thin Plates of Powder.....	289

# U. S. BOARD ON GEOGRAPHIC NAMES TRANSLITERATION SYSTEM

Block	Italic	Transliteration	Block	Italic	Transliteration
А а	<i>А а</i>	A, a	Р р	<i>Р р</i>	R, r
Б б	<i>Б б</i>	B, b	С с	<i>С с</i>	S, s
В в	<i>В в</i>	V, v	Т т	<i>Т т</i>	T, t
Г г	<i>Г г</i>	G, g	У у	<i>У у</i>	U, u
Д д	<i>Д д</i>	D, d	Ф ф	<i>Ф ф</i>	F, f
Е е	<i>Е е</i>	Ye, ye; E, e*	Х х	<i>Х х</i>	Kh, kh
Ж ж	<i>Ж ж</i>	Zh, zh	Ц ц	<i>Ц ц</i>	Ts, ts
З з	<i>З з</i>	Z, z	Ч ч	<i>Ч ч</i>	Ch, ch
И и	<i>И и</i>	I, i	Ш ш	<i>Ш ш</i>	Sh, sh
Й й	<i>Й й</i>	Y, y	Щ щ	<i>Щ щ</i>	Shch, shch
К к	<i>К к</i>	K, k	Ъ ъ	<i>Ъ ъ</i>	"
Л л	<i>Л л</i>	L, l	Ы ы	<i>Ы ы</i>	Y, y
М м	<i>М м</i>	M, m	Ь ь	<i>Ь ь</i>	'
Н н	<i>Н н</i>	N, n	Э э	<i>Э э</i>	E, e
О о	<i>О о</i>	O, o	Ю ю	<i>Ю ю</i>	Yu, yu
П п	<i>П п</i>	P, p	Я я	<i>Я я</i>	Ya, ya

\* ye initially, after vowels, and after ъ, ь; e elsewhere.  
 When written as ѐ in Russian, transliterate as yě or ě.  
 The use of diacritical marks is preferred, but such marks  
 may be omitted when expediency dictates.

FOLLOWING ARE THE CORRESPONDING RUSSIAN AND ENGLISH  
DESIGNATIONS OF THE TRIGONOMETRIC FUNCTIONS

Russian	English
sin	sin
cos	cos
tg	tan
ctg	cot
sec	sec
cosec	csc
sh	sinh
ch	cosh
th	tanh
cth	coth
sch	sech
csch	csch
arc sin	$\sin^{-1}$
arc cos	$\cos^{-1}$
arc tg	$\tan^{-1}$
arc ctg	$\cot^{-1}$
arc sec	$\sec^{-1}$
arc cosec	$\csc^{-1}$
arc sh	$\sinh^{-1}$
arc ch	$\cosh^{-1}$
arc th	$\tanh^{-1}$
arc cth	$\coth^{-1}$
arc sch	$\operatorname{sech}^{-1}$
arc csch	$\operatorname{csch}^{-1}$
<hr/>	
rot	curl
lg	log

FLOW AROUND A BODY BY A FLUX OF STRONGLY  
RAREFIED PLASMA

N. T. Pashchenko

(Moscow)

Motion of a body in strongly rarefied plasma was considered by a number of authors. One of the first in this direction was the work of Jastrow and Pearse [1]. In this work a steady-state solution for potential of electrical field in absence of magnetic field was found; however, a solution was sought possessing spherical symmetry, therefore actually motion of body thereby was disregarded. In [2] were investigated plasma oscillations in the trace after a slender body in the absence of a magnetic field, and it was considered that motion of particles is formed from two components - neutral, corresponding to free-molecular flow, and collective motion, analogous to the motion of a solid medium; when a body is dielectric collective oscillations are not limited to the narrow region of the Debye layer, but spread to the whole trace after the body. Effective solutions, however, are not obtained.

Plasma oscillations in the trace after a body in the presence of an external magnetic field were considered also in [3]; however it was assumed that the dimension of body was small as compared to Debye radius, which is inapplicable in examining motion of bodies in the ionosphere where the reverse relationship occurs. The body practically was considered a point and a problem without boundary conditions was considered.

Flow around a body by plasma was considered under analogous assumptions also in [4]. The nearest of all to this work with respect to the accepted assumptions are [5, 6], however the method of solution of the equation for potential utilized there did not give a possibility of revealing the phenomenon of "boundary" layer, characteristic for the considered case, giving a rather fast change of potential in environment of body, and expressions given in the mentioned works for potential are accurate only sufficiently far from body.

This work considers the problem of steady-state flow around a charged body by a high-speed flow of strongly rarefied plasma. Assuming perturbations caused by the body, charge of body, and Debye radius are small as compared to characteristic dimensions of body, field of potential, parameters of flow, and forces acting on the body.

1. Let us assume that in strongly rarefied plasma moves a charged body with constant speed  $\mathbf{V}$  relative to a certain system of reference fixed in space. By plasma we will understand gas consisting in general, of an electron, ion, and neutral component; undisturbed plasma is assumed quasineutral. Each of the components is characterized by its own distribution function of particles with respect to speeds satisfying the kinetic equation. Influence of external magnetic field and magnetic field due to motion of charges is disregarded.

As initial equations for distribution functions of each of the components and potential of electrical field we will take equations of self-consistent field of A. A. Vlasov [7]; plasma is considered sufficiently rarefied, so that it is possible to disregard interaction of particles by means of direct collisions, then the kinetic equation of each of the components does not contain an integral of collisions.

In a system of coordinates rigidly connected with a body, the system of equations of a self-consistent field has the form

$$c^2 \frac{\partial f_e}{\partial x^2} + \frac{e}{m_e} \frac{\partial \varphi}{\partial x^\beta} \frac{\partial f_e}{\partial c^\alpha} g^{\alpha\beta} = 0, \quad c^2 \frac{\partial f_i}{\partial x^2} - \frac{e}{m_i} \frac{\partial \varphi}{\partial x^\beta} \frac{\partial f_i}{\partial c^\alpha} g^{\alpha\beta} = 0 \quad (1.1)$$

$$c^2 \frac{\partial f}{\partial x^2} = 0, \quad \varphi_{;\alpha\beta} g^{\alpha\beta} = 4\pi e \left\{ \int_0 f_e dc - \int_0 f_i dc \right\} \quad (1.2)$$

Here  $f_e$ ,  $f_i$ ,  $f$  - distribution function of electron, ion, and neutral component correspondingly,  $c$  - speed of chaotic motion of particles in the accepted system of coordinates,  $e$  - charge of electron,  $\varphi$  - potential of electrical field,  $g^{\alpha\beta}$  - basic metric tensor of considered coordination,  $\varphi_{;\alpha\beta} g^{\alpha\beta}$  - Laplacian operator from function  $\varphi$ .

Boundary conditions for the distribution function are determined by the mechanism of interaction of particles during their collisions with the surface and in general can be written in the form

$$f_j^+(c, \mathbf{x}_s) = \int_{(c'n) < 0} K(c, c', \mathbf{x}_s) f_j^-(c', \mathbf{x}_s) dc' \quad (1.3)$$

$$f_j^-(c, \mathbf{x}_s) = f_j(c, \mathbf{x}_s) \text{ when } (c, \mathbf{n}) < 0, \quad f_j^+(c, \mathbf{x}_s) = f_j(c, \mathbf{x}_s) \text{ when } (c, \mathbf{n}) > 0$$

Here  $\mathbf{x}_s$  - radius vector of considered point of surface,  $\mathbf{n}$  - normal to surface

at point  $\mathbf{x}_s$ ,  $K(\mathbf{c}, \mathbf{c}', \mathbf{x}_s)$  — nucleus of interaction, characterizing probability that particles incident on surface with speed  $\mathbf{c}'$  will be reflected with speed  $\mathbf{c}$ ; when incident and reflected flows are independent (for instance diffuse reflection), expression  $K(\mathbf{c}, \mathbf{c}', \mathbf{x}_s)$  is represented in the form  $K_1(\mathbf{c}', \mathbf{x}_s)K_2(\mathbf{c}, \mathbf{x}_s)$ .

In general finding nucleus  $K(\mathbf{c}, \mathbf{c}', \mathbf{x}_s)$  presents an independent problem of investigation of mechanism of interaction of particles with surface. For simple cases of specular and diffuse reflection and their combination these nuclei can be written out [8]. As boundary values for distribution functions on infinity are taken their equilibrium values

$$f_j = n_0 \frac{1}{(\pi c_j^0)^{3/2}} \exp \left[ - \left( \frac{\mathbf{c} + \mathbf{V}}{c_j^0} \right)^2 \right] \quad (1.4)$$

Here  $n_0$  — numerical density of particles in undisturbed flow,  $c_j^0$  — average speed of thermal motion of particles of the  $j$ -th sort.

For the potential boundary conditions on body can be double depending upon physical properties of body; if the considered body is a conductor, its potential is constant  $\varphi = \varphi_0 = \text{const}$ , if the body is a dielectric, then on its surface is assigned either density of surface charge  $\sigma$ , connected with normal derivative from potential by the relationship

$$\sigma_s = - \frac{1}{4\pi} \frac{\partial \varphi}{\partial n} \Big|_{s=\mathbf{x}_s}$$

or potential as a function of a point of the surface.

Thus, the considered problem of flow around a charged body leads to joint solution of equations (1.1)-(1.2) with boundary conditions (1.3), (1.4) and corresponding boundary conditions for potential.

In general the solution of the problem in such a setting presents considerable difficulties, therefore for qualitative investigation of the phenomenon we will make a series of simplifications.

2. We will consider speed of body  $V$  great as compared to average thermal speed of ions  $c_i^0$ , and small as compared to electron thermal velocity  $c_e^0$

$$c_i^0 \ll V \ll c_e^0$$

we assume also that aerodynamic perturbations caused by the moving body are small,

and charge of body is small; then energy of electrical field  $e\phi$  can be considered small as compared to energy of thermal motion of particles  $kT$ . We will also consider Debye radius  $R_D$  small as compared to characteristic dimension of body  $R_0$ , which occurs in examining motion of body in the ionosphere. Under such assumptions the considered problem includes a series of small parameters

$$S_e = \frac{V}{c_e}, \quad \frac{1}{S_i} = \frac{c_i}{V}, \quad \mu = \max \left| \frac{e\phi}{kT} \right|, \quad \mu_0 = \frac{e\phi_0}{kT}, \quad \varepsilon = \frac{R_0}{R_D} \quad (2.1)$$

Let us introduce dimensionless variables

$$y^i = \frac{x^i}{R_0}, \quad \Phi = \frac{e\phi}{kT}, \quad F_j = \frac{f_j (c_j^2 \pi)^{1/2}}{n_0}, \quad v_j^a = \frac{c^a}{c_j} \quad (2.2)$$

and write in dimensionless form the equations

$$v_j^a \frac{\partial F_j}{\partial x^a} \pm \frac{1}{2} \frac{\partial \Phi}{\partial x^a} \frac{\partial F_j}{\partial v_j^a} g^{ab} = 0, \quad \varepsilon^2 \Phi_{,ab} g^{ab} = \frac{1}{\pi^{1/2}} \left\{ \int_0^\infty F_e dv_e - \int_0^\infty F_i dv_i \right\} \quad (2.3)$$

and boundary conditions

$$y = \infty, \quad \Phi = 0, \quad F_j = \exp [-(v_j + S_j)^2] \\ y = y_0, \quad F_j^+(v_j, y_0) = \frac{1}{\pi^{1/2}} \int_{(\vec{v}_j^0) < 0} K(v_j, v_j', y_0) F_j^-(y_0, v_j') dv_j' \quad (2.4)$$

Here, if the body is a conductor,

$$\Phi = \mu_0$$

and, if the body is a dielectric,

$$\Phi = \Phi(y_0), \quad \text{or} \quad \frac{\partial \Phi}{\partial n} \Big|_{y=y_0} = f_1(y_0) \quad (2.5)$$

Thus, solution of dimensionless system of equations (2.3) with boundary conditions (2.4), (2.5) is determined by system of small parameters  $S_e, 1/S_i, \mu, \mu_0, \varepsilon$ , where with such selection of variables equations contained only  $\mu$  and  $\varepsilon$ , and remaining parameters enter only in boundary conditions. Using smallness of shown parameters, we will introduce a series of simplifications.

In view of smallness  $S_e$  it is possible to take expression  $F_e = F_{e0} \exp \Phi$ ,

as distribution function of electrons  $F_e$ , and the equation for distribution function is satisfied with an accuracy of terms of the order  $\mu S_0 \ll 1$ ; boundary conditions here are satisfied exactly.<sup>1</sup>

In examining the kinetic equation for ions we will use smallness of parameter  $\mu$  — we will consider in the first approximation that in view of smallness of energy of electrical field, as compared to kinetic energy of heavy particles, the field does not act on ions, and as distribution function of ions it is possible to consider that incident ions have Maxwellian distribution

$$F_i = \exp[-(v_i + S_i)^2] \quad (2.6)$$

The equation is satisfied with an accuracy of terms of the order  $\mu$ .

Let us consider the kinetic equation for  $F_i$

$$v_i^2 \frac{\partial F_i}{\partial x^2} - \frac{1}{2} \mu \frac{\partial \psi}{\partial x^2} \frac{\partial F_i}{\partial v_i^2} g^{\alpha\beta} = 0 \quad (\Phi = \max |\Phi| \psi = \mu \psi) \quad (2.7)$$

The assumption that  $F_i$  with sufficient accuracy can be replaced by  $F_{01}$  means that, considering this equation as an equation with small parameter  $\mu$  in the region of small values of parameter, we are limited to the solution of a limiting equation (i.e., an equation obtained from the initial when  $\mu = 0$ ). Obviously, such an assumption will be sufficiently good everywhere, with the exception of the region of small values  $v_i^2$ , where both terms become comparable, and such linearization no longer is acceptable. Let us estimate this range of values  $v_i^2$ , for which we will resort to an extension of variable  $v_i$ . Equation (2.7) can be brought to the form

$$u^2 \frac{\partial F_i}{\partial x^2} - \frac{1}{2} \frac{\partial \psi}{\partial x^2} \frac{\partial F_i}{\partial u^2} g^{\alpha\beta} = 0 \quad \left(u = \frac{v}{\sqrt{\mu}}\right) \quad (2.8)$$

---

<sup>1</sup>It is necessary to note that Boltzmann distribution  $F_e = \exp[-v_e^2 + \Phi]$  usually taken, for instance in [2, 5], as electron distribution function, although it is an exact solution of the kinetic equation, boundary conditions for distribution function are not satisfied, and this introduces considerable errors in average magnitudes on infinity; in particular, for instance, the result of such an assumption are large currents on infinity in the absence of an electrical field (in the recently published monograph of Ya. L. Al'pert, A. V. Gurevich and L. P. Pitayevskiy "Artificial satellites in rarefied plasma," "Science," 1964 these inaccuracies are corrected. Remark during proofreading)

Let us estimate error introduced in average magnitudes by slow particles, for which asymptotic distribution of the kinetic operator is inapplicable. Let us consider moment of zero order from distribution function — numerical density

$$n_i = \int_0 f_i d\mathbf{c} = \frac{1}{\pi^{3/2}} \int_0 F_i(\mathbf{v}_i, \mathbf{y}) d\mathbf{v}_i = \left(\frac{\mu}{\pi}\right)^{3/2} \int_0 F_i(\mathbf{u}, \mathbf{y}) d\mathbf{u}$$

Thus, contribution at the time of zero order, given by slow particles, is proportional to  $\sim \mu^{3/2}$ ; obviously, contributions in moments of highest order will contain higher powers  $\mu$ , and, so that it was possible to use the zero term of asymptotic distribution, it is necessary that it was possible to disregard terms  $\sim \mu^{3/2}$ . This is the basis for linearization of the expression giving the distribution function of electrons  $F_e = F_{e0}(1 + \Phi)$ ; preservation of a large number of terms would signify calculation of terms whose order is higher than  $\mu^{3/2}$ . Thus, in accepted assumptions for particles not colliding with the body we have

$$F_i^- = F_{i0}^-, \quad F_e^- = F_{e0}^-(1 + \Phi) \quad (2.9)$$

Distribution functions of particles reflected from the body  $F_j^+$  are determined from boundary conditions (2.4). Consequently, at point of space for distribution function  $F_j$  there are given the relationships

$$F_j = F_{j0}^- \text{ when } \mathbf{v}_j \in \Omega_1, \quad F_j = F_{j0}^+ \text{ when } \mathbf{v}_j \in \Omega_2 \quad (2.10)$$

Here  $\Omega_1$  and  $\Omega_2$  — subspaces in space of speeds such that for the considered point  $\mathbf{y}$  of physical space speed  $\mathbf{u} \in \Omega_1$ , if a particle from this speed falls onto the considered point after a collision with the body;  $\Omega_2 = \Omega - \Omega_1$ , where  $\Omega$  — all the space of speeds.

Thus, the problem leads to determination of potential of electrical field

$$e^2 \Phi_{\text{el}} = \frac{1}{(\pi)^{3/2}} (n_e(1 + \Phi) - n_i) \quad \left( n_i = \int_0 F_i d\mathbf{v}_i, \quad n_e = \int_0 F_e d\mathbf{v}_e \right) \quad (2.11)$$

with boundary conditions (2.4). This is a linear elliptic second order equation with small parameter for higher derivatives. To the equation can be applied asymptotic methods; the problem allows regular degeneration in the sense of [9];

its solution can be represented in the form

$$\Phi^{(n)} = \Phi_0 + \Phi^{(0)(n)} \epsilon^{2n} + O(\epsilon^{2n}) \quad (2.12)$$

Here  $\Phi_0$  - solution of limiting problem ( $\epsilon = 0$ ) and  $\Phi^{(0)}$  - function of "boundary" layer, characterizing solution near boundaries. Depending upon smoothness of parameters of problem we obtain the character of asymptotic behavior also for derivative from potential. Solution of limiting problem is

$$\Phi_0 = \frac{n_1 - n_2}{n_2} = n_3 \quad (2.13)$$

Here  $n_3$  - relative excess density of ions in a flow disturbed by a body. This solution satisfies the boundary condition on infinity and does not satisfy, in general, the condition on the body (all further considerations will be carried out when the body is a conductor; however difficulties are not caused by consideration of a dielectric). Discrepancy in boundary conditions will compensate with the help of function of the "boundary layer"  $\Phi^{(0)}$ , which is the solution of equation

$$\epsilon^2 \Phi_{,\alpha\beta} g^{\alpha\beta} = \Phi_0 \quad (2.14)$$

under boundary conditions

$$\Phi^{(0)}|_{y=\infty} = -\Phi_0|_{y=\infty}, \quad \Phi_{y=y_0}^{(0)} = (\mu_0 - \Phi_0)_{y=y_0} \quad (2.15)$$

Thus, the solution with an accuracy of  $O(\epsilon)$  is represented in the form

$$\Phi = n_3 + \Phi^{(0)} \quad (2.16)$$

Here the limiting solution gives behavior of potential at a distance from the body, and function  $\Phi^{(0)}$  characterizes fast changing "boundary" layer near body. The problem of finding the potential leads, thus, to finding density of electrons and ions, solution of limiting equation, and equation of "boundary" layer.

3. As illustrative example we will consider the two-dimensional problem of flow around an infinite cylinder by a flow of strongly rarefied plasma. Let us find density of particles at point M outside the body. Obviously, region  $\Omega_1$  in

space of speeds is determined by system of inequalities

$$\left| \frac{(\mathbf{v} \times \mathbf{r})}{|\mathbf{v}|} \right| \leq 1, \quad (\mathbf{v} \cdot \mathbf{n}) > 0 \quad (3.1)$$

Or, passing to polar system of coordinates in physical space and space of speeds,

$$0 \leq v < \infty, \quad 0 - \delta \leq \beta \leq 0 + \delta, \quad \delta = \arcsin 1/r \quad (3.2)$$

Here  $r$  - dimensionless radius, in reference to radius of cylinder.

Density of particles is found from the relationship

$$\begin{aligned} n_j &= \frac{1}{\pi^3} \left\{ \int_{\Omega_1} F_j^+ d\mathbf{v}_j + \int_{\Omega_2} F_j^- d\mathbf{v}_j \right\} = \frac{1}{\pi^3} \left\{ \int_{\Omega} F_j^- d\mathbf{v}_j - \int_{\Omega_1} F_j^- d\mathbf{v}_j + \int_{\Omega_1} F_j^+ d\mathbf{v}_j \right\} = \\ &= n_0 + \frac{1}{\pi^3} \left[ \int_{\Omega_1} (F_j^+ - F_j^-) d\mathbf{v}_j \right] \end{aligned}$$

Since  $F_j^- = \exp[-(\mathbf{v}_j + \mathbf{S}_j)^2]$ , and in case of specular reflection we have

$$K(\mathbf{v}, \mathbf{v}', \mathbf{r}_0) = \delta[(\mathbf{v}'\mathbf{n}) + (\mathbf{v}\mathbf{n})]$$

that

$$F_j^+ = \exp[-(\mathbf{v}_j + \mathbf{S}_j - 2\mathbf{n}(\mathbf{v}\mathbf{n}))^2]$$

Here  $\mathbf{n}'$  - normal to considered point of circle with coordinates  $(1, \theta')$ . Thus, in polar system of coordinates

$$\begin{aligned} n_j &= 1 + \frac{1}{\pi} \int_{-\delta}^{0+\delta} \int_0^\infty \{ \exp[-(v_j^2 + 2v_j S_j \cos \beta + S_j^2 - \\ &\quad - 4v_j S_j \cos \theta' \cos(\beta - \theta'))] - \\ &\quad - \exp[-(v_j^2 + S_j^2 + 2v_j S_j \cos \beta)] \} r dr d\beta \end{aligned}$$

We will find the connection between  $\theta'$  and  $\beta$  for a molecule reflected from point  $(1, \theta')$  of a circle and falling onto the considered point of space  $(y, \theta)$ .

By the theorem of sines we find

$$\frac{r}{\sin[\pi - (\theta' - \beta)]} = \frac{1}{\sin(\theta - \beta)}, \quad \text{or} \quad \theta' = \beta + \arcsin[r \sin(\theta - \beta)] \quad (3.3)$$

Substituting the obtained expression (3.3) and calculating integrals, we will obtain for density of particles

$$n_1 = 1 + 1/4(\text{sign}(\theta + \delta - \varepsilon_1) - \text{sign}(\theta - \delta + \varepsilon_1) + \text{erf}[S \sin(\theta + \delta)] [1 - \text{sign} \cos(\theta + \delta - \varepsilon_1)] - \text{erf}[S \sin(\theta - \delta)] [1 - \text{sign} \cos(\theta - \delta + \varepsilon_1)]) + J_1$$

Here  $\varepsilon_1$  - as small as desired a small positive number

$$J_1 = \frac{1}{2\sqrt{\pi}} \int_{\alpha_1}^{\alpha_2} S \cos \alpha \exp[-S^2 \sin^2 \alpha] [1 + \text{erf}(S \cos \alpha)] d\alpha$$

$$\alpha = \beta + 2 \arcsin[r \sin(\theta - \delta)]$$

Thus, the solution of the limiting problem has the form

$$\Phi_0 = 1/4(\text{sign}(\theta + \delta - \varepsilon_1) - \text{sign}(\theta - \delta + \varepsilon_1) + \text{erf}[S \sin(\theta + \delta)] [1 - \text{sign} \cos(\theta + \delta - \varepsilon_1)] - \text{erf}[S \sin(\theta - \delta)] [1 - \text{sign} \cos(\theta - \delta + \varepsilon_1)]) + J_1$$

Let us find the function of the "boundary" layer, being limited to accuracy  $O(\varepsilon)$ . In the considered case of flow around circle  $\Phi^0$ , according to (2.7), solution of equation is

$$\varepsilon^2 d^2 \Phi^0 / dr^2 - \Phi^0 = 0$$

with boundary conditions  $\Phi^0|_{r=0} = 0$  and  $\Phi^0|_{r=1} = \mu_0 - \text{erf}(S \cos \theta)$ . This solution has the form

$$\Phi^0 = [\mu_0 - \text{erf}(S \cos \theta)] \exp\left[-\frac{r-1}{\varepsilon}\right]$$

As a result potential of the electrical field created by a charged body moving in rarefied plasma is given by the expression

$$\Phi = 1/4(\text{sign}(\theta + \delta - \varepsilon_1) - \text{sign}(\theta - \delta + \varepsilon_1) + \text{erf}[S \sin(\theta + \delta)] [1 - \text{sign} \cos(\theta + \delta - \varepsilon_1)] - \text{erf}[S \sin(\theta - \delta)] [1 - \text{sign} \cos(\theta - \delta + \varepsilon_1)]) + J_1 + [\mu_0 - \text{erf}(S \cos \theta)] \exp[-(r-1)/\varepsilon]$$

It is easy to see that influence of a fast changing exponential term appears only in direct proximity of boundary, and at sufficient distance from the body the expression for potential is given by the solution of the limiting problem. When  $\mu_0 = 0$  we obtain distribution of the electrical field created only due to purely aerodynamic perturbations, caused by motion of an uncharged body.

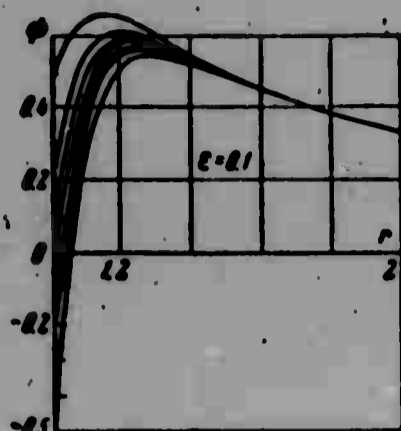


Fig. 1.

Figures 1, 2 give distribution of potential ahead of body ( $\theta = 0^\circ$ ) for values  $\epsilon = 0.1$  and  $\epsilon = 0.2$  correspondingly. Ahead of body potential attains certain positive maximum, after which it drops to zero. Positive maximum of potential ahead of body corresponds to region of maximum concentration of electrons, which will agree with the electron cloud observed before the moving body, shielding the charge of the body.

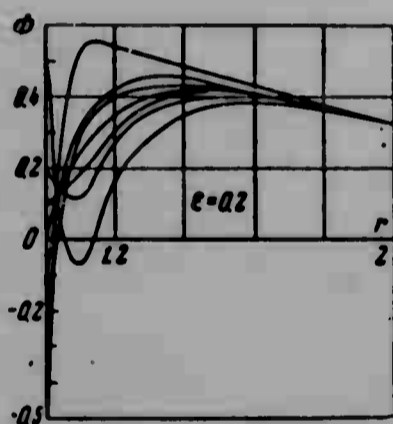


Fig. 2.

For a certain region of variables and parameters of the problem was found distribution of dimensionless potential  $\Phi$  depending upon  $r$  for different values  $\theta$  for cases of a positively and negatively charged body.

Results of calculations are given on Figs. 1-5, where there are constructed distribution curves of dimensionless potential  $\Phi = e\varphi/kT$  depending upon dimensionless radius  $r$ . These curves permit tracing influence of charge of body, and also Debye radius, on position and magnitude of extremum of potential.

On Figs. 3 and 4 is given distribution of potential for values  $\theta = 90^\circ$  and  $\theta = 150^\circ$ ; here curves 1, 2, 3, 4 correspond to the value  $\epsilon = 0.2$ ; curves 1', 2', 3', 4' - to the value  $\epsilon = 0.1$ . After the body (Fig. 5) potential attains considerable magnitude, remaining negative (region of "trace" having considerable extent). It is necessary to note that in the case of a cylinder conditions of smallness of aerodynamic perturbations are not carried out, and

therefore the obtained solution can give only a qualitative character of the phenomenon. For a quantitatively more precise determination it is necessary to consider ions on which the electrical field acts; obviously, in the region after the body will fall such particles, since filling of space after the body occurs basically due to particles whose speed is of the order of thermal velocity of motion. Therefore for a more exact quantitative description it is necessary to consider influence of field on heavy particles and in the region after the body to solve a nonlinear problem. It is possible, however, to show that qualitative behavior

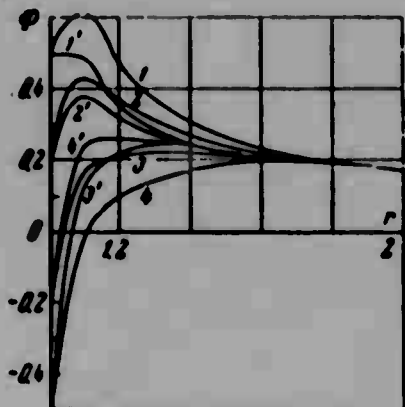


Fig. 3.

potential for body can be with sufficient accuracy replaced by an ordinary differential equation

$$\epsilon^2 \frac{d^2 \Phi}{dr^2} - \Phi = n_s$$

allowing direct integration.

Solution of this equation has the form

$$\Phi = \left[ \mu_0 + \frac{1}{2\epsilon} \int_1^\infty n_s \exp\left(-\frac{x-1}{\epsilon}\right) dx - \frac{1}{2\epsilon} \int_1^r n_s \exp\left(\frac{x-1}{\epsilon}\right) dx \right] \exp\left(-\frac{r-1}{\epsilon}\right) - \frac{1}{2\epsilon} \int_r^\infty n_s \exp\left(-\frac{x-1}{\epsilon}\right) dx \exp\left(\frac{r-1}{\epsilon}\right)$$

Hence for density of surface charge we will obtain the following expression

$$\sigma_s = \epsilon \left[ \mu_0 + \frac{1}{\epsilon} \int_1^\infty n_s \exp\left(-\frac{x-1}{\epsilon}\right) dx \right]$$

i.e., magnitude of surface charge is determined mainly by Debye radius, potential of body, and density of particles.

The value of surface charge permits obtaining the electrical force acting on the body. Force [10] acting on an element of the surface is determined by the

<sup>1</sup>In this connection it is necessary to note that the considered solution for a cylinder is incorrect in the case of diffuse reflection, since in assumption of diffuse reflection purely aerodynamic perturbations caused by the moving body are not small, and in order to clarify influence of mechanism of interaction of particles with surface it is necessary to consider flow around slender bodies, which perturbing the flow little. Let us note that here were not considered particles accomplishing finite motions.

relationship

$$F = -\frac{E^2}{8\pi} \Big|_{r=1}, \quad E = -\text{grad } \varphi$$

The full force acting on a body may be obtained by integration over surface of body.

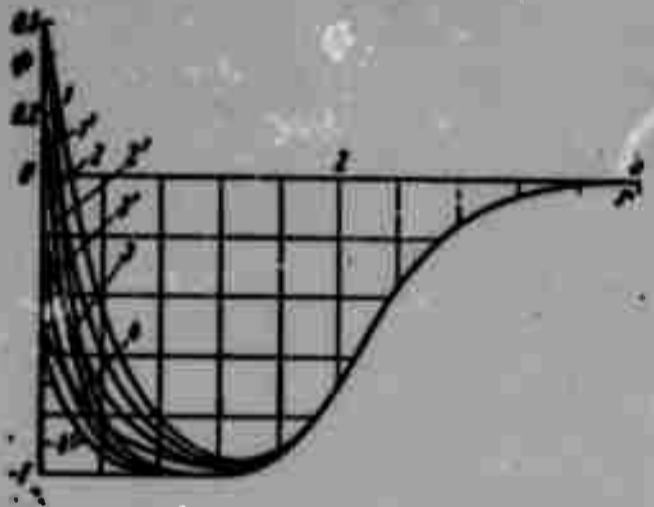


Fig. 4.

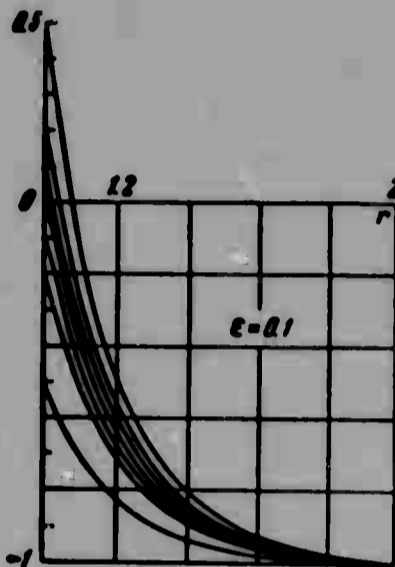


Fig. 5.

Aerodynamic forces acting on a body due to transmission of momentum by charged and neutral particles during their collisions with the surface can be obtained with the help of formulas presented, for instance, in [11]. It is possible to see that for a number of parameters of flow and field electrical forces can be comparable with aerodynamic forces.

Submitted  
14 May 1964

#### Literature

1. R. Jastrow and C. A. Pearse. Atmospheric Drag on the Satellite. J. Geophys. Res., 1957, Vol. 62, No. 3.
2. H. Joshihara. Motion of Thin Bodies in a Highly Rarefied Plasma. Phys. Fluids, 1961, Vol. 4, No. 1.
3. P. S. Greifinger. Induced Oscillations in a Rarefied Plasma in a Magnetic Field. Phys. Fluids, 1961, Vol. 4, No. 1.
4. L. Kraus and K. Watson. Plasma Motion Induced by Satellites in the Ionosphere. Phys. Fluids, 1958, Vol. 1, No. 6.
5. A. V. Gurevich. Perturbations in the ionosphere caused by a moving body. Artificial earth satellite, 1961, No. 7.

6. Ya. L. Al'pert, A. V. Gurevich and L. P. Pitayevskiy. Effects caused by an artificial satellite rapidly moving in the ionosphere and a magnetic medium. Prog. phys. sciences, 1963, Vol 79, No. 1.
7. A. A. Vlasov. Theory of many particles.
8. H. Grad. The Principles of Kinetic Theory of Gases. Handbuch der Physik, B. 12, 1958
9. M. I. Vishik and L. A. Lyusternik. Regular degeneration and the boundary layer for linear differential equations with small parameter. Prog. math. sciences, 1957, Vol. 12, Issue 5 (77).
10. L. D. Landau and Ye. M. Livshits. Electrodynamics of a solid media. Fizmatgiz, M., 1959.
11. N. T. Pashchenko. Flow around a fluctuating surface by a flow of strongly rarefied gas. PMM, 1959, Vol. 23, Issue 4.

**BLANK PAGE**

# DIFFUSION AND CONDUCTIVITY IN A PARTIALLY IONIZED MULTITEMPERATURE GAS MIXTURE

V. A. Polyanskiy

(Moscow)

In the work expressions are obtained for a diffusion flow of mass and generalized coefficients of diffusion in a partially ionized gas mixture with different temperatures of components occurring in an electromagnetic field. Equations of transfer, obtained from kinetic equations for each of the components of the mixture by the method of Gred using the "13 moments" approach [1] serve initially. Integrals of collisions in kinetic equations are taken in Landau form for particles interacting according to Coulomb law, and in Boltzmann form for other particles. Expressions are obtained for generalized Ohm's law and coefficients of mobility and conductivity in plasma with different sorts of ions. In § 2 are calculated coefficients of diffusion, mobility, and conductivity in a ditemperature partially ionized gas for the case when anisotropy of transfer phenomena can be disregarded ( $|\omega_e/\tau_e| \ll 1$ ). The coefficient of ambipolar diffusion in such gas is found. In § 3 is calculated conductivity of completely ionized plasma with two sorts of ions. If condition  $|\omega_e/\tau_e| \ll 1$  is not executed, results of §§ 2, 3 are accurate for diffusion coefficients along a magnetic field.

§ 1. Diffusion equations for a multitemperature gas mixture containing charged particles and being in an electromagnetic field, in hydrodynamic approximation<sup>1</sup> have the form

$$\begin{aligned} \sum_p (a_{ep} J^p + b_{ep} h^p) + \omega_e (J^e \times x) - c_e \sum_p \omega_p (J^p \times x) = \\ = \nabla p_e - c_e \nabla p + \operatorname{div} \pi^e - c_e \operatorname{div} \pi - \rho c_e \left( \frac{c_e}{m_e} - \sum_p \frac{c_p c_p}{m_p} \right) E^e \end{aligned} \quad (1.1)$$

<sup>1</sup>Macroscopic parameters of each of the components of the mixture change little at distances of the order of effective length of free path and in time of the order of time between collisions of particles.

Here

$$\begin{aligned} \mathbf{J}^\alpha &= \rho_\alpha (\mathbf{u}^\alpha - \mathbf{u}), & \rho_\alpha &= m_\alpha n_\alpha, & c_\alpha &= \rho_\alpha / \rho, & p_\alpha &= n_\alpha k T_\alpha \\ \mathbf{u} &= \sum_\alpha c_\alpha \mathbf{u}^\alpha, & \rho &= \sum_\alpha \rho_\alpha, & p &= \sum_\alpha p_\alpha, & \pi &= \sum_\alpha \pi^\alpha \\ \omega_\alpha &= e_\alpha |\mathbf{B}| / m_\alpha c, & \mathbf{E}^* &= \mathbf{E} + c^{-1} (\mathbf{u} \times \mathbf{B}), & \mathbf{x} &= \mathbf{B} / |\mathbf{B}| \end{aligned}$$

$\mathbf{J}^\alpha$  - diffusion flow of mass,  $\mathbf{h}^\alpha$  - flow of heat,  $p_\alpha$ ,  $\pi^\alpha$  and  $n_\alpha$  - correspondingly partial pressure, tensor of viscous stresses and number of particles in unit volume of the  $\alpha$  component of mixture,  $T_\alpha$  - temperature of  $\alpha$  component, in reference to average mass speed of mixture  $\mathbf{u}$ ,  $\omega_\alpha$  - cyclotron frequency of particle with charge  $e_\alpha$  and mass  $m_\alpha$ ,  $\mathbf{x}$  - unit vector in direction of magnetic field.

System (1.1) follows from the equation of motion of a gas mixture of the whole and from equations for flows  $\mathbf{J}^\alpha$ , which are obtained by the method of moments from kinetic equations for each of the components written in a system of coordinates which is motionless with respect to the mixture as a whole [1]. Integrals of collisions in kinetic equations are taken in Landau form for particles interacting according to Coulomb law, and in Boltzmann form for others. In accordance with this coefficients  $a_{\alpha\beta}$  and  $b_{\alpha\beta}$  are written in different form. For Coulomb interaction of particles we have

$$a_{\alpha\alpha} = - \sum_{\beta \neq \alpha} \frac{m_\beta}{m_\alpha + m_\beta} \frac{1}{\tau_{\alpha\beta}}, \quad a_{\alpha\beta} = \frac{m_\alpha}{m_\alpha + m_\beta} \frac{1}{\tau_{\beta\alpha}} \quad (\alpha \neq \beta) \quad (1.2)$$

$$b_{\alpha\alpha} = 0.6 \sum_{\beta \neq \alpha} \frac{m_\beta \tau_{\alpha\beta}}{m_\alpha + m_\beta} \frac{1}{\tau_{\alpha\beta}}, \quad b_{\alpha\beta} = - \frac{0.6 m_\alpha \tau_{\alpha\beta}}{m_\alpha + m_\beta} \frac{1}{\tau_{\beta\alpha}} \quad (\alpha \neq \beta) \quad (1.3)$$

Besides

$$\begin{aligned} \frac{1}{\tau_{\alpha\beta}} &= \frac{16}{3} n_\beta \left( \frac{1}{2\pi\gamma_{\alpha\beta}} \right)^{1/2} Q_{\alpha\beta}, & \frac{1}{\tau_{\beta\alpha}} &= \frac{n_\alpha}{n_\beta} \frac{1}{\tau_{\alpha\beta}}, & \gamma_{\alpha\beta} &= \frac{\gamma_\alpha \gamma_\beta}{\gamma_\alpha + \gamma_\beta} \\ Q_{\alpha\beta} &= \frac{\pi}{2} \left[ \frac{e_\alpha e_\beta \gamma_{\alpha\beta} (m_\alpha + m_\beta)}{m_\alpha m_\beta} \right]^2 \ln \Lambda_{\alpha\beta}, & \gamma_\alpha &= \frac{m_\alpha}{k T_\alpha}, \\ & (\Lambda_{\alpha\beta} - \text{Coulomb logarithm}) \end{aligned} \quad (1.4)$$

For other laws of interaction of particles coefficients  $a_{\alpha\beta}$  and  $b_{\alpha\beta}$  (and also  $c_{\alpha\beta}$ ,  $d_{\alpha\beta}$ ,  $\tau_\alpha^*$ , see below) are expressed through [2] of Chapman-Cauling integrals  $\Omega_{\alpha\beta}^n$ , where in quantities  $\tau_{\alpha\beta}^{-1}$

$$Q_{\alpha\beta} = (2\pi\gamma_{\alpha\beta})^{1/2} \Omega_{\alpha\beta}^{11} \quad (1.5)$$

The form of these coefficients is easy to establish, comparing (1.1) with corresponding expressions of [1]. System (1.1) is linearly dependent:

$$\sum_i a_{i\beta} = \sum_i b_{i\beta} = 0$$

Therefore for determination of  $J^\alpha$  it is necessary to add to (1.1) the evident equality

$$\sum_i J^i = 0 \quad (1.6)$$

Heat flow  $h^\beta$  can be excluded from (1.1) with the help of system [3]

$$\sum_\beta c_{\alpha\beta} h^\beta - \omega_\alpha \tau_\alpha^* (h^\alpha \times \kappa) = -\lambda_\alpha \nabla T_\alpha - \frac{0.4\lambda_\alpha}{k n_\alpha} \operatorname{div} \pi^\alpha + \sum_\beta d_{\alpha\beta} \tau_\alpha^* J^\beta$$

$$\lambda_\alpha = \frac{5k p_\alpha \tau_\alpha^*}{2m_\alpha} \quad (1.7)$$

Let us write quantities  $c_{\alpha\beta}$ ,  $\tau_\alpha^*$  and  $d_{\alpha\beta}$  in case of Coulomb interaction of particles

$$c_{\alpha\alpha} = 1, \quad c_{\alpha\beta} = -\frac{0.9m_\alpha \gamma_\beta^2 (3 + 2\delta_{\alpha\beta}) \tau_\alpha^*}{(m_\alpha + m_\beta) (\gamma_\alpha + \gamma_\beta)^2 \tau_{\alpha\beta}} \quad (\alpha \neq \beta) \quad (1.8)$$

$$\frac{1}{\tau_\alpha^*} = \frac{0.4}{\tau_{\alpha\alpha}} + \sum_{\beta \neq \alpha} \frac{m_\beta \gamma_\alpha \gamma_\beta}{(m_\alpha + m_\beta) (\gamma_\alpha + \gamma_\beta)^2 \tau_{\alpha\beta}} \left[ 3 \frac{\gamma_\alpha}{\gamma_\beta} + \right. \\ \left. + 1.3 \frac{\gamma_\beta}{\gamma_\alpha} + 1.6 - \delta_{\alpha\beta} (2.2 + 0.4 \frac{\gamma_\beta}{\gamma_\alpha}) \right] \quad (1.9)$$

$$d_{\alpha\alpha} = \sum_{\beta \neq \alpha} \frac{m_\beta \gamma_{\alpha\beta}}{(m_\alpha + m_\beta) \gamma_\alpha^2 \tau_{\alpha\beta}} \left[ 1.5 - \delta_{\alpha\beta} \left( 5 \frac{\gamma_\alpha}{\gamma_\beta} + 2 \right) \right] \quad (1.10)$$

$$d_{\alpha\beta} = -\frac{1.5m_\alpha \gamma_{\alpha\beta} (1 + 2\delta_{\alpha\beta})}{(m_\alpha + m_\beta) \gamma_\alpha^2 \tau_{\alpha\beta}} \quad (\alpha \neq \beta), \quad \delta_{\alpha\beta} = \frac{1 - T_\beta/T_\alpha}{1 + m_\beta/m_\alpha}$$

Expressions for  $c_{\alpha\beta}$ ,  $d_{\alpha\beta}$  and  $\tau_\alpha^*$  under other laws of interaction of particles can be written using corresponding results of [1, 3].

The solution of system (1.7) is written in the following way [3]:

$$h^\alpha = -\sum_\beta [\lambda_{\alpha\beta} \nabla_\parallel T_\beta + \lambda_{\alpha\beta} \nabla_\perp T_\beta + \lambda_{\alpha\beta} (\nabla T_\beta \times \kappa)] + \\ + \sum_\beta [\mu_{\alpha\beta} J_\parallel^\beta + \mu_{\alpha\beta} J_\perp^\beta + \mu_{\alpha\beta} (J^\beta \times \kappa)] - 0.4 \sum_\beta \frac{1}{k n_\beta} [(\lambda_{\alpha\beta}^\parallel - \lambda_{\alpha\beta}^\perp) \times \\ \times (\operatorname{div} \pi^\beta \cdot \kappa) \kappa + \lambda_{\alpha\beta}^\parallel \operatorname{div} \pi^\beta + \lambda_{\alpha\beta}^\perp (\operatorname{div} \pi^\beta \times \kappa)] \quad (1.11)$$

Here

$$\begin{aligned} \lambda_{\alpha\beta}^{\parallel} &= \frac{|c|_{\beta\alpha}}{|c|} \lambda_{\beta}, & \lambda_{\alpha\beta}^{\perp} &= \frac{|c^*|_{\beta\alpha}}{|c^*|} \lambda_{\beta}, & \lambda_{\alpha\beta}^{\cdot} &= \sum_{\gamma} \frac{\lambda_{\alpha\gamma}^{\perp} \lambda_{\gamma\beta}^{\parallel} \omega_{\gamma} \tau_{\gamma}^{\cdot}}{\lambda_{\gamma}} \\ \mu_{\alpha\beta}^{\parallel} &= \sum_{\gamma} \frac{\lambda_{\alpha\gamma}^{\perp} d_{\gamma\beta} \tau_{\gamma}^{\cdot}}{\lambda_{\gamma}} \end{aligned} \quad (1.12)$$

Expressions for  $\mu_{\alpha\beta}^{\perp}$  and  $\mu_{\alpha\beta}^{\cdot}$  are obtained from the formula for  $\mu_{\alpha\beta}^{\parallel}$  by means of replacement of the sign  $\parallel$  correspondingly by  $\perp$  and  $\cdot$ . The signs  $\parallel$ ,  $\perp$  for vectors mean that these vectors are directed along ( $\parallel$ ) and across ( $\perp$ ) of the magnetic field,  $|c|$  and  $|c^*|$  are determinants with elements  $c_{\alpha\beta}$  and  $c_{\alpha\beta}^*$ ,  $|c|_{\beta\alpha}$  and  $|c^*|_{\beta\alpha}$  are cofactors of elements ( $\beta\alpha$ ) of these determinants,  $\sigma^{ilm}$  is a permutable tensor,

$$\begin{aligned} \operatorname{div} \pi^{\beta} \times \kappa &= \sigma^{ilm} \kappa^m \frac{\partial \pi_{lr}^{\beta}}{\partial x_r}, & \operatorname{div} \pi^{\beta} \cdot \kappa &= \kappa^r \frac{\partial \pi_{rl}^{\beta}}{\partial x_l} \\ c_{\alpha\beta}^{\cdot} &= c_{\alpha\beta} + \frac{|c|_{\beta\alpha}}{|c|} \omega_{\alpha} \tau_{\alpha}^{\cdot} \omega_{\beta} \tau_{\beta}^{\cdot} \end{aligned}$$

Solution of system (1.1) can be obtained by substituting (1.11) in (1.1) and excluding with the help (1.6) from every equation of system (1.1) the quantity  $J^{\alpha}$ . Simple calculations show that diffusion flow of the mass of each component of the mixture is composed of several parts:

$$J = J_i^{\cdot} + J_i^{\perp} + J_i^{\parallel} + J_i^{\cdot} \quad (1.13)$$

Mass transfer, caused by gradients of densities of components of mixture,

$$J_i^{\cdot} = \sum_{\beta} \rho_{\beta} \frac{m_{\beta} T_{\beta}}{m_{\beta} T_{\alpha}} [G_{\alpha\beta}^{\parallel} \nabla_{\parallel} \ln \rho_{\beta} + G_{\alpha\beta}^{\perp} \nabla_{\perp} \ln \rho_{\beta} + G_{\alpha\beta}^{\cdot} (\ln \rho_{\beta} \times \kappa)] \quad (1.14)$$

Thermal diffusion mass transfer

$$\begin{aligned} J_i^{\perp} &= \sum_{\beta} \rho_{\beta} \frac{m_{\beta} T_{\beta}}{m_{\beta} T_{\alpha}} \left\{ \left( G_{\alpha\beta}^{\parallel} + \frac{1}{k n_{\beta}} \sum_{\gamma} b_{\gamma\beta} \lambda_{\gamma\beta}^{\parallel} D_{\alpha\gamma}^{\parallel} \right) \nabla_{\parallel} \ln T_{\beta} + \right. \\ &+ \left[ G_{\alpha\beta}^{\perp} + \frac{1}{k n_{\beta}} \sum_{\gamma} b_{\gamma\beta} (\lambda_{\gamma\beta}^{\perp} D_{\alpha\gamma}^{\perp} - \lambda_{\gamma\beta}^{\cdot} D_{\alpha\gamma}^{\cdot}) \right] \nabla_{\perp} \ln T_{\beta} + \\ &+ \left[ G_{\alpha\beta}^{\cdot} + \frac{1}{k n_{\beta}} \sum_{\gamma} b_{\gamma\beta} (\lambda_{\gamma\beta}^{\cdot} D_{\alpha\gamma}^{\perp} + \lambda_{\gamma\beta}^{\perp} D_{\alpha\gamma}^{\cdot}) \right] (\nabla \ln T_{\beta} \times \kappa) \left. \right\} \end{aligned} \quad (1.15)$$

Flow of mass due to viscous transfer of momentum

$$\begin{aligned}
J_s = \sum_{\beta} \frac{m_s}{kT_s} \{ & [G_{s\beta}^{\perp} + \frac{0.4}{k\eta_{\beta}} \sum_{\gamma, \delta} b_{\gamma\delta} (\lambda_{\delta\beta}^{\perp} D_{s\gamma}^{\perp} - \lambda_{\delta\beta}^{\wedge} D_{s\gamma}^{\wedge})] \operatorname{div} \pi^{\beta} + \\
& + [G_{s\beta}^{\parallel} - G_{s\beta}^{\perp} + \frac{0.4}{k\eta_{\beta}} \sum_{\gamma, \delta} b_{\gamma\delta} (\lambda_{\delta\beta}^{\parallel} D_{s\gamma}^{\parallel} - \lambda_{\delta\beta}^{\perp} D_{s\gamma}^{\perp} + \\
& + \lambda_{\delta\beta}^{\wedge} D_{s\gamma}^{\wedge})] (\operatorname{div} \pi^{\beta} \cdot \kappa) \kappa + [G_{s\beta}^{\wedge} + \frac{0.4}{k\eta_{\beta}} \sum_{\gamma, \delta} b_{\gamma\delta} (\lambda_{\delta\beta}^{\wedge} D_{s\gamma}^{\perp} + \\
& + \lambda_{\delta\beta}^{\perp} D_{s\gamma}^{\wedge})] (\operatorname{div} \pi^{\beta} \times \kappa) \}
\end{aligned} \quad (1.16)$$

Mass transfer by electromagnetic field

$$J_s = -\rho_s K_s^{\parallel} E_{\parallel}^* - \rho_s K_s^{\perp} E_{\perp}^* - \rho_s K_s^{\wedge} (E^* \times \kappa) \quad (1.17)$$

Here are introduced generalized coefficients of diffusion of multicomponent mixture  $D_{\alpha\beta}$  and mobility  $K_{\alpha}$

$$\begin{aligned}
D_{\alpha\beta}^{\parallel} &= \frac{kT_{\alpha}}{m_{\alpha}} \frac{|a^{(0)}|_{\beta\alpha} - |a^{(0)}|_{\alpha\alpha}}{|a^{(0)}|}, & D_{\alpha\beta}^{\perp} &= \frac{kT_{\alpha}}{m_{\alpha}} \frac{|a^{(0)}|_{\beta\alpha} - |a^{(0)}|_{\alpha\alpha}}{|a^{(0)}|}, \\
D_{\alpha\beta}^{\wedge} &= -\frac{kT_{\alpha}}{m_{\alpha}} \sum_{\gamma, \delta} a_{\gamma\delta}^{(2)} \frac{(|a^{(1)}|_{\beta\delta} - |a^{(1)}|_{\alpha\delta}) |a^{(3)}|_{\gamma\alpha}}{|a^{(1)}| |a^{(3)}|}, & G_{\alpha\beta}^{\parallel} &= D_{\alpha\beta}^{\parallel} - \sum_{\gamma} c_{\gamma} D_{s\gamma}^{\parallel}
\end{aligned} \quad (1.18)$$

$$K_s^{\parallel} = \sum_{\beta} \frac{n_{\beta}}{n_s kT_s} (c_{\beta} - \sum_{\gamma} \frac{m_{\beta}}{m_{\gamma}} c_{\gamma} c_{\gamma}) D_{s\beta}^{\parallel} \quad (1.19)$$

Here  $|a^{(p)}|$  - determinants with elements

$$\begin{aligned}
a_{\alpha\beta}^{(0)} &= a_{\alpha\beta} - a_{\alpha\alpha} + \sum_{\gamma} b_{s\gamma} (\mu_{\gamma\beta}^{\parallel} - \mu_{\gamma\alpha}^{\parallel}) \\
a_{\alpha\beta}^{(1)} &= a_{\alpha\beta} - a_{\alpha\alpha} + \sum_{\gamma} b_{s\gamma} (\mu_{\gamma\beta}^{\perp} - \mu_{\gamma\alpha}^{\perp}) \\
a_{\alpha\beta}^{(2)} &= \omega_{\alpha\beta}^* - \omega_{\alpha\alpha}^* + \sum_{\gamma} b_{s\gamma} (\mu_{\gamma\beta}^{\wedge} - \mu_{\gamma\alpha}^{\wedge}), & \omega_{\alpha\alpha}^* &= (1 - c_{\alpha}) \omega_{\alpha} \\
a_{\alpha\beta}^{(3)} &= a_{\alpha\beta}^{(1)} + \sum_{\gamma, \delta} \frac{|a^{(1)}|_{\gamma\delta}}{|a^{(2)}|} a_{\alpha\delta}^{(2)} a_{\gamma\beta}^{(2)}, & \omega_{\alpha\beta}^* &= -c_{\alpha} \omega_{\beta} \quad (\alpha \neq \beta)
\end{aligned} \quad (1.20)$$

$|a^{(p)}|_{\alpha\beta}$  - cofactor of elements  $a_{\alpha\beta}^{(p)}$  of these determinants. Expressions for quantities  $G_{\alpha\beta}^{\perp}$ ,  $G_{\alpha\beta}^{\wedge}$  and for mobility  $K_{\alpha}^{\perp}$ ,  $K_{\alpha}^{\wedge}$  are obtained from formulas for  $G_{\alpha\beta}^{\parallel}$ ,  $K_{\alpha}^{\parallel}$  by replacement in them of the sign  $\parallel$  correspondingly by the signs  $\perp$  and  $\wedge$ .

It is not difficult to see that coefficients  $D_{\alpha\beta}^{\parallel}$  for a mixture with identical temperatures of components coincide with generalized coefficients of diffusion

$D_{1j}$  given in [4], if coefficients of binary diffusion  $[D_{1j}]_k$  in  $D_{1j}$  are taken in the first approximation, and in quantities  $a_{\alpha\beta}^{(0)}$  terms of form  $b_{\alpha\beta}\mu_{\delta\gamma}^{\parallel}$  are omitted. Calculation of these terms, appearing due to heat transfer by diffusion, corresponds to the second approximation in coefficients of binary diffusion  $[D_{1j}]_k$ . From calculations made in [4] for certain potentials of interaction of particles of mixture, it is clear that the distinction of  $[D_{1j}]_2$  from  $[D_{1j}]_1$  composes only several percent (for instance, for the potential of Lennard-Jones this distinction does not exceed 3% for the majority of binary mixtures). However in the case of Coulomb interaction of charged particles the example of triple mixture considered below shows that calculation of diffusion heat transfer can lead to considerable change  $D_{\alpha\beta}$  (see also [5]).

The obtained expression (1.13) permits an easy writing of the generalized Ohm's law for plasma containing an arbitrary quantity of sorts of charged particles. Density of current

$$\mathbf{j} = \sum_i e_i n_i \mathbf{u}_i$$

Consequently, the generalized Ohm's law has the form

$$\mathbf{j} = \sum_i \frac{e_i}{m_i} \mathbf{J}^i + u \sum_i e_i n_i \quad (1.21)$$

Conductivity of such plasma is expressed by the formula

$$\sigma^{\parallel} = - \sum_i e_i n_i K_i^{\parallel} \quad (1.22)$$

Replacement of sign  $\parallel$  in (1.22) by signs  $\perp$  and  $\wedge$  gives expressions correspondingly for  $\sigma^{\perp}$  and  $\sigma^{\wedge}$ .

In conclusion of this section we will give the full system of hydrodynamic equations describing motion of a multitemperature partially ionized gas mixture in an electromagnetic field. The system is obtained by the method of moments from kinetic equations for each component of the mixture, written in a system of coordinates which is motionless with respect to the mixture as a whole. The system contains  $N - 1$  continuity equation of separate components ( $N$  - number of components of mixture), continuity equation and motion of mixture as a whole,  $N$  equations of energy and an "equation of state" mixture. In hydrodynamic

approximation (see footnote on p. 15) we have

$$\rho \frac{dc_a}{dt} + \operatorname{div} J^a = 0, \quad \frac{dp}{dt} + \rho \operatorname{div} u = 0 \quad (1.23)$$

$$\frac{du}{dt} = -\frac{1}{\rho} \nabla p - \frac{1}{\rho} \operatorname{div} \pi + \sum_{\beta} \frac{e_{\beta} c_{\beta}}{m_{\beta}} E + \frac{1}{\rho c} j \times B \quad (1.24)$$

$$\begin{aligned} \frac{3}{2} c_a \frac{dT_a}{dt} = & -c_a T_a \operatorname{div} u - \frac{m_a}{k\rho} \operatorname{div} h^a - \frac{T_a}{\rho} \operatorname{div} J^a - \frac{m_a}{k\rho} \pi_{ij}^a \frac{\partial u_i}{\partial x_j} + \\ & + \frac{m_a}{k\rho^2} J^a \cdot \nabla p - \frac{5}{2\rho} J^a \nabla T_a + \frac{m_a}{k\rho^2} J^a \operatorname{div} \pi + \frac{1}{k\rho} J^a \cdot \left[ \left( c_a - \sum_{\beta} \frac{m_a}{m_{\beta}} e_{\beta} c_{\beta} \right) E + \right. \\ & \left. + \frac{e_a}{c} u \times B - \frac{m_a}{\rho c} j \times B \right] + \sum_{\beta} \frac{3c_a m_a m_{\beta}}{(m_a + m_{\beta})^2 \tau_{a\beta}} (T_{\beta} - T_a) \end{aligned} \quad (1.25)$$

$$p = k\rho \sum_{\beta} \frac{c_{\beta} T_{\beta}}{m_{\beta}} \quad (1.26)$$

Tensors of viscous stresses of each component of the mixture  $\pi^{\alpha}$  in complicated form depend on tensor of speeds of deformations of all the mixture. Expressions for  $\pi^{\alpha}$  are obtained in [3]. Quantities  $J^{\alpha}$ ,  $j$ ,  $h^{\alpha}$  are given by formulas (1.13), (1.21) and (1.11).

§ 2. Below is considered a three-component mixture composed from ions (i), electrons (e), and neutral particles (a). Temperatures and mass of particles of heavy components are assumed identical ( $T_i = T_a = T$ ,  $m_i = m_a = m$ ). Temperature of electrons  $T_e \gg T$ , where is considered the executed condition

$$\epsilon \theta^{-1} \ll 1 \quad (\epsilon = m_e/m, \theta = T/T_e) \quad (2.1)$$

Coefficients  $a_{\alpha\beta}$  to  $d_{\alpha\beta}$  for such a mixture taking into account (2.1) take the form

$$\begin{aligned} a_{ee} &= -0.5\tau_{ei}^{-1} - \epsilon\tau_{ee}^{-1}, & a_{ei} &= 0.5\tau_{ie}^{-1}, & a_{ea} &= \tau_{ea}^{-1}, \\ a_{ii} &= -0.5\tau_{ie}^{-1} - \epsilon\tau_{ii}^{-1}, & a_{ie} &= 0.5\tau_{ei}^{-1}, & a_{ie} &= \tau_{ei}^{-1}, \\ a_{ee} &= -\tau_e^{-1}, & a_{ei} &= \tau_{ie}^{-1}, & a_{ea} &= \epsilon\tau_{ea}^{-1} \end{aligned} \quad (2.2)$$

$$\begin{aligned}
b_{ee} &= -\gamma b_1 \tau_{ei}^{-1}, & b_{ei} &= \gamma b_1 \tau_{ie}^{-1}, & b_{ee} &= e\theta \gamma b_2 \tau_{ee}^{-1} \\
b_{ii} &= -\gamma b_1 \tau_{ie}^{-1} + 0.6e^2 \theta \gamma \tau_{ie}^{-1}, & b_{ie} &= \gamma b_1 \tau_{ei}^{-1}, & b_{ie} &= -0.6e\theta \gamma \tau_{ei}^{-1} \\
b_{ee} &= -e\theta \gamma v, & b_{ee} &= e^2 \theta \gamma b_2 \tau_{ee}^{-1}, & b_{ei} &= -0.6e^2 \theta \gamma \tau_{ie}^{-1}
\end{aligned} \quad (2.3)$$

$$\begin{aligned}
d_{ee} &= -2.5b_1(\gamma \tau_{ei})^{-1} + 5e(1-\theta)(\gamma \theta \tau_{ee})^{-1}, & d_{ei} &= 2.5b_1(\gamma \tau_{ie})^{-1} \\
d_{ee} &= ed(\gamma \theta \tau_{ee})^{-1}, & d_{ii} &= -2.5b_1(\gamma \tau_{ie})^{-1} + 5e(1-\theta)(\gamma \theta \tau_{ie})^{-1} \\
d_{ie} &= 2.5b_1(\gamma \tau_{ei})^{-1}, & d_{ie} &= e(3-4.5\theta)(\gamma \tau_{ei})^{-1}, & d_{ee} &= -2.5(e\theta \gamma)^{-1}v \\
d_{ee} &= 2.5b_2(\gamma \theta \tau_{ee})^{-1}, & d_{ei} &= -1.5(\gamma \theta \tau_{ie})^{-1}
\end{aligned} \quad (2.4)$$

Here

$$\begin{aligned}
\tau_e^{-1} &= \tau_{ei}^{-1} + \tau_{ee}^{-1}, & v &= b_2 \tau_{ee}^{-1} - 0.6\tau_{ei}^{-1}, & \gamma &= m/kT \\
b_1 &= 0.25(1.2C_{ie}^* - 1), & b_2 &= (1.2C_{ee}^* - 1), \\
d &= 2.5\theta^2 b_2 - (1-\theta)(4A_{ee}^* - 12C_{ee}^* - 5\theta + 6\theta C_{ee}^*) \\
A_{ee}^* &= \Omega_{ee}^{(2)}/2\Omega_{ee}^{(1)}, & B_{ee}^* &= (5\Omega_{ee}^{(2)} - \Omega_{ee}^{(3)})/3\Omega_{ee}^{(1)}, & C_{ee}^* &= \Omega_{ee}^{(3)}/3\Omega_{ee}^{(1)}
\end{aligned}$$

Coefficients  $c_{\alpha\beta}$  and quantities  $\tau_{\alpha}^*$  for a triple mixture are written out in [3]. Let us give results of calculations of generalized coefficients of diffusion and conductivity for the case when anisotropy of phenomena of transfer can be disregarded ( $|\dot{\omega}_e| \tau_e^* \ll 1$ ). During calculations estimates of ratios of effective cross sections of collisions  $Q_{ee}/Q_{ei}$  for range of temperatures  $5 \cdot 10^2 \text{ K} \leq T \leq 10^4 \text{ K}$ ,  $5 \cdot 10^3 \text{ K} \leq T \leq 5 \cdot 10^4 \text{ K}$  given in § 2 of [3] were essentially used. Additional data confirming accuracy of these estimates can be found in [6]. These data permit a decrease of the lower bound of electron temperature  $T_e$  to  $2 \cdot 10^3 \text{ K}$  for certain gases. With an accuracy of quantities of the order  $e^{1/10}$  with respect to remaining coefficients  $D_{\alpha\beta}^I$  take the form

$$\begin{aligned}
D_{ee}^I &= \frac{\delta kT}{m} \left( \frac{a_1}{2\tau_{ie}} + \frac{a_2}{\tau_{ei}} \right), & D_{ee}^I &= \frac{\delta kT_e}{m_e} \left( \frac{a_1}{2\tau_{ei}} + \frac{a_2}{\tau_{ie}} \right), & D_{ei}^I &= \frac{\delta kT_e}{m_e} \left( \frac{a_1}{2\tau_{ei}} + \frac{a_2}{\tau_{ee}} \right) \\
D_{ei}^I &= D_{ie}^I = \frac{2\tau_{ei}}{a_1(1+\Delta)} \frac{kT}{m}, & D_{ie}^I &= \frac{\delta kT}{m} \left( \frac{a_1}{2\tau_{ei}} + \frac{a_2}{\tau_{ee}} \right)
\end{aligned} \quad (2.5)$$

Here

$$\begin{aligned}
(D_{ee}^I \approx D_{ei}^I, & D_{ei}^I \ll D_{ee}^I) \\
a &= \frac{n_i}{n_i + n_e}, & \delta &= \frac{2\tau_{ei}\tau_e}{a_{ee}(1+\Delta)}, & a_p &= 1 - f_p, & (p=0, 1, \dots, 5) \\
\Delta &= 2\tau_{ei}(1 - 2.5\tau_e v^{**}) \left[ \tau_{ee}\tau_{ei}a_1 \left( \frac{a_2}{\tau_e} + \frac{a_1}{2\tau_{ei}} \right) \right]^{-1} \\
f_0 &= 2.5v\tau_e\tau_{ee}, & f_1 &= \frac{5b_1}{\xi} \left( \frac{\tau_e^*}{\tau_{ei}} + \frac{\tau_i^*}{\tau_{ie}} - \frac{2g\tau_e^*\tau_i^*}{\tau_{ie}\tau_{ei}} \right), & f_2 &= -1.3v\tau_e, & f_3 &= 2.5b_2v\tau_{ee} \\
f_4 &= 1.5v\tau_e\tau_{ee} \frac{n_i}{n_e}, & f_5 &= \frac{2.5b_2v\tau_e\tau_{ee}n_e}{n_e}, & \xi &= 1 - \frac{g^2\tau_e^*\tau_i^*}{\tau_{ie}\tau_{ei}} \\
v^* &= \frac{b_1}{\tau_{ee}} + \frac{0.6}{\tau_{ie}}, & v^{**} &= \frac{b_1}{\tau_{ee}} + \frac{0.6}{\tau_{ei}}, & g &= 0.125(5.5 - 1.6A_{ei}^* - 1.2B_{ei}^*)
\end{aligned}$$

Calculations made on the assumption that degree of ionization is small and collisions of neutral - neutral, neutral - charged particle type predominate show that calculation of diffusion heat transfer introduces in  $D_{\alpha\beta}$  insignificant correction  $f_p \sim 0.01-0.08$  ( $p = 0, \dots, 5$ ). At a high degree of ionization, when collisions between charged particles become essential magnitude of correction increases:  $f_p \sim 0.5$  ( $p = 0, 2, 4$ ). This leads to considerable increase of certain diffusion coefficients  $D_{\alpha\beta}$ .

Mobility of charged particles

$$\begin{aligned} K_i^{\parallel} &= \frac{Ze}{kT} \alpha_i D_{ie}^{\parallel}, & K_e^{\parallel} &= \frac{e}{kT_e} \alpha_e D_{ei}^{\parallel} \\ \alpha_i &= \frac{n_e}{Zn_i} \left[ 1 - \frac{m_e}{p} (n_e - Zn_i) \right], & \alpha_e &= \frac{Zn_i}{n_e} \left[ 1 - \frac{m}{Zp} (Zn_i - n_e) \right] \end{aligned} \quad (2.6)$$

In (2.6) for convenience of writing mobility  $K_i^{\parallel}$  is taken with an opposite sign as compared to (1.19). Subsequently for simplicity we will consider that plasma is quasineutral. ( $Zn_i = n_e$ ,  $\alpha_i = \alpha_e = 1$ ). Simple computations taking into account estimates of ratios  $Q_{\alpha\beta}/Q_i$  from [3] give

$$K_i^{\parallel}/K_e^{\parallel} \sim e[a + (e\theta)^{-1/2}(1-a)]$$

Consequently, at a high degree of ionization ( $a \sim 1$ )  $K_i^{\parallel}/K_e^{\parallel} \sim e \ll 1$ . If  $a < 1$ , then inequality becomes less strong, since then  $K_i^{\parallel}/K_e^{\parallel} \sim e^{1/2}\theta^{-1/2}$ .

Conductivity of plasma

$$\sigma^{\parallel} = \frac{e^2 n_e \delta}{m_e} \left[ \frac{\alpha_i}{2\pi\tau_{ei}} + \frac{e}{\tau_{ee}} \left( \alpha_e + \frac{Z\alpha_i n_e}{n_e} \right) \right] \quad (2.7)$$

The expression for  $\sigma^{\parallel}$  becomes simpler if break away of temperature of electrons from temperature of heavy particles is not very great ( $e^{1/2}\theta^{-1/2} \ll 1$ )

$$\sigma^{\parallel} = \frac{e^2 n_e \tau_{ee}}{m_e (1 - 2.5v^2 \tau_{ee} \tau_{ei}^{-1})} \quad (2.8)$$

Formula (2.8) is analogous to expression (4.17) of [5], if in the latter quantity  $\tau_{e\beta}$  is determined at electron temperature  $T_e$ . This confirms the affirmation in [3] with respect to expression for density of current  $j$ .

We will consider ambipolar diffusion when  $|\omega_e| \tau_e \ll 1$ . Let us assume that, besides the condition of quasineutrality condition  $Z \nabla n_i = \nabla n_e \gg \nabla n_e$  is carried out and all currents are equal to zero ( $u' - u = u' - u = w_e$ ). Let us assume that, further, influence of viscous transfer of momentum and gradients of temperature on diffusion flows of ions and electrons can be disregarded. After exception from expressions for  $J^i$ ,  $J^e$  of electrical field  $E^*$  we will have

$$w_e = D_a \nabla \rho_i / \rho_i = D_a \nabla \rho_e / \rho_e \quad (2.9)$$

Here  $D_a$  - coefficient of ambipolar diffusion

$$D_a = \frac{20^{-1} G_{ie} K_i + Z^{-1} G_{ei} K_e}{K_i + K_e} \quad (2.10)$$

Calculations accurate to  $\epsilon^{1/2} \sim 1/2$  give

$$D_a = \frac{P_e \delta^0}{\rho} \left( \frac{a_1}{2\tau_{e1}} + \frac{a_2}{\tau_{e2}} \right) \left\{ 1 + \frac{1-\alpha}{\alpha} \left[ 1 - \frac{a_2}{\tau_0 (a_1 \tau_{e2}^{-1} + 0.5 a_2 \tau_{e1}^{-1})} - \frac{2a_2 \tau_{e1} \tau_{e2}}{Z a_1 \tau_{e1}} \right] \right\} \quad (2.11)$$

$$\delta^0 = 2\pi \tau_{e1} \tau_0 / a_2 a_1$$

3. Below formulas (1.19) and (1.22) are applied to ditemperature completely ionized plasma with two sorts of ions: (i) and (s). Let us assume that  $T$ ,  $m_i$ ,  $m_s$  ( $m_i \ll m_s$ ) - temperature and mass of ions,  $Z_i e$ ,  $Z_s e$  - their charges. When  $|\omega_e| \tau_e \ll 1$ , mobility of charges particles in such plasma are written in the following way:

$$K_i = e(Z_i n_i + Z_s n_s) \tau_0 / n_e m_e \quad (3.1)$$

$$K_a = \frac{e \tau_0 \tau_1}{n_e m_e} \left[ \frac{Z_p n_p}{\tau_0} - \frac{n_p}{\tau_{ap}} - \frac{n_s m_s}{(m_i + m_s) \tau_{ps}} \right] \quad \left( \begin{matrix} a, \beta = i, s \\ a \neq \beta \end{matrix} \right)$$

Now

$$\tau_0^{-1} = \tau_{e1}^{-1} + \tau_{e2}^{-1}, \quad \tau_1^{-1} = (m_s \tau_{ie}^{-1} + m_i \tau_{si}^{-1}) / (m_i + m_s)$$

Conductivity

$$\sigma = \frac{e^2 n_e \tau_0}{m_e} = \frac{3 n_e (k T_e)^{3/2}}{4 \sqrt{2\pi} e m_e^{1/2} (Z_i^2 n_i \ln \Lambda_{ei} + Z_s^2 n_s \ln \Lambda_{es})} \quad (3.2)$$

In (3.1), (3.2) calculations are made accurate to  $(m_e/m_i)^{1/2} \sim 1/2$ , and it is

considered that

$$\sum_a n_a e_a = 0, \quad b_{\alpha\beta} \mu_{\beta\gamma} = 0$$

If  $|\omega|v \geq 1$ , formulas (3.1), (3.2) are true for longitudinal coefficients.

Submitted  
16 June 1964

#### Literature

1. M. Ya. Aliyevskiy and V. M. Zhdanov. Equations of transfer for nonisothermal multisort plasma. PMTF, 1963, No. 5.
2. S. Chepman and T. Cauling. Mathematical theory of nonuniform gases. Publishing House of Foreign Literature, 1960.
3. M. Ya. Aliyevskiy, V. M. Zhdanov and V. A. Polyanskiy. Tensor of viscous stresses and heat flow in a two-temperature partially ionized gas. PMTF, 1964, No. 3.
4. J. Girshfel'der, Ch. Curtiss and R. Berd. Molecular theory of gases and liquids. Publishing House of Foreign Literature, 1961.
5. V. M. Zhdanov. Phenomena of transfer in partially ionized gas. PMM, 1962, Vol. 26, Issue 2.
6. Pen Tszay-chen and A. Pindrokh. Definitized calculation of properties of air at high temperatures. Problems of Rocket Technology. Coll. trans. and surv. for. period. lit., 1962, No. 12.

**BLANK PAGE**

# DISPERSION OF A HEATED MASS OF GAS IN REGULAR CONDITIONS

I. V. Nemchinov

(Moscow)

We consider motion of a given mass of gas, in particles of which energy is liberated, where intensity of energy release depends exponentially on temperature and density and arbitrarily on time. The analogy of the solution of L. I. Sedov of the problem about adiabatic dispersion, found earlier by the author is analyzed [1] — self-simulating solution, describing motion of gas with preheating in regular conditions [2], character of distribution of parameters with respect to particles of gas also in time for different indices of degree in the law of heat emission is investigated. The question about establishment of a self-simulating solution is discussed, and also its applicability to certain specific processes of gas-dynamic motion in the presence of intense heat addition.

§ 1. Let us consider the problem about nonadiabatic motion of a gas when intensity of energy release in particles  $Q$  [erg/g/sec] depends on thermodynamic parameters characterizing the state of the gas, for instance, on temperature and density — exponentially, and on time — arbitrarily. The equation of energy has the form

$$\frac{\partial e}{\partial t} + v \frac{\partial e}{\partial m} = Q = Q_* \left( \frac{e}{e_*} \right)^{-\alpha} \left( \frac{v}{v_*} \right)^{-\beta} \varphi \left( \frac{t}{t_*} \right) f \left( \frac{m}{m_*} \right) \quad (1.1)$$

$$\left( e = \frac{p v}{\kappa - 1}, \quad v = \frac{1}{\rho} \right)$$

Here  $e$  — energy of mass unit of gas,  $\kappa$  — constant adiabatic index,  $v$  — specific volume,  $\rho$  — density of substance,  $t$  — time,  $m$  — Lagrange (mass) coordinate of particle; the index  $*$  marks characteristic measured parameters in the law of heat emission,  $f$  and  $\varphi$  are arbitrary dimensionless assigned functions of arguments

characterizing change of intensity of source in time and energy release with respect to particles.

If the total mass of moving and heated gas is fixed, then there exists an analogy of the solution of L. I. Sedov of the problem about adiabatic dispersion [1] - self-simulating solution [2], describing regular conditions of motion and heating of gas.

In [2] was the case of plane motion of a gas when  $\alpha = 0$  and  $\beta = 0$  considered in detail, i.e., when intensity of energy release does not depend on thermodynamic parameters.

Such a case corresponds, for instance, to the rather wide-spread case of absorption of electromagnetic radiation by a substance, when the mass coefficient of absorption  $k\nu$  [ $\text{cm}^2/\text{g}$ ] does not depend on the state of the substance:  $k\nu = k_0\nu_0 = \text{const}$ . Then  $Q_0\tau = Ek_0\nu_0$ , where  $E$  is total energy of electromagnetic radiation incident per unit of surface [ $\text{erg}/\text{cm}^2$ ] and  $\tau$  - characteristic time of action of source of energy, where  $f = \exp(-k_0\nu_0 r_0)$  for absorption of monochromatic radiation. As  $m_*$  it is possible to select the quantity  $(k_0\nu_0)^{-1}$ . For the "transparent" region, dimensions of which  $r_0$  are such that  $k_0\nu_0 r_0 \ll 1$ , we will obtain  $f = 1$ .

Due to heating the coefficient of absorption can be changed, and, if its change can be described by the root law, then for transparent regions where  $f \approx 1$ , we will obtain

$$Q = \frac{E}{\tau} k\nu = \frac{E}{\tau} k_0\nu_0 \left(\frac{\nu}{\nu_0}\right)^{-\alpha} \left(\frac{\nu}{\nu_0}\right)^{-\beta} \varphi\left(\frac{\nu}{\nu_0}\right)$$

Completely ionized plasma with natural frequency  $\omega_0$  during calculation of energy transfer from electrons to ions with frequency of collisions  $\nu_1$  absorbs electromagnetic radiation with frequency  $\omega$ , where, if  $\nu_1 \ll \omega$  and  $\omega \gg \omega_0$ , then [3-6].

$$k = \frac{\nu_1}{c} \left(\frac{\omega_0}{\omega}\right)^3, \quad \omega_0 = \left(\frac{4\pi n_e e^2}{m_e}\right)^{1/2}, \quad \nu_1 = \frac{4\sqrt{2\pi} e^4 n_e L}{3(k_B T)^{1/2} m_e^{1/2}}$$

Here  $e$  and  $m_e$  - charge and mass of electron,  $n_e$  - number of electrons in unit volume,  $k_B$  - Boltzmann constant,  $T$  - temperature,  $L$  - Coulomb logarithm [6], which it is possible to consider approximately constant. Consequently, in this case  $\beta = 1$ ,  $\alpha = 3/2$ . N. G. Basov and O. N. Krokhin [3] proposed to use absorption of plasma by the

shown mechanism of a monochromatic pulsating light beam of great power to achieve very high temperatures of the order  $10^7$  degrees K.

During comparatively small changes of temperature near characteristic temperature  $T$ , the dependence of the rate of reactions and, consequently, dependence of heat emission on temperature and density may also be approximated by root law.

In the monograph of K. P. Stanyukovich [7] the problem about motion of gas driving a piston already was considered taking into account heat emission from pressure by the root law (dependence of burning rate of powders usually is approximated thus). It was assumed that pressure drop in moving gas is small, which is true only for a sufficiently heavy cast off body, i.e.,  $p = p(t)$ .

During thermonuclear reactions [8, 9] the law of heat emission has usually the form

$$Q = A \left( \frac{p}{p_0} \right) \left( \frac{T}{T_0} \right)^{-\chi} e^{-x} \quad \left( \chi = \frac{B}{T^{1/2}} \right) \\ (A = \text{const}, \quad B = \text{const})$$

Approximation by exponential dependence leads to the expression

$$Q = Q_0 \left( \frac{p}{p_0} \right) \left( \frac{T}{T_0} \right)^{\alpha}, \quad \alpha = \frac{-\chi_0 + 2}{3}, \quad \beta = 1, \quad \chi_0 = \frac{B}{T^{1/2}}$$

Electrical conductivity of strongly ionized gas changes by the law [10]

$$\sigma = \sigma_0(Z) \frac{T^{1/2}}{4e_0^2 \sqrt{2\pi m_e} L}$$

where  $\sigma_0(Z)$  — dimensionless coefficient of the order of unity depending on average charge of plasma  $Z$ . If electrical current  $j$  is constant with respect to cross section of discharge, then Joule heat liberated in it  $Q \sim T^{-1/2}$ .

For several physical and hydrodynamic problems (if relationship of parameters is such that regular conditions of dispersion) can be established consideration of the character of variation of parameters in time and their distribution with respect to particles for different values  $\alpha$  and  $\beta$  presents interest.

Equations of motion of gas and inseparability in the presence of preheating do not change form

$$\frac{\partial u}{\partial t} + \frac{\partial p}{\partial m} r^{-1} = 0, \quad \frac{\partial r}{\partial t} = u, \quad \frac{1}{v} \frac{\partial r^v}{\partial m} = v \quad (1.2)$$

Here  $u$  — speed of gas,  $r$  — Euler coordinate,  $m$  — is Lagrange coordinate,  
 $\nu = 1, 2, 3$  in flat, cylindrical, and spherical cases.

The problem about regular conditions of motion of gas of given mass has a solution in separable variables

$$\begin{aligned} p &= P(m) p^*(t), & v &= V(m) v^*(t) \\ u &= U(m) u^*(t), & r &= R(m) r^*(t) \end{aligned} \quad (1.3)$$

Putting (1.3) in system of partial differential equations (1.1) and (1.2), we will obtain two systems of ordinary differential equations, one of which serves for finding the dependence of variation of parameters on time, the other — for determination of distribution of parameters in regular conditions

$$\left(\frac{dv^*}{dt} + p^* \frac{dv^*}{dr^*}\right) \left(\frac{v^*}{v_0}\right)^{\alpha} \left(\frac{r^*}{r_0}\right)^{\beta} \varphi^{-1}\left(\frac{t}{\tau}\right) = Q_0 (PV)^{-(\alpha+1)} V^{-\beta} f\left(\frac{m}{m_0}\right) \quad (1.4)$$

$$\frac{du^*}{dt} \frac{1}{p^*(r^*)^{\gamma}} = \frac{dP}{dm} \frac{R^{\alpha-1}}{U} \quad (1.5)$$

$$\frac{dr^*}{dt} \frac{1}{u^*} = \frac{U}{R} \quad (1.6)$$

$$\frac{v^*}{(r^*)^{\gamma}} = \frac{1}{v} \frac{dR^*}{dm} \frac{1}{V} \quad (1.7)$$

Let us note that the obtained particular exact solution of equations of one-dimensional motion of gas taking into account preheating is a generalization (in the case of nonadiabatic motions of gas) of the solution of the problem about adiabatic dispersion of a fixed mass of gas [1], also being the solution in separable variables, where in this case the right side of the equation of energy is equal to zero, i.e.,

$$\frac{\partial}{\partial t} [\ln(pv^{\alpha})] = 0, \quad \text{or} \quad PV^{\alpha}/(m) = \text{const.}$$

In the considered solution with preheating from (1.5) it follows that

$$PV^{\gamma}/\left(\frac{m}{m_0}\right) = \text{const.}, \quad (\gamma-1)(1+\alpha) = \beta \quad (1.8)$$

However the degree of arbitrariness in the investigated solution is somewhat less than during adiabatic dispersion when  $f(m)$  determines possible arbitrariness in initial data, since in problems with preheating  $f(m)$  usually is fixed from physical considerations. Let us indicate that, in general,  $\gamma \neq \alpha$ . For  $\alpha = +\frac{1}{2}$ , and

$\beta = +1$  (heating plasma by electromagnetic radiation of constant frequency) magnitude  $\gamma = 1/2$  (whereas true adiabatic index of gas  $\kappa = 5/3$  appearing in left part of equation (1.1)).

It is natural that nonlinearity of system of equations (1.1) and (1.2) permits motion to be described by a solution in separable variables only if initial profile of parameters corresponds to solution of ordinary differential equations, obtained in assumption of self-simulation of motion. In the presence of prolonged energy release, when volume occupied by gas and its energy will become essentially larger than their initial values, it is possible to assume that motion will reach self-simulating conditions and during initial distribution of parameters, different from "self-simulating," i.e., self-simulating conditions will be asymptotic.

It is interesting to note that zero initial data (motion, starting from state of rest of absolutely cold gas) also satisfy separation of variables. Actually, when  $p^0(0) = 0$  and  $u^0(0) = 0$  arbitrary profile  $P(m)$  and  $U(m)$  satisfies condition  $p(0, m) = 0$ ,  $u(0, m) = 0$ . In such a case nonself-simulation of motion can take place only because initial distribution of density is different than self-simulating. However from intuitive ("physical") considerations it is clear that after as a result of heating a substance considerably expands, not only character of distribution of density, but also its absolute value is immaterial. As will be shown below, in many cases during prolonged energy release kinetic and thermal energy of moving gas are proportional to each other and have one order of magnitude. Therefore toward the end of energy release speed will be of order  $\sqrt{2E/M}$ , where  $E$  — total energy liberated in gas, and  $M$  — its mass. Consequently, dimension of region occupied by gas will be of order  $\sqrt{2E/M}$ , where  $\tau$  — full time of energy release, and average specific volume of order  $(\sqrt{2E/M}) \cdot M^{-1}$ .

It follows from this that for sufficiently small mass of moving gas  $M$ , sufficiently great liberated energy  $E$ , and sufficiently great duration of energy supply  $\tau$ , average density of substance  $\rho$  will be considerably less than initial density. It is clear that although in "absolute value"  $\tau$  can be a sufficiently small magnitude (as compared to "usual" scales), dispersion will take place in regular conditions of prolonged heat supply. It is natural that the criterion of duration of feed of energy is  $\tau \gg t_g$ , where  $t_g$  — characteristic gas-dynamic time of dispersion. If characteristic initial dimension  $r_0 = (M \rho_0)^{-1/2}$ , and characteristic rate of dispersion is of order  $\sqrt{2E/M}$ , then  $t_g \sqrt{2E/M} = r_0$ .

For parameters given in [3] and corresponding to preheating of plasma by light beam to  $T_0 = 10^7$  K, when at density  $\rho_0 = 10^{-7}$  g/cm<sup>3</sup>,  $r_0 \approx 1/k_0 = 10^{-2}$  cm and energy of mass unit of gas  $\epsilon_0 = 1.5 \cdot 10^{10}$  erg/g and therefore  $\sqrt{2\epsilon_0} = 5 \cdot 10^7$  cm/sec we will obtain that  $t_0 = 2 \cdot 10^{-10}$  sec. Consequently, already for an "extremely small" pulse duration of order  $10^{-8}$  sec one may assume that dispersion occurs in conditions of slow preheating.

On boundary of moving gas of total mass M during dispersion in vacuum, pressure  $p = 0$ . At point of symmetry (or for boundary with hard wall in flat case) speed of gas  $u = 0$ . Such boundary conditions correspond to self-simulating character of motion

$$m\zeta(\nu) = M, \quad P = 0; \quad m = 0, \quad U = 0, \quad P = 1$$

where  $\zeta(\nu) = 2.2\pi, 4\pi$  when  $\nu = 1, 2, 3$  correspondingly.

Dispersion of gas can be self-simulating also in the presence on its boundary of a projected plate (shell), i.e., when

$$m^0 \frac{du_0}{dt} = p_0 r_0^0 \quad (1.9)$$

where the index zero below designates parameters of gas on its edge, and  $m^0$  — mass of shell. Putting solution in form (1.3) in boundary condition (1.9), we will obtain

$$m^0 \left( \frac{dP}{dm} \right)_0 = P_0 \quad \left( P_0 = \frac{P_0}{r_0^0} \right) \quad (1.10)$$

Here and below by  $u^0$  was understood speed of gas on boundary ( $u_0 = u^0, U_0 = 1$ ), by  $r^0$  — radius of boundary ( $r^0 = r_0, R_0 = 1$ ), and by  $p^0$  — pressure in center of gas. From (1.10) it follows that with increase of mass of shell pressure drop decreases.

For  $\nu \neq 1$  sometimes it is natural to introduce such "elastic" shell, for instance, if heated gas is surrounded by cold unheated gas. Introduction of such thin shell ( $m^0 \ll M$ ) is convenient also for removal of infinite speeds of gas appearing in certain cases (for instance, when  $\alpha = 0, \beta = 0$ , when  $PV = 1$ ; it is natural that the appearing peculiarity will be integrable). Such a method can be applied also during calculations on [ETsVM] (ЭТМВМ) of nonself-modeling problems.

Below will be considered the case of dispersion in vacuum under the following boundary conditions:

$$\begin{aligned} P &= 0, & U &= 1, & R &= 1, & m\zeta(v) &= M \\ P &= 1, & V &= 1, & R &= 0, & U &= 0, & m &= 0 \end{aligned} \quad (1.11)$$

§ 2. Let us consider the case when an arbitrary function characterizing distribution of intensity of energy release with respect to particles of gas is constant:  $f = 1$ . Let us divide equation (1.5) by (1.6) and (1.7)

$$\frac{du^0 r^0 u^0}{dr^0 p v^0} = -\frac{U R}{U^2} \frac{dP}{dR} = C \quad (2.1)$$

Here  $C$  — constant of liberation. When  $C > 0$  pressure  $P$  drops with respect to radius  $R$ , and speed of gas  $u^0$  is increased with increase of dimensions of region  $r^0$ . From boundary conditions (1.11) and right sides of equations (1.4) and (1.6) it follows that speed is linearly distributed along radius, but density is connected with pressure by polytropic law

$$U = R, \quad PV^\gamma = 1 \quad (2.2)$$

Equation (2.1) under conditions (2.2) and (1.11) is integrated

$$P = (1 - R^2)^{\gamma/(\gamma-1)}, \quad PV = 1 - R^2, \quad C = \frac{2\gamma}{\gamma-1} \quad (2.3)$$

Kinetic energy of gas  $E_K$ , thermal energy  $E_T$  and total mass  $M$  are determined by expressions

$$\begin{aligned} E_K &= \frac{1}{2} \zeta(v) \rho^0 (u^0)^2 (r^0)^\gamma J_K \\ E_T &= \frac{1}{2} \zeta(v) p^0 (r^0)^\gamma J_T / (\gamma - 1) \\ M &= \zeta(v) \rho^0 (r^0)^\gamma J_M \end{aligned} \quad (2.4)$$

where for distribution of parameters (2.2) and (2.3) dimensionless integrals  $J_K$ ,  $J_T$  and  $J_M$  have form

$$\begin{aligned} J_K &= \int_0^1 R^2 (1 - R^2)^{\gamma/(\gamma-1)} R^{\gamma-1} dR \\ J_T &= \int_0^1 (1 - R^2)^{\gamma/(\gamma-1)} R^{\gamma-1} dR \\ J_M &= \int_0^1 (1 - R^2)^{\gamma/(\gamma-1)} R^{\gamma-1} dR \end{aligned} \quad (2.5)$$

Integrating all liberated energy, we will obtain

$$\frac{d(E_T + E_K)}{dt} = J_Q M Q_* \left(\frac{e^0}{e_*}\right)^{-\kappa} \left(\frac{v^0}{v_*}\right)^{-\beta} \varphi\left(\frac{t}{\tau}\right) \quad (2.6)$$

where  $J_Q$  turns out to equal  $J_T$ .

Expressions (2.5) can be calculated through gamma-function

$$J_M = \frac{\Gamma\left(\frac{\nu}{2}\right)\Gamma\left(\frac{\nu}{2-1}\right)}{2\Gamma\left(\frac{\nu}{2} + \frac{\nu}{2-1}\right)}, \quad J_K = \frac{\Gamma\left(\frac{\nu}{2} + 1\right)\Gamma\left(\frac{\nu}{2-1}\right)}{2\Gamma\left(\frac{\nu}{2} + \frac{\nu}{2-1} + 1\right)} \quad (2.7)$$

Maximum speed of edge of gas  $u^0$  and internal energy in center  $e^0$  are determined with respect to kinetic and thermal energy and total mass of gas

$$(u^0)^2 = \frac{2E_K J_M}{M J_K}, \quad e^0 = \frac{p^0 v^0}{(\kappa - 1)} = \frac{E_T J_M}{M J_T} \quad (2.8)$$

According to the general property of the gamma-function  $\Gamma(x+1) = x\Gamma(x)$ , and therefore

$$\frac{J_M}{J_K} = \frac{(\nu+2)\Gamma-\nu}{\nu(\Gamma-1)}, \quad \frac{J_T}{J_K} = \frac{2\Gamma}{\nu(\Gamma-1)} \quad (2.9)$$

Usual assumptions on possibility of introduction of average (constant) temperature and density of gas for estimate of parameters of gas in regular conditions lead to  $J_M = J_T = 1/\nu$ ,  $J_K = 1/(\nu+2)$ .

According to (2.9), the values  $J_M/J_K$  and  $J_T/J_K$  when  $\nu = 1/2$  equal accordingly  $10/3$  and  $7/10$ , instead of the estimated values  $5/3$  and  $1$ . We show that the obtained expressions can be used also for determination of magnitudes during adiabatic dispersion [1] with constant entropy of all particles, where in this case  $\nu = \kappa$ .

Let us note that in the case of cylindrical symmetry, when  $\nu = 2$ , we will obtain especially simple expressions

$$J_M = \frac{\Gamma-1}{2\Gamma}, \quad J_K = \frac{(\Gamma-1)^2}{2\Gamma(2\Gamma-1)}, \quad J_T = \frac{\Gamma-1}{2(2\Gamma-1)}$$

§ 3. Let us consider a variation of parameters in time. System of equations (1.4)-(1.7) taking into account results of § 1 will take the form

$$\begin{aligned} \frac{du}{dt} &= \frac{pv}{r}, \quad \frac{dr}{dt} = u, \quad r' = v \\ \frac{d\theta}{dt} &= \theta^{-\alpha} v^{-\beta} - (\kappa - 1) \frac{vu\theta}{r}, \quad \theta = pv \end{aligned} \quad (3.1)$$

Here as characteristic parameter  $\rho_* = v_*^{-1}$  is selected initial density in center,  $r_*$  - corresponding radius,  $p_*, v_*$ , corresponds to assigned characteristic temperature;  $Q_*, u_*, t_*$  are from relationships

$$u_* t_* = r_*, \quad 2\gamma u_*^2 = p_* v_* (\gamma - 1), \quad Q_* t_* (\kappa - 1) = p_* v_* \quad (3.2)$$

All magnitudes with index 0 and time  $t$  belong to corresponding measured parameters with index  $*$ , and for convenience in equations (3.1) all indices are omitted.

We will consider heating of initially cold and motionless gas. Initial values of system of equations have the form

$$u = 0, \quad \theta = 0, \quad v = 1, \quad r = 1 \quad (3.3)$$

At first heating and acceleration of gas occur for a small changing radius ( $r \approx 1$ ) and almost constant density ( $v \approx 1$ ). In this case dimensionless temperature and speed of gas grow by power law

$$\theta = [t(1 + \alpha)]^{1/(1+\alpha)}, \quad u = \frac{1}{2+\alpha} [t(1 + \alpha)]^{(2+\alpha)/(1+\alpha)} \quad (3.4)$$

It is clear that for times  $t$  of the order of unity motion of gas is impossible to disregard. Let us consider heating of gas when times are great taking into account motion of gas. System (3.1) has exponential solution

$$r = At^s, \quad \frac{dr}{dt} = u = sAt^{s-1}, \quad v' = r' = A^s t^{s-1}, \quad \theta = Bt^n \quad (3.5)$$

Indices of degree  $s$  and  $n$  and constants  $A$  and  $B$  are connected. From system (3.1) it follows that

$$B^{1+\alpha} [n + (\kappa - 1)s\beta] = A^{-\nu\beta}, \quad (\alpha + 1)n = 1 - s\beta \quad (3.6)$$

$$2s = n + 2, \quad s(s - 1)A^2 = B \quad (3.7)$$

Combination of these two conditions determines law of change of temperature

$$n(1 + \alpha + \frac{1}{2}\nu\beta) = 1 - \nu\beta \quad (3.8)$$

It is easy to see that temperature is increased only when  $\beta\nu < 1$  does not occur, for instance, in the above-mentioned case of preheating of plasma by luminous emittance of constant frequency. If according to (3.7) and (3.8), we will obtain  $s < 1$ , i.e., speed decreases, which is impossible, then in such case during determination of behavior of magnitudes for large times  $t$  one should set  $s = 1$ , since kinetic energy approaches a constant magnitude and is essentially larger than thermal energy (full liberated energy is limited). Inasmuch as proportionality of kinetic and thermal energy (the second of conditions (3.7)) does not occur, velocity (constant  $A$ ) can be determined only by means of numerical calculations of initial stage of heating. System of equations (3.1) is easily brought to system of two equations

$$\frac{dr}{du} = \frac{ur}{\theta}, \quad \frac{d\theta}{du} = \theta^{-(\alpha+1)} r^{1-\nu} - (\kappa - 1) \nu u \quad (3.9)$$

When  $\beta = 1$  for  $\nu = 1$  (when, according to (3.7), there should be  $n = 0$ ,  $\theta \rightarrow \text{const}$ ) both equations of (3.9) are integrated independently, and for large values the behavior of the solution is found from conditions of quasi-isothermality, i.e., by means of equating the right side of (3.9) to zero

$$\begin{aligned} \theta^{-(\alpha+1)} &= (\kappa - 1) \nu u \\ \frac{d\theta}{du} &= -\frac{\theta}{(1 + \alpha) u} \\ (u \rightarrow \infty, \theta \rightarrow 0) \end{aligned} \quad (3.10)$$

On Fig. 1 are shown dependences of  $\theta$ ,  $r$ ,  $u$  and  $p$  on  $t$  for three cases  $\nu = 1, 2, 3$  when  $\beta = 1$ ,  $\alpha = 3/2$  and  $\kappa = 5/3$  for initial data (3.3), obtained by means of numerical calculations of system (3.1), (3.2). Dimensionless temperature  $\theta$  has maximum equal to 1.20, 1.04 and 0.967 in moments of  $t$  equal to 1.13, 0.724 and 0.587 correspondingly when  $\nu = 1, 2$  and 3, when prior to moment  $t = 20$  values of  $u$  equal 2.75, 1.92 and 1.49, values of  $r$  equal 46.5, 34.7 and 28.2, and values of  $\theta$  of 0.813, 0.194 and 0.055. Presence of maximum of temperature distinguishes the results of this work from those of [3].



coefficient  $\lambda$  does not depend on  $\gamma$  and equals  $\sqrt{\nu/(\nu+2)}$ , and  $\eta$  weakly depends on  $\gamma$  and in general, on character of distribution of density. When  $\gamma$  changes from  $15/13$  to  $\gamma = \infty$ , which corresponds to the uniform distribution of density,  $\eta$  changes at  $\nu = 3$  from  $0.934$  to  $0.968$ , where for  $\gamma = 7/5$  it equals  $0.945$ , and with a shell-like distribution of density  $\eta = 1$ . Maximum  $\rho u^2$  is rather sharp which one may easily see from formula describing its change in time, if all energy passed into kinetic and  $u^0 \rightarrow u_\infty^0$

$$\frac{\rho u^2}{2} = \frac{E}{\zeta(\nu) r^\nu J_k} \left(1 - \frac{r^2}{u_\infty^2 t^2}\right)^{1/(\nu-1)} \left(\frac{r}{u_\infty t}\right)^{2+\nu}$$

The quantity  $u_\infty$  is determined with respect to  $E$  and  $M$  from relationships (2.7), (2.8). Another method of measurement of  $\overline{TEM}$  can be measurement of mechanical recoil impulse, appearing as a result of diffusion. It is necessary, however, to consider that when the heated diffusing gas does not abut directly with the hard wall where "measurement" of pressure is made, the measured magnitude of mechanical impulse can be larger than if there was not a layer of cold gas. However effects of "brief impact" [11] decrease with increase of duration of preheating. In the limiting case very "slow" preheating the cold gas is almost motionless, and additional energy is not introduced in it, consequently, increase of impulse is negligible.

§ 4. Motion of gas decreases its temperature, therefore for problems where magnitude of temperature attained as a result of preheating is essential, one should consider initial stage of heating of gas.

We will consider a problem about heating in the flat case of a motionless gas of constant density  $\rho_0$  by radiation. Equations of energy and law of heat emission have the form

$$\frac{\partial e}{\partial t} + \frac{\partial q}{\partial m} = 0, \quad \frac{\partial q}{\partial m} = -\frac{k}{\rho} q, \quad k = k_0 \left(\frac{e}{e_0}\right)^{-\alpha} \left(\frac{r_0}{r}\right)^{-\beta} = k_1 \left(\frac{e}{e_0}\right)^{-\alpha}$$

$$e(\kappa - 1) = p v_0, \quad \rho_0 x = m$$

Here  $q$  — flow of radiant energy, equal to given  $q_0$  on edge of substance (at point  $m = 0$ ).

If change of coefficient of absorption from parameters has exponential form, then as was shown in [12], region of initially cold ( $e = 0$ ) gas heated by unbalanced radiation is limited, in distinction from  $k = \text{const}$ , and distribution of parameters

in the "tongue of heating" carries the same character as in "thermal waves" [11] appearing during heating of a substance in conditions of radiant (nonlinear) thermal conduction. Solution of this self-modeling problem has form [12]

$$e = e_0 \left(1 - \frac{\xi \alpha}{1 + \alpha}\right)^{1/\alpha} \left(\frac{t}{t_0}\right)^{1/(\alpha+1)}, \quad q = q_0 \left(1 - \frac{\xi \alpha}{1 + \alpha}\right)^{1/\alpha}, \quad \xi = k_0 \left(\frac{t}{t_0}\right)^{\alpha/(\alpha+1)}$$

$$t_0 k_0 q_0 = e_0 \rho_0,$$

Thus, distribution of temperature near point  $m = 0$  carries the character of a plateau.

Increase of temperature and increase of pressure of gas proportional to it (during constant density of substance  $\rho_0$ ) lead to dispersion of gas in the direction of vacuum. Considering temperature in region of motionless gas as variable only in time, we will find that boundary of wave of rarefaction moves by the power law. For generality we will consider that intensity of source also changes by the power law. In this case equations of energy can be written in the form

$$\frac{\partial e}{\partial t} + p \frac{\partial v}{\partial t} = G t^b (pv)^{-\alpha} v^{-\beta} \quad (4.1)$$

where  $G$  — evident combination of measured parameters.

It is interesting to note that in regular conditions of dispersion with preheating, by such law temperature can increase if one selects sufficiently large quantity  $b$ , since instead of relationship (3.8) there will occur

$$n(1 + \alpha + 1/2 v \beta) = 1 - v \beta + b, \quad s = 1 + 1/2 n$$

In region of motionless gas  $v = v_0$ , therefore in this region

$$p^* = P t^{\frac{1+b}{1+\alpha}}, \quad v^* = v_0, \quad (a^*)^3 = \kappa p^* V^*$$

$$x^* = \int_0^t a^* dt = \sqrt{\kappa P v_0} \frac{2(1+\alpha)}{3+b+2\alpha} t^{\frac{2+b+2\alpha}{2(1+\alpha)}}$$

$$P^{1+\alpha} (1+b) = (1+\alpha) G v_0^{-(\beta+1+\alpha)} (\kappa - 1) \quad (4.2)$$

Such a problem is self-simulating [2]. Let us introduce new variables

$$p = p^* p^x, \quad u = a^* u^x, \quad v = v^* v^x, \quad x^* \mu = m v_0, \quad x = x^* x^x \quad (4.3)$$

System of equations (4.1) and (1.2) (when  $\nu = 1$ ) can be brought to a system of ordinary differential equations for  $p^x, u^x, v^x$  from  $\mu$  (indices above magnitudes subsequently will be omitted)

$$\mu \frac{d[\ln(pv^x)]}{d\mu} = -2C(p^{-(\alpha+1)}v^{-(\beta+\alpha+1)} - 1) \quad (4.4)$$

$$Cx - \mu \frac{du}{d\mu} + \frac{1}{x} \frac{dp}{d\mu} = 0, \quad \mu \frac{dv}{d\mu} + \frac{du}{d\mu} = 0$$

$$x - \mu v = u, \quad C(3 + \delta + 2\alpha) = 1 + \delta \quad (4.5)$$

$C = 0$  corresponds to the usual wave of rarefaction with respect to instantly heated gas. Boundary conditions of system (4.4) have the form

$$\mu = 1, \quad p = 1, \quad v = 1, \quad u = 0, \quad x = 1; \quad \mu = 0, \quad p = 0 \quad (4.6)$$

When  $\beta + \alpha + 1 = x(\alpha + 1)$ , i.e.,  $\gamma = \kappa$ , equation of energy of system (4.4) has exact solution  $pv^x = 1$ , however distribution of parameters with respect to  $\mu$  does not coincide with the case of an adiabatic wave of rarefaction, running along a region with constant parameters.

It is interesting to note that for  $\alpha = 3/2$  and  $\beta = 1$  when  $\kappa = 7/5$  variation of parameters is "adiabatic" ( $\gamma = \kappa$ ). The case of  $\alpha = 0, \beta = 0$  was considered earlier by the author and independently more specifically in [13]. In this case, as was shown by the author and A. A. Milyutin and independently by L. P. Feoktistov [13], temperature of gas on the edge differs from temperature of gas in motionless region by  $2C/(2C + x - 1)$  times, i.e., when  $\delta = 0$ , that corresponds to  $C = 1/3$  and  $\kappa = 5/3$  in all only 2 times. This accelerates appearance at regular conditions of dispersion, in which temperature of all points is identical.

During polytropic dependence  $pv^x = 1$  equation of impulses and inseparability of system (4.4) (second and third equation) can be by a change of variables brought to one equation not containing

$$v\mu^{2(1+\kappa)} = z, \quad u\mu^{(1-\kappa)(1+\kappa)} = y \quad (4.7)$$

$$\frac{z}{y} \frac{dy}{dz} = \left[ \left( C - \frac{x-1}{x+1} \right) z^{x+1} + \frac{x-1}{x+1} \right] \left[ \frac{2}{x+1} (z^{x+1} - 1) - C y z^x \right]^{-1}$$

Point  $y = 0, z = 1$ , corresponding to boundary of wave of rarefaction, where  $u = 0, \mu = 1, v = 1$ , is singular point of equation (4.7). Nearby its behavior of

integral curves is described by equation

$$Ky^{2C} = Cy + (C - 2)(z - 1) \quad (4.8)$$

where  $K$  - arbitrary coefficient. Slope of the general tangent to these curves entering node equal  $(-1 + 2/C)$ , is less than slope  $2/C$  of line of infinite derivatives, equation of which has the form

$$C(x + 1)yz^x = 2(z^{x+1} - 1) \quad (4.9)$$

On boundary of dispersion gas with vacuum  $\mu = 0$ , and speed is either bounded or infinite, therefore  $y \rightarrow -\infty$  (speed  $u < 0$ ). Consequently, near  $z = 1$   $|y|$  is increased, and  $z$  decreases. If  $y(z)$  intersects the line where  $y' = \infty$ , then integral curve gets in region  $y' = 0$ , i.e.,  $z$  starts to increase, and when  $y' \rightarrow -\infty$  there occurs  $z \rightarrow \infty$ . The second of equations (4.5) can be converted to the form

$$Cu - \mu \frac{du}{dz} [1 - z^{-(x+1)}] = 0 \quad (4.10)$$

It is easy to see that when  $z \rightarrow \infty$  there occurs  $u \sim \mu^C$ , and since when  $-1 < \alpha < \infty$  magnitude  $C$  lies in range  $0 < C < 1$ , then  $u \rightarrow 0$  for  $\mu \rightarrow 0$ , which is impossible. Consequently,  $z \rightarrow 0$ , where from the condition of nonintersection of line (4.9) we will obtain

$$C(-y)z^x < \frac{2}{(x-1)}$$

Behavior of solution of equation (4.7) when  $z \rightarrow 0$  can be found from the equation

$$\frac{z}{y} \frac{dy}{dz} = - \frac{(z-1)}{2 + (x+1)Cyz^x} \quad (4.11)$$

If  $yz^x \rightarrow 0$ , then  $(-y) \sim z^{-1/(x-1)}$  and, consequently,

$$(-u) \sim \nu^{-1/(x-1)}, \quad \text{or} \quad (-u) \sim \mu^{(x-1)/(x+1)}$$

what also is impossible. Therefore solution (4.7) has the form  $xCyz^x \rightarrow -1$  when  $z \rightarrow 0$ , and distribution of parameters on edge of wave of rarefaction is determined accurate to one constant  $D$  by expressions

$$u = -D + (CDx\mu)^{1/\alpha}(x-1)^{-1/\alpha}, \quad v^* = CDx\mu^{-(\alpha+1)} \quad (4.12)$$

Thus, speed of gas on edge turns out to be finite in distinction  $pv = \text{const}$ , when  $(-u) \sim (-\ln \mu)^{1/\alpha}$ . Speed of gas is proportional to the root of the liberated energy, therefore investigation of wave of rarefaction permits judging attained temperature.

Width of "tongue" of temperature increases according to the law  $x \sim t^{1/\alpha}$  when  $\alpha = 3/2$  and constant flow of heat ( $\delta = 0$ ). Boundary of wave of rarefaction in the beginning will lag behind "edge" of tongue  $-x \sim t^{1/\alpha}$ . If for  $t = t_*$  these magnitudes are of one order, then  $\sqrt{x p \cdot v \cdot t} \approx 1/k$ . Using (4.7), we will find that prior to the moment when hydrodynamic motion seizes region of the order of width of heated zone  $(\sqrt{x p \cdot v \cdot t})_{p, v} \approx q_0$  that determines necessary power  $q_0$  to achieve  $e_*$ . In accordance with estimate [3], for  $e_* = 1.5 \cdot 10^{15}$  erg/g there is required  $q_0 \approx 10^{14}$  joule/cm<sup>2</sup> sec for  $\rho_0 \approx 10^{-2}$  g/cm<sup>3</sup>.

Let us indicate that inasmuch as when  $\delta \neq 0$  edge of the tongue grows according to [12] by the power law with index  $\alpha(1 + \delta)/(1 + \alpha)$  when  $\delta = 3/(2\alpha - 1)$  the problem about heating and motion of gas connected with it is self-simulating (for  $\alpha = 3/2$  and  $\delta = 3/2$  the exponent for growth of edge of tongue is  $3/2$ ).

§ 5. Limitations put on applicability of obtained solutions due to disturbance of one-dimensional character of motion can be demonstrated in the following way.

Let us consider dispersion of a flat layer or cylinder of limited height, and let us assume that in the initial moment when parameters are distributed in "self-simulating" form, motion in lateral direction is absent. Temperature and speed of sound are maximum on line of symmetry (when  $\alpha = \beta = 0$  in regular conditions temperature of all points is identical). In the region where wave of rarefaction from ends still does not penetrate, and subsequently, the parameters are changed just as in the one-dimensional case. Let us assume that exponential conditions of change of temperature (and speed of sound) were established

$$T = T_m \left( \frac{t}{t_m} \right)^n, \quad a = \sqrt{x p v} = a_m \left( \frac{t}{t_m} \right)^{n/2} \quad (5.1)$$

Here  $t_m$  — characteristic time of change of temperature. When  $n > 0$  the quantity  $t_m$  is equal to characteristic time of action of source, and  $T_m$  — temperature toward the end of preheating. For  $n < 0$  the quantity  $t_m$  is equal to the order of

time when maximum temperature  $T_m$  is attained. During adiabatic dispersion without preheating  $t_m$  - characteristic time of dispersion of order  $r_0/a_m$  and  $a_m t_m = r_0$ , where  $r_0$  - initial dimension in "basic" direction a path  $x$  passed by wave of rarefaction is determined by the expression

$$x = \frac{a_m t_m}{(1 + 1/2n)} \left[ \left( \frac{t}{t_m} \right)^{1+1/2n} - 1 \right] \quad (5.2)$$

If  $n < -2$ , the path passed by the wave of rarefaction is bounded and for  $L(1 + 1/2n) > a_m t_m$  always the central part of the gas will scatter in one-dimensional form. This occurs, for instance, during adiabatic dispersion, when  $n = -v(x-1)$ , for  $x > 2$ , if height of cylinder ( $v = 2$ ) is somewhat larger than its initial radius. However, if  $n > -2$  (for  $v = 2$ ,  $\alpha = 3/2$  and  $\alpha = 1$  index  $n = -2/7$ ), then dispersion can become two-dimensional also after achievement of maximum. For  $n = 1$ , according to [2], change of internal energy of particles of flat layer is

$$e = \frac{E}{M} \frac{1}{\tau} \frac{2}{(3x-1)}, \quad a = \sqrt{x(x-1)} e \quad (5.3)$$

The moment when wave of rarefaction meets center  $t^*$  for a layer  $2L$  long is found from the expression

$$\frac{2}{3} a^* t^* = \frac{2}{3} t^* \left( \frac{E}{M} \frac{2x}{(3x-1)} \frac{t^*}{\tau} \right)^{1/2} = L \quad (5.4)$$

Consequently, during sufficiently prolonged or intense preheating dispersion will become two-dimensional (when thickness of dispersion layer becomes of the order of its initial height). At  $t^*$  pressure in center is

$$p^* = \frac{3^{1/2}(x-1)^{1/2}x^{1/2}}{(3x-1)^{1/2}\pi^{1/2}r_0^{1/2}} \left( \frac{E}{\tau} \right)^{1/2} \left( \frac{M}{L} \right)^{1/2} \quad (5.5)$$

Two-dimensional character of dispersion leads to increase of transparency of layer of mass  $M$  and advance of "wave of preheating" in depth of substance.

§ 6. The question about establishments of regular conditions can be solved only by means of numerical calculations of the problem with arbitrary "nonself-simulating" initial data. Such calculations for uniform preheating of initially cold gas of constant density  $\rho_0$  for intensity of feed, not depending either on

thermodynamic parameters or on time, were conducted at our request by A. S. Fonarev, and also A. A. Milyutin and V. L. Bodnevoy. Figure 2 shows change of pressure on a boundary with a hard wall. Pressure is referred to

$$p^{**} = \left( \frac{3E^2}{\tau^2} \frac{(x-1)^2}{(3x-1)^2} \right)^{1/2}$$

and time to

$$t^{**} = \frac{M}{2} \left( \frac{3\tau(3x-1)}{\rho_0^2 E(x-1)} \right)^{1/2}$$

Curve 1 - numerical calculation on ETsVM, curve 2 - self-simulating solution of problem about dispersion with preheating [1], curve 3 - exponential limiting law of pressure drop in regular conditions. As is easy to see, solution for "unself-simulating" initial data "emerges" on regular conditions.

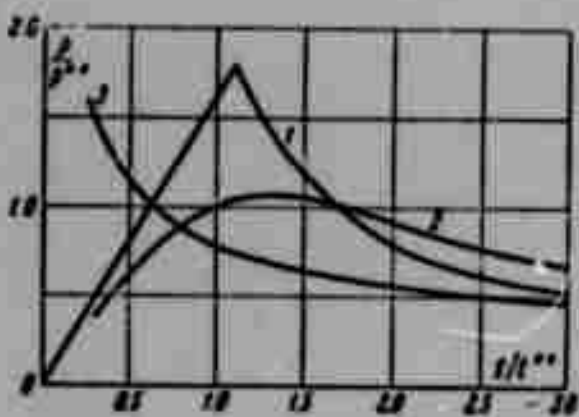


Fig. 2.

Indeed, maximum pressure at the time of approach of wave of rarefaction to a hard wall limiting gas when  $x = 7/5$ , is equal to  $1.73 p^{**}$ , whereas by self-simulating solution  $p = 1.36 p^{**}$  (moments of maximum correspondingly are  $t = 1.10 t^{**}$  and  $t = 1.30 t^{**}$ ), and already prior to moment  $t = 0.93 t^{**}$ , according to numerical calculation,  $p = 0.320 p^{**}$ , but by self-simulating solution  $p = 0.396 p^{**}$  (coincidence with limiting power law  $p = (2/\pi)^{1/2} p^{**} (t^{**}/t)^{1/2}$  is

still better:  $p = 0.312 p^{**}$ ; prior to moment  $t = 9.45 t^{**}$  by numerical calculation and by limiting law pressure  $p = 0.260 p^{**}$ , i.e., regular conditions of dispersion will be asymptotic.

I gratefully thank A. A. Milyutin and Yu. P. Rayzer for valuable discussions, V. L. Bodneva, A. N. Zimina and A. S. Fonarev for the conducted calculations.

Remark during proofreading. The author had the use of the known work of Dawson [14], in which are repeated rough estimates [3] of calculation of expansion of plasma during its heating. It is noted that with approach of transparency magnitude of energy release is impossible to consider constant and motion of substance should lead to cooling of plasma. In formulas of the work of Dawson it is not considered that after maximum of temperature in substance energy continues to

develop. However this, apparently, is considered in numerical calculations whose results are represented on graphs. Although methods of calculations are not set forth, apparently, they are in accordance with the self-simulating solution used in this work.

Submitted  
29 May 1964

#### Literature

1. L. I. Sedov. Methods of similarity and dimension in mechanics. Publication 3. State Technical Press, 1954, pp. 242-248.
2. I. V. Nemchinov. Dispersion of a flat layer of gas during gradual energy release. PMTF, 1961, No. 1, pp. 17-26.
3. N. G. Basov and O. N. Krokhin. Conditions of heating of plasma by radiation of optical generator. Jour. experim. and theor. physics, 1964, Vol. 46, No. 1, pp. 171-175.
4. L. D. Landau and Ye. M. Lifshits. Electrodynamics of solid media. State Technical Press, 1957, pp. 314-318, 333-337.
5. V. L. Ginzburg. Propagation of electromagnetic waves in plasma. Fizmatgiz, 1960, pp. 26-29.
6. L. Spittser. Physics of completely ionized gas. Publication of Foreign Literature, 1957.
7. K. P. Stanyukovich. Transient motions of solid medium. State Technical Press, 1954, pp. 646-656.
8. L. A. Artsimovich. Controlled thermonuclear reactions. Fizmatgiz, 1961.
9. D. A. Frank-Kamenetskiy. Physical processes inside stars. Fizmatgiz, 1959, pp. 278-304, 325-337.
10. S. I. Braginskiy. The theory of development of spark channel. Jour. experim. and theor. physics, 1958, Vol 34, No. 6, pp. 1548-1557.
11. Ya. B. Zel'dovich and Yu. P. Rayzer. Physics of shock waves and high-temperature hydrodynamic phenomena. Fizmatgiz, 1963.
12. I. V. Nemchinov. Certain nonsteady state problems of heat transfer by radiation. PMTF, 1960, No. 1, pp. 36-37.
13. V. Ye. Neuvazhayev. Expiration of gas in vacuum when root law of energy release applies. Reports Academy of Sciences of USSR, 1961, Vol. 141, No. 5, pp. 1058-1060.
14. J. M. Dawson. On the production of plasma by giant pulse lasers. The physics of fluids. July 1964, Vol. 7, No. 7, 981-987.

**BLANK PAGE**

NONLINEAR GEOMETRIC ACOUSTICS.  
WEAK SHOCK WAVES

P. F. Koromkov

(Moscow)

In geometric acoustics the position of rays is determined only by the medium. Intensity of wave is from the condition of constancy of energy of wave element during its motion along a beam tube [1, 2].

Propagation of weak shock waves differs from propagation of waves in acoustic approximation because there appear nonlinear effects, which appear in dissipation of energy on front of shock wave and in distortion of beams during change of pressure along front.

In preceding works were considered either only effects of dissipation [3-5], or only effects of additional distortion of rays [5-8]. The last ones were considered only in a uniform medium.

Below are considered simultaneously both these nonlinear effects, affecting propagation of weak shock waves in nonuniform moving medium.

In §§ 1-3 is obtained a closed system of equations of nonlinear geometric acoustics, in § 4 this system is considered when change of speed of sound and speed of medium are small. In § 5 are derived conditions on surface of discontinuity of functions. In §§ 6-8 are obtained certain solutions of the system of equations of nonlinear geometric acoustics.

§ 1. Let us assume that  $f(x_1, t) = 0$  is the equation of the surface of the front of a shock wave in a motionless system of coordinates. Differentiating, we will obtain

$$n_1 dx_1 + \frac{dt}{\sqrt{(\partial f / \partial x_k)^2}} \frac{\partial f}{\partial t} = 0 \quad (1.1)$$

Here  $n_1$  - unit vector of normal to front of shock wave

$$n_i = \frac{\partial f / \partial x_i}{\sqrt{(\partial f / \partial x_k)^2}} \quad (1.2)$$

In (1.1) the quantity  $n_i dx_i$  is displacement of surface in direction of normal during time  $dt$ . This displacement occurs because surface moves with respect to medium with speed  $D$  in the direction of the normal and contacts wind with speed  $w_i$ , i.e., speed of wave element  $V_i$  which is called radial velocity, is

$$V_i = Dn_i + w_i \quad (1.3)$$

Here for vectors and coordinates tensor designations are applied. The quantities  $i, k$  take the values 1, 2, 3. In the direction of the normal the surface is displaced with speed  $V_i n_i$ , so that we will obtain

$$n_i dx_i = (D + n_i w_i) dt \quad (1.4)$$

Putting (1.4) in (1.1), we will obtain the equation for the desired searched surface of the shock wave front

$$\frac{\partial f}{\partial t} + w_i \frac{\partial f}{\partial x_i} + D \sqrt{\left(\frac{\partial f}{\partial x_k}\right)^2} = 0 \quad \left( \begin{array}{l} w_i = w_i(x_k) \\ c = c(x_k) \\ D = D(x_k) \end{array} \right) \quad (1.5)$$

Let us note that speed of shock wave  $D$ , in distinction from the acoustic approach, depends on intensity of wave

$$D = Mc, \quad M = \left(1 + \frac{\gamma+1}{2} \frac{p'}{\rho c^2}\right)^{1/2}, \quad \gamma = \frac{c_p}{c_v} \quad (1.6)$$

Here  $c$  — speed of sound in medium,  $\rho$  — density of medium,  $p'$  — difference between pressure on front of shock wave and pressure before it.

Integration of equation (1.5) leads to integration of a characteristic system of equations, which we will write in the form

$$\begin{aligned} \frac{dx_i}{ds} &= M c n_i + w_i \\ \frac{d}{ds} \left( \frac{\partial f}{\partial x_i} \right) &= - \sqrt{\left(\frac{\partial f}{\partial x_k}\right)^2} \left( M \frac{\partial c}{\partial x_i} + n_k \frac{\partial w_k}{\partial x_i} + c \frac{\partial M}{\partial x_i} \right) \end{aligned} \quad (1.7)$$

From the first equation follows a relationship connecting time derivative along

beam and derivative with respect to coordinates

$$\frac{d}{dt} = (Mcn_i + w_i) \frac{\partial}{\partial x_i} \quad (1.8)$$

The second equation of (1.7) will be converted to more convenient form with the help of (1.2)

$$\begin{aligned} \frac{dn_i}{dt} &= (n_i n_k - \delta_{ik}) \left( M \frac{\partial c}{\partial x_k} + n_i \frac{\partial w_i}{\partial x_k} + c \frac{\partial M}{\partial x_k} \right) \\ \delta_{ik} &= 1 \text{ when } i = k, \quad \delta_{ik} = 0 \text{ when } i \neq k \end{aligned} \quad (1.9)$$

Thus, in the equation which determines direction of beams, as compared to geometric acoustics was added one more term  $c(\partial M / \partial x_k)$ . In acoustic approximation  $M \equiv 1$ , and this term is equal to zero.

Since  $M$  depends on pressure in shock wave, which beforehand is unknown, equation (1.9) is insufficient for determination of direction of beams. Necessary yet is an additional relationship.

§ 2. To produce the missing relationship we will consider short waves and will assume that motion of gas after front of shock wave occurs along beams formed by the front.

In this approximation along every beam tube occurs one-dimensional motion begun by the shock front. For this one-dimensional flow in a channel with variable area it is possible to write the equations of gas dynamics, which have to be solved jointly with equation (1.9), since position and area of every beam tube beforehand are unknown and are determined simultaneously with pressure on front. Thus, interaction of neighboring sections of shock wave occurs in the considered approach only through front of shock wave. Such beam approach can be made for shock waves of any intensity.

Below are considered only weak shock waves  $p' \ll \rho c^2$  with triangular profile of pressure, for which are obtained simpler equations. For such waves the solution can be obtained in evident form, if position of beams is determined only by properties of medium [3-5]

$$\begin{aligned} p' &= \frac{a \sqrt{\rho c}}{L} \left( \int_0^l \frac{dl}{L q q_n \sqrt{\rho c}} \right)^{-1/2}, \quad \lambda = \frac{\gamma + 1}{2} a q_n \left( \int_0^l \frac{dl}{L q q_n \sqrt{\rho c}} \right)^{1/2} \\ L &= \left( 1 + \frac{w_i n_i}{c} \right) \sqrt{S}, \quad q = \sqrt{(cn_i + w_i)^2}, \quad q_n = c + n_i w_i \end{aligned} \quad (2.1)$$

Here  $l$  - distance along beam,  $\lambda$  - length of positive phase of wave along normal to front,  $S$  - area of front of wave included in beam tube,  $a$  and  $l_0$  - constants determined by initial data.

Excluding from these relationships  $a$  and  $l_0$ , we will obtain equation

$$\frac{d}{dt} \left[ \frac{p'^2 S}{\rho c} \left( 1 + \frac{w_1 n_1}{c} \right)^2 \right] = - \frac{\gamma+1}{2} \frac{p'^2 S}{\rho^2 c^2 \lambda} \left( 1 + \frac{w_1 n_1}{c} \right)^2 \quad (2.2)$$

$$\frac{d\lambda}{dt} = \frac{\lambda}{c + w_1 n_1} \frac{d}{dt} (c + w_1 n_1) + \frac{\gamma+1}{4} \frac{p'}{\rho c} \quad (2.3)$$

We will apply these equations to weak shock wave propagating along beams determined by equation (1.9). Thus, we will consider that in the initial moment a wave has triangular profile of pressure. Equations (2.1)-(2.3) show that in the considered approach profile remains triangular and for the whole time of motion along beam.

Let us note that the triangular profile is considered as initial profile not by random choice. The fact is that when position of beams does not depend on intensity of wave, profile of pressure of weak shock waves at large distance from source tends to triangular, independently of initial distribution of pressure [9-10]. In particular, weak shock waves caused by explosion have triangular profile of positive phase ( $p' > 0$ ).

Equation (2.2) has a simple physical meaning [11]. In the acoustic approach in its right side stands zero, so that along the beam is kept the magnitude standing in left part, which is proportional to energy of wave element. In nonlinear geometric acoustics energy of wave decreases due to dissipation on the front, but influence of this dissipation on magnitude of pressure depends on wavelength: the longer, the less this influence.

Equation (2.3) describes change of length of shock wave.

§ 3. In the considered case, when beams are distorted due to change of pressure along front of shock wave, magnitude of area of beam tube  $S$  is unknown and should be determined with the help of equation (1.9). For this we will find the connection between  $S$  and  $n_1$ .

Let us apply the formula of Ostrogradskiy-Gauss to vector  $V_1/Mc$  and volume inside beam tube

$$\iiint_V \frac{\partial}{\partial x_i} \frac{V_i}{Mc} d\tau = \iint_{\Sigma} \frac{V_i ds_i}{Mc} \quad (3.1)$$

Here  $T, \Sigma$  - volume and surface of beam tube,  $d\tau$  and  $do_k$  - small elements of volume and surface. Let us consider small segment of beam tube  $dl$  in length and area of normal section  $\sigma$ . Since  $T = \sigma dl$  and  $dl = V|dt$ , from (3.1) we will obtain

$$\frac{\partial}{\partial x_i} \frac{V_i}{Mc} = \frac{1}{\sigma|V|} \frac{d}{dt} \frac{\sigma|V|}{Mc} \quad (3.2)$$

Using relationship  $\sigma|V| = SV_1 n_1$ , we will obtain

$$\frac{1}{S} \frac{dS}{dt} = Mc \frac{\partial}{\partial x_i} \left( n_i + \frac{w_i}{Mc} \right) - \frac{Mc}{Mc + w_i n_i} \frac{d}{dt} \frac{w_i n_i}{Mc} \quad (3.3)$$

The quantities  $p'$  and  $M$  are connected by relationship (1.6) which for weak shock waves is written in the form

$$p' = \frac{4}{\gamma + 1} \rho c^2 m, \quad m = M - 1, \quad m \ll 1 \quad (3.4)$$

Let us change variables according to these formulas in equations (1.8), (1.9), (2.2), (2.3), and (3.3) and consider that  $m$  is small as compared to unity. After such transformations we will obtain the system of equations of nonlinear geometric acoustics in final form

$$\begin{aligned} \left( n_k + \frac{w_k}{c} \right) \frac{\partial n_i}{\partial x_k} - (n_i n_k - \delta_{ik}) \frac{\partial m}{\partial x_k} = \\ = (n_i n_k - \delta_{ik}) \left( \frac{1}{c} \frac{\partial c}{\partial x_k} + \frac{n_i}{c} \frac{\partial w_i}{\partial x_k} \right) \quad (n_i^2 = 1) \end{aligned} \quad (3.5)$$

$$\begin{aligned} 2 \left( n_k + \frac{w_k}{c} \right) \frac{\partial m}{\partial x_k} + m \frac{\partial}{\partial x_k} \left( n_k + \frac{w_k}{c} \right) = \\ = -m \left( n_k + \frac{w_k}{c} \right) \left[ \frac{1}{\rho} \frac{\partial \rho}{\partial x_k} + \frac{3}{c} \frac{\partial c}{\partial x_k} + \frac{c}{c + w_i n_i} \frac{\partial}{\partial x_k} \left( \frac{w_i n_i}{c} \right) \right] - \frac{2m^2}{\lambda} \end{aligned} \quad (3.6)$$

$$\left( n_k + \frac{w_k}{c} \right) \frac{\partial \lambda}{\partial x_k} = \frac{c n_k + w_k}{c + w_i n_i} \frac{\lambda}{c} \frac{\partial}{\partial x_k} (c + w_i n_i) + m \quad (3.7)$$

Here  $n_i, m$  and  $\lambda$  - unknown magnitudes, and  $c, w_k, \rho$  - functions of coordinates and have to be assigned; they determine the state of the undisturbed medium.

Thus, in nonlinear geometric acoustics the equation for determination of direction of beams (2.5) turned out to be connected with equations for determination of intensity of wave (3.6), (3.7). This connection exists due to the presence of a second term in the left part of equation (3.5). When gradients of pressure are small

as compared to gradients of speed of sound and speed of wind, this term may be disregarded, then equation of beams (3.5) ceases to depend on equations (3.6), (3.7) and it may be integrated separately. In turn, equations (3.6), (3.7) in this case are integrated and obtain form (2.1).

§ 4. Speed of sound in atmosphere is changed insignificantly up to a height of approximately 100 km, so that it is possible to take

$$c = c_0 + c'(x_i), \quad c_0 = \text{const}, \quad c' \ll c_0 \quad (4.1)$$

Speed of wind usually is small as compared to speed of sound, and therefore it is possible to take also

$$w_h(x_i) \ll c_0 \quad (4.2)$$

Under conditions (4.1), (4.2) system (3.5)-(3.7)

$$\begin{aligned} n_k \frac{\partial n_i}{\partial x_k} - (n_i n_k - \delta_{ik}) \frac{\partial m}{\partial x_k} &= (n_i n_k - \delta_{ik}) \left( \frac{1}{c_0} \frac{\partial c}{\partial x_k} + \frac{n_i}{c_0} \frac{\partial w_i}{\partial x_k} \right) \\ 2n_k \frac{\partial m}{\partial x_k} + m \frac{\partial n_k}{\partial x_k} &= -\frac{n_k}{\rho} \frac{\partial \rho}{\partial x_k} m - \frac{2m^2}{\lambda}, \quad n_k \frac{\partial \lambda}{\partial x_k} = m \end{aligned} \quad (4.3)$$

Now we will consider cases when initial data possess cylindrical symmetry, and speed of sound, speed of wind, and air density depend only on one coordinate  $z$ , directed along axis of symmetry.

In the presence of wind initial symmetry of shock wave will not be kept during motion of wave, since beams are bent not only in the direction to plane  $z = 0$  (which, let us assume, corresponds to surface of earth), but also to the side. However, as follows from analysis of equations (4.3), these deflections to the side almost do not affect changes of pressure in wave (these changes are of the second order of smallness as compared to changes of pressure due to distortion of beam in the direction to the earth). This occurs because neighboring beams also deviate to the side approximately in the same magnitude, therefore changes of area of beam tubes with such deflection are small. Consequently, change of pressure is small. The principal value is in distortion of beam in the direction to the earth. Beam proceeding along the earth cannot deviate. Therefore here occurs strong change of relative position of beams and strong change of pressure. Thus, in equations it is possible to consider only that value of projection of wind speed which leads to

curving of beams to the earth (or from the earth). The equation determining beam deflection to the side, i.e., the equation for  $n_\varphi$  will not be considered, since it does not affect pressure in wave.

Let us write equation (4.3) in cylindrical coordinates and consider the remarks which were made. We will consider only beams near plane  $z = 0$ , so that  $n_r \simeq 1$ ,  $n_z \simeq \alpha$  and  $\alpha^2 \ll 1$ .

The system of equations of nonlinear geometric acoustics for stratified atmosphere with small changes of speed of sound and speed of wind for beams propagating along the earth has the form

$$\begin{aligned} \frac{\partial m}{\partial z} + \frac{\partial \alpha}{\partial r} + \alpha \frac{\partial \alpha}{\partial z} &= -\omega, & \omega(z) &= \frac{1}{c_0} \frac{dc}{dz} + \frac{1}{c_0} \frac{dw}{dz} \cos \varphi \\ 2 \frac{\partial m}{\partial r} + 2\alpha \frac{\partial m}{\partial z} + m \frac{\partial \alpha}{\partial z} &= -m \frac{v}{r} - m\alpha\delta - \frac{2m^2}{\lambda}, & \delta(z) &= \frac{1}{\rho} \frac{d\rho}{dz} \\ \frac{\partial \lambda}{\partial r} + \alpha \frac{\partial \lambda}{\partial z} &= m \end{aligned}$$

Here  $\varphi$  — angle between direction on considered point from origin of coordinates and velocity vector of wind,  $\omega$  — total gradient of speed of sound and speed of wind,  $v = 1$ , if initial data possess cylindrical symmetry with the  $z$  axis as axis of symmetry, and  $v = 0$  for two-dimensional problem.

Let us note that substitution  $\xi = mr^{-1/2}$  may be freed from free term  $\sim 1/r$ , which appears in equation (4.5) when  $v = 1$ . But equations (4.4) and (4.6) are changed here. Therefore such a substitution is not considered.

System of equations (4.4)-(4.6) will be hyperbolic. Directions of characteristics of this system such

$$dz/dr = \alpha \pm \sqrt{1/2m}, \quad dz/dr = \alpha \quad (4.7)$$

Along the first pair of characteristics there are executed correspondingly the relationships

$$d\alpha \pm \sqrt{2/m} dm = -\omega dr \mp \sqrt{1/2m} (v/r + \alpha\delta + 2m/\lambda) dr \quad (4.8)$$

Along the third characteristic is executed the relationship

$$d\lambda = mdr \quad (4.9)$$

We will introduce new variable  $\beta = 2\sqrt{2m}$ . Equations (4.7)-(4.9) will take form

$$\frac{ds}{dr} = \alpha \pm \frac{\beta}{4}, \quad d\alpha \pm d\beta = -\omega dr \mp \frac{\beta}{4} \left( \frac{v}{r} + \alpha\delta + \frac{\beta^2}{4\lambda} \right) dr \quad (4.10)$$

$$\frac{ds}{dr} = \alpha, \quad d\lambda = \frac{\beta^2}{8} dr \quad (4.11)$$

The quantity  $\beta$  constitutes critical angle of inclination of wall during Mach reflection of plane shock wave of intensity  $m$  (see (3.4)).

§ 5. Certain solutions of equations of hyperbolic type possess the feature that characteristics of one family intersect and the solution becomes ambiguous. In gas dynamics to the intersection of characteristics corresponds the appearance of a shock wave, which removes ambiguity. In equations of nonlinear geometric acoustics intersection of the characteristics of one family is also possible — this was revealed during numerical calculation of certain problems. The ambiguity which appears may be removed by introducing a discontinuity of functions  $m$ ,  $n_1$ ,  $\lambda$ .

Conditions on surface of discontinuity of functions can be obtained from the same physical considerations as the derivation of the equations of nonlinear geometric acoustics themselves [6-8].

The unit normal to the surface of discontinuity is designated  $\nu_1$ . From the condition that surface of front of shock wave is continuous on surface of discontinuity, it follows that speed of wave along surface of discontinuity on the left and on the right from the discontinuity is identical. This condition gives the relationship

$$\left( \frac{v \times \mu}{\nu_1 n_1} \right)_1 = \left( \frac{v \times \mu}{\nu_1 n_1} \right)_2, \quad \mu = \frac{v}{|v|} \quad (5.1)$$

During transition through the discontinuity the area of the beam tube is changed in accordance with change of angle of its slope. From this condition we will obtain

$$\left( s \frac{\mu_2 n_2}{\mu_1 \nu_1} \right)_1 = \left( s \frac{\mu_2 n_2}{\mu_1 \nu_1} \right)_2 \quad (5.2)$$

Finally, along beam tube are executed the following relationships, which are obtained during integration of equations (2.2) and (2.3) on a small segment of the beam tube containing the discontinuity of functions

$$\left[ m^2 S \left( 1 + \frac{w_1 n_1}{c} \right) \right]_1 = \left[ m^2 S \left( 1 + \frac{w_1 n_1}{c} \right) \right]_2, \quad \lambda_1 = \lambda_2 \quad (5.3)$$

The first relationship of (5.3) expresses conservation of energy during transition of shock wave through surface of discontinuity of functions. Putting it in (5.2) and considering that parameters of medium are continuous on surface of discontinuity of functions and that  $M$  is close to unity, we will obtain

$$\left[ m^2 \left( n_1 v_1 + \frac{v_1 w_1}{c} \right) \left( 1 + \frac{n_1 w_1}{c} \right) \right]_1 = \left[ m^2 \left( n_1 v_1 + \frac{v_1 w_1}{c} \right) \left( 1 + \frac{n_1 w_1}{c} \right) \right]_2 \quad (5.4)$$

Relationships (5.1), (5.4) and the second equality in (5.3) are also necessary conditions on surface of discontinuity.

For simplified equations (4.4)-(4.6) conditions on surface of discontinuity of functions are also obtained more simply

$$x = a_1 + V \sqrt{2m_1} \frac{\pi^2}{V(1+\pi^2)(1+\pi)}, \quad a_2 = a_1 + V \sqrt{2m_1} \frac{\pi^2 - 1}{V(1+\pi^2)(1+\pi)}, \quad (5.5)$$

$$\lambda_1 = \lambda_2, \quad \pi = \frac{m_2}{m_1}$$

Here  $\pi$  - angle of inclination of surface of discontinuity of functions to plane  $z = 0$ . This angle determines "speed" of propagation of discontinuity in plane of variables  $r, z$  since in the accepted approximation of small angles,  $\pi$  coincides with the derivative  $dz/dr$ . From the first relationship of (5.5) it follows that "speed" of weak discontinuity ( $\pi \rightarrow 1$ ) coincides with "speed" of first pair of characteristics (4.7).

Physical meaning of the appearance of discontinuities in equations of nonlinear geometric acoustics is that in reality (i.e., in more exact formulation of problem than beam approximation) there appears a reflected shock wave, since "break" of shock wave (i.e., discontinuity  $n_1$ ) is possible only during triple configuration. The stronger the discontinuity of functions which appears, the stronger should be the reflected wave. Thus, actual equations indicate appearance of a superfluous shock wave, for which besides calculation is conducted. In certain problems this reflected wave plays an essential role, as, for instance, during regular reflection. But, using on the discontinuity the first relationship of (5.3), thereby we will disregard the reflected wave, inasmuch as this relationship expresses conservation of energy along beam tube. For a reflected wave no energy remains.

For this reason during achievement of defined intensity of discontinuity in equations of nonlinear geometric acoustics it is necessary to stop calculation. This is necessary to do where reflection will be obviously regular, and namely, where during transition through discontinuity the beam changes angle of inclination by a magnitude larger than critical. It is possible to continue calculation further, if the reflected wave is "inserted" in suitable form.

§ 6. Let us note particular cases of the solution of system of equations (4.4)-(4.6) in a homogeneous atmosphere, i.e., when  $\omega = 0$  and  $\delta = 0$ . At first we will indicate the solution of equations (4.5), (4.6) for rectilinear beams. In the case of a plane wave propagating along the earth

$$\lambda = \sqrt{c_1 r + c_2}, \quad m = c_1 / 2\sqrt{c_1 r + c_2}, \quad a = 0, \quad v = 0$$

In the case of a divergent spherical wave

$$\lambda = \sqrt{c_1 \ln r + c_2}, \quad m = c_1 / 2r\sqrt{c_1 \ln r + c_2}, \quad a = z/r, \quad v = 1$$

Thus, in these cases known solutions are obtained for damping of weak shock waves in homogeneous atmosphere [9].

Now we will consider the solution of equation (4.4) in an unhomogeneous atmosphere, and when pressure along front of shock wave changes little, so that derivative  $\partial m / \partial z$  is small as compared to derivatives of speed of sound and speed of wind, which enter the total gradient  $\omega$ . Disregarding in equation (4.4) the first term, we will obtain

$$\partial a / \partial r + a \partial a / \partial z = -\omega(z) \quad (6.1)$$

Hence we obtain equations of beams

$$ds/dr = a, \quad da/dr = -\omega(z) \quad (6.2)$$

For a constant total gradient  $\omega = \omega_0$  we will obtain known equations of beams in the form of parabolas

$$s = z_0 + a_0 r - 1/2 \omega_0 r^2 \quad (6.3)$$

§ 7. The above considered beam approximation for weak shock waves can be checked by means of comparison of obtained solutions with exact. There is special

interest in amplification or weakening of pressure on front of shock wave during its propagation along a wall (along earth).

Pressure on the wall of a wedge during self-simulating reflection of a flat weak shock wave for small angles ( $\alpha < \beta_1$ ) is obtained in [13]:

$$\zeta = 1 + \frac{16}{3\pi} \frac{\alpha}{\beta_1} \approx 1 + 1.7 \frac{\alpha}{\beta_1}, \quad \zeta = \frac{m}{m_1} \quad (7.1)$$

Here  $\zeta$  - reflectivity,  $\alpha$  - half-angle of solution of wedge or angle of inclination of wall, the index 1 pertains to an incident wave. On the other hand, from the second relationship on discontinuity (5.5), in deriving which equation (2.2) was used, for small angles  $\alpha = \alpha_2 - \alpha_1 < \beta_1$  we will obtain

$$\zeta = 1 + 2 \frac{\alpha}{\beta_1} \quad (7.2)$$

If the wall is inclined gradually, so that the discontinuity of functions starts not in the place of beginning of distortion of wall, but at a certain distance, or if the wall is bent to the other side (in this case occurs weakening of wave), then for long waves  $\lambda = \alpha$  a solution is obtained in the form of a simple wave, and pressure on wall is from relationship (4.8). Let us obtain

$$\zeta = \left(1 + \frac{\alpha}{\beta_1}\right)^2 \quad (7.3)$$

Here is considered a uniform medium. When  $\alpha < \beta_1$  (7.3) coincides with (7.2).

Thus, for small angles of inclination of beams equations of nonlinear geometric acoustics give satisfactory results.

Now we will compare solutions for large angles (but not larger than critical). In [14, 15] is obtained the exact value of reflectivity for critical angle of slope of wall  $\zeta = 5$ . On the other hand, from the second relationship on discontinuity (5.5) when  $\alpha_2 - \alpha_1 = \beta_1$  we will obtain  $\zeta = 5.3$ . This is higher than the exact value in all by 6%.

Thus, nonlinear geometric acoustics sufficiently well determines magnitude of pressure on wall in the whole range of Mach reflection from small angles to critical.

Let us note that it is impossible to use formula (7.3), when  $\alpha$  is positive and close to  $\beta_1$ , since in the solution appears intersection of the characteristics of

one family. To remove ambiguity it is necessary to introduce discontinuity of functions, and the simple wave is destroyed.

§ 8. System of equations (4.4)-(4.6) was calculated by the method of characteristics on an electron computer for different values of parameters  $\omega(z)$ ,  $b(z)$ ,  $\nu$ ,  $\lambda$ . The figure shows the result of calculation of amplification factor  $\zeta$  for the symmetric case of initial data corresponding to a point source of a shock wave on plane  $z = 0$ , for constant total gradient  $\omega = \omega_0$  and  $\nu = 1$ ,  $b = 0$ ,  $\lambda = \omega$ .

Along the axis of the ordinates is plotted the value of amplification factor  $\zeta = p'/p_0'$ . Here  $p'$  — pressure in weak shock wave, which is obtained as a result of calculation,  $p_0'$  — pressure which would be at the same distance during propagation of a wave in a uniform medium, i.e.,  $p_0' = kpc^2/r$ .

Along the axis of abscissas is plotted the distance to the source (explosion), in reference to magnitude of critical distance  $r_*$ , which is equal to

$$r_* = 2(\gamma + 1)k^{1/2} |\omega_0|^{-1/2} \quad (8.1)$$

For a positive total gradient amplification of pressure is obtained and for negative — weakening. The first case usually is observed down wind, and the second — against the wind.

Let us note that all cases of constant gradients both of the speed of sound and also the speed of wind lead to two cases:  $\omega_0 > 0$  and  $\omega_0 < 0$ . Therefore values of  $\zeta$  in various directions from the explosion for various relationships between gradients of speed of sound and speed of wind are obtained by simple recalculation of results presented on the figure.

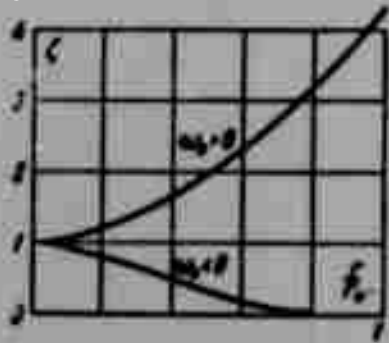


Fig. 1.

Furthermore, let us note that in the whole region; influencing at shown distances the quantity  $\zeta$  when  $z = 0$  (on the earth), discontinuity of functions did not appear. During calculations of the flat case discontinuity of functions appears earlier and affects the magnitude  $\zeta$  at  $r = 0.14 r_*$ , on which  $\zeta = 1.65$ .

The author thanks O. S. Ryzhov for useful comments made during consideration of work and V. I. Kozhevnikov for help during carrying out calculations.

Submitted  
9 June 1964

#### Literature

1. D. I. Blokhintsev. Acoustics of a nonuniform moving medium. State Technical Press, 1946.
2. J. B. Keller. Geometrical acoustics. I. The theory of weak shock waves. J. Appl. Phys., 1954, Vol. 25, No. 8.
3. K. Ye. Gubkin. Propagation of discontinuities in sound waves. PMM, 1958, Vol 22, Issue 4.
4. O. S. Ryzhov. Damping of shock waves in nonuniform media. PMTF, 1961, No. 2.
5. K. Ye. Gubkin. Nonlinear geometric acoustics and its application. Collection "Certain problems of mathematics and mechanics," Novosibirsk, 1961.
6. G. B. Whitham. A new approach to problems of shock dynamics. Part 1. Two-dimensional problems. J. Fluid Mech., Vol. 2, Part 4.
7. G. B. Whitham. On the propagation of shock waves through regions of nonuniform area of flow. J. Fluid Mech., 1958, Part 4.
8. G. B. Whitham. A new approach to problems of shock dynamics. Part 2. Three-dimensional problems. J. Fluid Mech., 1959, Vol. 5, Part 3.
9. L. D. Landau. Shock waves at great distances from the place of their appearance. PMM, 1945, Vol. 9, Issue 4.
10. P. F. Korotkov. Shock waves at a considerable distance from the place of explosion. Izv. AN SSSR, OTN, 1958, No. 3.
11. O. S. Ryzhov and G. M. Shefter. Energy of sound waves propagating in moving media. PMM, 1962, Vol. 26, No. 5.
12. P. F. Korotkov. Increase of pressure in the shock wave of an explosion in direction of wind. PMTF, 1961, No. 3.
13. M. J. Lighthill. The diffraction of blast. I. Proc. Roy. Soc., ser. A., 1949, Vol. 198, No. 1055.
14. O. S. Ryzhov and S. A. Khristianovich. Nonlinear reflection of weak shock waves. PMM, 1958, Vol. 22, Issue 5.
15. P. F. Korotkov. On Mach reflection of shock waves. PMTF, 1964, No. 1.

**BLANK PAGE**

## BURNING STABILITY OF POWDER

A. G. Istratov and V. B. Librovich

(Moscow)

In the theory of burning of powders and explosives, Ya. B. Zel'dovich [1] obtained a unique dependence of burning rate on initial temperature of the substance: with decrease of temperature there occurs decrease of this rate only up to a definite limit, and then stable burning becomes impossible; powder, after igniting, gives only isolated flashes. This temperature limit of possible burning is inherent only to the burning of condensed substances. In distinction from the limit of propagation of flame in gasses, a steady-state solution exists at low temperatures, but turns out to be unstable (in gas flame under the limit, steady-state solutions do not exist at all).

In work [1] there is given a criterion which establishes the possibility of steady-state burning of powder.

$$\gamma = \frac{E_2(T_b - T_0)}{2RT_b^2} \frac{c_{p1}}{c_{p2}} < 1 \quad (1)$$

Here  $T_b$ ,  $T_s$ ,  $T_0$  are burning temperature, surface temperature and initial temperature of powder respectively;  $E_2$  is activation energy of chemical reaction in gas;  $c_{p1}$  and  $c_{p2}$  are heat capacities of powder and gas respectively.

However, in experiments it has been noted [2] that for real powders criterion (1) is not satisfied. It is possible to name the following causes of this: First, the criterion of Ya. B. Zel'dovich was derived on the assumption that gasification of solid matter occurs in an infinitely narrow, inertialess zone of chemical transformation (vaporization); only in this case may one assume that burning rate is determined by the gradient of the Michelson distribution of temperature in the condensed phase (k-phase) of powder at its surface. In reality, the zone of chemical reaction has finite extent and inertness. Because of this, the hypothesis of Ya. B. Zel'dovich about the decisive role of temperature gradient was modified by A. D. Margolin, who assumed that burning rate is determined by temperature gradient in the end of the reaction zone, where the chemical transformation of solid matter into gaseous products is completed. Thus the stability criterion takes the form

$$\gamma = \frac{E_2(T_b - T_0)}{2RT_b^2} \frac{c_{p1}}{c_{p2}} < \left[ 1 - \frac{q_1}{c_{p1}(T_b - T_0)} \right]^{-1} \quad (2)$$

where  $q_1$  is heat of reaction in the k-phase.

Secondly, during derivation of the criterion, Ya. B. Zel'dovich considered that temperature of surface of powder is constant. However, fast changes of it even small ones, render a considerable influence on the section of the thermal layer adjacent to the surface, thereby strongly changing the temperature gradient; this affects the stability of burning. Investigation of burning stability taking into account this second circumstance is conducted below.

Let us note that another approach to the study of burning stability of liquid systems was applied by L. D. Landau. He considered the hydrodynamic aspect of stability. He assumed that flame is located directly on the surface of the burning substance, and that burning rate does not depend on perturbations (perturbations were considered to be two-dimensional) and is a known constant. Thus, in the very formulation of the problem L. D. Landau excluded the structure of the powder flame, with which the instability revealed by Ya. B. Zel'dovich is connected.

Separation of stable burning can occur also due to the interaction of oscillations of pressure in the combustion chamber and oscillations of burning rate of the powder (see, for instance, the work of Ya. B. Zel'dovich [4]). This question is not considered here.

Investigation of stability of the solution describing steady-state burning of powder will be conducted by the method applied by G. I. Barenblatt, Ya. B. Zel'dovich and A. G. Istratov for investigation of thermal diffusion stability of a laminar flame [5]. In the method there is used the assumption that chemical reactions are concentrated in narrow regions, which are negligibly thin as compared to preheating zones. This corresponds to chemical reactions with very high activation energies.

Let us assume that during burning, distributions of temperature and concentration have the form depicted in Fig. 1. There are distinguished three regions. In region

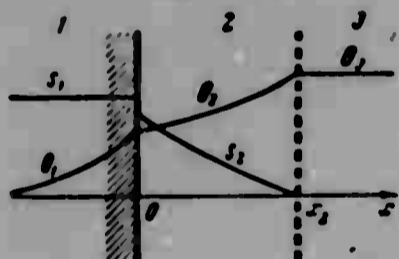


Fig. 1.

1 there occurs heating of solid powder from initial temperature  $T_0$  to surface temperature  $T_s$ ; then on the boundary between regions 1 and 2 in a narrow zone there occurs the chemical reaction of decomposition of powder into a gaseous substance. Gasification products, which are mixed with products of burning of the powder which are diffusing to the surface, move through region 2 and are heated from

surface temperature to combustion temperature  $T_b$  by heat proceeding from the zone reaction toward the junction of zones 2 and 3. Zone 3 is filled only with combustion products of the powder.

We will consider all perturbations to be one-dimensional. Furthermore, following work [1], we will assume that processes in the gas are inertialess as compared to processes in the condensed phase. This corresponds to the condition that ratio of density of gas to density of powder is minute.

In region 1 perturbations of temperature have to satisfy the usual heat-conduction equation, which in dimensionless form is

$$\frac{\partial \theta_1'}{\partial \tau} + \frac{\partial \theta_1'}{\partial \xi} = \frac{\partial^2 \theta_1'}{\partial \xi^2} \quad (3)$$

$$\left( \theta = \theta^0 + \theta' = \frac{T - T_0}{T_0 - T_0}, \xi = \frac{u_1 \rho_1 c_{p1}}{\lambda_1} x, \tau = \frac{u_1 \rho_1 c_{p1}}{\lambda_1} t \right)$$

Here  $x$  is the coordinate along the normal to the surface of the powder,  $t$  — is time,  $\rho_1$ ,  $c_{p1}$ ,  $\lambda_1$  are density, heat capacity and thermal conductivity of the powder,  $u_1$  is linear rate of steady-state burning. Subscript 1 pertains to k-phase of powder; subscripts 2, 3 pertain respectively to the gas phase in zones 2 and 3. Superscript  $^0$  pertains to steady-state values; the prime signifies perturbation. For perturbations of concentration of reactant  $s_1'$  we will obtain, after setting diffusion coefficient in the k-phase equal to zero,  $s_1' \equiv 0$ . Density in region 1 obviously can also be considered to be constant.

In regions 2 and 3, which are occupied with gas, for perturbations of temperature and concentration we will obtain the equations

$$\begin{aligned} \frac{\partial \theta_2'}{\partial \xi} + j' \frac{\partial \theta_2'}{\partial \xi} &= \frac{\lambda}{c_p} \frac{\partial^2 \theta_2'}{\partial \xi^2}, \quad \frac{\partial s_2'}{\partial \xi} + j' \frac{\partial s_2'}{\partial \xi} = \frac{\lambda}{c_p} \frac{\partial^2 s_2'}{\partial \xi^2} \\ \frac{\partial \theta_3'}{\partial \xi} &= \frac{\lambda}{c_p} \frac{\partial^2 \theta_3'}{\partial \xi^2} \end{aligned} \quad (4)$$

$$\left( \lambda = \frac{\lambda_2}{\lambda_1} = \frac{\lambda_3}{\lambda_1}, c_p = \frac{c_{p2}}{c_{p1}} = \frac{c_{p3}}{c_{p1}}, j' = \frac{(\rho_2 u_2)'}{\rho_1 u_1} \right)$$

The absence in equations (4) of terms with time derivatives is due to the assumption of relatively low density of gas; as it is easy to verify, these terms are of the order of  $\rho_2/\rho_1 \ll 1$ . For the same reason, from the continuity equation it follows that perturbation of mass flow  $j' = (\rho_2 u_2)'/\rho_1 u_1$  is constant along zones 2 and 3. Dependence of perturbations on time in these regions is quasi-steady-state — time enters in as a parameter through the boundary conditions. In spite of the low density of gas, mass flow of substance from surface of the powder should be considered to be finite, since it is equal to the mass burning rate. The introduction of infinitely large linear rate of outflow of gasses does not at all mean that the gas flame must be far removed from the powder surface; the essential parameter here is the mass rate, and not the linear rate.

It is not necessary to write diffusion equations in zone 3, since in this region concentration of reactant is equal to zero (total combustion).

It is also assumed that heat capacities and transfer coefficients are constant, where the Lewis number is equal to unity.

Let us note the steady-state distributions of temperature and concentration [1]

$$\begin{aligned}
\theta_1^* &= \theta_1^* e^{\xi} \quad \left( \theta_1^* = \frac{T_b - T_0}{T_b - T_0} \right) \\
\theta_1^* &= 1 - \frac{\Delta_2}{c_p} \left[ 1 - \exp \frac{c_p}{\lambda} (\xi - \xi^0) \right] \quad \left( \Delta_2 = \frac{q_2}{c_{p1}(T_b - T_0)} \right) \\
\theta_2^* &= 1 - \exp \frac{c_p}{\lambda} (\xi - \xi^0), \quad \theta_3^* = 1
\end{aligned} \tag{5}$$

Here  $q_2$  is heat of reaction in gas;  $\xi^0$  is distance between reaction zone in gas and powder surface during steady-state burning.

Solutions of equations (3), (4) have to satisfy, besides natural conditions at infinity, also joining conditions on boundaries between zones, i.e., conditions on reaction zones. As in work [5], we assume that reaction zones are first-order discontinuity surfaces of temperature and concentration, and will write for them linearized conservation laws. Thus, we will consider the following circumstances:

Actual reaction surfaces can undergo small displacements. Let us assume therefore that coordinate of zone of reaction in the k-phase (between zones 1 and 2) will be  $\zeta_1 = \zeta_1^0 + \zeta_1'(\tau)$  (stationary position of zone  $\zeta_1^0 = 0$ ); for the gas accordingly  $\zeta_2 = \zeta_2^0 + \zeta_2'(\tau)$ ; ( $\zeta_2^0 = \xi^0$ ).

We will consider that changes of chemical reaction rates  $w_1$  and  $w_2$ , to which perturbations of the steady state will lead, are caused wholly by change of temperatures  $T_s$  and  $T_r$  on the corresponding surfaces in the k-phase and in the gas. Such an assumption is natural for high activation energies of chemical reactions  $E_1$  and  $E_2$ . In the steady state reaction rates are equal to mass burning rate; therefore, reaction rates in the k-phase and in the gas respectively can be written in the form

$$\begin{aligned}
\rho_1 w_1^* &= \rho_1 w_1 \left( 1 + \frac{d \ln w_1^*}{dT_s} T_s' \right) \quad \left( \frac{d \ln w_1^*}{dT_s} = \frac{E_1}{2RT_s^2} \right) \\
\rho_2 w_2 &= \rho_2 w_2 \left( 1 + \frac{d \ln w_2^*}{dT_r} T_r' \right) \quad \left( \frac{d \ln w_2^*}{dT_r} = \frac{E_2}{2RT_b^2} \right)
\end{aligned}$$

or in dimensionless form

$$\begin{aligned}
m_1 &= \frac{\rho_1 w_1}{\rho_1 w_1} = 1 + z_1 \theta_s' \quad \left( z_1 = \frac{E_1 (T_b - T_0)}{2RT_b^2} \right) \\
m_2 &= \frac{\rho_2 w_2}{\rho_1 w_1} = 1 + z_2 \theta_r' \quad \left( z_2 = \frac{E_2 (T_b - T_0)}{2RT_b^2} \right)
\end{aligned} \tag{6}$$

In the depth of the powder perturbations must be damped; condition of damping of perturbations in the gas far from the powder surface is stringent too, due to the assumption of infinite linear rate of gas flow; it is sufficient to consider perturbations to be finite.

Thus,

$$\theta_1' \rightarrow 0 \text{ as } \xi \rightarrow -\infty, \quad \theta_3' < \infty \text{ as } \xi \rightarrow +\infty \quad (7)$$

On the powder surface ( $\xi = 0$ ) there must be realized:

continuity of temperature

$$\frac{d\theta_1}{d\xi} \zeta_1' + \theta_1' = \frac{d\theta_3}{d\xi} \zeta_1' + \theta_3' = \theta_0' \quad (8)$$

conservation of heat flow (taking into account heat emission in reaction zone)

$$(1 - c_p)(\theta_0' + \theta_0'') \frac{d\zeta_1'}{d\tau} - (1 - c_p)\theta_0' + \frac{d^2\theta_1}{d\xi^2} \zeta_1' + \frac{\partial\theta_1'}{\partial\xi} - \lambda \frac{d^2\theta_3}{d\xi^2} \zeta_1' - \lambda \frac{\partial\theta_3'}{\partial\xi} = \Delta_1 z_1 \theta_0' \quad (9)$$

$$\left( \theta_0' = \frac{T_0}{T_b - T_0}, \quad \Delta_1 = \frac{q_1}{c_{p1}(T_b - T_0)} \right)$$

the condition of total consumption of reactant

$$-d\zeta_1' / d\tau = z_1 \theta_0' \quad (10)$$

conservation of mass flow  $s_2$  (taking into account its production the powder surface)

$$-s_2 \frac{d\zeta_1'}{d\tau} + \frac{ds_2}{d\xi} \zeta_1' + s_2' - \frac{\lambda}{c_p} \frac{d^2 s_2}{d\xi^2} \zeta_1' - \frac{\lambda}{c_p} \frac{\partial s_2'}{\partial\xi} = z_1 \theta_0' \quad (11)$$

continuity of mass flow

$$f' = -d\zeta_1' / d\tau \quad (12)$$

On the surface of the reaction zone in the gas ( $\xi = \xi^0$ ) it is necessary to consider: continuity of temperature

$$\frac{d\theta_2}{d\xi} \zeta_2' + \theta_2' = \theta_3' = \theta_0' \quad (13)$$

continuity of concentration of substance  $s_2$

$$\zeta_2' ds_2' / d\xi + s_2' = 0 \quad (14)$$

conservation of heat flow (taking into account heat emission in reaction zone)

$$\lambda \frac{d^2\theta_2}{d\xi^2} \zeta_2' + \lambda \frac{\partial\theta_2'}{\partial\xi} - \lambda \frac{\partial\theta_3'}{\partial\xi} = \Delta_2 z_2 \theta_0' \quad (15)$$

condition of total consumption of substance  $s_2$

$$-\frac{\lambda}{c_p} \frac{d^2 s_2}{d\xi^2} \zeta_2' - \frac{\lambda}{c_p} \frac{\partial s_2'}{\partial\xi} = z_2 \theta_0' \quad (16)$$

In conditions (8)-(16), ratio of density of gas to density of powder was assumed equal to zero.

Let us note that for the scheme of burning of powder of Ya. B. Zel'dovich (constant temperature of powder surface, powder is gasified under influence only of the external flow of heat), equations (3), (4) remain the same. There are changed only certain conditions on the powder surface. Instead of conditions (8)-(11), we should write:

conditions of constancy of temperature of powder surface

$$\frac{d\theta_1'}{d\xi} \zeta_1' + \theta_1' = 0, \quad \frac{d\theta_2'}{d\xi} \zeta_1' + \theta_2' = 0 \quad (17)$$

conditions of conservation of heat flow (taking into account its consumption in zone of gasification of powder)

$$(1 - \epsilon_p)(\theta_1' + \theta_2') \frac{d\zeta_1'}{d\xi} + \frac{d^2\theta_1'}{d\xi^2} \zeta_1' + \frac{\partial\theta_1'}{\partial\xi} - \lambda \frac{d^2\theta_2'}{d\xi^2} \zeta_1' - \lambda \frac{\partial\theta_2'}{\partial\xi} = \Delta_1 \frac{d\zeta_1'}{d\xi} \quad (18)$$

conditions of conservation of mass flow  $s_2$  (taking into account its production during gasification)

$$-s_2' \frac{d\zeta_1'}{d\xi} + \frac{ds_2'}{d\xi} \zeta_1' + s_2' - \frac{\lambda}{c_p} \frac{d^2\theta_1'}{d\xi^2} \zeta_1' - \frac{\lambda}{c_p} \frac{\partial\theta_1'}{\partial\xi} = -\frac{d\zeta_1'}{d\xi} \quad (19)$$

Solutions of equations (3), (4) and displacements of combustion surfaces can be written in the form

$$\begin{aligned} \theta_1' &= a \exp(r\xi + \omega\tau) \quad (r = 1/2(1 + \sqrt{1 + 4\omega})) \\ \theta_2' &= b e^{r\xi} + c \exp\left(\frac{c_p}{\lambda} \xi + \omega\tau\right) - f \frac{\Delta_1}{\lambda} \omega \xi \exp\left[\frac{c_p}{\lambda} (\xi - \xi^0) + \omega\tau\right] \\ s_2' &= k e^{r\xi} + l \exp\left(\frac{c_p}{\lambda} \xi + \omega\tau\right) + j \frac{c_p}{\lambda} \omega \xi \exp\left[\frac{c_p}{\lambda} (\xi - \xi^0) + \omega\tau\right] \\ \theta_3' &= d e^{r\xi}, \quad \zeta_1' = f e^{r\xi}, \quad \zeta_2' = g e^{r\xi} \end{aligned} \quad (20)$$

Solutions (20) already satisfy conditions at infinity (7); the sign of  $r$  is selected in such a way that the unstable solution ( $R_e \omega > 0$ ) which is being sought tends to zero as  $\xi \rightarrow -\infty$ .

After substitution of solutions (20) and (5) into conditions (8)-(16), we will find an algebraic system of linear homogeneous equations for determination of constants  $a, b, c, d, f, g, k, l$ . Equating the determinant of the system to zero and expanding it, we obtain an equation in complex frequency  $\omega$ :

$$\begin{aligned} 2\omega(\gamma - 1) + \gamma + \sigma\omega &= (\gamma + \sigma\omega)(1 + 4\omega)^{1/2} \\ \left(\gamma - \frac{s_2\theta_1^0}{c_p} - \frac{E_1(T_0 - T_0^0)}{2RT_0^0} \frac{c_{p1}}{c_{p2}}, \quad \sigma = \frac{s_1}{s_1 c_p} - \frac{E_1 T_0^0}{E_1 T_0^0} \frac{c_{p1}}{c_{p2}}\right) \end{aligned} \quad (21)$$

Roots of this equation are

$$\omega_1 = 0, \quad \omega_{2,3} = \frac{1}{2}\sigma^2\{(\gamma - 1)^2 - (\gamma + 1)\sigma \pm [(\gamma - 1)^2(\sigma^2 - 2(\gamma + 1)\sigma + (\gamma - 1)^2)]^{1/2}\} \quad (22)$$

Let us note that perturbations corresponding to the root  $\omega_1 = 0$  appear when initial steady-state distributions of quantities are displaced along axis  $x$  without change of their shape. The possibility of such perturbations directly follows from the utilized equations of diffusion and thermal conduction, which are invariant with respect to displacement of axis  $x$ . This property of invariance was used in work [6] for investigation of stability of a laminar flame. In this work for the first time there was turned attention to the fact that the presence of "translational" perturbations does not indicate instability of the solution.

In view of the fact that in the process of solution of equation (21) it was necessary to take the square, the obtained roots must be checked by substitution into the initial equation for the purpose of elimination of extraneous roots. It turns out that for  $\gamma > 1$ ,  $\sigma \leq 2(\gamma + 1)$  the equation has all three roots, for  $\gamma > 1$ ,  $\sigma > 2(\gamma + 1)$  it has two roots  $-\omega_1$  and  $\omega_2$  (with the sign +); for  $\gamma < 1$ ,  $\sigma \leq 2(\gamma + 1)$  it has one root  $-\omega_1$ ; for  $\gamma < 1$ ,  $\sigma > 2(\gamma + 1)$  — two roots  $-\omega_1$  and  $\omega_3$  (with the sign -); for the value  $\gamma = 1$ , the equation is satisfied by roots  $\omega_1$  and  $\omega_2 = \omega_3 = -1/\sigma$ .

From (22) it follows that instability of solutions ( $\text{Re } \omega > 0$ ) appears if there is satisfied the inequality

$$(\gamma - 1)^2 > (\gamma + 1)\sigma \quad (23)$$

For  $\gamma > 1$  this is equivalent to the inequality

$$\gamma > 1 + \sigma/2 + \frac{1}{2}[\sigma(\sigma + 8)]^{1/2} \quad (24)$$

for  $\gamma < 1$ ,  $\sigma > 2(\gamma + 1)$

$$\gamma < 1 + \sigma/2 - \frac{1}{2}[\sigma(\sigma + 8)]^{1/2} \quad (25)$$

for  $\gamma < 1$ ,  $\sigma \geq 2(\gamma + 1)$  there is no unstable regime.

Let us note, however, that of the conditions (24) and (25) only condition (24) has physical meaning, since there should additionally be observed the evident condition  $\gamma > 0$ .

In Fig. 2 there is depicted the dependence (24) (curve 1) which bounds the region of stable burning of powder (region under the curve).

The obtained condition of stable burning of powder (24) differs from the criterion of stability of Ya. B. Zel'dovich (1); the essential parameter influencing burning

stability also turns out to be the quantity  $\sigma = E_2 T_s^2 c_{p1} / E_1 T_b^2 c_{p2}$ . The influence of ratio of activation energies of reactions in gas and condensed phases of powder on stability of burning, as already was indicated, is explained by the strong influence of changes in temperature of the surface on the gradient near it. For very high activation energy of reaction in the k-phase ( $\sigma \rightarrow 0$ ), temperature of powder surface remains practically constant, and criterion (24) becomes (1).

Criterion of stability (1) is also obtained if we consider the scheme of burning with vaporization on the surface of the k-phase (conditions (17)-(19)). In work [1] this criterion is obtained from several other considerations.

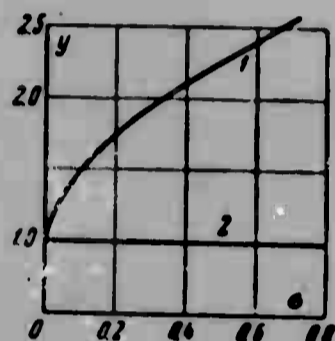


Fig. 2.

For real powders  $\sigma \approx 0.1$ . For such  $\sigma$  it is possible to use the approximate expression for the stability criterion

$$y < 1 + \sqrt{2\sigma} \quad (26)$$

It is necessary to pay attention to the fact that in the region of stable burning of powder which is above the straight line  $y = 1$  (Fig. 2), onset of oscillations of burning rate is possible, since the frequency in this region is complex.

In conclusion we thank G. I. Barenblatt, Ya. B. Zel'dovich and O. I. Leypunskiy for formulation and discussion of the problem.

Submitted  
6 March 1964

#### Literature

1. Ya. B. Zel'dovich. On the theory of burning of powders and explosives. Journal of Experimental and Theoretical Physics, 1942, Vol. 12, No. 11-12.
2. A. I. Korotkov and O. I. Leypunskiy. Dependence of temperature coefficient of burning rate of powder at atmospheric pressure on temperature of powder. Collection "The Physics of Explosions." No. 2, 1953.
3. L. D. Landau and Ye. M. Lifshits. Mechanics of continuous media. Gostekhizdat, 1954.
4. Ya. B. Zel'dovich. On the stability of burning of powder in a semiclosed volume. Applied Mechanics and Technical Physics, 1963, No. 1.
5. G. I. Barenblatt, Ya. B. Zel'dovich and A. G. Istratov. In thermal diffusion stability of a laminar flame. Applied Mechanics and Technical Physics, 1962, No. 4.
6. G. I. Barenblatt and Ya. B. Zel'dovich. On the stability of propagation of flame. Applied Mathematics and Mechanics, 1957, Vol. 21, Issue 6.

ASYMPTOTIC METHODS OF HYDRODYNAMIC  
THEORY OF STABILITY

G. M. Zaslavskiy, S. S. Moiseyev  
and R. Z. Saldeyev

(Novosibirsk)

We consider the asymptotic method of solution of a differential equation of the fourth order with two small parameters. An equation of such type is frequently the result of different problems of the hydrodynamic theory of stability, and also problems of transformation of oscillations in magnetohydrodynamics and plasma. In particular, the character of a special region where different solutions of geometric-optical approach "cross" is investigated. Rules of bypass of singular points are clarified and in different cases for finite solutions formulas are cited for calculation of the spectrum of oscillations. The proposed method can be applied also to analogous differential equations of higher order. The theory is applied to investigation of instability of plasma in the field of gravity.

Designations

- $\rho$  - amplitude of perturbation;
- $\alpha, \beta$  - small parameters;
- $\xi$  - coordinate in direction of heterogeneity;
- $x, y, z$  - dimensionless coordinates in direction of heterogeneity;
- $k$  - wave vector of perturbation;
- $\omega$  - frequency;
- $L$  - characteristic dimension;
- $P, p^0, q, q^0, w$  - derivative from amplitude phases of perturbation;
- $H_{1/3}^{(1)(2)}$  - Hankel function of 1 stand 2nd kind;
- $L_1$  - contours of integration in phases of solution;

$n_0$  - density of medium;  
 $g$  - potential of field of gravity;  
 $c$  - velocity of light;  
 $T$  - temperature;  
 $e$  - charge of electron;  
 $H$  - magnetic field strength;  
 $V$  - speed;  
 $q$  - heat flow;  
 $E$  - electric field strength;  
 $r_1$  - Larmor radius of ions;  
 $\Pi$  - pre-exponential factor of solution.

1. State of problem. Use of asymptotic methods in the linear hydrodynamic theory of stability are well-known, for instance, in connection with the problem of stability of Poiseuille flow (for detailed survey of works see [1]). The essence of the matter is that it is necessary to construct a solution and to find eigenvalues  $\omega = \omega(k)$  for assigned boundary conditions of equation

$$\alpha \frac{d^2 \varphi}{d\xi^2} - U_0(\xi, k, \omega) \frac{d^2 \varphi}{d\xi^2} + U_1(\xi, k, \omega) \varphi = 0 \quad (1.1)$$

where  $\alpha$  - small parameter,  $\xi$  - coordinate (in the case of Poiseuille flow  $\alpha$  is proportional to viscosity). The presence of small parameter  $\alpha$  ensured possibility of construction of a formal asymptotic series for solution with respect to a successfully selected power of  $\alpha$ .

Recently there appeared a large number of works for the study of stability of weak-nonuniform plasma. Where a detailed investigation was conducted the problem lead to the equation

$$\frac{d^2 \varphi}{d\xi^2} - U(\xi, k, \omega) \varphi = 0 \quad (1.2)$$

In order to introduce in (1.2) evidently small parameter  $\beta$ , characterizing weak heterogeneity, we will introduce dimensionless coordinate  $x = \xi/L$  ( $L$  - characteristic dimension of problem). Let us set  $U = k_0^2 U$ , where  $U \sim 1$  everywhere, with the exception of the region near point  $x_0$ , where  $U(x_0) = 0$ . Then we have instead of (1.2)

$$\beta \frac{d^2 \varphi}{dx^2} - U(x, k, \omega) \varphi = 0, \quad \beta = \frac{1}{k_0^2 L^2} \ll 1 \quad (1.3)$$

In [2] it was proposed to use smallness  $\beta$  for construction of asymptotic solutions, well-known in quantum mechanics under the name "quasiclassical".<sup>1</sup>

In a number of cases the following situation appears: in the considered region exists a point in which  $U$  turns into  $\infty$ . This circumstance was studied in connection with the problem on transformation of waves in plasma [5]. Pole  $U$  in cases studied in [5] was fictitious and vanished during calculation of the higher derivative with small parameter of type  $\alpha$  for it.<sup>2</sup> For problems connected with transformation of waves in plasma the method of successive approximations was used [6].

Asymptotic method, near on one hand, to [6] and on the other — to [1], was applied in [7] for an equation of type (1.1) during investigation of stability of inhomogeneous plasma taking into account final conductivity. This method, as one will see subsequently, has very limited applicability.

Below is considered the possibility of a single asymptotic approach to investigation of the equation which models the above-mentioned problems under the condition of weak heterogeneity of medium.

2. Formulation of problem. Physical questions considered in the introduction lead to the necessity of investigating the equation

$$\alpha \beta^2 \frac{d^2 \varphi}{dx^2} - \beta U_1(x, k, \omega) \frac{d^2 \varphi}{dx^2} + U_2(x, k, \omega) \varphi = 0 \quad (\alpha, \beta \ll 1) \quad (2.1)$$

where  $x$  — dimensionless coordinate,  $k, \omega$  — parameters of problem,  $\alpha$  and  $\beta$  — small parameters.

Usually in the physical statement of a problem parameter  $\alpha$  is connected taking into account weak dissipative process, and  $\beta$  is the parameter of "quasiclassicality," constituting ratio of characteristic length of change  $\varphi$  to characteristic length of change  $U_1, U_2$ ; in equation (2.1) functions  $U_1$  and  $U_2$  are dimensionless values where

$$U_1, U_2 \sim 1 \quad (2.2)$$

<sup>1</sup>For a detailed survey of works in this area see [3, 4].

<sup>2</sup>The given reasoning somewhat roughly transmits situation studied in [5].

with the exception of points where they turn into zero.

Solutions tending to zero on  $\pm\infty$  we call subsequently finite, or local.

Otherwise the solution is called nonlocal.

When  $\beta = 1$  in (2.1) investigation of equation was conducted in works of Lin' Tszya-tszyao [1] and Vazov [8] in connection with the problem of stability of Poiseuille flow. When  $\alpha = 0$  the equation passes into an equation of the 2nd order, in detail investigated in numerous works, especially in connection with the quasiclassical approach in quantum mechanics (see for instance, [9]).

The solution of equation (2.1) is sought in the form

$$\varphi(x) = C \exp \left\{ \frac{1}{V\beta} \int q(x) dx \right\}, \quad q(x) = q^{(0)}(x) + V\beta q^{(1)}(x) + \dots \quad (2.3)$$

Substitution of (2.3) in (2.1) taking into account (2.2) gives

$$q^{(0)2} - \frac{U_2}{\alpha} q^{(0)} + \frac{U_1}{\alpha} = 0 \quad (2.4)$$

$$4q^{(1)}q^{(0)} + 6q^{(0)} \frac{dq^{(0)}}{dx} - \frac{U_2}{\alpha} \left( \frac{dq^{(0)}}{dx} + 2pq^{(1)}q^{(0)} \right) = 0 \quad (2.5)$$

From equation (2.4) we find

$$q^{(0)} = \pm \left[ \frac{U_2}{2\alpha} \pm \left( \frac{U_2^2}{4\alpha^2} - \frac{U_1}{\alpha} \right)^{1/2} \right]^{1/2}$$

or, considering smallness  $\alpha$ , we have two pairs of values

$$q_i^{(0)} = \pm \sqrt{U_1/U_2} \quad (i=1, 2), \quad q_i^{(0)} = \pm \sqrt{U_2/\alpha} \quad (i=3, 4) \quad (2.6)$$

Analogously from (2.5) we find:

$$q_i^{(1)} = -\frac{1}{2} \frac{dq_i^{(0)}}{dx} \frac{1}{q_i^{(0)}} \quad (i=1, 2), \quad q_i^{(1)} = -\frac{5}{2} \frac{dq_i^{(0)}}{dx} \frac{1}{q_i^{(0)}} \quad (i=3, 4) \quad (2.7)$$

Formulas (2.6), (2.7) permit writing the solution of (2.4) for  $\varphi$  in the form (accurate to following terms in expansion (2.3) for  $q$ )

$$\varphi_i = \frac{C}{V\beta_i} \exp \int p_i dx \quad (i=1, 2) \quad (2.8)$$

$$\varphi_i = \frac{C}{V\beta_i} \exp \int p_i dx \quad (i=3, 4) \quad \left( p_i = \frac{q_i^{(0)}}{V\beta} \right) \quad (2.9)$$

The obtained solution of (2.8) will be asymptotic, and its accuracy is limited by the domain of applicability of expansion of (2.3), which will be subsequently called external. It is obvious that the solution of (2.8), (2.9) is inapplicable in regions near points where  $U_1$  and  $U_2$  turn into zero; these regions subsequently will be called internal. The solution must be sought separately. In connection with this the solution of equation (2.1) under assigned boundary conditions leads to the following three procedures: 1) construction of solution in internal and external regions; 2) indication of condition of joining of solutions (this question appears in connection with presence of Stokes lines during use of asymptotic expressions); 3) satisfaction of boundary conditions (this leads also to the equation for eigenvalues of problem). Let us note that the point where  $U_1 = 0$  does not merit special attention, since near this point the role of the term with  $\varphi^{IV}$  in (2.1) is immaterial, and behavior of solution near this point is determined by the theory well-developed for equation (2.1) with  $\alpha = 0$ .



Fig. 1.

Subsequently, without loss of generality of the method developed below, we will select for convenience a specific form of functions  $U_1(x)$  and  $U_2(x)$  (Fig. 1). On Fig. 2 domains 1, 2 are external, and domain 3 is internal.

The above reasoning finishes formulation of the problem, solution of which will be carried out in §§ 3-5.

3. Weak case. For selected form  $U_1(x)$  and  $U_2(x)$  (Fig. 1)  $U_1$ ,  $U_2$  turn into zero correspondingly in points A, B and  $O_1$ ,  $O_2$ . We will assume<sup>1</sup>, that the distance between B and  $O_2$  is larger than unity. Near point  $O_2$  it is possible to represent

$$U_2 = Ux, \quad x < 1, \quad U \sim 1 \quad (3.1)$$

and to consider  $U_1$  constant.

On Fig. 3 are depicted domains of applicability of different approaches.



Fig. 2.

Expansion (3.1) is valid on segment  $(O_2, 1)$ ; solution (2.8), (2.9) are correspondingly valid on segments 1 and 3.

When  $x < 1$  equation (2.1) takes the form

$$\alpha\beta^2\varphi^{IV} - \beta Ux\varphi'' + U_1\varphi = 0 \quad (3.2)$$

<sup>1</sup>If the conducted reasoning is invariant with respect to replacement  $(O_1, A) \leftrightarrow (O_2, B)$ , then we will speak only about points  $(O_2, B)$ .

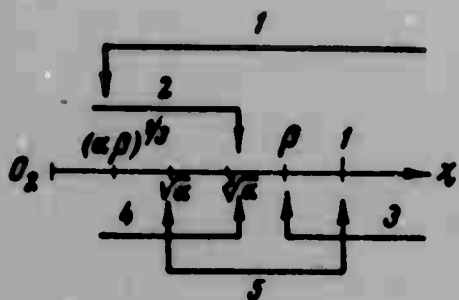


Fig. 3.

Let us make, as in [1], the substitution  $x = a^{1/2}y$  and consider the solution of the obtained equation

$$\beta \frac{d^2 \varphi}{dy^2} - Uy \frac{d^2 \varphi}{dy^2} + \frac{a^{1/2}}{\beta} U_1 \varphi = 0 \quad (3.3)$$

near  $y \sim 1$ . In this section we will be limited to

$a^{1/2}/\beta < 1$ . Then it is possible to construct a solution analogous to [1], in the form of asymptotic series

$$\varphi = \varphi^{(0)} + \frac{a^{1/2}}{\beta} \varphi^{(1)} + \dots \quad (3.4)$$

Substitution of (3.4) in (3.3) gives

$$\beta \frac{d^2 \varphi^{(0)}}{dy^2} - Uy \frac{d^2 \varphi^{(0)}}{dy^2} = 0 \quad (3.5)$$

Domain of applicability of solutions of equation (3.5) on the right is determined by values  $x \sim a^{1/2}$  and on Fig. 3 is designated by segment 2 (or 4). Equation (3.5) has four solutions [1]:

$$\varphi_1 = 1, \quad \varphi_2 = x \quad (3.6)$$

$$\begin{aligned} \varphi_3 &= \int dy \int dy V \bar{y} H_{1/2}^{(1)} \left[ \frac{2}{3} (iy)^{1/2} \left( \frac{U}{\beta} \right)^{1/2} \right] \\ \varphi_4 &= \int dy \int dy V \bar{y} H_{1/2}^{(2)} \left[ \frac{2}{3} (iy)^{1/2} \left( \frac{U}{\beta} \right)^{1/2} \right] \end{aligned} \quad (3.7)$$

Here  $H^{(1)}$ ,  $H^{(2)}$  — Hankel functions correspondingly of the first and second kind. Considering that the argument of Hankel functions in (3.7) is great it is possible to write for solutions  $\varphi_3$ ,  $\varphi_4$ , turning on  $\pm\infty$  into zero

$$\begin{aligned} \varphi &\sim x^{-1/2} \exp \left\{ -\frac{2}{3} \left( \frac{U}{\beta} \right)^{1/2} x^{1/2} \right\} \quad (x > 0) \\ \varphi &\sim |x|^{-1/2} \sin \left\{ \frac{2}{3} \left( \frac{U}{\beta} \right)^{1/2} (x)^{1/2} + \frac{\pi}{4} \right\} \quad (x < 0) \end{aligned} \quad (3.8)$$

If  $\varphi$  does not have to turn on  $\pm\infty$  into zero, when  $x > 0$  solution consists also of a growing exponential, and the solution when  $x < 0$  is determined by the usual rules, considering that  $x = 0$  is the reversal point [10]. Solutions (3.8) pass into

solutions determined by equation (2.9), and they, consequently, may be joined. Possibility of joining is ensured because segments 1 and 2 on Fig. 3 have a common part, inside which occurs the joining. There is quite another picture for solutions (3.6) and (2.8), which do not pass into one another and therefore are directly unjoinable. This is connected with the following circumstance. Pair of solutions (3.6) in principle does not have quasiclassical form and for it

$$k_y^2 = \varphi^{-1} d^2 \varphi / dy^2 = 0 \quad (3.9)$$

In fact equality (3.9) is determined accurate to  $\alpha^{1/2} \beta^{-1} \ll 1$ . This inequality means that domains of applicability of solutions (2.8) and (3.6) (on Fig. 3 - this is correspondingly segments 3 and 4) do not overlap.

To remove the shown difficulty we will consider equation

$$\beta U x \varphi'' - U_1 \varphi = 0 \quad (3.10)$$

valid as a zero approximation in the domain  $\sqrt{\alpha} < x < 1$ . (segment 5 on Fig. 3). Solution of this equation has the form

$$\varphi = \sqrt{x} Z_1(-2\sqrt{U_1 x / U \beta}) \quad (3.11)$$

where  $Z_1$  - one of two linearly independent cylindrical functions (for instance,  $I_1$  and  $N_1$ ). For small values of the argument in (3.11) we have  $\varphi_1 = 1$ ,  $\varphi_2 = x$ , i.e., (3.11) passes into (3.6). For large values of the argument the asymptotic behavior of  $Z_1$  coincides with (2.8). This finishes the first procedure, shown in § 2. The answer to the second part of the problem shown in the same place is contained in theorems of Wasow [8], which in the considered case preserve their force.

Equations for eigenvalues in the case of local solutions can easily be written immediately, proceeding just as in the quasiclassical approach for a second order equation [9] in deriving "rules of quantization":

$$\int_{\alpha}^{\infty} \sqrt{\frac{U_1}{\varphi}} dx = (n + \frac{1}{2})\pi, \quad \int_{\alpha}^{\infty} \sqrt{\frac{U_1}{\beta U_1}} dx = (n + \frac{1}{2})\pi \quad (3.12)$$

Expressions (3.12) give two independent solutions for eigenvalues. This corresponds to the fact that on  $+\infty$  (or  $-\infty$ ) we have two linearly independent solutions, determined by (2.8) or (2.9), which subsequently are "extended" to  $-\infty$  (or  $+\infty$ ) each

independently (the connection appears only in following order with respect to  $\alpha/\beta^2$ ).

4. Classification. In equation (3.2), valid when  $x < 1$ , we make the substitution

$$x = \beta y \quad (4.1)$$

This gives

$$\frac{\alpha}{\beta^2} \frac{d^2 \varphi}{dy^2} - U y \frac{d\varphi}{dy} + U_1 \varphi = 0 \quad (4.2)$$

Solution of this equation is obtained by applying the method of Laplace

$$\varphi(y) = \int \frac{1}{t} \exp \left\{ y t - \frac{\alpha}{\beta^2} \frac{t^2}{3U} + \frac{1}{t} \frac{U_1}{U} \right\} dt \quad (4.3)$$

where the integral is taken in the plane of complex variable  $t$  by the contour on whose ends function

$$\exp \left\{ y t - \frac{\alpha}{\beta^2} \frac{t^2}{3U} + \frac{1}{t} \frac{U_1}{U} \right\}$$

turns into zero. The solution of (4.3), in accordance with (4.1) and (3.1), is valid in domain  $y < 1/\beta > 1$ . Let us be limited to consideration of domain

$$1 < y < 1/\beta > 1, \text{ when } \beta < x < 1 \quad (4.4)$$

In the considered domain  $y > 1$ , therefore for calculation of the integral in (4.3) it is possible to use the method of steepest descents. We have four crossing points

$$t_0 \equiv q_i^*(y) = \pm \left( \frac{\beta^2 U}{2\alpha} \right)^{1/2} \left( y \pm \left( y^2 - \frac{\alpha}{\beta^2} \frac{4U_1}{U^2} \right)^{1/2} \right)^{1/2} \quad (4.5)$$

This determines four contours, integration over which gives four linearly independent solutions. Choosing in the appropriate way contours, we obtain solutions

$$\varphi_i(y) \sim \sqrt{\pi} \left[ y \left( \frac{U_1}{U} \frac{1}{q_i^{*2}} - \frac{\alpha}{\beta^2} \frac{q_i^*}{U} \right) \right]^{-1/2} \frac{1}{q_i^{*2}} \exp \int q_i^*(y) dy \quad (i = 1, 2, 3, 4) \quad (4.6)$$

Determining

$$\begin{aligned} q_1^* &= \pm \left( \frac{\beta^2 U}{2\alpha} \right)^{1/2} \left( y - \left( y^2 - \frac{\alpha}{\beta^2} \frac{4U_1}{U^2} \right)^{1/2} \right)^{1/2} & (i = 1, 2) \\ q_3^* &= \pm \left( \frac{\beta^2 U}{2\alpha} \right)^{1/2} \left( y + \left( y^2 - \frac{\alpha}{\beta^2} \frac{4U_1}{U^2} \right)^{1/2} \right)^{1/2} & (i = 3, 4) \end{aligned} \quad (4.7)$$

we obtain from (4.6)<sup>1</sup>

$$\begin{aligned}\varphi_i(y) &\sim (q_i^0)^{-1/2} \exp \int^y q_i^0(y) dy \quad (i=1,2) \\ \varphi_i(y) &\sim (q_i^0)^{-1/2} \exp \int^y q_i^0(y) dy \quad (i=3,4)\end{aligned}\quad (4.8)$$

For large values of  $y$  solutions (4.8), as is simple to verify, pass into corresponding solutions in external region (2.8), (2.9).

Let us consider the value of  $y$  turning into zero internal root in (4.7)

$$y_0 = \pm ia = \pm 2\gamma(\alpha/\beta^2)U_1/U \quad (4.9)$$

(for the considered form of functions  $U_1(x)$  and  $U_2(x)$  in points  $y_0$   $U_1 < 0$  and  $y_0$  is purely imaginary). Points  $y_0$  we will subsequently call branch points. Considering (2.2) and (4.1), we see that the value in branch points  $x \sim \gamma\alpha$  and distance between branch points  $\sim \sqrt{\gamma\alpha}$ . From (4.9) immediately it follows that

$$\alpha < 1 \quad (\alpha/\beta^2 < 1), \quad \alpha > 1 \quad (\alpha/\beta^2 > 1) \quad (4.10)$$

When  $\alpha < 1$  branch points do not enter domain (4.4), where solution (4.8), is valid, and they do not need attention. When  $\alpha > 1$  this is not so and, as we will see subsequently, calculation of branch points essentially changes all consideration and can lead to a qualitatively new physical picture of the process. The case  $\alpha < 1$  we will call weak, and  $\alpha > 1$  strong.

Solution of the problem, carried out in § 3, was valid for  $\alpha/\beta^2 < \beta < 1$ , therefore it is valid to carry it to the weak case.

If one were to introduce the idea of wavelengths

$$\lambda \sim \varphi / \frac{d\varphi}{dx}$$

in the strong case between branch points is "packed" many wavelengths, of which there are none in the weak case. Thus, classification is conducted with respect to the number of wavelengths, which is placed between branch points (i.e., by the

<sup>1</sup>Here and further for simplicity of writing the pre-exponential factor is designated by the same letter as the integrand expression in phase; in reality they differ by terms  $\sim \alpha$ , immaterial when  $x > \gamma\alpha$ .

relationship between parameters  $\alpha$  and  $\beta$ ), although the distance between branch points in both cases is the same ( $\sim \sqrt{\alpha}$ ).

5. Strong case. As already was noted the necessity of calculation of branch points  $a_1, a_2, b_1$  and  $b_2$  (Fig. 4) quite changes the rule of transition from, for instance, the domain  $x < 0_1$  into the domain  $x > 0_1$ .

In order to obtain these rules for (4.8), we will determine the branch of roots in (4.7) in the following way (near point  $0_1$ ):

$$\pm \sqrt{y - \sqrt{y^2 + \alpha}} \begin{cases} \pm \frac{1}{2} \sqrt{2} (\sqrt{y + ia} - \sqrt{y - ia}) & (y > 0) \\ \pm \frac{1}{2} i \sqrt{2} (\sqrt{|y| + ia} - \sqrt{|y| - ia}) & (y < 0) \end{cases} \quad (5.1)$$

$$\pm \sqrt{y + \sqrt{y^2 + \alpha}} \begin{cases} \pm \frac{1}{2} \sqrt{2} (\sqrt{y + ia} + \sqrt{y - ia}) & (y > 0) \\ \pm \frac{1}{2} i \sqrt{2} (\sqrt{|y| + ia} + \sqrt{|y| - ia}) & (y < 0) \end{cases} \quad (5.2)$$

After that solutions (4.8) are written in the form

$$\varphi_{1,2} = \begin{cases} (q_1^*)^{-1/2} \exp \left\{ \pm \int (w_1(y) - w_2(y)) dy \right\} & (y > 0) \\ (q_1^*)^{-1/2} \exp \left\{ \pm i \int (w_1(|y|) - w_2(|y|)) dy \right\} & (y < 0) \end{cases} \quad (5.3)$$

$$\varphi_{3,4} = \begin{cases} (q_2^*)^{-1/2} \exp \left\{ \pm \int (w_1(y) + w_2(y)) dy \right\} & (y > 0) \\ (q_2^*)^{-1/2} \exp \left\{ \pm i \int (w_1(|y|) + w_2(|y|)) dy \right\} & (y < 0) \end{cases} \quad (5.4)$$

where

$$w_1 = \sqrt{\gamma^{1/2} \beta^2 U / \alpha \gamma y - ia}, \quad w_2 = \sqrt{\gamma^{1/2} \beta^2 U / \alpha \gamma y + ia} \quad (5.5)$$

In expressions (5.3), (5.4) the exponential is factored for both branch points, that will allow subsequent use of rules of type [10].

On the left from point A we write an arbitrary solution,<sup>1</sup> turning on  $-\infty$  into zero

$$\begin{aligned} \varphi = & |q_1^*|^{-1/2} \exp \left( -i \int_{\lambda}^y w_1(y) dy + i \int_{\lambda}^y w_2(y) dy \right) + \\ & + D |q_2^*|^{-1/2} \exp \left( \int_{\lambda}^y w_1(y) dy + \int_{\lambda}^y w_2(y) dy \right) \end{aligned} \quad (5.6)$$

<sup>1</sup>The meaning of designations and letters, not specified in this section, is clarified on Fig. 4.

Let us note, however, that of the conditions (24) and (25) only condition (24) has physical meaning, since there should additionally be observed the evident condition  $y > 0$ .

In Fig. 2 there is depicted the dependence (24) (curve 1) which bounds the region of stable burning of powder (region under the curve).

The obtained condition of stable burning of powder (24) differs from the criterion of stability of Ya. B. Zel'dovich (1); the essential parameter influencing burning

-67-

On the right from point A the second term in (5.6) does not change, and the first will be converted according to rules (5.1). This gives

$$\varphi(y) = |q_1^*|^{-1/2} \left[ \exp \left( -i \frac{\pi}{4} + i \int_A^y q_1^* dy \right) + \exp \left( i \frac{\pi}{4} - i \int_A^y q_1^* dy \right) \right] + D |q_2^*|^{-1/2} \exp \left( \int_A^y w_1(y) dy + \int_A^y w_2(y) dy \right) \quad (5.7)$$

Considering formulas (5.3)-(5.5), it is possible to construct a picture of level lines for each of the branch points separately (Fig. 4). Level lines from two neighboring branch points cross on the real axis in points  $C_1, C_2$ . Then solution (5.7) can be rewritten in the following form for  $A < y < C_1$ :

$$\begin{aligned} \varphi(y) = & \frac{1}{|q_1^*|^{1/2}} e^{i\pi/4} \exp \left( -\int_A^y w_1(y) dy + \int_A^y w_2(y) dy \right) + \\ & + \frac{1}{|q_1^*|^{1/2}} e^{-i\pi/4} \exp \left( \int_A^y w_1(y) dy - \int_A^y w_2(y) dy \right) + \\ & + D |\bar{q}_2^*|^{-1/2} \exp \left( \int_A^y w_1(y) dy + \int_A^y w_2(y) dy \right) \end{aligned} \quad (5.8)$$

where

$$\begin{aligned} i\varphi_1 = & \frac{\beta}{V^{2\alpha}} \left\{ \int_{L_1} \sqrt{U_2(z) - V^4 U_1(z) \alpha / \beta^2} dz - \right. \\ & \left. - \int_{L_2} \sqrt{U_2(z) + V^4 U_1(z) \alpha / \beta^2} dz \right\} - i \frac{\pi}{4} \end{aligned} \quad (5.9)$$

Integrals in (5.8) are taken from branch point  $a_1(a_2)$  along the line where  $w_1(w_2)$  is purely imaginary to point  $C_1$  and further with respect to the real axis. Contours  $L_1$  and  $L_2$  in (5.9) start at point A, go along real axis to point  $C_1$  and further with respect to lines where  $w_1$  and  $w_2$  are correspondingly purely imaginary, to branch points  $a_1, a_2$ . In writing (5.9) it is considered also that near point  $O_1$ , where  $U_2 = 0$ , expressions under the sign of the integral pass correspondingly into

$$\begin{aligned} p_1^* &= \sqrt[3]{\beta^2 U / \alpha} (z - ia) \\ p_2^* &= \sqrt[3]{\beta^2 U / \alpha} (z + ia) \end{aligned}$$

Cuts are selected with respect to lines 1. It is not difficult to verify that  $\varphi_1$ , determined by expression (5.9), is purely real.

-79-

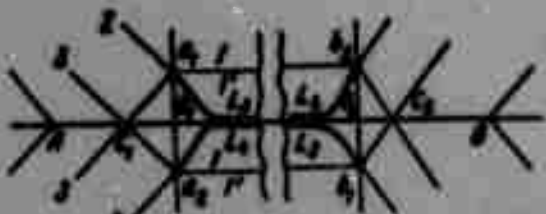


Fig. 4.

So that solution (5.8), determined on the left from point  $O_1$ , is written on the right from  $O_1$ , we will use rules of bypass given in the appendix. It is convenient to introduce designations:

$$p_1 = \sqrt[1/2]{(\beta^2/a)(U_2 - \gamma^2 U_1 a / \beta^2)}, \quad p_2 = \sqrt[1/2]{(\beta^2/a)(U_2 + \gamma^2 U_1 a / \beta^2)} \quad (5.10)$$

Then for  $O_1 < y < O_2$  we have accurate to a constant factor

$$\begin{aligned} \varphi(y) = & i e^{i\varphi_1} |p_1 + p_2|^{-1/2} \exp\left(i \int_{a_1}^y p_1(z) dz + i \int_{a_2}^y p_2(z) dz\right) - \\ & - (i e^{i\varphi_1} + D) |p_1 + p_2|^{-1/2} \exp\left(-i \int_{a_1}^y p_1(z) dz - i \int_{a_2}^y p_2(z) dz\right) + \\ & + e^{i\varphi_1} |p_1 - p_2|^{-1/2} \exp\left(i \int_{a_1}^y p_1(z) dz - i \int_{a_2}^y p_2(z) dz\right) + \\ & + (2 \cos \varphi_1 - i D) |p_1 - p_2|^{-1/2} \exp\left(-i \int_{a_1}^y p_1(z) dz + i \int_{a_2}^y p_2(z) dz\right) \end{aligned} \quad (5.11)$$

Here integration is done from  $a_1, a_2$  correspondingly over lines  $L_3, L_4$  (Fig. 4), descending to the real axis and proceeding along it to point  $y$ . Transporting solution (5.11) to point  $O_2$ , we rewrite it in the form

$$\begin{aligned} \varphi(y) = & i e^{i\varphi_1} \frac{\Phi}{|p_1 + p_2|^{1/2}} \exp\left(-i \int_y^{a_1} p_1(z) dz - i \int_y^{a_2} p_2(z) dz\right) - \\ & - \frac{i e^{i\varphi_1} + D}{|p_1 + p_2|^{1/2}} \exp\left(i \int_y^{a_1} p_1(z) dz + i \int_y^{a_2} p_2(z) dz\right) + \\ & + \frac{e^{i\varphi_1} \Psi}{|p_1 - p_2|^{1/2}} \exp\left(-i \int_y^{a_1} p_1(z) dz + i \int_y^{a_2} p_2(z) dz\right) + \\ & + \frac{2 \cos \varphi_1 - i D}{|p_1 - p_2|^{1/2}} \exp\left(i \int_y^{a_1} p_1(z) dz - i \int_y^{a_2} p_2(z) dz\right) \end{aligned} \quad (5.12)$$

Integrals from  $y$  to  $b$  decrease in the same meaning as from  $y$  to  $a$ . Furthermore, we will put:

$$\Phi \equiv e^{i\varphi_1} = \exp\left(i \int_{L_3} p_1(z) dz + i \int_{L_4} p_2(z) dz\right) \quad (5.13)$$

$$\Psi = \exp\left(-i \int_{L_3} p_1(z) dz + i \int_{L_4} p_2(z) dz\right) \quad (5.14)$$

Contours  $L_3$  and  $L_4$  are designated on Fig. 4. It is easy to verify that index of the exponential in (5.14) is purely real, and  $\varphi_2$  in (5.13) is purely imaginary. For this we will bend contour  $L_3$  so that it goes from  $a_1$  to  $O_1$ , then along the real axis and further from  $O_2$  to  $b_1$ .

An analogous procedure will be carried out also with  $L_4$ . Then, according to (5.10), on the real axis where  $L_3$  and  $L_4$  coincide, we have

$$\int_{a_1}^{a_2} (p_1 - p_2) dy - \text{purely imaginary} \quad \int_{a_1}^{a_2} (p_1 + p_2) dy - \text{purely real}$$

Considering that

$$\int_{a_1}^{a_2} \sqrt{z + ia} dz = (ia)^{1/2}, \quad \int_{a_1}^{a_2} \sqrt{z - ia} dz = (-ia)^{1/2}$$

we arrive immediately to the above affirmation.

On the right from point  $O_2$ , using again the rules of bypass (see appendix), we obtain

$$\begin{aligned} \varphi(y) = & |p_1 + p_2|^{-1/2} \left( i\Phi e^{i\varphi_1} - i \frac{2\cos\varphi_1 - iD}{\Psi} \right) \exp \left( \int_{a_1}^y p_1(z) dz + \int_{a_2}^y p_2(z) dz \right) + \\ & + |p_1 + p_2|^{-1/2} \left( \frac{2\cos\varphi_1 - iD}{\Psi} - \frac{ie^{i\varphi_1} + D}{\Phi} \right) \exp \left( \int_{a_1}^y p_1(z) dz + \int_{a_2}^y p_2(z) dz \right) + \\ & + |p_1 - p_2|^{-1/2} \left( -e^{i\varphi_1}\Phi + e^{i\varphi_1}\Psi - \frac{e^{i\varphi_1} - iD}{\Phi} + \frac{2\cos\varphi_1 - iD}{\Psi} \right) \times \\ & \times \exp \left( -\int_{a_1}^y p_1(z) dz + \int_{a_2}^y p_2(z) dz \right) + |p_1 - p_2|^{-1/2} \frac{2\cos\varphi_1 - iD}{\Psi} \times \\ & \times \exp \left( \int_{a_1}^y p_1(z) dz - \int_{a_2}^y p_2(z) dz \right) \end{aligned} \quad (5.15)$$

The condition of absence on  $+\infty$  of growing solutions gives

$$\begin{aligned} e^{i\varphi_1}\Phi\Psi &= 2\cos\varphi_1 - iD \\ (\Psi - \Phi)e^{i\varphi_1} - \frac{e^{i\varphi_1} - iD}{\Phi} + \frac{2\cos\varphi_1 - iD}{\Psi} &= e^{i\varphi_1} \frac{2\cos\varphi_1 - iD}{\Psi} \end{aligned} \quad (5.16)$$

$$i\varphi_2 = - \int_{L_1'} p_1(z) dz + \int_{L_2'} p_2(z) dz \quad (5.17)$$

Here contours  $L_1'$  and  $L_2'$  are analogous to contours  $L_1$ ,  $L_2$  and are taken correspondingly from  $b_1$ ,  $b_2$  through point  $C_2$  to  $B$ . Let us note that  $\varphi_3$ , as also  $\varphi_2$ , is purely real and positive. Solving system (5.16), we find

$$e^{i(\varphi_1 + \varphi_2 + \varphi_3)} = \pm 1, \quad \text{or} \quad \varphi_1 + \varphi_2 + \varphi_3 = n\pi \quad (5.18)$$

Hence

$$i \int_{L_1} p_1 dz - i \int_{L_2} p_2 dz + \int_{L_3} p_1 dz + \int_{L_4} p_2 dz - i \int_{L_1'} p_1 dz + i \int_{L_2'} p_2 dz = \left(n + \frac{1}{2}\right) \pi \quad (5.19)$$

Equation (5.19) constitutes the generalized "rule of quantization" for the strong case. The left part of (5.19) constitutes a full advance of phase, consisting of three parts: 1) advance of phase in domain  $AO_1$ ; 2) advance of phase in domain  $O_1O_2$ ; 3) advance of phase in domain  $O_2B$ .

Length of waves in these regions

$$\lambda_z \sim \left(\int \sqrt{U_1/\beta U_2} dx\right)^{-1} \quad \text{in } AO_1 \text{ and } O_2B, \quad \lambda_x \sim \left(\int \sqrt{U_2/\alpha\beta} dx\right)^{-1} \quad \text{in } O_1O_2$$

Such strong "cohesion" of oscillations is characteristic for the strong case, and in this meaning condition (5.19) expresses this fact.

6. Note. 1. According to classification conducted in § 4, when  $\alpha/\beta^2 < 1$  we have a weak case. The solution conducted in § 3 is valid when  $\alpha/\beta^2 < \alpha$ . Thus, for the weak case domain  $\beta \leq \alpha/\beta^2 < 1$  remains unconsidered. The solution given in § 3, as was shown, is a generalization of known solution [1] on a quasiclassical case. It is possible, however, to construct a solution when  $\alpha/\beta^2 < 1$ , including, as particular case  $\alpha/\beta^2 < \beta$ . For this we will turn to formulas (4.6)-(4.9). Solutions (4.8) are desired for  $\alpha/\beta^2 < 1$ . Rules of joining for them are the same as in § 3, inasmuch as branch points (4.9) do not lie in domain of validity (4.8). "Rules of quantization" (3.12) remain as before.

The given arguments unify the method well-developed in §§ 4 and 5. A purely technical distinction is connected with the purpose that the constructed asymptotic solutions (4.8) have different structure of Stokes lines depending upon whether or not branch points (4.9) fall into the domain where solution (4.8) is valid.

2. Given asymptotic method is easily generalized on that case when behavior  $U_2(x)$  near zero  $U_2$  has the form  $U_2 \sim U_2 x^m$ . Besides it is natural that conditions of joining solutions change; however equations (3.12) and (5.18) remain as before. The case  $m = 2$  for weak coupling was considered in [7]. For instance, the "gravitational mode," found in [7], is obtained immediately from second condition (3.12).

3. As is known [5, 6, 11] presence of heterogeneity in medium can lead to one type of oscillations in a certain domain creates a new type of oscillations (effect of "transformation" of waves). A detailed physical picture of this phenomenon is in [5]. The method well-developed above can be applied to this phenomenon. Effect of transformation already is contained in the solution. Thus for instance, in a strong case (§ 5) the presence of oscillatory solution  $\varphi_{3,4}$  in domain  $O_1O_2$  leads to the appearance of oscillatory solution  $\varphi_{1,2}$  in domain  $AO_1$ . It is possible to say that points leading to transformation are branch points. Coefficient of transformation is obtained as the ratio of amplitudes  $\varphi_1$  to  $\varphi_3$ . It is natural that in the weak case the effect of transformation is small since "birth" of a new solution occurs with respect to small parameter  $\alpha/\beta^2$ . Essential in the strong case is strong transformation. Coefficient of transformation can be in this case  $\sim 1$ .

7. Certain peculiarities of instability of plasma in field of gravity. An example of application of the above theory is peculiarities of stabilization of the so-called "groove" instability of plasma during calculation of finiteness of Larmor radius of ions [12].

The differential equation for perturbed magnitudes in an interesting case has, as is known [3], form

$$\beta \varphi'' - \left\{ 1 - \frac{G}{r(r-1)} \right\} \varphi = 0 \quad (7.1)$$

$$\beta = \frac{1}{(kL)^2}, \quad r = \frac{\omega}{\omega_i}, \quad \omega_i = \frac{eT}{mH_0} k_y \frac{n_0'}{n_0}, \quad G = \frac{g}{\omega_i^2} \frac{n_0'}{n_0}, \quad n_0' = \frac{dn_0}{dx}$$

Here  $L$  - characteristic dimension,  $g$  - acceleration due to gravity,  $n_0$  - density,  $T$  - temperature,  $H_0$  - magnetic field strength. Here instability is stabilized, if  $G \lesssim 1$ , and the consideration may be regarded as correct when existence of finite solutions is shown. However, as follows from (7.1), at the point where  $r = 1$ , the coefficient with  $\varphi$  undergoes a discontinuity, and it is necessary to substantiate the existence of finite solutions. We will therefore originate from wider assumptions in deriving the equation for perturbed magnitudes and will consider perturbation of temperature  $T$ , satisfying in the quasiclassical approach the equation

$$\frac{3}{2} n_0 \left( \frac{\partial T}{\partial t} + (\mathbf{V}_0 \nabla) T \right) + n_0 T_0 \operatorname{div} \mathbf{V}_1 = - \operatorname{div} \mathbf{q}_1 \quad (7.2)$$

$$\mathbf{q}_1 = \frac{5}{2} \frac{en_0 T_0}{eH_0} (h \nabla T) \quad \left( h = \frac{H_0}{H} \right)$$

Here  $V_{01}$ ,  $T_0$  - correspondingly undisturbed speed and temperature of ions. Electrons for simplicity will be considered cold. Choosing perturbation in the form  $\varphi(x) \exp(iyk_y + i\omega t)$  and conducting standard simple calculations, distinguished from the conclusion (7.1) only by calculation of perturbation of temperature, we will obtain in the system of coordinates where ions are at rest, the equation

$$\varphi^{IV} - \left\{ \frac{2}{\beta} + (r-1) \left[ 3rR^2 - \frac{G}{\beta(r-1)^2} \right] \right\} \varphi'' + \left\{ \frac{1}{\beta^2} + \frac{(r-1)}{\beta} \left[ 3rR^2 - \frac{G}{\beta(r-1)^2} \right] - 3 \frac{R^2 G}{\beta} \right\} \varphi = 0 \quad (R = \frac{L}{r_1}) \quad (7.3)$$

Here  $r_1$  - Larmor radius of ions.

Let us consider for simplicity the case of weak connection, corresponding to two separate equations for finding natural frequencies (3.12). The second of equation (3.12) corresponds to the case of usual groove perturbations, where role of the second "reversal point" is played by the point where  $U_2 = 0$ , and finite solutions exist if the outside interval between "reversal points" potential  $U_1/U_2$  leads to fading solutions. If

$$rR^2 > \frac{G}{\beta(r-1)^2} \quad (G \leq 1)$$

from (7.3) we will obtain a result corresponding to (7.1), i.e., stabilization of instability. Let us consider now what the second equation for natural frequencies leads to, i.e.,

$$\int_0^{a_2} \sqrt{U_2} dx = (n + 1/2) \pi$$

Qualitatively the correct result will be obtained from the condition  $U_2 \approx 0$ . Using  $U_2$  from (7.3) when  $r = 1 + r_1$  ( $r_1 \ll 1$ ), we will find that

$$r_1 = \frac{1}{2}(k_y r_1)^2 \pm \sqrt{\frac{1}{4}(k_y r_1)^4 + (k_y r_1)^2 G} \quad (7.4)$$

From (7.4) we see that calculation of perturbations of temperature leads to instability if

$$|G| > k_y^2 r_1^2 \quad (7.5)$$

and stabilization of instability imposes harder conditions on Larmor radius than is

required according to analysis of equation (7.1).

Distance between points of "intersection" of solutions in this case

$$x \sim k_y r_i L \quad (7.6)$$

and the conducted consideration is valid if  $L r_i^{-1} (k_y r_i)^{1/2} < 1$ .

8. Application. Let us derive a rule of joining solutions for  $\varphi_1$  during bypass around branch points; to be specific we will take points  $a_1, a_2$  on Fig. 4. Let us start from line 1, outgoing from point  $a_1$ . On this line the solution will be written in the form

$$\begin{aligned} \varphi(y) = & A_1 \Pi_1 \exp \left( i \int^y (\omega_1(z) - \omega_2(z)) dz \right) + B_1 \Pi_2 \exp \left( -i \int^y (\omega_1(z) - \omega_2(z)) dz \right) + \\ & + C_1 \Pi_3 \exp \left( i \int^y (\omega_1(z) + \omega_2(z)) dz \right) + D_1 \Pi_4 \exp \left( -i \int^y (\omega_1(z) + \omega_2(z)) dz \right) \end{aligned} \quad (8.1)$$

where preexponents  $\Pi_i$  are determined from (4.6). We have

$$\begin{aligned} & \text{in passing around point } a_1 \\ & \Pi_1 = \Pi_2 = \exp(-1/2 \ln(\omega_1 - \omega_2)), \quad \Pi_3 = \Pi_4 = \exp(-1/2 \ln(\omega_1 + \omega_2)), \\ & \text{in passing around point } a_2 \\ & \Pi_1 = \Pi_2 = \exp(-1/2 \ln(\omega_2 - \omega_1)), \quad \Pi_3 = \Pi_4 = \exp(-1/2 \ln(\omega_2 + \omega_1)) \end{aligned}$$

From (8.1) it is clear that it is possible to bypass points  $a_1$  and  $a_2$ . To bypass every branch point separately the same rules of joining are obtained as in [10] (one should note that in [13] is given another method of simultaneous bypass of points of intersection of solutions).

Let us note that around point  $a_1$  independently is carried out bypass of the pair of solutions for  $A_1$  and  $D_1$ ; around point  $a_2$  - bypass of the pair of solutions for  $A_1$  and  $C_1$  and the pair of solutions for  $B_1$  and  $D_1$  is analogously independent. Let us designate by  $A_1, B_1, C_1, D_1$  the system of coefficients of solution near lines with the number 1, outgoing from points  $a_1, a_2$ . Then the result of simultaneous bypass around  $a_1, a_2$  gives the desired formulas of joining

$$\begin{aligned} A_2 &= A_1 + iD_1, & B_2 &= B_1 + iD_1, & C_2 &= iA_1 + iB_1 + C_1 - D_1, & D_2 &= D_1 \\ A_3 &= A_2 + iC_2, & B_3 &= B_2 + iC_2, & C_3 &= C_2, & D_3 &= iA_2 + iB_2 - C_2 + D_2 \\ A_1' &= A_3 + iD_3, & B_1' &= B_3 + iD_3, & C_1' &= iA_3 + iB_3 + C_3 - D_3, & D_1' &= D_3 \\ A_1' &= -B_1, & B_1' &= -A_1, & C_1' &= -D_1, & D_1' &= -C_1 \end{aligned} \quad (8.2)$$

In writing the last line in (8.2) it is considered that the solution of equation (2.1) should be analytic in complex plane  $y$ .

The authors thank A. A. Galeev, V. N. Orayevskiy for valuable discussions.

Submitted  
27 May 1964

#### Literature

1. Lin' Tszya-tszyao. Theory of hydrodynamic stability. Publishing House of Foreign Literature, M., 1958.
2. L. I. Rudakov and R. Z. Sagdeyev. Instability of inhomogeneous rarefied plasma in strong magnetic field. Reports of Academy of Sciences. USSR, 1961, Vol. 138, p. 581.
3. A. A. Galeev, S. S. Moiseyev and R. Z. Sagdeyev. Theory of stability of inhomogeneous plasma. Atomic energy, 1963, Vol. 15, p. 451.
4. V. P. Silin and A. A. Rukhadze. Method of geometric optics in electrodynamics of inhomogeneous plasma. Progress phys. sciences, 1964, Vol. 82, p. 499.
5. V. L. Ginzburg. Propagation of electromagnetic waves in plasma. Fizmatgiz, M., 1960.
6. N. G. Denisov. Dis. Gorkiy State University, 1954; V. V. Zheleznyakov and Ye. A. Zlotnik. Transition of plasma waves into electromagnetic waves in inhomogeneous isotropic plasma. Pub. higher educ. inst. (Radio physics), 1962, Vol. 5, p. 644.
7. H. Furth, I. Killen and M. Rosenbluth. Finite resistivity instabilities of a sheet pichn. Phys. fluids, 1963, Vol. 6, 459.
8. M. Wasow. The complex asymptotic theory of a fourth order differential equation of hydrodynamics. Ann. Math., 1948, Vol. 49, p. 852.
9. L. D. Landau and Ye. M. Lifshits. Quantum mechanics. Fizmatgiz, M., 1963.
10. Furry. Two notes on phase-integral methods. Phys. Rev., 1957, Vol. 71, p. 360.
11. D. A. Tidman. Radio emission by plasma oscillations in nonuniform plasmas. Phys. Rev., 1960, Vol. 117, p. 366.
12. M. Rosenbluth, N. Krall and N. Rostoker. Finite Larmor radius stabilization. Nuclear fusion, 1962, Supplement, 1, 143.
13. E. C. Stueckelberg. Theorie der unelastischen Stösse zwischen Atomen. Helv. Phys. Acta, 1932, Vol. 5, p. 369.

ONE CASE OF FREE CONVECTION OF A LIQUID  
IN THE PRESENCE OF DISSOLVING  
AND ABSORBING WALLS

G. A. Bugayenko

(Cherkassy)

Convection of a liquid is considered in specific conditions when among bodies bounding the flow are those which dissolve and those which absorb the diffusing substance, but practically change neither geometric dimensions nor form. The exact solution is found for the problem on convection for the middle part of the space between vertical coaxial cylinders heated to different temperatures.

The presence of dissolved bodies in liquid makes it inhomogeneous in composition. Macroscopic motion of liquid and molecular transfer of substance change the composition of the solution. In such conditions the liquid is a binary mixture [1].

Equations of stationary convection of a binary liquid mixture taking into account thermal diffusion and diffusion thermal conduction have the form [2]

$$\begin{aligned}(\nabla) \mathbf{v} &= -\rho_0^{-1} \nabla p + \nu \nabla^2 \mathbf{v} + g(\beta_1 T + \beta_2 C) \mathbf{r} \\(\nabla) T &= (\chi + N\lambda^2 D) \nabla^2 T + N\lambda D \nabla^2 C \\(\nabla) C &= \lambda D \nabla^2 T + D \nabla^2 C \\\operatorname{div} \mathbf{v} &= 0\end{aligned}\tag{1}$$

Here  $\mathbf{v}$  — hydrodynamic speed;  $T$  and  $C$  — deviation of temperature and concentration of light component of mixture from their mean values  $\langle T \rangle$  and  $\langle C \rangle$  correspondingly;  $p$  — pressure counted from hydrostatic when  $T = \langle T \rangle$  and  $C = \langle C \rangle$ ; coefficients of kinematic viscosity  $\nu$ , temperature transfer  $\chi$ , diffusion  $D$  and thermal diffusion  $\lambda$

and expansion of liquid  $\beta_1$  and  $\beta_2$  are taken for  $\langle T \rangle$  and  $\langle C \rangle$ ; thermodynamic coefficient  $N$  determines (together with  $\lambda$ ) diffusion thermal conduction of medium;  $\gamma$  - unit vector, directed vertically upwards;  $g$  - strength of gravity field.

Let us assume that liquid fills space between two coaxial cylindrical surfaces, temperatures of which are maintained constant. Let us study established convection flow of liquid on the assumption that one of the cylinders is dissolved in a liquid, and the other absorbs the diffusing substance which gets on it.

Let us formulate at first boundary conditions of the problem. Speed on surface of internal (radius  $R_1$ ) and external (radius  $R_2$ ) cylinders is equal to zero; temperature on surface of internal cylinder is constant and equals  $T_0$ ; temperature on surface of external cylinder  $T_1$ ; space between cylinders is closed, and quantity of liquid flowing in a unit of time through normal to axis section is equal to zero; external cylinder is dissolved, so that nearby its surface when  $r = R_2$  equilibrium exists, at which concentration of liquid adjoining surface of cylinder is equal to concentration of saturated solution  $C = C_*$  (diffusion of substance from the layer adjoining the body occurs slower than process of dissolution can occur), and surface of internal cylinder  $r = R_1$  absorbs the diffusing substance getting on it, so that on this surface  $C = 0$  (as in chemical reactions occurring on the surface of a solid body) [1].

We will use the cylindrical system of coordinates  $r, \phi, z$ ; a axis is directed along the common axis of the cylinders vertically upwards.

From considerations of symmetries we look for solution of the problem in the form

$$\begin{aligned} v_r = v_\phi = 0, \quad T = T(r), \quad C = C(r) \\ v_z = v_z(r, z), \quad p = p(r, z) \end{aligned}$$

In these assumptions equations (1) are considerably simplified. From the continuity equation it follows that  $dv_z/dz = 0$ , and this means  $v_z = v(r)$ . From the first equation of system (1) we find that  $dp/dr = 0$  and  $dp/d\phi = 0$ , whence it follows that  $p$  depends only on  $z$ . System (1) in the considered case is brought to

$$\begin{aligned} \frac{1}{\rho_0} \frac{dp}{dz} = \frac{\gamma}{r} \frac{d}{dr} \left( r \frac{dv}{dr} \right) + g(\beta_1 T + \beta_2 C) \\ \frac{d}{dr} \left( r \frac{dT}{dr} \right) = 0, \quad \frac{d}{dr} \left( r \frac{dC}{dr} \right) = 0 \end{aligned} \quad (2)$$

Boundary conditions

$$\begin{aligned} v(R_1) = v(R_2) = 0, \quad T(R_1) = T_0, \quad T(R_2) = T_1, \\ C(R_1) = 0 \quad C(R_2) = C_0 \end{aligned} \quad (3)$$

Since in the first equation of system (2) the left part does not depend on  $r$ , and the right on  $z$ , both parts are equal to a constant.

Integrating the second and third equation of system (2) under boundary conditions (3), we find

$$T = \frac{T_1 - T_0}{\ln(R_2/R_1)} \ln \frac{r}{R_1} + T_0, \quad C = \frac{C_0}{\ln(R_2/R_1)} \ln \frac{r}{R_1} \quad (4)$$

Consequently, distribution of temperature and concentration turns out to be the same as in the case of a motionless medium; this circumstance is connected with the fact that hydrodynamic speed is perpendicular to gradient of temperature and concentration.

The first equation of (2) we rewrite so

$$\frac{1}{r} \frac{d}{dr} \left( r \frac{dv}{dr} \right) + \frac{\epsilon}{v} (\beta_1 T + \beta_2 C) = A \quad (5)$$

where  $A$  — constant.

Placing (4) in (5), we will obtain

$$\frac{1}{r} \frac{d}{dr} \left( r \frac{dv}{dr} \right) + a \ln \frac{r}{R_1} + b = 0 \quad (6)$$

where

$$a = \left( \beta_1 \frac{T_1 - T_0}{\ln(R_2/R_1)} + \beta_2 \frac{C_0}{\ln(R_2/R_1)} \right) \frac{\epsilon}{v}, \quad b = \beta_1 T_0 \frac{\epsilon}{v} - A \quad (7)$$

Integrating (6) under boundary conditions (3), we will find speed

$$v = 1/4 r^2 [a (1 - \ln \frac{r}{R_1}) - b] + k \ln \frac{r}{R_1} + k_1 \quad (8)$$

Constants of integration  $k$  and  $k_1$  will be determined from three conditions:

$$v(R_1) = 0, \quad v(R_2) = 0, \quad \int_{R_1}^{R_2} v r dr = 0$$

the last of them is the condition of closure of flow.

As a result we will obtain the values

$$k_1 = \frac{R_1^3}{4\Delta} \left( P \ln \frac{R_2}{R_1} - MQ \right), \quad k = \frac{1}{\ln(R_2/R_1)} \left[ M + k_1 \left( \frac{R_2^3}{R_1^3} - 1 \right) \right]$$

Here

$$4\Delta = \frac{1}{2} (R_2^4 - R_1^4) \ln \frac{R_2}{R_1} + \frac{1}{2} (R_2^3 - R_1^3) R_1^2 \ln \frac{R_2}{R_1} + Q (R_2^3 - R_1^3)$$

$$M = \frac{1}{2} \epsilon R_2^3 \ln \frac{R_2}{R_1}$$

$$P = a/16 [R_2^4 \ln \frac{R_2}{R_1} - \frac{1}{2} (R_2^4 - R_1^4)]$$

$$Q = \frac{1}{2} [R_2^3 \ln \frac{R_2}{R_1} - \frac{1}{2} (R_2^3 - R_1^3)]$$

Constant A in (5) turns out to be

$$A = \frac{\epsilon R_2 T_0}{v_0} - \epsilon + \frac{1}{\Delta} \left\{ P \ln \frac{R_2}{R_1} + MQ \right\}$$

From the solution, in particular, it follows that the law of distribution of concentration is analogous to the law of distribution of temperature (both logarithmic) and that heat transfer from a hot cylinder to a cold cylinder is determined (as also in the absence of dissolving and absorbing bodies) only by molecular thermal conduction of liquid. The diffusion flow of the dissolved substance is radial and is equal to

$$J_r = -\rho_0 D \left( \frac{\partial C}{\partial r} + \lambda \frac{\partial T}{\partial r} \right) = -\frac{\rho_0 D}{\ln(R_2/R_1)} [(T_1 - T_0)\lambda + C_0]$$

The quantity of substance absorbed in a unit of time in area per unit of length of absorbing cylinder, is constant and equal to  $2\pi r J_r$ . The same quantity of substance enters the liquid from the dissolved cylinder.

Submitted  
29 January 1964

#### Literature

1. L. D. Landau and Ye. M. Lifshits. Mechanics of solid media. Gostekhteorizdat, 1953, Ch. VI.
2. I. G. Shaposhnikov. The theory of convection phenomena in a binary mixture. PMM, 1953, Vol. 17, Issue 5.
3. G. Z. Gershuni. Free thermal convection in the space between vertical coaxial cylinders. Reports of Academy of Sciences of USSR, 1952, Vol. 86, No. 4.

SPLITTING A STREAM OF LIQUID,  
STREAMLINED BY A GAS FLOW

V. A. Borodin, L. N. Britneva,  
Yu. F. Dityakin and  
V. I. Yagodkin

(Moscow)

The problem about disintegration of a cylindrical stream of ideal liquid, transversely streamlined by the flow of another ideal liquid, has both independent and also auxiliary value during the analysis of oscillations and splitting of a liquid torus [1].

This work studies two forms of waves propagating along the surface of a stream: a) tangential waves, deforming the stream in the plane of its cross section and leading to its splitting of into longitudinal threads; b) longitudinal waves.

There are two works [2, 3] in which influence on a cylindrical stream of liquid by a plane shock wave directed normally to the axis of the stream was studied.

Experiments showed that for a given speed of gas flowing around the stream there exists a certain critical diameter of the stream; when values of diameter are smaller than critical, the stream turns out to be stable and cannot be destroyed by a shock wave of given intensity. Evidently, this conclusion is analogous to the conclusion concerning the existence of a critical value of Weber number ( $W = aU_0^2\rho_2/\sigma$ ,  $a$  - radius of drop,  $U_0$  - relative speed of drop,  $\rho_2$  - density of liquid of external medium,  $\sigma$  - coefficient of surface tension of liquid of medium) during disintegration of a drop in a flow of gas [4, 5, 6].

The mentioned experiments substantiate applicability of the method of small perturbations to solution of the problem about splitting of a stream.

1. Let us assume that a stream of ideal liquid of radius  $a$  (density  $\rho_1$ ) is flowed around normally to the axis by a flow of another liquid (density  $\rho_2$ ) with constant speed  $U_0$ .

Velocity potential of perturbations will be designated for the stream through

$\Phi_1(r, \varphi, t)$ , for the medium — through  $\Phi_2(r, \varphi, t)$ , where  $r, \varphi$  — cylindrical coordinates,  $t$  — time. Speed on boundary when  $r = a$   $U_\varphi = 2U_0 \sin \varphi$ .

Velocity potential of perturbed motion of liquid satisfies Laplace equation

$$\frac{\partial}{\partial r} \left( r \frac{\partial \Phi}{\partial r} \right) + \frac{1}{r^2} \frac{\partial^2 \Phi}{\partial \varphi^2} = 0 \quad (1.1)$$

Speeds of perturbations are expressed through

$$v_r = \partial \Phi / \partial r, \quad v_\varphi = r^{-1} \partial \Phi / \partial \varphi \quad (1.2)$$

Pressure during perturbed motion of liquid is determined by Lagrange-Cauchy integral

$$\frac{p}{\rho} = - \frac{\partial \Phi}{\partial t} - U_\infty v_\varphi \quad (1.3)$$

Let us assume that dependence of potential of speeds on time has the form

$$\Phi(r, \varphi, t) = u(r, \varphi) e^{-i\beta t} \quad (1.4)$$

where  $\beta$  — complex frequency of oscillations. Boundary conditions are the following.

1. Continuity of normal components of speeds on boundary

$$v_r = v_r' + U_n, \quad r = a + \zeta \quad (1.5)$$

Here  $\zeta$  — radial deflection of perturbed surface from cylinder,  $U_n$  — projection of flow rate on normal to perturbed surface of stream

$$U_n = \frac{2U_0}{\beta a} \sin \varphi \frac{\partial u_1}{\partial r \partial \varphi} \quad (1.6)$$

Radial deflection  $\zeta$  is determined from relationship

$$\frac{\partial \zeta}{\partial t} = \left( \frac{\partial \Phi_1}{\partial r} \right)_{r=a} \quad (\zeta = \zeta^*(\varphi) e^{-i\beta t}) \quad (1.7)$$

From (1.6) and (1.7) we will obtain the first boundary condition in the form

$$\frac{\partial u_1}{\partial r} - \frac{\partial u_2}{\partial r} - \frac{2U_0}{\beta a} \sin \varphi \frac{\partial u_1}{\partial r \partial \varphi} = 0 \quad \text{when } r = a \quad (1.8)$$

2. Equality of difference of perturbed pressures on surface of flow to pressure of surface tension

$$p_1 - p_2 = \sigma H \quad \left( H = -\frac{\zeta}{a^3} - \frac{1}{a^3} \frac{\partial^2 \zeta}{\partial \varphi^2} \right) \quad (1.9)$$

Here  $H$  — perturbation of mean curvature of interface.

From relationships (1.2)-(1.4), (1.7) and the equation  $\Delta u_1 = 0$  we will obtain the second boundary condition in the form

$$i\beta u_{,r_1} - i\beta u_{,r_2} + 2U_0 \sin \varphi \frac{r_2}{a} \frac{\partial u_1}{\partial \varphi} = -\frac{\sigma}{i\beta_2} \left( \frac{\partial^2 u_1}{\partial r^2} + \frac{3}{a} \frac{\partial^2 u_1}{\partial r^2} \right) \quad \text{when } r = a \quad (1.10)$$

Let us introduce dimensionless parameters

$$R = \frac{r}{a}, \quad Z = i\beta \left( \frac{a^3 \rho_1}{\sigma} \right)^{1/2}, \quad M = \frac{\rho_2}{\rho_1}, \quad W = \frac{\sigma U_0^2 \rho_2}{\sigma} \quad (1.11)$$

$$\Psi = 2U_0 \left( \frac{a \rho_1}{\sigma} \right)^{1/2} \sin \varphi = \psi_0 \sin \varphi, \quad \psi_0 = 2 \left( \frac{W}{M} \right)^{1/2}$$

boundary conditions will be converted to the form

$$\frac{\partial u_1}{\partial R} - \frac{\partial u_1}{\partial R} - \frac{\psi_0 \sin \varphi}{Z} \frac{\partial u_1}{\partial R \partial \varphi} = 0 \quad \text{when } R = 1 \quad (1.12)$$

$$Z^2 u_1 - M Z^2 u_2 + M \psi_0 Z \sin \varphi \frac{\partial u_1}{\partial \varphi} + \frac{\partial^2 u_1}{\partial R^2} + 3 \frac{\partial^2 u_1}{\partial R^2} = 0 \quad \text{when } R = 1 \quad (1.13)$$

Quotients (bounded) of the solution of Laplace equation will be written in the form

$$u_1 = \sum_{m=0}^{\infty} A_m R^m e^{im\varphi}, \quad u_2 = \sum_{m=0}^{\infty} B_m R^{-m} e^{im\varphi} \quad (1.14)$$

For  $\psi_0 = 0$  we will obtain eigenvalues (frequency of oscillations of stream)

$$Z^2 = -\frac{m(m^2 - 1)}{M + 1} \quad (1.15)$$

analogous to oscillations of a spherical drop (Rayleigh case). Placing (1.14) in (1.12) and (1.13), we will obtain for the general case ( $\psi_0 \neq 0$ )

$$\sum_{m=0}^{\infty} \left[ m A_m e^{im\varphi} + m B_m e^{im\varphi} - \frac{\psi_0}{2Z} m^3 A_m e^{i(m+1)\varphi} + \frac{\psi_0}{2Z} m^3 B_m e^{i(m-1)\varphi} \right] = 0 \quad (1.16)$$

$$\sum_{m=0}^{\infty} \left[ Z^2 A_m e^{im\varphi} - MZ^2 B_m e^{im\varphi} + \frac{M\psi_0 Z}{2} m B_m e^{i(m+1)\varphi} - \frac{M\psi_0 Z}{2} m B_m e^{i(m-1)\varphi} + m(m^2 - 1) A_m e^{im\varphi} \right] = 0 \quad (1.17)$$

So that equalities (1.16) and (1.17) are identities with respect to coordinate  $\varphi$ , it is necessary that coefficients for exponentials be zeroes for all shown values of index  $m$ . This gives an infinite linear system of equations for  $A_m, B_m$

$$m A_m + m B_m - \frac{\psi_0}{2Z} (m-1)^2 A_{m-1} + \frac{\psi_0}{2Z} (m+1)^2 A_{m+1} = 0 \quad (m=1, 2, \dots) \quad (1.18)$$

$$Z^2 A_m - MZ^2 B_m + \frac{M\psi_0 Z}{2} (m-1) B_{m-1} - \frac{M\psi_0 Z}{2} (m+1) B_{m+1} + m(m^2 - 1) A_m = 0 \quad (m=0, 1, 2, \dots) \quad (1.19)$$

Excluding from (1.18) and (1.19)  $B_m$  and disregarding components containing small  $M$ , after the substitution  $\psi_0 = 2(W/M)^{1/2}$ , we will obtain

$$c_{m,m-2} A_{m-2} + c_{m,m} A_m + c_{m,m+2} A_{m+2} = 0 \quad (1.20)$$

$$\begin{aligned} c_{m,m} &= \chi + R_m - D_m W, & R_m &= m(m^2 - 1) \\ c_{m,m-2} &= C_{m-2} W, & D_m &= 2m^2, & C_m &= m^2 \\ c_{m,m+2} &= E_m W, & E_m &= (m+2)^2, & \chi &= Z^2 \end{aligned} \quad (1.21)$$

System (1.20) is broken two independent systems for even and odd values of index  $m$ . Dividing left and right side of equations of system (1.20) by  $c_{m,m}$ , we will obtain

$$A_m = \alpha_m A_{m-2} + \beta_m A_{m+2} \quad (m=0, 1, 2, \dots) \quad (1.22)$$

Here

$$\alpha_m = -\frac{c_{m,m-2}}{c_{m,m}}, \quad \beta_m = -\frac{c_{m,m+2}}{c_{m,m}} \quad (1.23)$$

For large values of  $m$   $\alpha_m$  and  $\beta_m$  have order  $O(W/m)$ , i.e., the considered system is fully regular, starting from certain sufficiently large  $m$  [7]. Putting

$$\begin{aligned} A_{2k+1}/A_1 &= \alpha_1 \alpha_3 \dots \alpha_{2k+1} S_{2k+1}, & \gamma_{2k+1} &= \alpha_{2k+1} \beta_{2k+1} \\ A_{2k}/A_2 &= \alpha_2 \alpha_4 \dots \alpha_{2k} S_{2k}, & \gamma_{2k} &= \alpha_{2k} \beta_{2k-1} \end{aligned} \quad (1.24)$$

considering coefficients  $A_1$  and  $A_2$  as known and rejecting equations corresponding to  $m = 0, 2$  and  $m = 1$ , from (1.22) we will obtain

$$\begin{aligned} s_3 &= 1 + \gamma_3 s_1, & s_4 &= 1 + \gamma_4 s_2 \\ s_5 &= s_3 + \gamma_5 s_7, & s_6 &= s_4 + \gamma_6 s_8 \\ &\dots\dots\dots & &\dots\dots\dots \\ s_{2k+1} &= s_{2k-1} + \gamma_{2k+1} s_{2k+3}, & s_{2k} &= s_{2k-2} + \gamma_{2k+2} s_{2k+2} \end{aligned} \quad (1.25)$$

The solution of system (1.25) can be represented in the form of continued fractions

$$\begin{aligned} s_{2k+1} &= s_{2k-1} \left( \frac{1}{1} - \frac{\gamma_{2k+3}}{1} - \frac{\gamma_{2k+5}}{1} - \dots \right) \\ s_{2k} &= s_{2k-2} \left( \frac{1}{1} - \frac{\gamma_{2k+2}}{1} - \frac{\gamma_{2k+4}}{1} - \dots \right) \end{aligned}$$

Equations of eigenvalue in the form of continued fractions have form

$$1 = \frac{\gamma_3}{1} - \frac{\gamma_5}{1} - \dots, \quad 1 = \frac{\gamma_4}{1} - \frac{\gamma_6}{1} - \dots \quad (1.26)$$

Equations (1.26) were solved by the method of successive approximations. Successive approximations of  $1$  of values of roots  $W_*$ <sup>(1)</sup> when  $Z = 0$  are given in the table.

Table

i	m = 3,5,...				m = 4,6,...				
	0	—	—	—	0.75	—	—	—	—
2	0	1.778	—	—	0.661	2.839	—	—	—
3	0	1.285	1.9813	—	0.6576	1.8502	6.7422	—	—
4	0	1.247	2.3173	10.8813	0.6556	1.741	3.4350	13.1676	—
5	0	1.2445	2.379	4.675	0.6560	1.7082	2.570	6.0935	145.213

For determination of forms of perturbations we will obtain the equation of nodal lines on the perturbed surface of the stream. From (1.2), considering (1.4) and (1.14), when  $m = 0$  (symmetry relative to average plane) and  $R = 1$  we will obtain speed of lifting of surface of stream

$$v_r = \frac{1}{2} \sum_{m=0}^{\infty} m A_m R^{m-1} \cos m\varphi e^{-4\eta} \quad (1.27)$$

If transition to instability occurs when  $\chi = 0$ , then  $\beta = 0$ , coefficients  $A_m$  are real, and equations of nodal lines on perturbed surface of stream take form

$$\sum_{k=0}^{\infty} m A_m \cos m\varphi = 0 \quad (1.28)$$

$$m = 2k \text{ or } m = 2k + 1$$

if eigenvalues and values of  $W_*$ <sup>(1)</sup> are determined from system (1.20). Since system (1.20) is uniform, then coefficients  $A_{2m}$  are proportional to  $A_2$ , and coefficients  $A_{2k+1}$  are proportional to  $A_1$ . From equation (1.28) one can determine value of angle  $\varphi$ , corresponding to nodal lines of neutral perturbation.

Equations (1.28) give the value of angle  $\varphi = 90^\circ$ , corresponding to  $W_* = 1.2445$  when  $m = 2k + 1$  and  $\varphi = 58^\circ$ , corresponding to  $W_* = 0.656$  when  $m = 2k$ . On Fig. 1 are given diagrams of forms of perturbations of the surface of a stream, corresponding to different eigenvalues  $W$ , obtained with respect to speed of deformation of surface stream from (1.27).

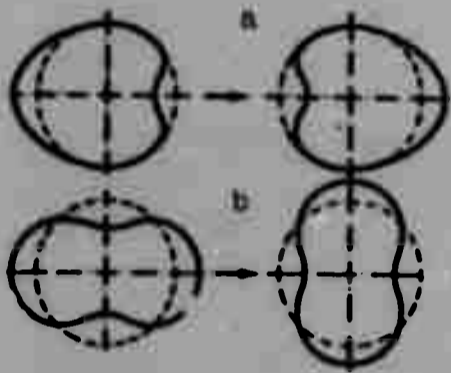


Fig. 1.

As can be seen on Fig. 1, to the case  $m = 2k + 1$  corresponds only the form of perturbation which is a shift parallel to the direction of the circumfluent flow. To the case  $m = 2k$  correspond different forms of perturbations, which can lead to formation of two, four, and more streams. Magnitude of least critical Weber number turned out to be  $W_*$ <sup>(5)</sup> = 0.656.

Let us find the dependence on  $W$  number of nodal lines for the case of growing perturbations, possessing the biggest increment  $Z$ . Since of all forms of growing perturbations, in reality only a form corresponding to the biggest value of increment  $\chi = Z^2$  is carried out, for determination of forms of perturbations for an assigned value of  $\chi$  from the equation of eigenvalues one should find the least value of root  $W$ .

We cite with the help of the second equation (1.26) values of minimum  $W$  roots for assigned values  $\chi$  and angles of nodal lines on surface of stream

$\chi = 0$	5	50	100	1000
min $W = 0.656$	1.045	2.086	2.540	27.6
$\varphi = 58$	58	30 and 75	40 and 80	35 and 85

Hence it is clear that when  $2 \leq W \leq 27.6$  on the perturbed surface of the stream appear four nodal lines.

Comparison of these data and the table shows that for  $0.656 < W < 1.24$  on the

stream appear two nodal lines, and the main stream is split, consequently, into two longitudinal streams. How the split occurs when  $W > 1.24$  has not yet been established in view of difficulties during calculation of forms of perturbations for odd  $m$ .

2. Let us consider waves propagating along the stream. This question is essential for study of disintegration of a liquid torus whose radius is sufficiently great as compared to dimensions of the cross section [1]. In this case it is possible to disregard curvature of ring and to be limited to consideration of influence of flow around a rectilinear liquid cylinder. It is necessary, however, to consider that on the torus can exist only waves whose length is confined to the length of the torus a whole number of times.

The Laplace equation for this case will have the form

$$\frac{\partial}{\partial r} \left( r \frac{\partial \Phi}{\partial r} \right) + \frac{1}{r^2} \frac{\partial^2 \Phi}{\partial \varphi^2} + \frac{\partial^2 \Phi}{\partial z^2} = 0 \quad (2.1)$$

Putting

$$\Phi(r, \varphi, z, t) = u(r, \varphi) e^{-i\beta t + i\lambda z} \quad (2.2)$$

we will obtain

$$\frac{\partial}{\partial r} \left( r \frac{\partial u}{\partial r} \right) + \frac{1}{r^2} \frac{\partial^2 u}{\partial \varphi^2} - k^2 u = 0 \quad (2.3)$$

Equation (2.3) has the particular solution

$$u = u_m(r) \cos m\varphi, \quad u_m(r) = A_m I_m(kr) + B_m K_m(kr) \quad (2.4)$$

Here  $I_m(kr)$ ,  $K_m(kr)$  - Bessel function of imaginary argument. Putting

$$ka = \alpha, \quad r = aR \quad (2.5)$$

the solution for stream  $U_1$  and for external medium  $U_2$  is written in the form

$$U_1 = \sum_{m=0}^{\infty} A_m I_m(\alpha R) \cos m\varphi, \quad U_2 = \sum_{m=0}^{\infty} B_m K_m(\alpha R) \cos m\varphi \quad (2.6)$$

Boundary conditions of problem will have the form

$$\begin{aligned} \frac{\partial U_1}{\partial R} - \frac{\partial U_2}{\partial R} - \frac{\psi_0 \sin \varphi}{Z} \frac{\partial^2 U_1}{\partial R \partial \varphi} &= 0, \quad (R=1) \\ Z^2 U_1 - M Z^2 U_2 + M \psi_0 Z \sin \varphi \frac{\partial U_2}{\partial \varphi} - \frac{\partial U_1}{\partial R} - \frac{\partial^2 U_1}{\partial R \partial \varphi} + \alpha^2 \frac{\partial U_1}{\partial R} &= 0, \quad R=1 \end{aligned} \quad (2.7)$$

Here  $Z$ ,  $M$ ,  $\psi_0$  are as in (1.11). After substitution of (2.5), (2.6) in (2.7) and after certain transformations we will obtain

$$\begin{aligned} 2Z I_m'(\alpha) A_m - 2Z K_m'(\alpha) B_m + (m+1) \psi_0 I_{m+1}'(\alpha) A_{m+1} - \\ - (m-1) \psi_0 I_{m-1}'(\alpha) A_{m-1} &= 0 \\ 2Z^2 I_m(\alpha) A_m - 2M Z^2 K_m(\alpha) B_m + 2\alpha(\alpha^2 + m^2 - 1) I_m'(\alpha) A_m - \\ - M \psi_0 Z (m+1) K_{m+1}(\alpha) B_{m+1} + M \psi_0 Z (m-1) K_{m-1}(\alpha) B_{m-1} &= 0 \\ (m=0, 1, 2, \dots) \end{aligned} \quad (2.8)$$

Excluding from system (2.8) coefficients  $B_m$ , we will obtain system

$$A_m [Z^2 + R_m + P_m W] - A_{m+2} Q_m W - A_{m-2} S_m W = 0 \quad (m=0, 1, 2, \dots) \quad (2.9)$$

$$\begin{aligned} R_m &= \alpha(\alpha^2 + m^2 - 1) \frac{I_m'(\alpha)}{I_m(\alpha)}, \quad S_m = (m-1)(m-2) \frac{K_{m-1}(\alpha) I_{m-2}'(\alpha)}{K_{m-1}(\alpha) I_m(\alpha)} \\ P_m &= m \frac{I_m'(\alpha)}{I_m(\alpha)} \left[ (m+1) \frac{K_{m+1}(\alpha)}{K_{m+1}(\alpha)} + (m-1) \frac{K_{m-1}(\alpha)}{K_{m-1}(\alpha)} \right] \\ Q_m &= (m+1)(m+2) \frac{K_{m+1}(\alpha) I_{m+2}'(\alpha)}{K_{m+1}(\alpha) I_m(\alpha)} \end{aligned} \quad (2.10)$$

Analogous to the conclusion § 1, we will obtain

$$\begin{aligned} A_m &= \alpha_m A_{m-2} + \beta_m A_{m+2} \quad (m=0, 1, 2, \dots) \\ \left( \alpha_m &= \frac{S_m W}{\xi + R_m + P_m W}, \quad \beta_m = \frac{Q_m W}{\xi + R_m + P_m W} \right) \end{aligned} \quad (2.11)$$

Using designations (1.24) and analogous considerations, we will come to the same equations of eigenvalues as in (1.26)

$$1 = \frac{\gamma_0}{1} - \frac{\gamma_0}{1} - \dots, \quad 1 = \frac{\gamma_0}{1} - \frac{\gamma_0}{1} - \dots \quad (2.12)$$

However, for the considered problem the constructed algorithm of continued fractions gives somewhat slow convergence. For reliability of the calculated values it is required to conduct calculations to  $m = 40$ , and they become visible. Let us introduce certain simplifications.

We will use the first approximation from the formula of Meissel for Bessel

functions with large index [8]

$$I_\nu(vZ) \approx \frac{Z^\nu \exp(v(1-Z)^{1/2})}{(2\pi\nu)^{1/2} (1-Z)^{1/2} (1+(1-Z)^{1/2})^\nu} \quad \text{for } \nu \gg 1 \quad (2.13)$$

Then

$$I_n(nZ) = i^{-n} J_n(inZ) = \frac{Z^n \exp(n(1-Z)^{1/2})}{(2\pi n)^{1/2} (1-Z)^{1/2} (1+(1-Z)^{1/2})^n} \quad (2.14)$$

From the recurrent relationship [8] for Bessel functions we have

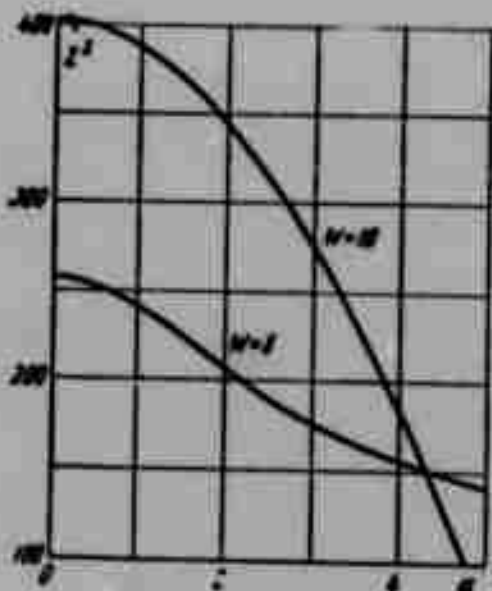


Fig. 2.

$$\begin{aligned} \frac{I'_n(a)}{I_n(a)} &= \frac{I'_{n-1}(a)}{I_{n-1}(a)} - \frac{n}{a} \\ \frac{K_n(a)}{K'_n(a)} &= - \left( \frac{K_{n-1}(a)}{K'_{n-1}(a)} + \frac{n}{a} \right)^{-1} \end{aligned} \quad (2.15)$$

Applying formula (2.14) to (2.15), we will obtain

$$M_n = \frac{I'_n(a)}{I_n(a)} = \frac{2}{\pi} \frac{n^2}{a(n-1)^{n-1}} - \frac{n}{a}$$

and, since  $n^2 / (n-1)^{n-1} \sim e(n-1)$  when  $n \gg 1$ , then

$$M_n = \frac{n-2}{a} \sim \frac{n}{a} \quad (2.16)$$

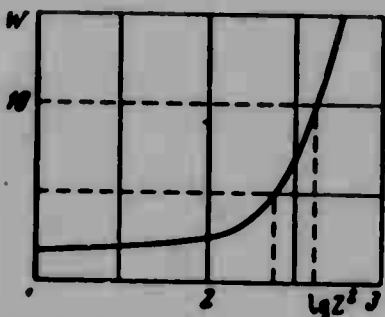


Fig. 3.

Analogously it is possible to show that for large indices

$$N_n = \frac{K_n(a)}{K'_n(a)} \sim - \frac{a}{n} \quad (2.17)$$

If one were to use (2.15)-(2.17), then it is possible instead of (1.21)-(1.24) to obtain such algorithm for calculation  $\gamma_n$

$$\gamma_n = W^n \frac{n(n-1)^2(n-2) M_n M_{n-2} N_{n-1}^2}{EF}$$

$$\begin{aligned} E &= \zeta + a(a^2 + n^2 - 1)M_n + nWM_n[(n+1)N_{n+1} + (n-1)N_{n-1}] \\ F &= \zeta + a[a^2 + (n-2)^2 - 1]M_{n-2} + W(n-2)M_{n-2}[(n-1)N_{n-1} + \\ &\quad + (n-3)N_{n-3}] \end{aligned} \quad (2.18)$$

where when  $n < 20$  formulas (2.15) are used, and when  $n > 20$ , — formulas (2.16) and (2.17).

We give the calculated values of root  $\zeta = Z^2$  of the equation of eigenvalues (2.12) for two values of Weber number (Fig. 2).

$\alpha = 0$	1	2	5	
$\zeta = 257.8$	241.8	205	140.3	for $W = 5$
$\zeta = 402.3$	386.3	343.5	74.5	for $W = 10$

As can be seen from this graph,  $\zeta = 256$  and  $403$  when  $\alpha = 0$ . If one were to depict on the graph according to the given data the curve  $W = f(\zeta)$  (Fig. 3), then one can be certain that increment  $\zeta$  when  $\alpha = 0$  according to Fig. 2 will agree well with the above results on Fig. 3. Thus, results of the solution of the first and second problems, carried out in this work, will agree well. Curves of Fig. 2 give maximum of increment when  $\alpha = 0$ , which corresponds to wave length  $\lambda = \infty$ .

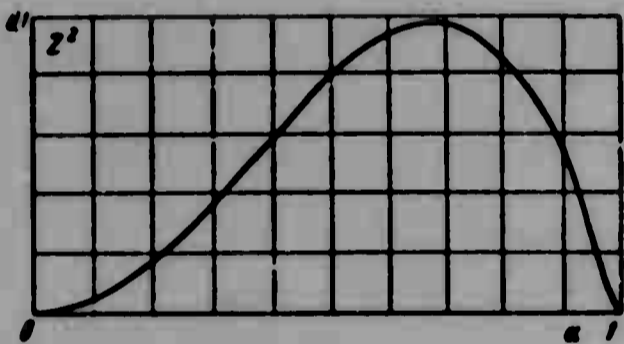


Fig. 4.

Figure 4 gives curve of increment with respect to wave number for  $W = 0$ , i.e., for a case analogous to Rayleigh cases in problems about oscillation of a spherical drop. As can be seen, the maximum point corresponds to  $\zeta = Z^2 < 0.1$ , and, thus influence of the flow around (Fig. 2) increases value of increment of oscillations many times.

If one were to apply obtained results to the problem about oscillations of torus [10, 1], then it is possible, apparently, to affirm the following: Since on the torus can appear only waves whose length is confined on it a whole number of times, then the least number of parts into which the torus can be split is two. Figure 2 shows that two waves on the torus indeed can appear and, moreover, that chiefly two waves will appear. This is confirmed also experimentally. On photographs given in the work of Lane [11], one may see distinctly the appearance of two nodes on the liquid torus being blown by a flow of air.

Submitted  
22 May 1964

### Literature

1. V. A. Borodin, Yu. F. Dityakin and V. I. Yagodkin. Mechanisms of disintegration of a drop moving in a gas flow. Jour. applied mech. and tech. physics, 1964, No. 3.
2. J. Priem. Break up of water drops and sprays with a shock wave. Jet Propuls., 1957, Vol. 27, No. 10, p. 1084.
3. G. Morell. Break up of liquid jets by transverse shocks. Eighth symposium on combustion, Baltimore, 1962.
4. V. A. Borodin, Yu. F. Dityakin and V. I. Yagodkin. Splitting of a spherical drop in a gas flow. Jour. applied mech. and tech. physics, 1962, No. 1, p. 85.
5. M. S. Volynskiy. Splitting of a drop in a flow of air. Reports of Academy of Sciences of USSR, 1948, Vol. 62, No. 3, p. 301.
6. M. S. Volynskiy. Study of splitting of drops in a gas flow. Reports of Academy of Sciences of USSR, 1949, Vol. 63, No. 2.
7. L. V. Kantorovich and V. I. Krylov. Methods of approximate solution of partial differential equations. ONTI, M.-L., 1936.
8. G. N. Watson. Theory of Bessel functions, Chapter I. Publishing House of Foreign Literature, M., 1949, p. 254.
9. I. S. Gradshteyn and I. M. Ryzhik. Tables of integrals, sums of series and products. Fizmatgiz, 1962.
10. S. Oka. On the instability and breaking up of a ring of liquid into small drops. Proc. Phys. Math. Soc. Japan, 2nd ser., 1936, Vol. 18, No. 9, p. 524.
11. W. R. Lane. Shatter of drops in streams. Ind. Engng. Chem., 1951, Vol. 43, No. 6, p. 1312.

**BLANK PAGE**

## RHEOLOGICAL PROPERTIES OF POLYMERS IN THE FLUID STATE

G. V. Vinogradov and A. Ya. Malkin

(Moscow)

The most essential peculiarities of rheological properties of polymers in the fluid state are described and it appears that functions characterizing these properties can be represented in the form of temperature-invariant dependencies, which furthermore, at least for linear polymers, turn out to be universal, i.e., not depending on nature of polymers. A description of the complex of rheological properties is given on the example of experimental investigation of industrial polymers of Soviet production: polyisobutylene [P-20] ( $\Pi$ -20) with molecular weight 100 thousand, and polypropylene [OP-30] ( $OP$ -30) with molecular weight 700 thousand. Furthermore, to check the obtained conclusions results of investigation of polyethylene ("alkatin-2" and others), block polystyrene, etc, were used.

To produce a possibly more full characteristics in the fluid state results were used of experiments conducted on rotary elastoviscosimeter [REV-1] (PЭВ-1) [1] and capillary viscosimeter of constant pressures [2]. On the REV-1 was obtained a large part of the data considered below. This instrument realizes stress field with high degree of homogeneity of strain state ( $\sim 98\%$ ); the dynamometric arrangement of the instrument possesses extraordinarily high rigidity ( $\sim 1 \cdot 10^{10}$  dyne cm/rdn), due to which it is possible to disregard influence of deformation of the actual dynamometer on results of rheological investigations (see [3]); constant speed of shift in investigated polymer and cessation of deformation are carried out for 0.1 sec. Stresses during assigned kinematic conditions of flow are fixed continuously; error in thermostatic control does not exceed  $\pm 1^\circ\text{C}$ . A capillary viscosimeter was used for production of data on viscosity of polymers in steady-state operating conditions of flow at higher speeds of shift than were attained on the rotary instrument.

Typical deformation characteristics of polymers, obtained on the REV-1, are represented on Fig. 1. Here the left part of the figure shows the dependence of shift stresses  $\tau$  on magnitude of relative deformation  $\gamma$  at different constant speeds

of deformation  $\dot{\gamma} = \text{const}$  and different temperatures, and the right part shows dependence of stresses  $\tau$  on time  $t$  for conditions of relaxation of stresses (when  $\dot{\gamma} = \text{const}$ ) after cessation of established flow. For small values  $\dot{\gamma}$  curves  $\tau(\dot{\gamma})$  are monotonic; increase of  $\dot{\gamma}$  is accompanied by formation on these curves of evidently expressed maxima  $\tau_m$ . In all cases for sufficiently large  $\dot{\gamma}$  are attained constant values of stresses  $\tau_s$ .

Character of dependence  $\tau(\dot{\gamma})$  is conditioned by relationship between speeds of growth of shift stresses with increase of deformation in system and their relaxation, corresponding to change of intermolecular interaction and transition of forced deformed macromolecules and the most probable conformations.

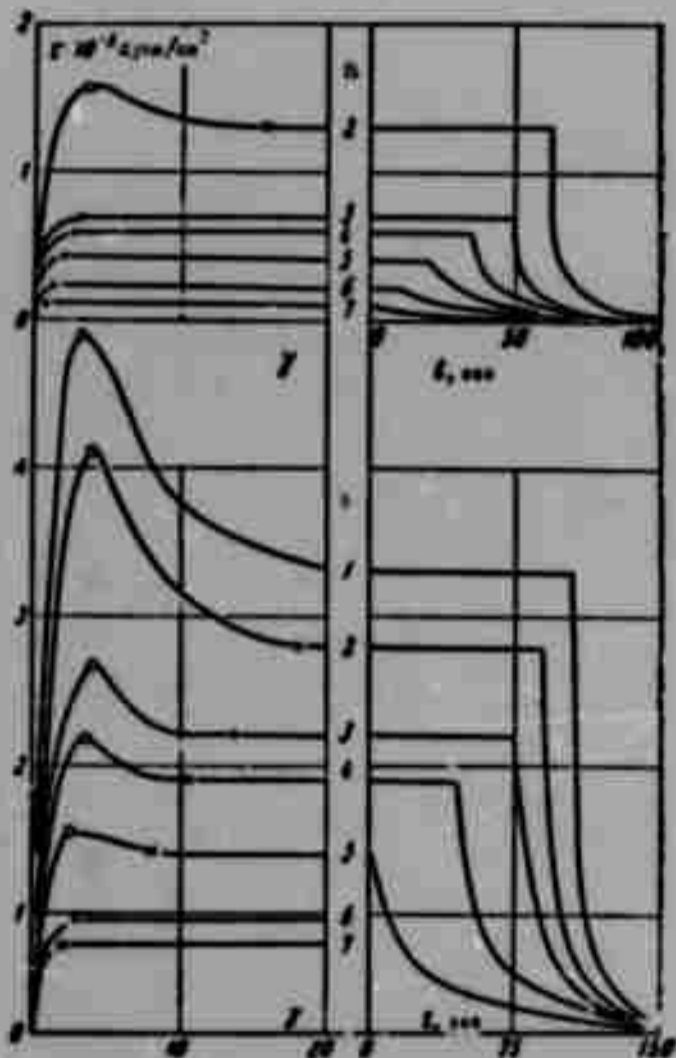


Fig. 1. Typical experimental results  
a) polypropylene, 230°C; b) polyisobutylene 10°C; speed of shift, sec<sup>-1</sup>;  
1 - 0.80, 2 - 0.40, 3 - 0.12,  
4 - 0.08, 5 - 0.04, 6 - 0.016,  
7 - 0.008.

During repeated deformation the following characteristic effects are observed: if flow stops prior to  $\tau_m$ , then form of dependence  $\tau(\dot{\gamma})$  practically does not change; during transition through  $\tau_m$  for a repeated experiment a gradual lowering of  $\tau_m$  was observed, and this lowering is greater the more  $\dot{\gamma}$  corresponded to moment of stopping of flow. If, however, the polymer after cessation of deformation "rests" a more or less prolonged time, then gradual restoration of initial form of the curve  $\tau(\dot{\gamma})$  is observed, which in described experiments always was complete.

Thus, deformation of polymers in fluid state is accompanied by change of their structure, appearing in change of mechanical properties. Therefore  $\tau_m$  can be considered as the limit of shift strength of the structure of a polymer, transition through which is accompanied by intense reversible destructions of

this structure (at very high values of  $\dot{\gamma}$  these changes can also be irreversible),

and drop of stresses after  $\tau_m$  can be considered as structural relaxation of stresses [4].

Experimental data shown on Fig. 1 permit quantitatively determining parameters characterizing strength properties of melts of polymers. Here belong all quantities connected with transition through limit of shift strength and appearance at conditions of established flow. In this relation the ratio  $\tau_m/\tau_s$  is significant. Namely, this quantity should be considered as a measure of structure strength.

For certain polymers (plasticized polyvinylchloride) this quantity with increase of  $\dot{\gamma}$  to several hundreds  $\text{sec}^{-1}$  can attain values of 2-3, although usually  $\tau_m/\tau_s$  is lower. Thus, for polypropylene  $\tau_m/\tau_s$  attains a constant value, equal (at  $190^\circ$ ) to 1.35 already when  $\dot{\gamma} = 3 \text{ sec}^{-1}$ , and does not increase with further increase of  $\dot{\gamma}$ .

Magnitudes of relative deformations, corresponding to transition through limit of shift strength and appearance at conditions of established flow (in conformity with  $\gamma_m$  and  $\gamma_s$ ) have important value. As data of Fig. 1 show,  $\gamma_s$  rapidly increases with increase of  $\dot{\gamma}$ , attaining thousands of percents. These enormous values of  $\gamma_s$  correspond to considerable time intervals which are required for achievement of steady-state conditions of flow of polymer in different channels.

For further systematization and generalization of experimental data the method of construction of temperature-invariant characteristics, described for the example of viscosity properties in [5, 6] is important. It was shown that it was possible to obtain representations of viscosity properties invariant with respect to temperature and universal with respect to a great group of polymers [7] if one considers the dependence of  $\eta/\eta_0$  on  $\dot{\gamma}\eta_0$ , where  $\eta$  is effective viscosity of a given polymer for a certain value  $\dot{\gamma}$ , and  $\eta_0$  is the biggest Newton viscosity of the same polymer. By definition,  $\eta = \tau_s/\dot{\gamma}$ , and  $\eta_0 = \lim \eta$  when  $\dot{\gamma} \rightarrow 0$ . This method of construction of temperature-invariant characteristics is easily generalized also on the dependence of  $\gamma_m$  and  $\gamma_s$  on  $\dot{\gamma}$ . Use of  $\dot{\gamma}\eta_0$  as an argument permits obtaining temperature-invariant presentation and these properties of polymer.

The most important characteristic of polymeric systems is their effective viscosity. On Fig. 2 it is shown that viscosity properties of investigated polymers can be represented in temperature-invariant form, which, as one may see from this figure, is universal. In the field of experimental points on Fig. 2 it is possible to average the curve (shown by dotted line), which we will call the universal

temperature-invariant characteristic of viscosity of polymers in the fluid state. This is curve sufficiently well described by the empirical formula

$$\eta_0/\eta = 1 + 6.12 \cdot 10^{-3} \gamma \eta_0^{0.355} + 2.35 \cdot 10^{-4} (\gamma \eta_0)^{0.71} \quad (1)$$

The quantity  $\eta_0$  characterizes individual peculiarities of given polymer, with respect to  $\eta_0$  is determined dependence of viscosity of polymer on molecular weight and temperature.

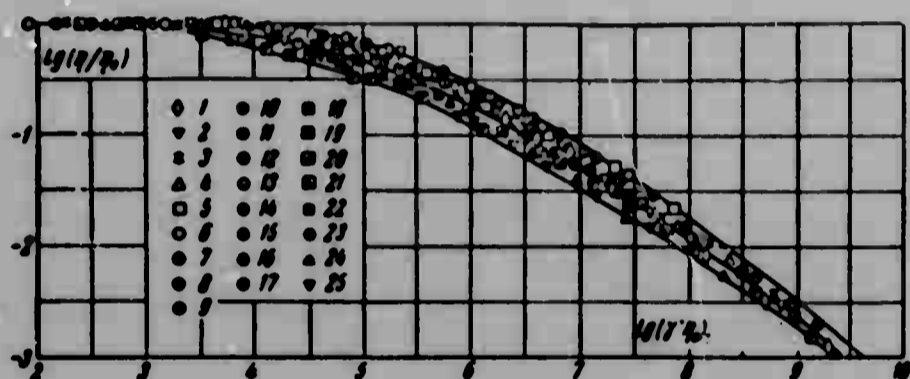


Fig. 2. Universal temperature-invariant characteristics of viscosity; polypropylene: 1 - 190°, 2 - 210°, 3 - 230°, 4 - 250°, 5 - 270°, 6 - 290°; polyisobutylene: 7 - 20°, 8 - 10°, 9 - 0°, 10 - 10°, 11 - 40°, 12 - 60°, 13 - 80°; polystyrene (according to N. V. Prozorovskoy): 14 - 150°, 15 - 170°, 16 - 210°, 17 - 230°; polyethylene: 18 - 150°, 19 - 170°, 20 - 190°, 21 - 210°, 22 - 230°; polyvinylbutyral (see in [6]); 23 - 119°, 24 - 125°, 25 - 155°.

In many cases it has been experimentally possible to reach directly the region of direct ratio between  $\tau_s$  and  $\gamma'$  (i.e., deviations from condition  $\tau_s/\gamma' = \text{const}$  do not exceed the bounds of experimental errors). In other cases for determination of  $\eta_0$  it is necessary to resort to one or another method of extrapolation (see, for instance, [6]). However proceeding from Fig. 2, it is possible to affirm that existence of region of Newton flow for considered polymers is an experimental fact, i.e., polymers behave not as plastic, but as truly viscous media. Anomaly of viscosity appears with increase  $\gamma'$  (or  $\tau_s$ ) gradually, i.e., in region of anomalous viscosity to growth of  $\gamma'$  corresponds gradual reversible (thixotropic) and all deeper destruction of initial structure of polymer.

What was said justifies the idea of anomaly of viscosity as on the region of "structural" viscosity. However, as occurs in organic polymeric systems, in distinction, for instance, from bentonitic clays, this region stretches many hundred orders in shift stress (speeds), and regions of completely destroyed structure (least Newton viscosity) in melted polymers experimentally this has never been reached, probably connected with the fact that during further increase of  $\dot{\gamma}$  there starts to occur not only reversible (thixotropic) destruction of structures in polymer, but also irreversible changes of macromolecules themselves (mechanical-destruction) are developed. Furthermore, with increase of rate large dissipative losses are developed and the appearance of unstable conditions of flow (elastic turbulence [8]) becomes possible. Relative influence of these factors for different polymers can be different, however at present it is not possible to increase speed of shift higher than the limit speed, corresponding to maximum values of  $\dot{\gamma} \cdot \eta_0$  on Fig. 2.

Use of temperature-invariant characteristics of viscosity permits essential expansion of range of change  $\dot{\gamma}$  during construction of curves of flow, under which is understood dependence  $\dot{\gamma}(\tau_s)$ . On Fig. 3 are shown curves of flow of polypropylene at different temperatures. Part of the points (shown on this figure by light signs) is obtained directly experimentally, the other (blackened signs) are obtained by extrapolation with use of temperature-invariant characteristics of viscosity of polypropylene. As can be seen from Fig. 3, curves of flow cover range of change of speeds of shift  $10^8$  times and shift stresses — more than  $10^3$  times, besides effective viscosity of polymer decreases more than  $10^3$  times. It is essential also that experimentally it is possible to observe a rather considerable section of Newton flow (lower branches of curves of flow). For the right side of Fig. 1 the dependencies of  $\lg(\tau/\tau_s)$  on  $t$  are represented on Fig. 4; these relaxation curves turn out to be depending on  $\tau_s$  (i.e., relaxation properties of polymers are nonlinear with respect to stress) and do not obey the exponential law of Maxwellian relaxation. Only for sufficiently small  $\dot{\gamma}$ , corresponding to region of Newton flows, do relaxation properties of the considered systems turn out to be linear, i.e., relaxation curves become not depending on stress and can directly be considered as real characteristics of relaxation properties of a polymer. Another experimental proof of the linearity of binding elastic properties for sufficiently

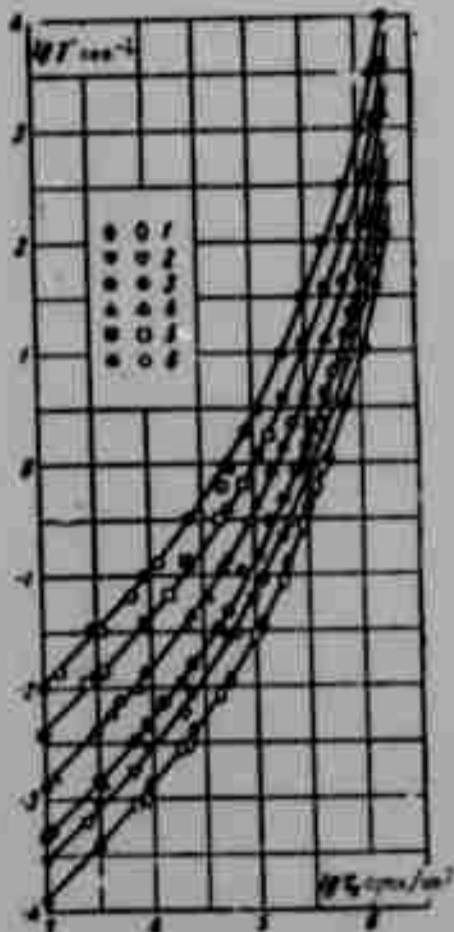


Fig. 3. Curves of flow of polypropylene:  
1 - 190°, 2 - 210°, 3 - 230°, 4 - 250°, 5 - 270°, 6 - 290°.

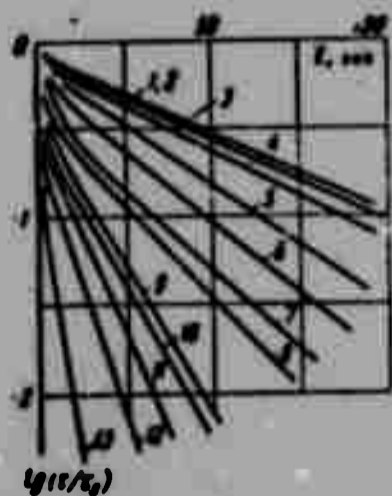


Fig. 4. Typical relaxation curves; polypropylene. 230°; speed of shift (sec<sup>-1</sup>):

1 - 0.004, 2 - 0.008, 3 - 0.012,  
4 - 0.016, 5 - 0.02, 6 - 0.03,  
7 - 0.12, 8 - 0.16, 9 - 0.32,  
10 - 0.60, 11 - 0.80, 12 - 1.00, 13 - 4.0

small  $\gamma'$  is comparison of relaxation curves with curved development of stress appearance at conditions of established flow: in the case of linear viscoelasticity one curve should be the mirror image of the other.

Relaxation properties of polymers in the linear region (for small  $\gamma'$ ) are not described by value of time of relaxation. However, it is characteristic that curvature of dependence of  $\lg(\tau/\tau_s)$  on  $t$  essentially shows only for small  $t$ , then these dependencies become practically rectilinear, i.e., over a certain time behavior of polymer during relaxation can be simulated by one Maxwellian element with characteristic time  $\theta_0$ , determined with respect to tangent of angle of inclination of rectilinear section of graph of dependence of  $\lg(\tau/\tau_s)$  on  $t$ .

Most likely, for sufficiently large  $t$  the rectilinear section again passes into curvilinear, corresponding to large relaxation times. However, experimentally such a section has not been shown, which, most probably, is connected not with its fundamental absence, but with difficulties of measurement of very small stress with the help of a dynamometer of high rigidity, and lowering of rigidity of dynamometer leads to appearance of large and indeterminate errors, caused by its deformations [3].

On Fig. 5 is represented the dependence of  $\eta_0/\theta_0$  on  $\gamma'\eta_0$  (in logarithmic coordinates). And in this case it is possible to construct a temperature-invariant characteristic which, as Fig. 5 shows, turns out to be universal with respect to the considered polymers.

It is obvious that Fig. 5 characterizes regularity of change of relaxation spectrum during growth of  $\gamma'$ .

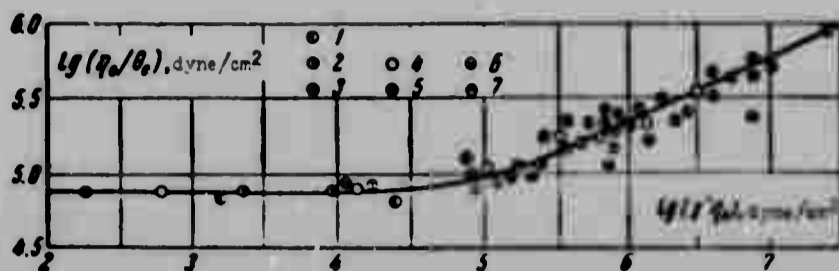


Fig. 5. Dependence of relaxation properties (with respect to  $\eta_0$ ) on conditions of determining conditions of deformation; polypropylene: 1 -  $190^\circ$ , 2 -  $250^\circ$ , 3 -  $290^\circ$ ; polyethylene: 4 -  $150^\circ$ ; polyisobutylene: 5 -  $10^\circ$ , 6 -  $0^\circ$ , 7 -  $10^\circ$ .

following: both effective viscosity and characteristic relaxation times decrease, while both process possess the same regularities. It is natural then to assume that change of relaxation (viscoelastic) properties of polymers in the current state, flowing with increase of speed of deformation in the direction of decrease of characteristic relaxation times, is the cause of anomaly of viscosity. Universality of temperature-invariant characteristic of viscosity is determined by universal character of change of relaxation properties with increase of speed of shift.

No matter how the theory of nonlinear behavior of polymers was constructed, in any case for sufficiently small values of parameters the relationships of linear theory of viscoelasticity must be executed; therefore for all cases the relaxation spectrum, characterizing linear region of mechanical behavior, remains a property of the system. Usually spectral functions are found according to data of dynamic (frequency) or other tests conducted in a more or less narrow range of change of frequency (or time), using those or other methods of approximation of conversion of known integral transforms [9]. Thus, in particular, knowing dynamic viscosity  $\eta_d$  as a function of frequency  $\omega$ , it is possible to calculate the frequency spectrum by the formula

$$N(\omega) = \frac{2}{\pi} \operatorname{Re} [i\eta_d(i\omega)] \quad (2)$$

where by  $N(\omega)$  is understood [9] a function determined as an original of the Laplace transform, where the representation of this original constitutes a relaxation function of stress after instantaneous assignment of constant deformation. Here it would be interesting, not turning to special dynamic tests, to find function

Let us note two experimental facts. First, these changes occur equally for different polymers, outside the dependence on temperature. Secondly, these changes occur so that characteristic times of relaxation decrease with growth of  $\gamma'$ . Thus, with increase of speed of shift occurs the

$N(\omega)$ , applying the above generalization of data on viscosity properties of considered systems. It is possible to use the following known and repeatedly checked experimental fact (see, for instance, [10]): dependencies  $\eta_d(\omega)$  and  $\eta(\gamma^*)$  - are equivalent. This permits immediate representation of dependence  $\eta_d(\omega)$  in a very wide range of change of frequency by the formula

$$\eta_0/\eta_d = 1 + 6.12 \cdot 10^{-3}(\omega\eta_0)^{0.335} + 2.35 \cdot 10^{-4}(\omega\eta_0)^{0.71} \quad (3)$$

It follows from this also that from the above proved possibility of construction of temperature-invariant characteristics of viscosity and their universality follows the possibility of representation of all relaxation and dynamic characteristics of polymers in the fluid state, including here the very same spectrum in temperature-invariant form. The first part of this affirmation, directly following as a particular case from the above results, was repeatedly confirmed experimentally in the works of Ferry [11] on the example of different amorphous polymers. Here it is affirmed and below certain examples will illustrate not only the possibility of construction of temperature-invariant characteristics of viscoelastic behavior of polymers in the fluid state, but also their universality at least with respect to line polymers.

Placing now (3) in (2) and executing all operations, we will obtain the dependence  $N/\eta_0$  on  $\omega\eta_0$ , i.e., temperature-invariant representation of relaxation (frequency) spectrum. The expression for  $N(\omega)$ , found by (2), has the form

$$N(\omega) = \eta_0 \left[ \sum_{k=1}^3 L_k (\omega\eta_0)^{0.335k} \right] : \left[ \sum_{k=0}^3 M_k (\omega\eta_0)^{0.335k} \right] \quad (4)$$

Values of constants  $L_k$  and  $M_k$  are expressed through coefficients and indices of formula (3). The maximum, function (4) lies at value  $\omega\eta_0$ , intermediate between  $8 \cdot 10^4$  and  $1 \cdot 10^5$  dynes/cm<sup>2</sup>. It is interesting to note that this value  $\omega\eta_0$  is well correlated with data of Fig. 5. Namely, if one were to consider limiting value  $\theta_0$ , which is obtained when  $\gamma^* \rightarrow 0$ , then it is possible to see that for sufficiently small  $\gamma^*$  (in linear region)  $(\eta_0/\theta_0) = (\omega\eta_0) = 8 \cdot 10^4$  dynes/cm<sup>2</sup> (one should consider that relaxation time  $\theta$  is simply the inverse of relaxation frequency  $\omega$ ). Thus, indeed, a considerable part of relaxation occurs in a time which corresponds to the

maximum of the relaxation spectrum. Thereby are confirmed validity of temperature-invariant representation of spectrum, position of maximum along the axis  $\omega\eta_0$  and stability of this position, at least, for those polymers for which experimental data are represented on Fig. 5.

The analytic expression  $N(\omega)$ , determined by (4), turns out to be rather complicated for further use. However, as consideration of specific values of function  $N/\eta_0(\omega\eta_0)$ , shows, it can be represented — in a very wide range of change of argument — in the form of the more convenient, and qualitatively and quantitatively sufficiently accurate expression

$$N/\eta_0 = \begin{cases} 2.24 \cdot 10^{-2} (\omega\eta_0)^{0.40} & (0 < \omega\eta_0 < 4.68 \cdot 10^4) \\ 0.166 & (4.68 \cdot 10^4 < \omega\eta_0 < 3.80 \cdot 10^5) \\ 7.1 \cdot 10^3 (\omega\eta_0)^{-0.66} & (3.80 \cdot 10^5 < \omega\eta_0 < \infty) \end{cases} \quad (5)$$

This function satisfies the known relationship of the theory of linear viscoelasticity

$$\int_0^\infty \frac{N(\omega)}{\omega} d\omega = \eta_0$$

Formula (5) determines the universal relaxation spectrum of polymers which are in the fluid state, for the linear region of their mechanical behavior. An independent experimental check of particular cases of deformation concludes the possibility of testing the validity of conclusions obtained above. Certainly, already the fact itself of equivalence of functions  $\eta_d(\omega)$  and  $\eta(\gamma')$  predetermines accuracy of further conclusions about universality of relaxation properties of polymers in the fluid state and following from a fixed form of dependence  $N(\omega)$  forms of different viscoelastic functions (relaxation, dynamic, and delay). Nevertheless, there is a special interest in principally an independent experiment. Such an experiment, in accordance with the above material may be relaxation of stress after stopping an established flow with preservation of constant deformation.

Using the principle of Boltzmann-Volterra, it is possible to show that for the considered case dependence of stress on time  $\tau(t)$  is expressed through  $N(\omega)$  by an integral transform of the form

$$\tau(t) = \gamma \int_0^\infty \frac{N(\omega)}{\omega} e^{-i\omega t} d\omega \quad (6)$$

or in universalized temperature-invariant form

$$\frac{\tau(t/\eta_0)}{\tau_0} = \int_{x=0}^{\infty} \frac{N(x)/\eta_0}{x} e^{-(t/\eta_0)x} dx \quad (7)$$

Let us note that, as follows from comparison of determination of function  $N(\omega)$  with expression (6), the case of relaxation of stress after instantaneous assignment of a constant deformation, held constant during the experiment, is not equivalent to the case of relaxation of stress after instantaneous stopping of established flow also keeping constant deformation.

Results of calculation of dependence  $(\tau/\tau_0)$  on  $t/\eta_0$  by formula (7) are represented on Fig. 6 in the form of a solid line. Experimental data for certain

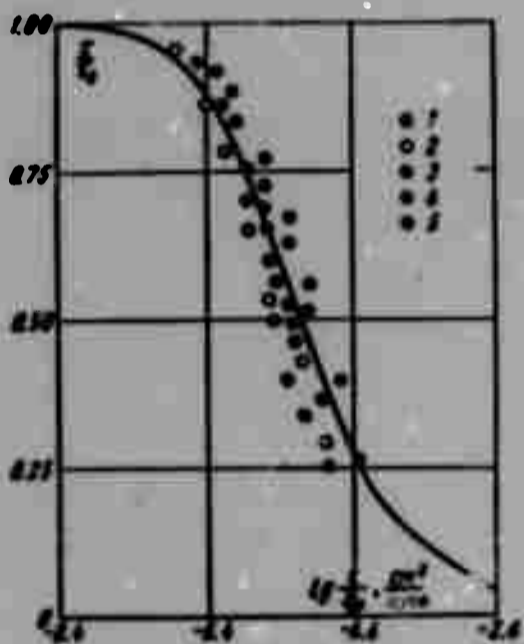


Fig. 6. Stress relaxation after instantaneous stopping of established flow;

polyisobutylene: 1 - 22°;  
polypropylene: 2 - 190°,  
3 - 230°, 4 - 250°, 5 - 270°.

typical cases, obtained in the linear region in the form of separate points. As can be seen, the analytic curve will agree satisfactorily with experimental data obtained for polymers different in chemical nature, for which, however, the principle of universality of the temperature-invariant characteristic of viscosity holds. The same data of Fig. 6 confirm the above principle of universality of temperature-invariant relaxation spectrum for polymers which are in the fluid state, and its found analytic representation.

Above was obtained the universal relaxation spectrum of polymers for the linear region and it was shown that with increase of  $\gamma'$  and transition into the nonlinear region the spectrum is changed so that there occurs a decrease of characteristic relaxation times. The experiment does not correspond quantitatively on the question of how changes of  $N(\omega)$  occur, indicating only the direction of this process. However a phenomenological theory [12] was proposed, as whose basis was the above proved fact of decrease of characteristic relaxation times with growth of  $\gamma'$ . According to this theory, decrease of  $\eta$  with increase of  $\gamma'$  is caused by

"truncation" of the relaxation (frequency) spectrum to small  $\omega$ . Then it is possible to write

$$\eta(\dot{\gamma}) = \int_{\omega_0(\dot{\gamma})}^{\infty} \frac{N(\omega)}{\omega} d\omega \quad (8)$$

where function  $\omega_0(\dot{\gamma})$ , playing a central role in the theory [12], shows up to what frequency  $\omega_0$  the spectrum is cut off at an assigned rate of deformation, i.e., constitutes the function of change of relaxation spectrum. Let us determine  $\omega_0(\dot{\gamma})$ , proceeding from equation (8) and above-obtained expressions  $\eta(\dot{\gamma})$  (see (1)) and  $N(\omega)$  (see (5)). Obviously, we will obtain a universal temperature-invariant function  $\omega_0\eta_0(\dot{\gamma}\eta_0)$ , inasmuch as in (1) and (5) in such a form are represented arguments  $\eta$  and  $N$ . The numerical solution of equation (8) relative to  $\omega_0(\dot{\gamma})$  showed that  $\omega_0\eta_0 = \dot{\gamma}\eta_0$ , i.e., in all cases  $\omega_0 = \dot{\gamma}$ , and function of change of spectrum  $\omega_0(\dot{\gamma})$  turns out to be in general, a universal function, not depending on individual parameters of polymer. Such a form of function  $\omega_0(\dot{\gamma})$  means that during transition to steady-state operating conditions of flow of viscoelastic polymers, occurring with speed of shift  $\dot{\gamma}$ , there occurs destruction of those structural elements of the polymer which are responsible for relaxation processes occurring with frequencies smaller than this speed of shift.

In [12] the connection between  $N(\omega)$ ,  $\eta(\dot{\gamma})$  and  $\omega_0(\dot{\gamma})$  was considered in the most general form. When the obtained relationships were made more specific it was assumed that destruction of the spectrum is described by the formula  $\omega_0(\dot{\gamma}) = \dot{\gamma}/R_{e*}$ , where  $R_{e*} = 5-6$  is the critical value of criterion of elastic turbulence [8], inasmuch as it was supposed that destruction of viscoelastic elements of structure of the polymer initiates development of elastic turbulence. The result obtained above is based on direct treatment of experimental data and is not connected with additional assumptions. This result accurate to a constant factor coincides with the assumption accepted in [12]. Noncoincidence of factors in the expression for  $\omega_0(\dot{\gamma})$  is caused, judging by obtained results, most probably by the fact that local changes of structure when  $R_e = 1$  appear earlier than the developed well noticeable macroscopic unstable flow of polymers is observed (when  $R_e = R_{e*} = 5-6$ ).

The argument, of the above-obtained temperature-invariant characteristics  $\dot{\gamma}\eta_0$  equals  $\tau_g(\eta_0/\eta)$ , and from the existence of temperature-invariant universal characteristic of viscosity it follows that  $\eta/\eta_0$  is an implicit function of  $\tau_g$ ,

i.e., the argument of considered characteristics will be a single-valued function of shearing stresses.

Thus, change of viscoelastic characteristics of polymers in the fluid state is determined only by effective stresses.

Submitted  
17 June 1964

#### Literature

1. G. V. Vinogradov, I. M. Belkin, A. A. Konstantinov, S. K. Krashenninnikov, B. A. Rogov, A. Ya. Malkin and I. V. Konyukh. Rotational elastoviscosimeters for the investigation of polymeric systems. Plant laboratory, 1964, Vo. 30, No. 3, p. 364.
2. G. V. Vinogradov and N. V. Prozorovskaya. Investigation of melts of polymers on a constant pressures capillary viscosimeter. Plastics, 1964, No. 5, p. 50.
3. A. I. Leonov, A. Ya. Malkin and G. V. Vinogradov. The influence of rigidity of dynamometric devices on results of rheological measurements. Colloid Jour., 1964, Vol. 26, No. 3, p. 335.
4. C. G. Vinogradov, A. Ya. Malkin, Ye. P. Plotnidova and V. A. Kargin. The thixotropy of polymers in a viscofluid state. Reports of Academy of Sciences of USSR, 1964, Vol. 154, No. 6, p. 1421.
5. G. V. Vinogradov, A. Ya. Malkin, N. V. Prozorovskaya and V. A. Kargin. Rheology of polymers. Temperature-invariant characteristic of anomalous-viscous systems. Reports of Academy of Sciences of USSR, 1963, Vol. 150, No. 3, p. 574.
6. G. V. Vinogradov and A. Ya. Malkin. Temperature-independent Viscosity Characteristics of Polymer Systems, J. Polymer Sci., 1964, A2, No. 5, p. 2357.
7. G. V. Vinogradov, A. Ya. Malkin, N. V. Prozorovskaya and V. A. Kargin. Rheology of polymers. Universality of the temperature-invariant characteristic of viscosity of polymeric systems. Reports of Academy of Sciences of USSR, 1964, Vol. 154, No. 4, p. 890.
8. A. Ya. Malkin and A. I. Leonov. Criteria of instability of conditions of shearing strains of elastoviscous polymeric systems. Reports of Academy of Sciences of USSR, 1963, Vol. 151, No. 2, p. 380.
9. B. Gross. Mathematical Structure of the Theories of Viscoelasticity, Hermann, Paris, 1953.
10. F. J. Padden and T. W. De Witt. Some Rheological Properties of Concentrated Polyisobutylene Solutions. J. Appl. Phys., 1954, Vol 25, No. 9, p. 1086.
11. J. Ferry. Viscoelastic properties of polymers, Publishing House of Foreign Literature, M., 1963.
12. A. I. Leonov. Theory of thixotropy of viscoelastic media with continuous distribution of relaxation times. PMTF, 1964, No. 4.

## POLYMER CREEP IN THE VITREOUS STATE

A. V. Dolgov and N. I. Malinin

(Novosibirsk, Moscow)

The theory of linear heredity (viscoelasticity) was widely used for description of deformation properties of polymers in a highly elastic state, and also in the region of transition from a vitreous to a highly elastic state [1-5].

At sufficiently high stress levels creep of polymers and plastics appears also in the vitreous state [6-8]. However, as is noted in [6] (p. 126), the theory of linear heredity does not give satisfactory results during description of behavior of vitreous polymers.

Unfortunately, up to now, apparently, there have been no attempts to apply theories of nonlinear heredity for description of creep of amorphous vitreous polymers and plastics on their basis. There are however several works in which nonlinear theories of viscoelasticity were successfully applied for crystal polymers (caprone [9], a monofiber of polypropylene [10]), and also for amorphous polymers in a highly elastic state (plasticized polyvinylchloride [11, 12]).

Of a number of works dedicated to development of theories of nonlinear heredity, useful in this or that measure for vitreous polymers, are noteworthy the following. Yu. N. Rabotnov [13] proposed a generalization of the line integral of the Volterra equation for nonlinear hereditary material in the form

$$\varphi(t) = \sigma + E \int_0^t \sigma(\theta) J(t-\theta) d\theta \quad (1)$$

Here  $\sigma$  — stress,  $\varepsilon$  — deformation,  $t$  — time,  $E$  — elastic modulus,  $J$  — kernel of equation of heredity,  $\varphi(\varepsilon)$  — certain nonlinear function, determined experimentally. For bodies whose deformation properties are described by equation (1), isochronous curves of deformation, obtained from family of curves of creep, taken at various stresses, have to be similar to the curve of "instantaneous" deformation. According to [9], this principle with sufficient degree of accuracy is also satisfied for certain plastics, in particular caprone.

Leaderman [14] wrote the equation of nonlinear heredity in the form

$$\varepsilon(t) = \frac{\sigma(t)}{E} + \int_0^t \frac{d[\sigma(\theta)]}{d\theta} J_0(t-\theta) d\theta \quad (2)$$

Here  $J_0$  — kernel and  $f(\sigma)$  — nonlinear function of stresses, determined by experimental means. Leaderman applied equation (2) for description of the creep of fibers and other polymer materials. M. I. Rozovskiy in [15] proposed a relationship of the nonlinear theory of heredity in the form

$$\varepsilon = \frac{\sigma}{E} + \int_0^t f[\sigma(\theta)] J^*(t-\theta) d\theta \quad (3)$$

It is not difficult to show that equation (3) by partial integration can be obtained from relationship (2), if one sets  $J_0(x) = df/dx$ .

For material, the time of elastic consequence (or its symbatic relaxation time) which depends on stresses, M. I. Rozovskiy proposed the equation [15]

$$\varepsilon = \frac{\sigma}{E} + \int_0^t J(t-\theta; \sigma) \sigma(\theta) d\theta \quad (4)$$

The assumption about existence of dependence of time of relaxation of polymers on magnitude of effective stress was expressed by A. P. Aleksandrov [16].

This hypothesis was used by Yu. S. Lazurkin for explanation of phenomenon of "forced elasticity" of polymers [17]. The dependence of relaxation time of polymers on the magnitude of effective stress was directly observed by B. A. Dogadkin, G. M. Bartenev and M. M. Reznikovskiy for smoked sheets of natural rubber [18]. Ideas on the dependence of time of relaxation of polymers on stress were used in the investigations of A. L. Rabinovich [18], P. M. Ogibalov [20]. It is necessary to note that such dependence can be obtained from schematic consideration of the

molecular process of deformation of polymers, when under the action of applied stresses every molecular polymer chain accomplishes a gradual transition from initial unbalanced to final equilibrium configuration. This transition constitutes the totality of acts of turn of the molecular segments of the chain relative to their neighbors, where a separate act is accomplished under the action of fluctuations of thermal motion and is accompanied by transition through the energy barrier, which is caused by influence of adjoining groups.

Possibility of construction of functional dependence of general form by a representation in the form of the sum of integral operators of first and highest degrees by analogy with expansion of the usual function in a power series by the Taylor formula was noted in the monograph of V. Volterra [21] (pp. 19-21). This possibility for nonlinear hereditary media was realized by Nakada [22], by obtaining the equation

$$\begin{aligned} \sigma(t) = & \int_0^t \sigma(\theta_1) J_1(t - \theta_1) d\theta_1 + \int_0^t \int_0^t \sigma(\theta_1) \sigma(\theta_2) J_2(t - \theta_1, t - \theta_2) d\theta_1 d\theta_2 + \\ & + \int_0^t \int_0^t \int_0^t \sigma(\theta_1) \sigma(\theta_2) \sigma(\theta_3) J_3(t - \theta_1, t - \theta_2, t - \theta_3) d\theta_1 d\theta_2 d\theta_3 + \dots \end{aligned} \quad (5)$$

Here  $J_1, J_2, J_3$ , etc., are experimentally determinable functions,<sup>1</sup> symmetric relative to their arguments (it is assumed that prior to  $t = 0$  stresses  $\sigma = 0$ ). The possibility of very accurately describing the deformation behavior of high polymers using equation (5) was confirmed in [10, 12], the authors of which kept terms up to the third order inclusively. However it is necessary to note that dependence (5) is more complicated than the foregoing. This fact can cause in certain cases insurmountable difficulties of mathematical character in solving specific problems using equation (5); the difficulties arise also when seeking functions  $J_1, J_2, J_3$ , etc., from experimental data.

In this work an attempt is made to describe deformation properties of amorphous vitreous polymer (unplasticized polyvinylchloride at  $T = 19^\circ\text{C}$ ) during uniaxial extension with the help of equation (4).

Hereditary media differ from "nonhereditary" because their deformations depend

<sup>1</sup>Functions  $J_1, J_2$ , etc., can have strong peculiarities, for instance, in the form of a  $\delta$ -Dirac function; these peculiarities will also determine "instantaneous" deformation.

on the whole past of the stressed-deformed state of a body up to considered moment of time  $t$ . Let us imagine that the past of a stressed-deformed state of a body began at time  $t_0$ , when the body was first subjected to a load. Interval of time  $t - t_0$  by points  $\theta_1$  on the time axis we take on periods  $\Delta\theta_1 = \theta_1 - \theta_{1-1}$ . For a linear body it is possible to assume, following Volterra [21] (p. 194), that during the period of  $\Delta\theta_1$  stresses  $\sigma$  introduce a contribution in the magnitude of deformation  $\epsilon(t)$ , equal to

$$\Delta\epsilon_i = \sigma J(t - \theta) \Delta\theta_i, \quad \theta_{i-1} < \theta < \theta_i \quad (6)$$

Directing  $\Delta\theta_1$  to 0 and integrating from  $t_0$  to  $t$ , we obtain the Volterra equation of the theory of linear heredity.

For a linear body the principle described by expression (6) no longer is satisfied. Instead of (6) we will formulate a new principle, determined by relationship

$$\Delta\epsilon_i = K(\sigma, t - \theta) \Delta\theta_i \quad (7)$$

Let us note that, in virtue of the principle of invariance relative to the beginning of the reading, time as an argument of functions  $J$  and  $K$  can appear only in the form of the difference  $t - \theta$ . Directing  $\Delta\theta_1$  to zero and integrating from  $t_0$  to  $t$ , we obtain the equation of dependence of deformations on stresses in the form

$$\epsilon = F(\sigma) + \int_{t_0}^t K(\sigma, t - \theta) d\theta \quad (8)$$

where  $F(\sigma)$  is a function determining "instantaneous" deformation.

It is necessary to note that the principle described by relationship (7), does not possess sufficient generality for derivation of equation (5)

Because of the selection of form of function  $F(\sigma)$  it is necessary to note the following. Deformation  $F(\sigma)$  is developed practically instantly (more exactly, with the speed of sound). If time of observations is much larger than time of passage of elastic waves through sample, then  $F(\sigma)$  can be considered not dependent on the prehistory of the stressed-deformed state of the body. The magnitude of the instantaneous elastic deformation of polymers is connected with change of interatomic distances and valence angles [1] (p. 117), [23] (pp. 149-150).

The instantaneous-elastic modulus, determined by the ratio of effective stress to the magnitude of conditionally-instantaneous deformation, does not depend on temperature [23] (p. 150), or insignificantly drops with a temperature rise [1] (p. 118). Thus, form of function  $F(\sigma)$  can be determined either by a curve of deformation, taken at low temperatures when the material is "frozen" and highly elastic deformation practically does not develop, or when influence is sufficiently fast.

In the book of T. Alfrey [1] (p. 537) are given curves of deformation for samples of polymethyl methacrylate, a filamentous amorphous polymer (as is polyvinylchloride), at temperatures up to  $-40^{\circ}\text{C}$ . When  $T = -40^{\circ}\text{C}$  the diagram of elongation constituted a straight line up to destruction. Taking into account these data, one may assume that "instantaneous" deformation obeys the law of Hooke, i.e.,  $F(\sigma) = \sigma/E$ . This conclusion is confirmed also by results of A. L. Rabinovich,<sup>1</sup> establishing independence of modulus  $E$  from stress for a series of polymers when load is removed very rapidly. Thus, equation (8) will be written in the form

$$\epsilon = \frac{\sigma}{E} \int_0^t K(\sigma, t - \theta) d\theta \quad (9)$$

Dependence (9) constitutes a nonlinear Volterra equation [24] (pp. 61-68), and coincides with the equation of M. I. Rozovskiy (4), proposed for a material whose relaxation times depend on stress, since it is always possible to assume that  $K(\sigma; t - \theta) = \sigma(\theta)J(\sigma; t - \theta)$ .

In this work unplasticized polyvinylchloride [PVC] (ПВХ) was investigated at  $T = 19^{\circ}\text{C}$ . The material was in the vitreous state, since its temperature of vitrification is  $80^{\circ}\text{C}$  (according to [6] (p. 18)). According to results of investigations of short-term (up to 2500 sec) creeps are determined by the modulus  $E$  and form of function  $K(\sigma, t - \theta)$ . Then with the help of equation (9) behavior of material during other programs of deformation is predicted when, for instance, load increases by the linear law with time or changes intermittently. Obtained results were compared with corresponding experimental data.

Tests were conducted on a program machine with magnetic load, described in

---

<sup>1</sup>Report on Second All-Union conference on theoretical and applied mechanics  
4 February, 1964, Moscow.

article [25]. Deformations were measured on the working part of the sample on a base of 60 mm. Every experiment of the number described below was repeated 3-4 times, and deviation in results of repeated experiments did not exceed 3-4%.

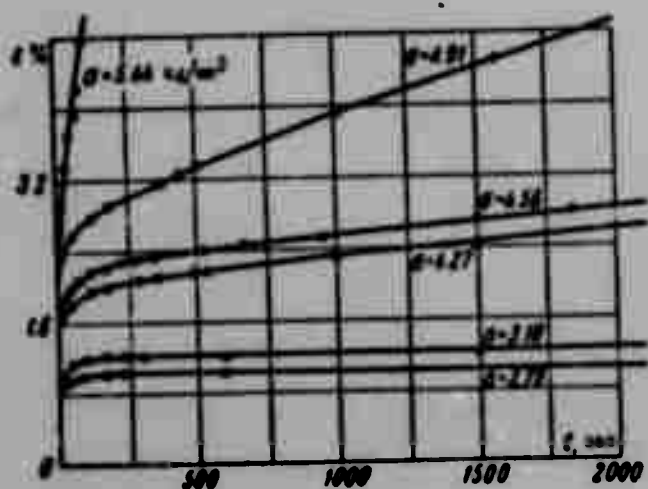


Fig. 1. Curves of creep for PVC at  $T = 19^{\circ}\text{C}$ .

On Fig. 1 are represented curves of creep for PVC, written in coordinates  $\epsilon - t$ . Instantaneous deformation  $\epsilon^{[e]}$  was determined in accordance with the above-stated, Hooke law.

The modulus of "instantaneous" elasticity was calculated by three methods. It was possible to determine it by the magnitude of "instantaneous" deformation during tests on creep conducted for loads which were not too high. With high loads of creep grew very fast and separation of

"instantaneous-elastic" deformation from creep was difficult. By the second method the modulus  $E$  was determined as the tangent of the angle of inclination of the initial linear section of the curve of deformation (solid curves, represented on Fig. 2), taken with a constant rate of load. And, finally, it was possible to determine modulus  $E$  by the magnitude of "instantaneous" return as the load was removed. All these three methods gave the same value of modulus  $E$ .

On Fig. 3 are given curves of deformation for PVC under loading at constant rate  $\sigma$  and subsequent removal of load, taken at  $15^{\circ}\text{C}$ .

Removal of load was done over 0.03 sec, i.e., practically instantly. After removal of load the curve of return was taken in coordinates  $\epsilon - t$  (diagram was recorded on tape of oscillograph H-700) as long as rate of return did not decrease to a minute, almost elusive magnitude. On Fig. 3 return is represented by heavy lines proceeding along the axis of abscissas. For sample No. 82 return is fixed over 0.1 sec for samples 49 and 80 - over 0.5 and 2 sec correspondingly. From Fig. 3 it is clear that the straight line corresponding to "instantaneous" return is parallel to the initial linear section of the load curve that confirms the above position, and also results obtained by A. L. Rabinovich. From diagrams, represented on Fig. 3, is obtained the value of elastic modulus  $E = 3 \cdot 10^4 \text{ kg/mm}^2$  at  $T = 15^{\circ}\text{C}$ ,

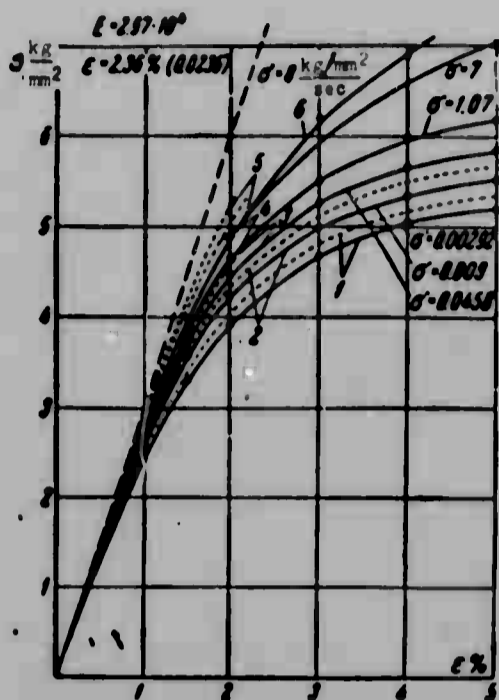


Fig. 2. Curves of elongation PVC,  $E = 2.97 \cdot 10^4$ ; 1 -  $\sigma = 2.92 \cdot 10^{-3}$  kg/mm<sup>2</sup> sec, 2 -  $\sigma = 9 \cdot 10^{-3}$  kg/mm<sup>2</sup> sec, 3 -  $\sigma = 4.58 \cdot 10^{-2}$  kg/mm<sup>2</sup> sec, 4 -  $\sigma = 1.07$  kg/mm<sup>2</sup> sec, 5 -  $\sigma = 7$  kg/mm<sup>2</sup> sec, 6 -  $\sigma = 8$  kg/mm<sup>2</sup> sec;  $T = 19^\circ\text{C}$ .

the end sharply deviated from the initial rectilinear dependence. With high loads and small times the third period of creep was finished by a brittle break of the sample, and for smaller loads and sufficiently large durations it finished by formation of a neck in accordance with mechanism of "forced elasticity". Both these mechanisms are studied in detail for amorphous polymers in [17]. On Figs. 1 and 4 sections corresponding to the third period of creep are absent. Theory, equations of which are given below, does not describe creep of material on the third section.

The empirical formula, corresponding to rectilinear in coordinates  $\lg \epsilon^{[c]}$ ,  $\lg t$  of the diagrams (Fig. 4), has the form

$$\epsilon^{[c]} = A_1 t^n \quad (10)$$

where  $A_1$  and  $n$  are tension functions of  $\sigma$ . The last one during the period of the experiment was kept on a constant (if we disregard insignificant transverse

practically not differing from modulus

$E = 2.97 \cdot 10^4$  kg/mm<sup>2</sup> at  $T = 19^\circ\text{C}$ . Nonlinear sections of diagrams on Figs. 2 and 3 differed considerably, caused by higher creep at  $T = 19^\circ\text{C}$ .

Creep  $\epsilon^{[c]}$  was determined by the difference of full and "instantaneous-elastic" deformations. On Fig. 4 curves of creep (the same, as on Fig. 1) are depicted in logarithmic coordinates  $\lg \epsilon^{[c]} - \lg t$  (as the beginning of the time reading, as usual, the moment of application of load is taken). In these coordinates diagrams of creep are well approximated by straight lines. This result will agree with data of the work of Findley [8], which graphs of  $\lg \epsilon^{[c]} - \lg t$  were also very well contained on straight lines up to  $t = 100,000$  hours and more.

Here one should note that in certain cases, when on curves of creep for PVC a third section was observed, the diagram of  $\lg \epsilon^{[c]} - \lg t$  at

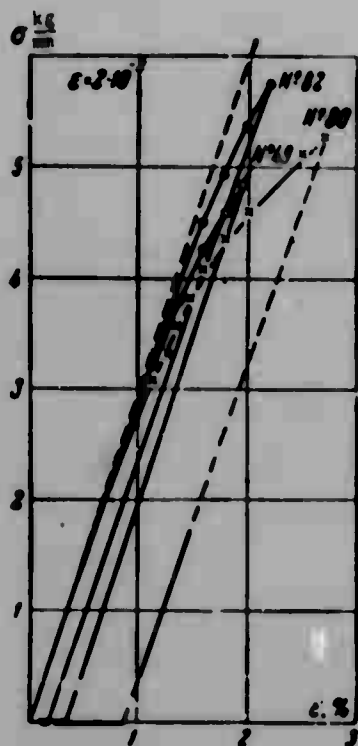


Fig. 3. Curves of loading and removal of load for PVC at  $T = 15^{\circ}\text{C}$  for samples No. 49, 80 and 82 correspondingly:  
 $\sigma' = 8.6 \cdot 10^{-3} \text{ kg/mm}^2 \text{ sec}$ ,  $\sigma' = 3.86 \cdot 10^{-3} \text{ kg/mm}^2 \text{ sec}$ ,  $\sigma' = 6.6 \text{ kg/mm}^2 \text{ sec}$ .

compression of sample) level and therefore can be considered as a parameter. For convenience it is possible to set  $n = 1 - f_2(\sigma)$ ,  $A_1 = f_1(\sigma)/(1 - f_2(\sigma))$ ; equation (9) will take the form

$$\epsilon = \frac{\sigma}{E} + \int_0^t \frac{f_1(\sigma)}{(t-\theta)^{1/n}} d\theta \quad (11)$$

On Fig. 5 small crosses represent results of experimental determination of function  $f_1(\sigma)$ , points - corresponding results for  $f_2(\sigma)$ . Dependence  $f_1(\sigma)$  is rather well approximated by the function

$$f_1(\sigma) = A_2 \text{sh} \frac{\sigma}{\sigma_0} \quad (12)$$

where  $A_2$  and  $\sigma_0$  are parameters. This one may well see on Fig. 5, where the broken line depicts function (12), while  $A_2 = 1.64 \cdot 10^5$  and  $\sigma_0 = 1.086 \text{ kg/mm}^2$ . Values of  $f_2$  for stresses lower than  $\sigma = 2.79 \text{ kg/mm}^2$  were not determined, since with such low  $\sigma$  creep was insignificant, and accuracy of determination of  $f_2$  is insufficient. For stresses  $\sigma = 2.79, 3.18$  and  $4.27 \text{ kg/mm}^2$  is obtained the same value

$f_2$ , equal to 0.8. In order to estimate movement of function  $f_2(\sigma)$  at lower stresses, we will take into account experimental data of Findley [8], obtained for a large number of polymeric materials, including polyvinylchloride. Findley established that, at least at not too high stresses, not provoking destruction or cold extraction of sample over  $\sim 10^5$  hours, straight lines approximating diagram of creep in coordinates  $\lg \epsilon^{[c]} - \lg t$ , are parallel. On the basis of these results Findley considered parameter  $n$  in the empirical equation assumed by him for the family of curves of creep of form

$$\epsilon^{[c]} = A_3^n \text{sh} \frac{\sigma}{\sigma_0} \quad (13)$$

as constant. Really, for stresses  $\sigma = 2.79, 3.18$  and  $4.27 \text{ kg/mm}^2$  function  $f_2(\sigma)$ , and consequently also  $n$  practically do not change with change of stress. In connection with the above-stated we will consider that  $f_2(\sigma)$  when stresses are below  $2.79 \text{ kg/mm}^2$  will keep a constant value.

Thus, the region of stresses from  $\sigma = 0$  to a certain critical stress provoking

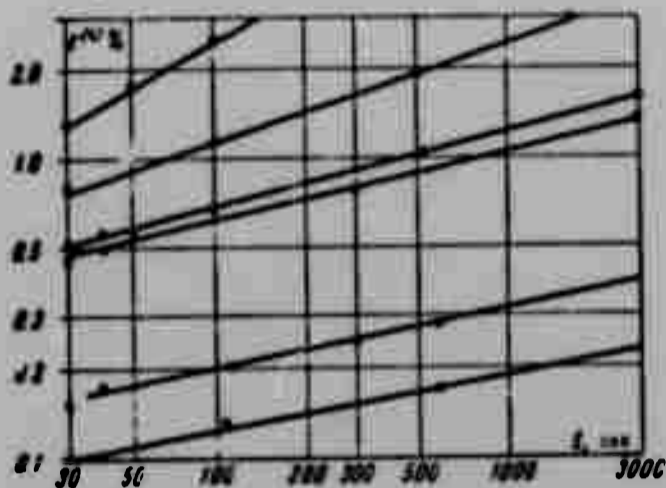


Fig. 4. Curves of creep for PVC (the same as on Fig. 1) in  $\lg \epsilon^{[c]} - \lg t$ .

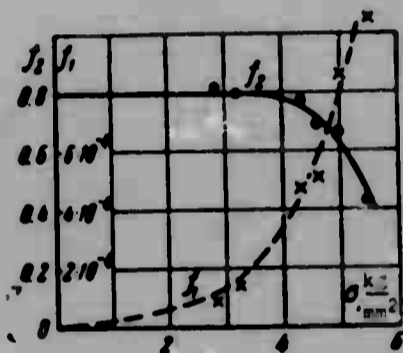


Fig. 5. Graph of functions  $f_1(\sigma)$  and  $f_2(\sigma)$ .

theory described by the equation of M. I. Rozovski (3).<sup>1</sup> And, finally, in the subdomain of still higher voltages it is necessary to take into account dependence of relaxation times on effective stress, and for calculations of creeps to use relationships (4) or (9). Check of applicability of equation (11) for description of creep processes during other programs of change of stresses in time was conducted in experiments illustrated below.

<sup>1</sup>Findley considers that "instantaneous" deformations change with change of stress by a nonlinear law. Considering the above considerations, data of the work of A. L. Rabinovich and our data, represented on Fig. 3, the conclusion can be made that for "instantaneous" deformations Hooke's law is satisfied. Nonlinearity of diagrams of "instantaneous" deformation, obtained by Findley was, apparently, caused by the fact that the load was applied not instantly, and creep appeared in the process of loading, as for instance, in our experiments represented on Figs. 2 and 3.

destruction or "cold extraction" of sample, can be divided into three subdomains. At the lowest stresses, when  $\ln(\sigma/\sigma_0) \approx \sigma$ , we have a linear subdomain. This result coincides with data of the work of G. I. Bryzgalin [26], establishing that at sufficiently low stresses plastic on the basis of glasslike polymers behave as linear hereditary bodies. In this subdomain for determination of creeps of plastics and polymers it is possible to use theories of linear creep. For curves of creep corresponding to the second subdomain, one should consider nonlinearity of the dependence of deformations  $\epsilon^{[c]}$  on stresses, but it is possible to use the dependence of Findley (13) and to consider  $n$  constant. If in this subdomain the principle described by equation (7) is satisfied, it is possible to show that for calculation of deformations of plastics it is possible to use the

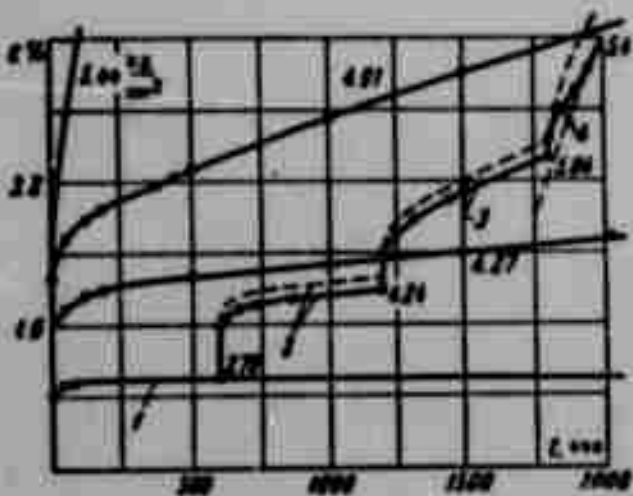


Fig. 6. Curve of creep under step loading:

1 —  $\sigma = 2.79 \text{ kg/mm}^2$ , 2 —  $\sigma = 4.24 \text{ kg/mm}^2$ , 3 —  $\sigma = 5.04 \text{ kg/mm}^2$ , 4 —  $\sigma = 5.4 \text{ kg/mm}^2$ ;  $T = 19^\circ \text{C}$

On Fig. 2 solid lines depict curves of deformation for PVC, obtained during constant loading rates. The dotted line represents analytic curves built according to equation (11) with use of functions  $f_1(\sigma)$  and  $f_2(\sigma)$ , depicted on Fig. 5. Construction of analytic curves was connected with calculation of magnitude of integral in the right part of equation (11). During determination of magnitude of integral, which was conducted by numerical methods, it was taken into

account that the integrand expression had a weak peculiarity at  $t = 0$ . Dotted curves go only to stresses  $\sigma = 5.5 \text{ kg/mm}^2$ . For higher stresses usually processes began connected with the third stage of creep, illustrated above. These processes, as was noted earlier, are not described by theories considered here. From Fig. 2 it is clear that during low loading rates  $\sigma' = 4.58 \cdot 10^{-2}$ ,  $9 \cdot 10^{-3}$ ,  $2.92 \cdot 10^{-3} \text{ kg/mm}^2 \text{ sec}$  deviations of experimental curves from calculated curves do not exceed 3%, if one considers deviations with respect to stresses.

If, however, these deflections are considered deformations, then they will be sometimes higher, since curves of deformation are at the end rather hollow. During high loading rates ( $\sigma = 1.07$ ,  $7$ ,  $8 \text{ kg/mm}^2 \text{ sec}$ ) deflections of analytic curves from experimental is somewhat higher and attain 8%, if one were to determine them with respect to stresses. But if deflection for deformation, then they turn out to be somewhat lower.

Higher deflections of analytic curves from those determined experimentally at high loading rates can be explained by the following circumstance. Dependencies (10) and (12) are built by points corresponding to values  $t \gg 1 \text{ sec}$  (for instance  $t = 10 \text{ sec}$  and more).

It is necessary to expect that dependence (11), in which these data were, will be with sufficient degree of accuracy satisfied only for sufficiently large values of time. But there are no bases to extrapolate this dependence on times measured in tenths of a second and less, for which exact values of  $\epsilon^{[c]}$  and  $\sigma$  by fully

understandable causes connected with inertness of machine, in experiments on creep were not obtained. Moreover, extrapolation of rectilinear sections of diagrams of creep, represented on Fig. 4, on region of lower values of  $t$  will lead to contradiction, since these straight lines will cross, which is improbable. Therefore good coincidence of analytic curves with experimental can be expected only for sufficiently large  $t$ , for instance, when  $t > 10$  sec.

On Fig. 6 is represented curve of creep in coordinates  $\epsilon$ ,  $t$ , obtained for a step increasing load. Solid lines — experimental data, hachured — calculation by equation (11) taking into account (10) and (12). For a step variable load equation (11) is integrated easily. Let us assume that the initial step (which subsequently we will consider for simplicity as zero) was applied at time  $t_0 = 0$ , the  $i$ -th step — at time  $t = t_i$ . Deformation on  $k$ -th step of stress is

$$\epsilon(t) = \frac{\sigma_k}{E} + \sum_{i=1}^k \frac{f_1(\sigma_i)}{1 - f_1(\sigma_i)} \left[ (t - t_i)^{f_1(\sigma_i)} - (t - t_{i-1})^{f_1(\sigma_i)} \right] \quad (14)$$

where we will consider  $t - t_{k+1} = 0$ . On the initial section, corresponding to stress  $\sigma = 2.79 \text{ kg/mm}^2$ , experimental and analytic curves coincided. From Fig. 6 it is clear that analytic curves within limits of band of scattering are near the experimental curves.

On Fig. 7 are represented curves of deformation for PVC during repeated cycles of loading — load removal. Magnitude of load was  $4.35 \text{ kg/mm}^2$ . Under a load



Fig. 7. Curves of creep for PVC under deformation in coordinates  $\epsilon\%$  —  $t$ ;  $T = 19^\circ \text{C}$

deformation increased, during removal of load it fell. Calculations were conducted by formula (14), useful for the considered case. Solid line — experiment, dotted line — analytic curve. As can be seen from Fig. 7, under a load during the first cycle deformations, corresponding to the analytic curve, are lower than

corresponding experimental magnitudes approximately by 4%. This small divergence is fully explained by scattering of experimental data, since the analytic curve is built according to the basic experiment, results of which accurate to the magnitude

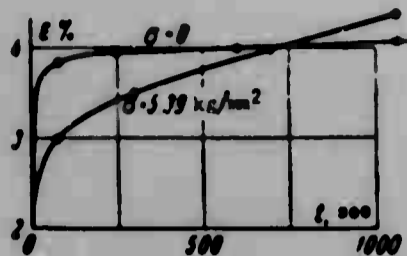


Fig. 8. 1 - curve of creep for PVC,  $\sigma = 5.39$  kg/mm<sup>2</sup>, 2 - curve of return after experiment on creep 1060 sec long of the type represented on Fig. 1;  $T = 16^{\circ}\text{C}$ .

of scattering can deviate from data of control experiment, represented on Fig. 7. Subsequently on sections of curve (Fig. 7), where the load acted, the analytic curve deviates from the experimental also insignificantly.

Analytic curves, corresponding to return (when load is removed), will deviate considerably more from experimental curves. However during the design of constructions this experimental fact cannot have a large value on creep and strength, since during the period when the load does not act on construction danger of its destruction is absent.

If one were to use the ideas well-developed in [10-12], then it is possible to construct curves of creep and return. They will have the form represented on Fig. 8. Return in the beginning occurs faster than creep, but then deformations of creep exceed deformations of return. The theory described by equations (4), (8) and (9) does not explain this effect. As it was shown in [10, 12], the theory described by equation (5) possesses generality sufficient for prediction of such effects.

In conclusion one should note that the solution of nonlinear integral Volterra equation(9), important for applications, may be obtained by the method of successive approximations described in the monograph of F. Trikomí [24] (pp. 61-68).

Submitted  
10 June 1964

#### Literature

1. T. Alfrey. Mechanical properties of high polymers. Publishing House of Foreign Literature, M., 1952.
2. J. Ferry. Viscoelastic properties of polymers. Publishing House of Foreign Literature, M., 1963.
3. G. L. Slonimskiy. \*Laws of deformation of real materials. I. Jour. tech. physics, 1939, Vol. 9, No. 20, p. 1791.
4. A. P. Bronskiy. Phenomenon of after-effect in a solid body. PMM, 1941, Vol. 5, Issue 1.
5. N. I. Malinin. Creep and relaxation of polymers in the transition state. PMTF, 1961, No. 1, p. 56.

6. H. Stuart (Redakteur). Die Physik der Hochpolymeren. Bd. IV, Berlin, Springer-Verlag, 1956.
7. J. Marin, Y. H. Pao and G. Cuff. Creep properties of lucite and plexiglas for tension, compression, bending and torsion. Trans. ASME, 1951, Vol. 73, No. 5, p. 705.
8. W. N. Findley. Creep and relaxation of plastics. Machine Design, 1960, Vol. 32, No. 10, p. 205.
9. M. A. Koltunov and V. N. Bezukhov. Thermomechanical behavior of caprone. Herald of Moscow University, 1962, No. 6, p. 51.
10. I. M. Ward and E. T. Onat. Non-linear mechanical behavior of oriented polypropylene. J. Mech. and Phys. Solids, 1963, Vol. 11, No. 4, p. 217.
11. H. Leaderman. Large longitudinal retarded elastic deformation of rubberlike network polymers. Trans. Soc. Rheol., 1962, Vol. 6, p. 361.
12. H. Leaderman, F. McCrackin and O. Nakada. Large longitudinal retarded elastic deformation of rubberlike network polymers. II. Application of a general formulation of nonlinear response. Trans. Soc. Rheol., 1963, Vol. 7, p. 111.
13. Yu. N. Rabotnov. Certain questions on the theory of creep. Herald of Moscow University, 1948, No. 10, p. 81.
14. H. Leaderman. Elastic and creep properties of filamentous and other high polymers. Washington, Textile Foundation, 1943.
15. M. I. Rozovskiy. Creep and prolonged destruction of materials. Jour. tech. physics, 1951, Vol. 21, No. 11, p. 1311.
16. A. P. Aleksandrov. Frost-resistance of high-molecular compounds. Transactions of I and II conferences on high-molecular compounds. Publishing House of Academy of Sciences of USSR, M.-L., 1945, p. 49.
17. Yu. S. Lazurkin and R. L. Fogel'son. The nature of large deformations of high-molecular substances in the glasslike state. Jour. tech. physics, 1951, Vol. 21, No. 3, p. 267.
18. B. A. Dogadkin, G. M. Bartenev and M. M. Reznikovskiy. Investigation of the role of molecular forces in the mechanism of highly elastic deformation. I. Molecular mechanism and the equation of kinetics of highly elastic deformation. Colloid Jour., 1949, Vol. 11, No. 5.
19. A. L. Rabinovich and A. V. Turazyan. Influence of rate of deformation on magnitude of deformation and strength of oriented glass plastics. Reports of Academy of Sciences of USSR, 1963, Vol. 148, No. 6, p. 1350.
20. P. M. Ogibalov and I. M. Tyuneyeva. Theoretical treatment of experimental data about elastic after-effect of glass plastics. Herald of Moscow University, 1964, No. 2, p. 58.
21. V. Volterra. Theory of functionals and of integral and integro-differential equations. London and Glasgow, Blackie and Son Limited, 1931.
22. O. Nakada. Theory of non-linear responses. J. Phys. Soc. Japan, 1960, Vol. 15, No. 12, p. 2280.
23. P. P. Kobeko. Amorphous substances. Publishing House of Academy of Sciences of USSR, M., 1952.
24. F. Tricomì. Integral equations. Publishing House of Foreign Literature, M., 1960.
25. S. T. Mileyko and V. I. Telenkov. Short-term creep of aluminum alloys. PMTF, 1962, No. 5, p. 168.

26. G. I. Bryzgalin. The description of anisotropic creep of glass plastics.  
PMTF, 1963, No. 6, p. 117.

## RUPTURE OF A BODY WITH LINEAR DISLOCATION

M. Ya. Leonov and K. N. Rusinko

(Frunze)

Brittle rupture of an unbounded body with introduced material half-plane is investigated (edge dislocation) during its uniform extension to infinity by forces perpendicular to the shown half-plane. The basic purpose of this work is clarification of the influence of different laws of interaction of opposite edges of cracks on conditions of brittle rupture. In this meaning it is the continuation and development of [1].

§ 1. Initial model of a solid body. We consider an ideally uniform model of a fragile body possessing the following properties: 1) maximum tensile stresses do not exceed certain constant of material ( $\sigma_0$ ), called resistance to breaking away; 2) dependence between deformations and stresses is described by the law of Hooke, if tensile stresses do not attain magnitude  $\sigma_0$ ; 3) in the model cracks are formed when maximum normal stress in the body, deformations of which everywhere obey the law of Hooke, exceeds  $\sigma_0$ ; 4) edges of crack are attracted by stress  $\sigma$  which is an arbitrary continuous nonnegative nonincreasing function  $\sigma(h)$  of the distance  $h$  between edges of slot (Fig. 1), where it is considered that

$$\sigma(0) = \sigma_0, \quad \int_0^\infty \sigma(h) dh < \infty \quad (1.1)$$

As in [1], here there are made no assumptions relative to smallness of area of interacting part of surface of crack.

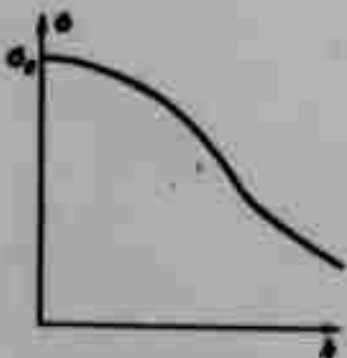


Fig. 1.

## § 2. Formulation of problem. Let us consider in

conditions of flat deformation an unbounded body into which is introduced a material half-plane of thickness  $\mu$ ; at infinity normal stresses  $s$ , perpendicular to the introduced half-plane are applied to the body.

If the indicated body remained continuous and its deformation everywhere obeyed Hooke's law, then normal stresses  $\sigma_y$  in points lying on the continuation of the

implanted half-plane would be represented in the form [2]

$$\sigma_y = s + \frac{E\mu}{4\pi(1-\nu^2)l} \quad (2.1)$$

Here  $l$  — distance from boundary of introduced half-plane,  $E$  — elastic modulus,  $\nu$  — Poisson's ratio. For sufficiently small  $l$  stresses determined by the formula, will exceed resistance to breaking away. Consequently, in this region of the considered model will be formed a crack.

Under the action of tensile stresses  $s$ , applied to the body at infinity, the shown crack will be developed. Under assigned, fixed power  $\mu$  of the introduced layer it is required to determine maximum intensity of load  $s$  (limiting intensity of load  $s$ ), at which is possible equilibrium of the considered body. Origin of coordinates is selected in the center of the crack, axis  $x$  is directed along crack, axis  $y$  — in the direction of extension of body (Fig. 2). Distance between edges of slot is equal to doubled displacement along  $y$  axis of surface points of crack from action of pressure  $p(x)$ , supplementing stress (2.1) to stresses  $\sigma(h)$ , i.e.,

$$p(x) = s + \frac{E\mu}{4\pi(1-\nu^2)(x+L)} - \sigma[2v(x, +0)] \quad (2.2)$$

Here  $v(x, +0)$  — normal displacement of shore of crack,  $L$  — half-length of crack. For determination  $v(x, +0)$ , following [2], we will obtain

$$v(x, +0) = \frac{1-\nu^2}{\pi E} \int_{-L}^L p(\xi) \Lambda(x) d\xi, \quad \Lambda(x) = \ln \frac{L^2 - x\xi + \sqrt{(L^2 - x^2)(L^2 - \xi^2)}}{L^2 - x\xi - \sqrt{(L^2 - x^2)(L^2 - \xi^2)}}$$

Placing here the value of pressure given by formula (2.2), and calculating corresponding integrals, we will obtain [2]

$$v(x, +0) = \frac{2(1-\nu^2)}{E} s \sqrt{L^2 - x^2} + \frac{\mu}{2\pi} \arccos \frac{x}{L} - \frac{1-\nu^2}{\pi E} \int_{-L}^L \sigma[2v(\xi, +0)] \Lambda(x) d\xi \quad (2.3)$$

If in the last formula function  $\sigma[2v(x, +0)]$  is given in evident form through  $2v(x, +0)$ , we will obtain the integral equation for finding displacement  $v(x, +0)$ .

In this equation<sup>1</sup> also unknown is parameter  $L$ . This parameter will be found from the condition of boundedness of tensile stresses, which is equivalent [3] to relationship

$$\frac{\partial v(x, +0)}{\partial x} \Big|_{x=L} = 0 \quad (2.4)$$

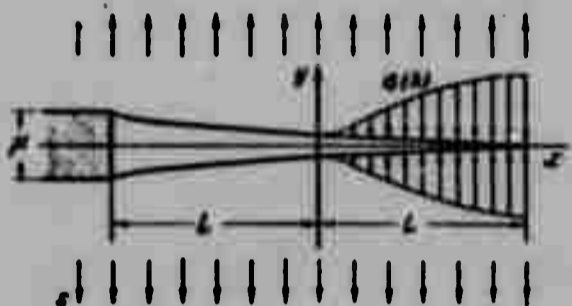


Fig. 2.

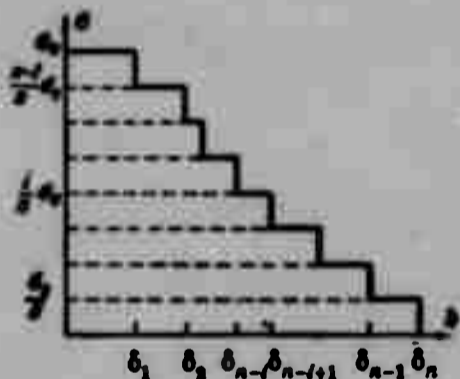


Fig. 3.

Let us note that under load  $s$ , less than limiting, at point  $x = -L$ ,  $y = 0$  normal stresses are infinite.<sup>2</sup> These stresses, however, are negative (compressing), and therefore during investigation of crackformation are not taken into account.

Equation (2.3) and condition (2.4) are sufficient for determination of displacement of edge of crack.

§ 3. Multistage law of attraction of opposite edges of crack. Let us replace temporarily dependence  $\sigma(h)$  (Fig. 1) by a broken line, as was shown on Fig. 3. For the present we will consider that edges of slot either are attracted with stress  $\sigma_{0i}/n$  ( $i = 1, 2, \dots, n$ ), if distance

<sup>1</sup>In [2] is expounded the approximate solution of this equation for the case of linear dependence  $\sigma[2v]$ .

<sup>2</sup>As we will see subsequently, during the action of a limit load normal stress  $\sigma_y$  is bounded also at point  $x = -L$ ,  $y = 0$ .

between them is within the limits from  $\delta_{n-1}$  to  $\delta_{n-1+1}$ , or do not interact otherwise; here  $n$  - arbitrary integer,  $\delta_1$  - any magnitudes (with the dimension of length), satisfying inequalities

$$\delta_0 = 0 < \delta_1 < \delta_2 < \dots < \delta_n$$

Let us consider at first the case  $\mu < \delta_n$ . In this case edges of slot interact, as is shown on Fig. 4. Boundary conditions for this slot will be

$$\sigma[2v(x, +0)] = \begin{cases} \alpha_0/n & \text{when } -L < x < b_{r+1} \\ \alpha_0(r+1)/n & \text{when } b_{r+1} < x < b_{r+2} \quad (r \leq n) \\ \alpha_0(r+2)/n & \text{when } b_{r+2} < x < b_{r+3} \\ \alpha_0 & \text{when } b_n < x < L \end{cases} \quad (3.1)$$

where  $r$  - integer depending on  $\mu$ ,  $b_i$  ( $i = r+1, r+2, \dots, n$ ) - an unknown magnitude; equations for their determination will be composed below.

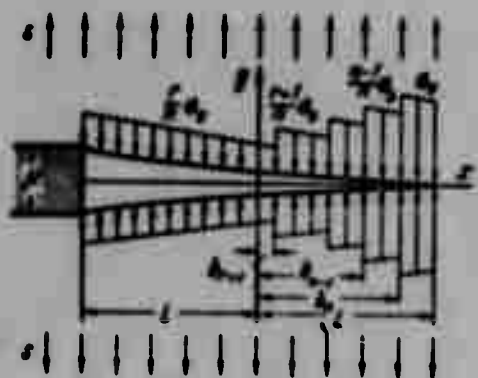


Fig. 4.

With such a law of interaction by formula (2.3) it is easy to find displacement of points of edge of crack. In this case

$$\begin{aligned} v(x, +0) = & \frac{1-v^2}{\pi E} \left\{ 2\pi s \sqrt{L^2 - x^2} + \right. \\ & + \frac{E\mu}{2(1-v^2)} \arccos \frac{x}{L} - \frac{2\pi r \alpha_0}{n} \sqrt{L^2 - x^2} - \\ & - \frac{\alpha_0}{n} \sum_{j=r+1}^n \left[ 2 \sqrt{L^2 - x^2} \arccos \frac{b_j}{L} + \right. \\ & \left. \left. + (x-b_j) \ln \frac{L^2 - bx + \sqrt{(L^2 - b_j^2)(L^2 - x^2)}}{L^2 - bx - \sqrt{(L^2 - b_j^2)(L^2 - x^2)}} \right] \right\} \end{aligned} \quad (3.2)$$

Here and subsequently we consider principal values of the function  $\arccos x/L$ .

Stress on end of slot  $x = L$  must be finite, that is equivalent to condition (2.4). This condition gives

$$\pi s L + \frac{E\mu}{4(1-v^2)} - \frac{\alpha_0 L}{n} \sum_{j=r+1}^n (\sin \gamma_j + \gamma_j) - \frac{\pi r \alpha_0 L}{n} = 0 \quad (3.3)$$

$$\gamma_i = \arccos \frac{b_i}{L} \quad (i = r+1, r+2, \dots, n) \quad (3.4)$$

Relationship (3.3) may be converted to the form

$$L = \frac{E\mu}{4(1-\nu^2)} \frac{n}{s_0} \left[ \sum_{j=r+1}^n (\sin \gamma_j + \gamma_j) + \pi r - \frac{\pi n s}{c_0} \right]^{-1} \quad (3.5)$$

In order to compose  $n - r$  equations for  $n - r$  unknowns of the quantities  $b_1$ , we will turn to the law of attraction between surfaces of crack. Dependence of intensity of interaction of edges of slot on distance  $h$  between them is represented on Fig. 3. In points where  $2v = h = \delta_{n-i+1}$  ( $i = r+1, r+2, \dots, n$ ), the indicated force of interaction changes by the quantity  $\sigma_0/n$ . Abscissas of these points on Fig. 4 are designated by  $b_1$ . Equating doubled displacement  $2v(x, +0)$  of the shown points to corresponding values  $\delta_1$ , we will obtain equations for determination of unknowns

$$\begin{aligned} 2v(b_{r+1}, +0) &= \delta_{n-r} \\ 2v(b_{r+2}, +0) &= \delta_{n-r-1} \\ 2v(b_{r+3}, +0) &= \delta_{n-r-2} \\ 2v(b_n, +0) &= \delta_1 \end{aligned} \quad (3.6)$$

Using formula (3.2), we will write these equations in expanded form:

$$\begin{aligned} \frac{\pi E}{1-\nu^2} \delta_{n-r} &= 4L \sin \gamma_{r+1} \left( \pi s - \frac{c_0}{n} \sum_{j=r+1}^n \gamma_j - \frac{\pi r c_0}{n} \right) + \\ &+ \frac{E\mu}{1-\nu^2} \gamma_{r+1} - \frac{2c_0}{n} \sum_{j=r+1}^n (b_{r+1} - b_j) \ln \frac{1 - \cos(\gamma_{r+1} - \gamma_j)}{1 - \cos(\gamma_{r+1} + \gamma_j)} \\ \frac{\pi E}{1-\nu^2} \delta_{n-r-1} &= 4L \sin \gamma_{r+2} \left( \pi s - \frac{c_0}{n} \sum_{j=r+1}^n \gamma_j - \frac{\pi r c_0}{n} \right) + \\ &+ \frac{E\mu}{1-\nu^2} \gamma_{r+2} - \frac{2c_0}{n} \sum_{j=r+1}^n (b_{r+2} - b_j) \ln \frac{1 - \cos(\gamma_{r+2} - \gamma_j)}{1 - \cos(\gamma_{r+2} + \gamma_j)} \\ &\dots \dots \dots \\ \frac{\pi E}{1-\nu^2} \delta_1 &= 4L \sin \gamma_n \left( \pi s - \frac{c_0}{n} \sum_{j=r+1}^n \gamma_j - \frac{\pi r c_0}{n} \right) + \\ &+ \frac{E\mu}{1-\nu^2} \gamma_n - \frac{2c_0}{n} \sum_{j=r+1}^n (b_n - b_j) \ln \frac{1 - \cos(\gamma_n - \gamma_j)}{1 - \cos(\gamma_n + \gamma_j)} \end{aligned} \quad (3.7)$$

Adding the left and right side of the last equalities (including, also those passed through, designated by dots), we will obtain

$$\frac{\pi E}{1-\nu^2} \sum_{j=1}^{n-r} \delta_j = \frac{E\mu}{1-\nu^2} \sum_{j=r+1}^n \gamma_j + 4L \left( \pi s - \frac{c_0}{n} \sum_{j=r+1}^n \gamma_j - \frac{\pi r c_0}{n} \right) \quad (3.8)$$

Excluding parameter  $L$  from formulas (3.5) and (3.8), we find

$$\begin{aligned} s = \frac{\sigma_0}{\pi n} \left\{ a_1 \left[ \pi r + \sum_{j=r+1}^n (\sin \gamma_j + \gamma_j) \right] + \pi r \sum_{j=r+1}^n (\sin \gamma_j - \gamma_j) - \right. \\ \left. - \left( \sum_{j=r+1}^n \gamma_j \right)^2 \right\} \left[ \sum_{j=r+1}^n (\sin \gamma_j - \gamma_j) + a_1 \right]^{-1} \quad \left( a_1 = \frac{\pi}{\mu} \sum_{j=1}^{n-r} \delta_j \right) \end{aligned} \quad (3.9)$$

Dependence (3.9) is basic during further investigation of destruction of a body with dislocation.

Let us consider now the case  $\mu > \delta_n$ . In this case edges of crack do not interact on certain section  $-L < x < b_1$ , and on remaining section of surface of slot are attracted, as is shown on Fig. 5. Boundary conditions for this slot will be

$$\sigma[2\nu(x, +0)] = \begin{cases} 0 & \text{when } -L < x < b_1 \\ \sigma_0/n & \text{when } b_1 < x < b_2 \\ 2\sigma_0/n & \text{when } b_2 < x < b_3 \\ \dots\dots\dots & \dots\dots\dots \\ \sigma_0 & \text{when } b_n < x < L \end{cases} \quad (3.10)$$

From comparison of formulas (3.1) and (3.10) we conclude that in this case ( $\mu > \delta_n$ ) the connection between stress  $s$  and parameters of crack  $\gamma_1$  is expressed by the formula (3.9), in which one should consider  $r = 0$ .

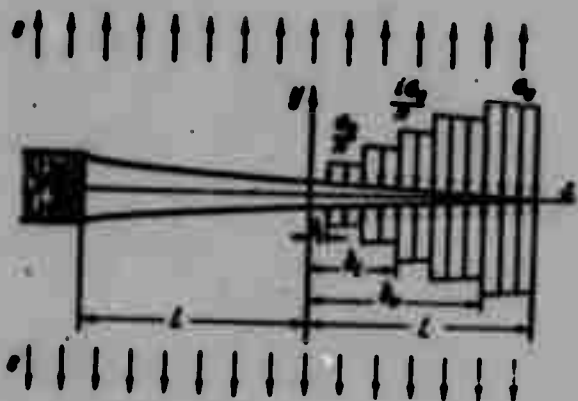


Fig. 5.

§ 4. Determination of limit load. Let us assume that  $\mu < \delta_n$ . From formulas (3.5), (3.7), obtained in assumption that  $\delta_{n-r} < \mu < \delta_{n-r+1}$ , it is possible, in general, to determine dimensions of slot ( $L, b_{r+1}, b_{r+2}, \dots, b_n$ ), corresponding to given load  $s$  and power of dislocation  $\mu$ . However subsequently we will

find the maximum value of load  $s$  (limiting intensity of load  $s$ ), at which is possible equilibrium of considered model of body, having dislocation of assigned power  $\mu$ .

In this case ( $\mu < \delta_n$ ) the limit load is maximum of magnitude  $s$ , determined by formula (3.9) as a function of variables  $\gamma_i$  ( $i = r+1, r+2, \dots, n$ ), where the quantities  $\gamma_1$  are connected by  $n - r$  relationships (3.7), of which  $n - r - 1$  are

independent.<sup>1</sup>

For determination of maximum of right side of formula (3.9) we will introduce new variables

$$z_1 = \sum_{j=r+1}^n \gamma_j, \quad z_2 = \sum_{j=r+1}^n \sin \gamma_j \quad (4.1)$$

The quantities  $\gamma_i$ , determined by formula (3.4), satisfy inequalities  $0 < \gamma_i < \pi$  ( $i = r+1, r+2, \dots, n$ ). Consequently, variables  $z_1$  and  $z_2$  can take only positive values.<sup>2</sup>

During substitution (4.1) formula (3.9) will be converted to the form

$$s = a_0 \frac{a_1(\pi r + z_1 + z_2) + \pi r(z_2 - z_1) - z_1^2}{\pi a(z_2 - z_1 + a_1)} \quad (4.2)$$

The right side of this formula is equal to zero when

$$a_1(\pi r + z_1 + z_2) + \pi r(z_2 - z_1) - z_1^2 = 0 \quad (4.3)$$

Subsequently under region of variation of variables  $z_1, z_2$  we will consider the region (in plane  $z_1, z_2$ ) bounded by curve (4.3) and positive direction of axes  $z_1$  and  $z_2$ .

From formula (4.2) it follows that when  $z_1 = a_1$  the right side of this formula does not depend on  $z_2$ . Furthermore, independently of the value  $z_2 > 0$  we have

$$\left. \frac{\partial s}{\partial z_1} \right|_{z_1=a_1} = 0, \quad \left. \frac{\partial^2 s}{\partial z_1^2} \right|_{z_1=a_1} < 0$$

Hence we conclude that the right side of formula (4.2) has maximum at an arbitrary value of  $z_2 > 0$ , if

$$z_1 = \sum_{j=r+1}^n \gamma_j = a_1 \quad (4.4)$$

<sup>1</sup>Formula (3.9) is obtained from relationships (3.7), therefore equations (3.7) and (3.9) are linearly dependent.

<sup>2</sup>Formulas (3.4) and (4.1) put additional limitation on variables  $z_1$  and  $z_2$  (namely,  $z_1 < \pi(n-r)$ ,  $z_2 < n-r$ ), which, however, during investigation of maximum of right side of relationship (4.2) need not be considered.

This maximum (limit load) is in the form

$$S_{\max} = \frac{\sigma_0}{n} \left( \frac{1}{\mu} \sum_{j=1}^{n-r} \delta_j + r \right) \quad (4.5)$$

It is easy to establish that function  $s$ , determined by formula (4.2), does not have other maxima.

Formula (4.4) together with  $n - r - 1$  independent equalities (3.7) serves for finding the quantities  $b_i$  ( $i = r+1, r+2, \dots, n$ ), corresponding to limit load, which have no interest here.

Let us consider now the case  $\mu > \delta_n$ . In this case the limit load coincides with maximum of magnitude  $s$ , determined by formula (3.9) as a function of variables  $\gamma_i$ . This maximum is found by formula (4.5), in which one should consider  $r = 0$ . Thus, under the multistage law of attraction of opposite edges of crack limiting intensity  $S_*$  of load  $s$  will be

$$\begin{aligned} S_* &= \frac{\sigma_0}{n} \left( \frac{1}{\mu} \sum_{j=1}^{n-r} \delta_j + r \right) && \begin{aligned} &(r = 1, \dots, n) \\ &\text{when } \delta_{n-r} < \mu < \delta_{n-r+1} \end{aligned} \\ S_* &= \frac{\sigma_0}{n\mu} \sum_{j=1}^n \delta_j && \text{when } \mu > \delta_n \end{aligned} \quad (4.6)$$

Remark. From equalities (3.2) and (3.3) it is easy to find that during action of limit load we have formulas

$$\frac{\partial v(x, +0)}{\partial x} = 0 \quad \text{when } x = -L, \quad \frac{\partial v(x, +0)}{\partial x} < 0 \quad \text{when } -L < x < L \quad (4.7)$$

Hence we conclude that under limit load (and consequently, under a load less than limit) displacement of edge of crack  $v(x, +0)$  is a diminishing function of  $x$ . Thus, the taken diagram of interaction of edges of crack, depicted on Figs. 4, 5, is correct.

Futhermore, from the first formula of (4.7) it may be concluded that under the action of a limit load normal stresses are bounded also at point  $x = -L, y = 0$ .

§ 5. Dislocatory theorem. Work  $T_0$ , which it is necessary to expend on surmounting internal forces during formation of a unit of free surface of crack in a solid body, is called surface energy of a solid body, i.e.,

$$T_0 = \frac{1}{2} \int_0^{\infty} \sigma(h) dh \quad (5.1)$$

Particular surface energy will be the quantity

$$T(H) = \frac{1}{2} \int_0^H \sigma(h) dh \quad (5.2)$$

Under the multistage law of interaction of edges of a crack (Fig. 3) doubled surface energy is the area bounded by coordinate axes ( $\sigma$ ,  $h$ ) and broken line  $\sigma(h)$ , i.e.,

$$2T_0 = \int_0^{\delta_n} \sigma(h) dh = \frac{\sigma_0}{n} \sum_{i=1}^n \delta_i \quad (5.3)$$

and doubled particular surface energy is the area shaded on Fig. 6. We assume that  $H$  satisfies inequalities

$$\delta_{n-r} < H < \delta_{n-r+1}$$

In this case we have

$$2T(H) = \frac{\sigma_0}{n} \left( \sum_{i=1}^{n-r} \delta_i + Hr \right) \quad (5.4)$$

It is obvious that when  $H \geq \delta_n$  we have

$$T(H) = T_0 \quad (5.5)$$

Comparing equalities (4.6) with relationships (5.3), (5.4), (5.5), under the multistage law of attraction of opposite edges of a crack we arrive at the following value of limiting intensity of tearing load, applied to a body with dislocation of assigned power  $\mu$ :

$$S_0 = \frac{2T(\mu)}{\mu} \quad \left( 2T(\mu) = \int_0^{\mu} \sigma(h) dh \right) \quad (5.6)$$

Formula (5.6) is obtained with an arbitrary value of  $n$ ,  $\delta_i$  ( $i = 1, \dots, n$ ), characterizing multistage law of attraction of edges of crack (Fig. 3). Setting by corresponding value  $n$  and law of change  $\delta_i$  (as a function of  $i$ ), from the multistage law of attraction of edges of a crack can be obtained any assigned

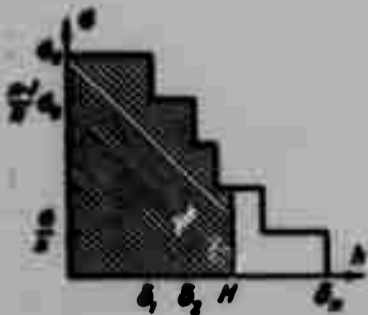


Fig. 6.

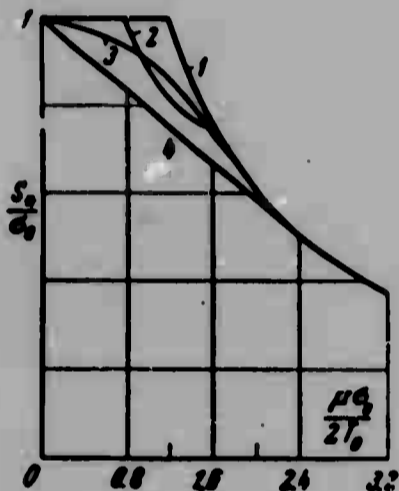


Fig. 7.

dependence of interaction of surfaces of slot. This proves accuracy of formula (5.6) under an arbitrary (physically acceptable) law of attraction of opposite edges of a crack. This result can be formulated in the following way.

Dislocatory theorem. Limit load during extension of body, containing edge dislocation of power  $\mu$ , is determined by formula

$$S_0 = \frac{1}{\mu} \int_0^\mu \sigma(h) dh \quad (5.7)$$

i.e., it is equal to the average intensity of attractive forces, acting on opposite edges of crack from 0 to  $\mu$ .

§ 6. Comparison of limit load under various laws of interaction of edges of slot. 1. Single-stage law of interaction

$$\sigma(h) = \sigma_0 \quad \text{when } h < \delta_1, \quad \sigma(h) = 0 \quad \text{when } h > \delta_1 \quad (6.1)$$

A body whose edges of the crack are attracted according to law (6.1) is called [1] a simplified model of a fragile body. For this model from formula (5.7) we have

$$S_0 = \sigma_0 \quad \text{when } \mu < \frac{2T_0}{\sigma_0}, \quad S_0 = 2T_0/\mu \quad \text{when } \mu > 2T_0/\sigma_0 \quad (6.2)$$

Relationships (6.2) were obtained by other method in [1, 4].

2. Two-stage law of interaction

$$\sigma(h) = \begin{cases} \sigma_0 & \text{when } h < \delta_1 \\ 1/2 \sigma_0 & \text{when } \delta_1 < h < \delta_2 \\ 0 & \text{when } h > \delta_2 \end{cases} \quad (6.3)$$

Let us consider the case  $\delta_2 = 2\delta_1$ . Here from formula (5.3) we obtain

$$\delta_1 = 1/3 T_0 / \sigma_0, \quad \delta_2 = 2/3 T_0 / \sigma_0$$

Under a two-stage law of interaction the limit load is in the form

$$\frac{S_0}{\sigma_0} = \begin{cases} 1 & \text{when } \mu < 1/2 T_0/\sigma_0 \\ 1/2 + 1/2 T_0/\sigma_0 \mu & \text{when } 1/2 T_0/\sigma_0 < \mu < 2 T_0/\sigma_0 \\ 2 T_0/\sigma_0 \mu & \text{when } \mu > 2 T_0/\sigma_0 \end{cases} \quad (6.4)$$

3. Cosinusoidal law of attraction of edges of crack

$$\sigma(h) = \sigma_0 \cos(\pi h/2\delta) \quad \text{when } h < \delta, \quad \sigma(h) = 0 \quad \text{when } h > \delta \quad (6.5)$$

From condition (5.3) follows  $\delta = \pi T_0/\sigma_0$ . In this case

$$\begin{aligned} S_0 &= 2T_0/\mu \sin(1/2 \sigma_0 \mu/T_0) \quad \text{when } \mu < \pi T_0/\sigma_0 \\ S_0 &= 2T_0/\mu \quad \text{when } \mu > \pi T_0/\sigma_0 \end{aligned} \quad (6.6)$$

4. Linear law of interaction of edges of cracks

$$\sigma(h) = \sigma_0(1 - h/\delta) \quad \text{when } h < \delta, \quad \sigma(h) = 0 \quad \text{when } h > \delta \quad (6.7)$$

In this case from condition (5.3)  $\delta$  is obtained in the form

$$\delta = 4T_0/\sigma_0$$

here

$$\frac{S_0}{\sigma_0} = \begin{cases} 1 - 1/2 \sigma_0 \mu/T_0 & \text{when } \mu < 4T_0/\sigma_0 \\ 2T_0/\sigma_0 \mu & \text{when } \mu > 4T_0/\sigma_0 \end{cases} \quad (6.8)$$

Dependence (6.2) on Fig. 7 is given by curve 1, dependence (6.4) — by curve 2, dependence (6.6) — by curve 3, and dependence (6.8) — by curve 4.

Submitted  
11 March 1964

#### Literature

1. M. Ya. Leonov. Elements of the theory of brittle rupture. PMTF, 1961, No. 3.
2. M. Ya. Leonov and V. V. Panasyuk. "Razvytok naydribnishykh trishchyn v tverdomu tili. Prykl. mekhanika," Vol. V, Issue 4, 1959.
3. Yu. P. Zheltov and S. A. Khrystianovich. Hydraulic break of an oil-bearing layer. News AS USSR, OTN, 1955, No. 5.
4. M. Ya. Leonov and L. V. Onishko. "Pro vplyv liniynoi dyslokatsii na mitsnist' vidryvu." Dopovidі AN UkrSSR, 1961, No. 4.

**BLANK PAGE**

STUDY OF DESTRUCTION OF BRITTLE BONDINGS  
BY METHODS OF THE THEORY OF CRACKS

B. M. Malyshev and R. L. Salganik

(Moscow)

Bonding parts of construction by means of gluing has found wide application. This is explained by a number of advantages which gluing possesses as compared to other forms of bonding, and also by the fact that in certain cases, as for example, in bonding polymers with metals or polymers to polymers, it turns out to be the only acceptable form of bonding. There is extensive literature about gluing, its application and methods of calculation and tests of glue compounds (see [1-8]).

A basic characteristic of a glue bonding is its strength. The strength of a glue bonding is determined by adhesion of glue to glued surfaces — adhesion and natural strength of glue — cohesion. Correspondingly we distinguish adhesive (peeling without destruction of glue layer) and cohesive (destruction of glue layer) types of destruction of glue bondings. Quantitatively adhesion (cohesion) is characterized by work expended on ungluing a unit area of glued surface — the work of adhesion (cohesion). This magnitude can be equal in the case of a breakaway, shift or their combination.

At present there is a method of its determination only for the case of ungluing a thin film from a sufficiently flexible material. On use of this method are based standard instruments, in which peeling of film is produced by a certain method. Methods of determination of work of adhesion (cohesion) for bonding

relatively hard bodies are unknown. In connection with this the bonding strength of such bodies is characterized by another magnitude – specific adhesion, by which is understood crushing stress in bonding during strictly normal and uniform (occurring immediately in all points) breakaway. An analogous characteristic is introduced for shift. Accordingly basic forms of tests are a break of samples which are glued end to end and overlapping (Fig. 1a and b).

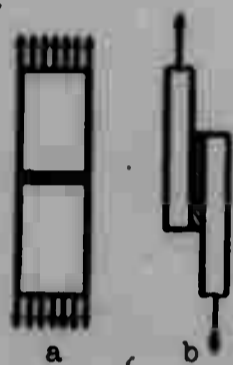


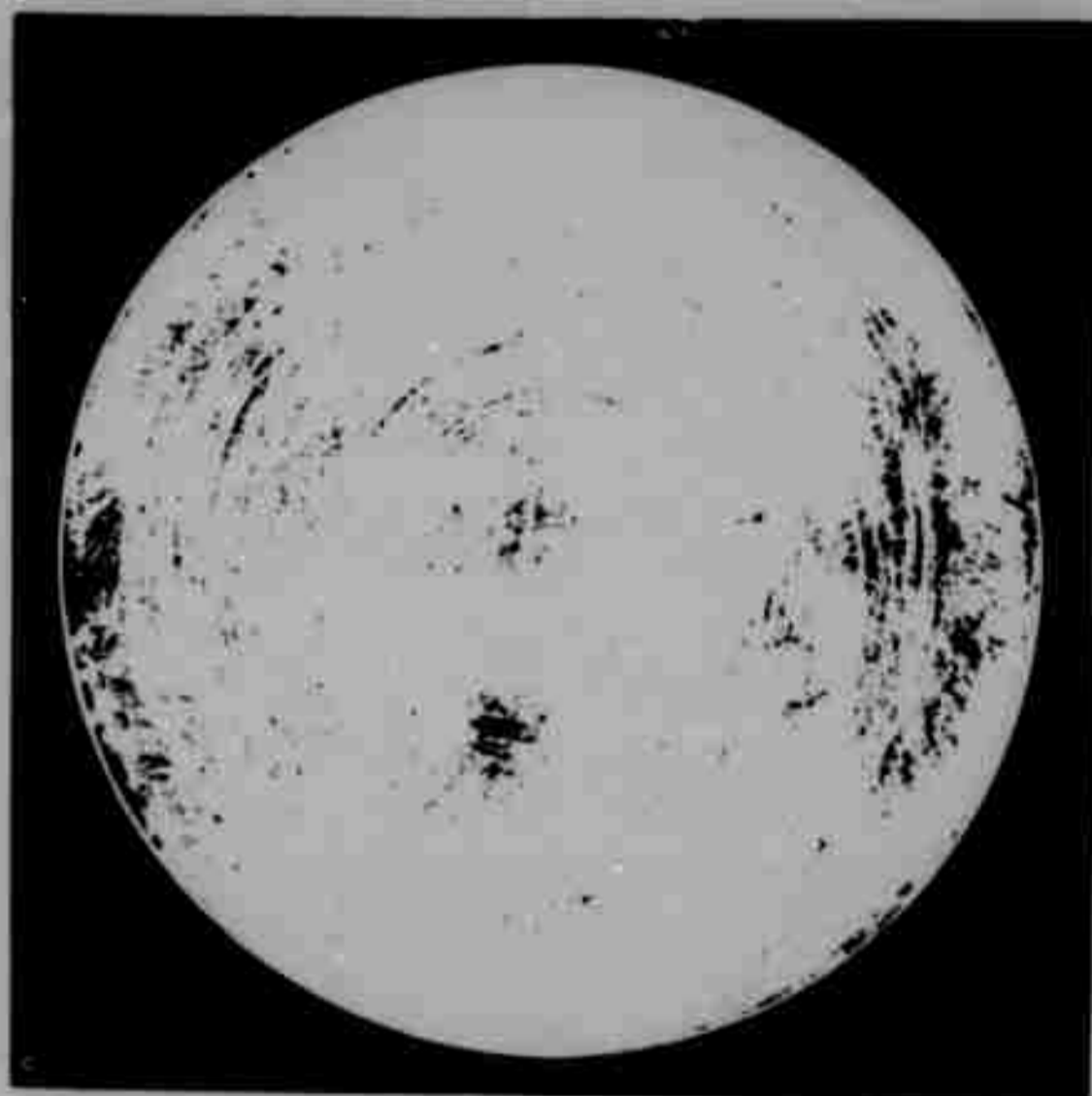
Fig. 1.

During tests of samples glued end to end, because of difficulties of creation of a uniform breakaway, there is usually obtained a great scattering of experimental data for specific adhesion (see, for instance, [9]). These difficulties led to an attempt to reach uniform breakaway by means of a realization so fast that speed of development of cracks appearing in weak places did not exceed the speed with which other sections of contacting surfaces are disconnected, and breakaway occurred in the first approximation evenly over all points of the area [10].

During tests of overlapping bonding scattering of destroying stress of shift averaged over the whole area usually is not so great. However this is not connected with uniformity of breakaway, which in this case evidently occurs by means of spread of cracks, but is connected with the fact that, in contrast to the preceding case, a crack always appears in a defined place – near end of overlap. On Fig. 2 are given photographs of surfaces glued by epoxy after breakaway: a, b) for the case of a bonding of overlapping lines from plastic, c) for the case of a round plate from plastic which was glued flatwise to a hard surface and was detached by a concentrated force.

Under a certain load near ends of overlap it was possible to observe appearance of cracks, which then with great speed spread through the whole bond. In case a through the whole bond passed one crack, appearing near the left end of the overlap, which it is possible to see, along characteristic traces which usually remained on the surface of the bonding after passage of crack. On photographs these traces constitute transverse lines arched in the direction of motion of the crack. In case b a crack was formed at first near left end of overlap, then – near the right (meeting point of these cracks is marked by an arrow).

Appearance of crack near ends of overlap can be explained, proceeding from



available theoretical results [3, 5] including the fact that for a sufficiently long overlap stresses are concentrated near its ends, and in the middle part are distributed practically evenly. If one were to consider that the bonding is destroyed when stresses in it attain a defined magnitude, there will follow a conclusion concerning the appearance of a crack near ends of overlap, where stresses are maximum. Hence there also is obtained a tendency of the breaking load to a certain constant value with increase of length of overlap, observed in reality. Crushing stress averaged over the whole area will decrease and, consequently, cannot serve as a characteristic of bonding strength.

The examined examples illustrate a general case. Most frequently destruction of bondings occurs by means of spread of cracks along it. Therefore for determination of strength of glue bondings destroyed thus it is natural to use methods of the theory of cracks [11], applied until recently to uniform materials. We note immediately that this theory permits tracing development of cracks already present and does not touch the problem of their onset, which should be considered separately.

Application of this theory for determination of strength of bondings is justified because not always is the appearance of a crack or the beginning of development of an already present crack (for instance, "ungluing") equivalent to destruction of the whole bonding, as occurred in the example of bond overlap which was examined. Frequently due to stability of cracks for their advance it is required to increase applied loads so that the breaking loads for the body as a whole do not depend on dimensions of initial cracks and can be considerably larger than those loads which correspond to beginning of movement of cracks [12].

In spite of the essential role of cracks in destruction of glue bonds, in existing methods of calculation and test of glue bonds the mechanism of destruction by means of propagation of cracks is not considered.

In the proposed work is given a method of determination of energy of destruction (work of adhesion, cohesion) founded on the study of propagation of cracks in a bonding in the case of bonding hard bodies to each other. It is shown that during normal breakaway of samples glued and hardened in approximately the same conditions and tested by setups with essentially different geometry, energy of destruction remained practically constant during stable propagation of a crack and did not depend either on dimensions of samples or on test setup.

Constancy of energy of destruction in propagation of a crack most graphically appeared in a setup using breakaway by a normal concentrated force of a thin transparent plate glued flatwise to a hard surface. In this setup due to axial symmetry a disk-like crack was obtained and on a considerable intermediate section spread under an almost constant force that, as analysis showed, verifies constancy of energy of destruction.

The revealed behavior of energy of destruction during normal breakaway fully agrees with that taken in the theory of cracks spreading in uniform materials, assumption on autonomy, i.e., independence of state of strain near the end of a quasistatically advancing crack from applied loads and geometry of system. In general, when in the undestroyed bonding near the end of the crack act both normal and also tangential stress, it is possible to expect dependence of energy of destruction on ratio of these stresses autonomous in that same meaning. One of the proposed setups permits determining such a dependence.

This dependence universal for a given bonding is the only characteristic of bonding necessary for application of the theory of cracks to calculation of strength of fragile and quasifragile glue bondings.

#### § 1. Results of theoretical investigation and basic assumptions.

1<sup>0</sup>. Preliminarily we will give basic positions of the theory of propagation of cracks in uniform material [11].

In a uniform material (for simplicity we consider a plate) cracks spread so that in the undestroyed body near the end of the crack on a place located along direction of propagation of crack, there act only tensile stresses, which create a normal break.

Experimentally it has been confirmed that development of cracks in uniform material will agree with basic hypotheses taken in the theory of cracks.

1. Sections of crack near ends, where internal bondings are still not finally destroyed and interaction (cohesion) of its opposite edges is essential (end regions), are small compared with dimension of crack.

2. End of crack starts to advance deep into the body only after achievement by cohesive forces of certain maximum magnitude, where further quasistatic motion of this end occurs so that distribution of cohesive forces, and together with it a certain integral characteristic of their intensity — modulus of cohesion, and form of crack in end region are autonomous, i.e., are not changed during change of

applied loads and geometry.

Work expended on destruction, proceeding on formation of a new surface (energy of destruction), is expressed through the modulus of cohesion, elastic modulus, and Poisson's ratio and therefore, according to the second hypothesis, should remain constant during propagation of crack.

With the help of the shown hypotheses determination of equilibrium of a plate with cracks leads to the mathematically exact problem at hand.

It is essential that such an approach will apply not only to truly fragile materials (comparatively not numerous), but also to the case when propagation of crack is accompanied by plastic deformations in the narrow zone just before the surface (quasibrittle rupture). This case is realized for the majority of structural materials.

2°. Let us consider propagation of cracks along bonding, using certain results of [13]. A distinction of propagation of a crack along bonding between two sufficiently durable bodies first of all is that the crack is restricted in selection of direction and therefore in its mobile end, in general, no longer will be a purely normal break.

To study such a crack by suitable mathematical model there is a cut, located along the boundary of bonding of two elastic bodies, between which outside the cut there is full cohesion. In the considered case, as also for a crack in a uniform material, investigation of distribution of stresses and displacements in the small neighborhood of the end of the cut plays a basic role. Therefore, without loss of generality, it is possible to consider cut of length  $l$ , located along rectilinear boundary of bonding (axis  $x$ ) of two infinite plates. Analysis of solution of corresponding problem of theory of elasticity [14] shows that on continuation of a cut nearby its end distribution of normal  $\sigma_y$  and tangent  $\tau_{xy}$  stresses, caused by applied loads, is determined by the expressions

$$\begin{aligned}\sigma_y &= -\frac{1}{\sqrt{r}} \left[ A_0 \cos \left( \beta \ln \frac{r}{l+s} \right) - B_0 \sin \left( \beta \ln \frac{r}{l+s} \right) + o(1) \right] \\ \tau_{xy} &= -\frac{1}{\sqrt{r}} \left[ A_0 \sin \left( \beta \ln \frac{r}{l+s} \right) + B_0 \cos \left( \beta \ln \frac{r}{l+s} \right) + o(1) \right] \\ \beta &= \frac{1}{2\pi} \ln \frac{\mu_1 + \mu_2 \kappa_1}{\mu_2 + \mu_1 \kappa_1}, \quad \kappa_{1,2} = 3 - 4\nu_{1,2}\end{aligned}\tag{1.1}$$

Here  $\mu_1, \mu_2$  - shear moduli,  $\nu_1, \nu_2$  - Poisson's ratio of glued materials,  $s$  - distance from considered point on continuation of cut to end of cut,  $A_0$ ,  $B_0$  - "coefficients of intensity of stresses," calculated through applied loads;  $\beta$  serves as an index of distinction of properties of glued materials; it turns into zero when these properties coincide.

When materials are identical ( $\beta = 0$ ), stresses near end of cut change monotonically, infinitely increasing when  $s \rightarrow 0$ . Normal stresses are proportional to coefficient  $A_0$ , tangent stresses - to  $B_0$ .

When materials are different ( $\beta \neq 0$ ), character of dependence qualitatively remains as before at distances from end of cut exceeding certain  $x$ .

$$x_* \approx l \exp(-\pi/2\beta) \quad (1.2)$$

At closer distances ( $s < x_*$ ) character of dependence essentially changes: stress, infinitely increasing in absolute value, will with infinitely increased frequency change sign according to approach toward end of cut, and normal and tangential stress, as one may see from formula (1.1), depend on both coefficients  $A_0, B_0$ . For opposite edges of cut is obtained a physically absurd result - that they penetrate each other (this occurs with a frequency increasing with approach toward end of cut). This deficiency of the mathematical model will be removed if one assumes that opposite edges, bulging, press one another and form a contact site. Region of propagation of these sites near end of cut, just as region of fluctuations of stresses on its continuation, has an extent of order  $x_*$ . A maximum estimate for  $x_*$  is obtained if one assumes the least of Poisson's ratio of glued materials equal to zero. Then  $\beta < 0.17$  and  $x_* < 10^{-4}l$ . In the real case one may assume that this coefficient is not less than 0.2, and then  $x_* < 10^{-6}l$ .

On contact sites appear forces of reaction, which for determination of state of strain near end of crack have to be considered along with applied forces. Furthermore, in a real crack forces of interaction of opposite edges must be considered, effective from the side of strongly deformed but still undestroyed glue. All these forces give on continuation of the crack stresses also expressed by the formulas (1.1), but with their own values of coefficients of intensity  $A', B'$ . Under equilibrium the action of these forces should compensate the action of applied loads. This is expressed by equalities

$$A_0 + A' = 0, \quad B_0 + B' = 0 \quad (1.3)$$

which, as one may see from expressions (1.1), ensure on a certain length  $\lambda$  compensation of stresses appearing from applied loads, so that stresses on continuation of crack are finite, and there occurs a smooth closing of the opposite edges of the crack on the ends.

Length  $\lambda$  in a real crack corresponds to section of transition from completely destroyed bonding to undestroyed bonding and for sufficiently fragile bondings has order of thickness  $\delta$  of glue layer. If  $\lambda < x_*$ , then fluctuation of stresses  $\sigma_y$  and  $\tau_{xy}$  in an undestroyed bonding determined by formulas (1.1) will take place only at distances from end of crack exceeding  $\lambda$ . When  $\lambda > x_*$  these fluctuations will not occur at all, and during description of phenomena in end region the distinction of index  $\beta$  from zero can be disregarded. As can be seen from given estimates for  $x_*$ , this case occurs in real bondings, since thickness of glue layer does not occur less than 0.01 mm.

The two hypotheses used for cracks in a homogeneous body can be extended to the considered case of a crack in a bonding. The first hypothesis on smallness of end region is transferred without change. The second hypothesis is generalized and is that a quasistatic advance of the crack starts and occurs during achievement of a certain limiting state in the undestroyed bonding near end of crack at which normal and tangential stress in this place are connected by a functional dependence, autonomous in former meaning, i.e., not changing form during change of applied loads and geometry of system. In virtue of equalities (1.3) and the fact that it is possible to disregard  $\beta$  in (1.1), stresses in bonding near equilibrium end of crack are expressed through coefficients of intensity  $A_0$ ,  $B_0$ , so that there is an autonomous dependence among these coefficients.

Propagation of crack is accompanied by irreversible processes of destruction of bonding. Certain work is expended on this. This work of adhesion (cohesion), for a unit area of new surface, described by contour of crack during its displacement in neighborhood of given point in depth of bonding, constitutes the specific surface energy of destruction, which will designate by  $T$ . Energy of destruction  $T$  is simply determined by forces of interaction of opposite edges of crack in end region and in the case of quasistatic propagation of crack is expressed through  $A_0$ ,  $B_0$  by the formula

$$T = \frac{\pi}{2} \frac{(\mu_1 + \mu_2 \kappa_1)(\mu_2 + \mu_1 \kappa_2)}{\mu_1 \mu_2 [\mu_1 (\kappa_2 + 1) + \mu_2 (\kappa_1 + 1)]} (A_0^2 + B_0^2) \quad (1.4)$$

Therefore the shown dependence between  $A_0$  and  $B_0$  can be recorded as the dependence of energy of destruction  $T$  on any combination  $A_0$  and  $B_0$ , not being a function of  $A_0^2 + B_0^2$ .

Considering that in examining phenomena near end of crack in real bonding the distinction of index  $\beta$  from zero can be disregarded, from formulas (1.1) we obtain proportionality of normal stresses in bonding to coefficient  $A_0$ , and tangent stresses to coefficient  $B_0$ , up to end of crack. Therefore it is convenient to select as the argument on which depends energy of destruction  $T$  in state of mobile equilibrium,  $A_0/B_0$ , equal to the ratio of normal  $\sigma_y$  and tangent  $\tau_{xy}$  stresses in bonding near end of crack. Thus, we obtain the autonomous dependence<sup>1</sup>

$$T = T_*/(A_0/B_0) = T_*/(\sigma_y/\tau_{xy}) \quad (1.5)$$

where  $T_*$  - any characteristic value of  $T$ , for instance, corresponding to normal breakaway ( $A_0/B_0 = \infty$ ).

This dependence will exist also for space cracks under the condition that stresses of shift along contour are absent. Calculation of the latter does not present difficulties and leads to the addition of one more coefficient of intensity  $C_0$ , so that in expression (1.5) there will be two arguments:  $A_0/B_0$  and  $A_0/C_0$ , equal to ratio of normal stresses in bonding to tangent stresses, directed correspondingly perpendicular to contour of crack and along it.

§ 2. Formulation of problem of experimental investigation. For an experimental check of the existence of dependence (1.5) a setup is needed which allows simple determination of coefficients of intensity  $A_0$  and  $B_0$  through measured magnitudes.

1°. As such a setup it is possible to propose the breakaway of two thin end-to-end plates by concentrated forces applied to opposite edges of crack (Fig. 3). For not very small angles  $\alpha$  between directions of force and crack this setup is easily realizable, and in the case of lengths of cracks which are small as compared

---

<sup>1</sup>If during description of phenomena in end region it was impossible to consider  $\beta = 0$ , then in expressions (1.1) the dimension of crack  $l$  essentially would enter and then the autonomous dependence between coefficients  $A_0$ ,  $B_0$  either would not exist at all or would have to be brought to constancy of energy of destruction  $T$  for any values of ratio  $A_0/B_0$ .

with dimensions of plates, very simple analytic dependencies can be obtained.

For left end we obtain

$$T = \frac{\pi}{2} \frac{(\mu_1 + \mu_2 x_1)(\mu_2 + \mu_1 x_2)}{\mu_1 \mu_2 [\mu_2(x_1 + 1) + \mu_1(x_2 + 1)]} \frac{P l_1}{(l_1 + l_2) l_1 b^2} \cdot \frac{A_0}{B_0} = \operatorname{tg} \alpha \quad (2.1)$$

where  $b$  — thickness of plates; remaining designations are shown on Fig. 3. In order to obtain hence the formula for the right end, it is necessary for indices 1, 2 to change places and to replace  $\alpha$  by  $\pi - \alpha$ .

Thus, in the considered setup normal and tangential stress in bonding near end of crack are related to one another just as normal and tangent components of the applied concentrated force.

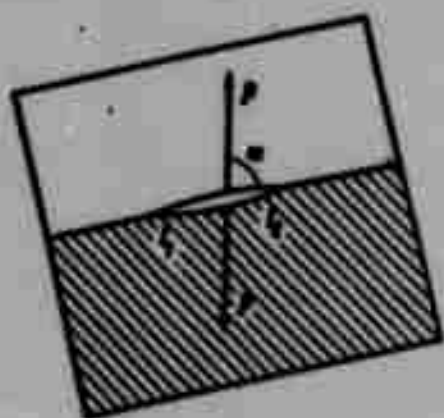


Fig. 3.

From resulting expressions it is clear that in this setup check of existence of dependence (1.5) leads to check of constancy of energy of destruction  $T$  as each end of crack advances under a given value of angle  $\alpha$ .

If this constancy is established with different  $\alpha$ , the actual dependence (1.5) can be found by constructing the graph of

$$T = T(\operatorname{tg} \alpha) = T(A_0/B_0).$$

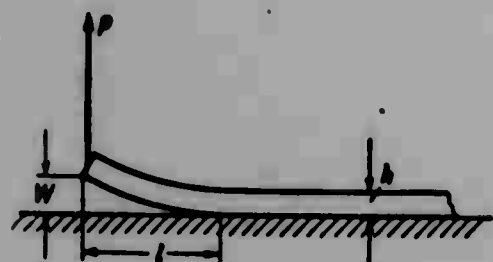


Fig. 4.

2<sup>c</sup>. If one were to be limited to only finding the characteristic points of dependence (1.5), in particular, energy of destruction, corresponding to normal breakaway, then a simpler setup can be proposed involving the breakaway of a thin beam glued to an undeformed surface by a normal concentrated force (Fig. 4). This setup

is analogous to setups applied for determination of energy of destruction of homogeneous bodies. For the first time<sup>1</sup> such a setup was used for determination of surface tension of mica [15]. The expression for  $T$  is obtained from the equation

<sup>1</sup>For other purposes similar setups were considered in connection with questions of adhesion in articles of collection [16], pp. 101-145. (Remark during proofreading.)

of conservation of energy

$$P\delta w = \delta \Pi + T\delta l \quad (2.2)$$

Here  $P$  — force,  $w$  — displacement of unbent end,  $\Pi$  — elastic energy stored in beam,  $l$  — length of crack,  $b$  — width of beam. Because the surface from which occurs breakaway cannot be deformed, the beam can be considered rigidly fixed at the end of crack (console). Then

$$w = \frac{Pl^3}{3EI}, \quad \Pi = \frac{3Elw^3}{2l^3} \left(1 - \frac{bh^3}{12}\right) \quad (2.3)$$

where  $E$  — elastic modulus,  $h$  — height of beam. From relationships (2.2), (2.3) we find

$$T = \frac{3Pw}{2bl} = \frac{Pl^2}{2bEI} = \frac{9Elw^3}{2bl^4} = \left(\frac{9P^4w^3}{8bEI}\right)^{1/4} \quad (2.4)$$

3°. Another setup is much more convenient than determination of energy of destruction during normal breakaway. This setup consists in the breakaway of a thin plate glued flatwise to a hard surface by a concentrated force (Fig. 5).

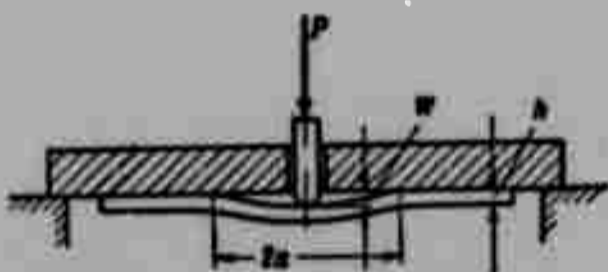


Fig. 5.

Due to axial symmetry the crack will be disk-like. Taking, as in the preceding setup, rigid fixing of plate along contour of crack, we will obtain for bend  $w$  and potential energy  $\Pi$  the expressions.

$$w = \frac{Pa^3}{16\pi D}, \quad \Pi = \frac{8\pi Dw^3}{a^3} \quad (2.5)$$

$$\left(D = \frac{Eh^3}{12(1-\nu^2)}\right)$$

where  $h$  — thickness of plate,  $a$  — radius of crack. Hence from equation of conservation of energy (2.2), in which it is necessary to replace  $b\delta l$  by  $2\pi a\delta a$ , we will obtain

$$T = \frac{P^2}{32\pi D^3} = \frac{P^2}{2\pi a^3} = \frac{8Dw^3}{a^3} \quad (2.6)$$

so that energy of destruction  $T$  is expressed only through load  $P$  and constant rigidity of plate  $D$ . Thus, constancy of energy of destruction in this case involves constancy of detaching force  $P$ .

§ 3. Setting up experiments and results of tests.<sup>1</sup> For possibly sharper development of distinction of elastic properties of glued materials tests were conducted with bondings of plastic with plastic and plastic with steel, elastic modulus of which is approximately 70 times more than the elastic modulus of plastic. Selection of plastic as one of the glued materials was so that it was possible to observe and to measure crack easily.

1°. Gluing. Since samples were glued from nonporous materials and were tested at room temperature, for equal distribution of glue layer and to prevent appearance in it of temperature stresses a low-viscosity glue was necessary with small contents of volatile substances, hardening at room temperature. Such a glue was made on the basis of epoxy resin [ED-6] (ЭД-6) (10 g) with the additive polyethylene polyamine (0.8 or 1 g) as solidifier. In certain cases acetone was applied as diluent of resin (0.5 or 1 g) or plasticizer — dibutylphthalate (5, 10%). Surfaces of samples subjected to gluing were thoroughly mechanically processed, including rubbing the plate with fine emery powder. Then these surfaces were defatted by carbon tetrachloride and acetone. Epoxy resin before gluing was heated to 50-60°C. The samples were also heated to this temperature. After pouring in resin of solidifier the composition was thoroughly mixed and the mixture placed on the glued surfaces in as even a layer as possible after which parts of sample were connected, placed on an even horizontal surface, and a load placed on them, so that hardening occurred at room temperature under a pressure of 0.5-1 kg/cm<sup>2</sup>. After hardening, continuing in various cases from a few to ten twenty-four-hour periods, the pressed glue was cleaned, and the samples tested. Thickness of glue layer was tenths of a millimeter.

2°. Tests of plates glued end to end. Plates 0.5, 0.6, 0.8 cm thick were used having a length of 30 cm and width of 6 and 12 cm for steel and plastic correspondingly. Plates of identical thickness were glued together in pairs (along the long side). Tests were conducted on standard rupture-test machine of kinematic type with lever dynamometer. Concentrated forces were applied to edges of crack with the help of steel wires. Wires were passed through holes specially drilled near boundary of bonding and were unbent along plate, forming  $\Pi$ -shaped loops. Ends of wires were secured in clamps of machine. At a certain tension,

---

<sup>1</sup>In carrying out of experiments much help was given by G.V. Bychkov, N. S. Turbanova, D. I. Generalov and S. G. Kartashev.

usually exceeding 30 kg, a crack started to form. Propagation of this crack was caused by further increase of force. Force was measured by scale of dynamometer, distance from ends of crack to place of application of force — by a ruler. The majority of experiments was conducted for the case of a normal break, when direction of crack and force composed a right angle. A series of experiments was conducted for angles which were not right angles (oblique breakaway). The latter was achieved by turning the plate, which during propagation of crack formed an angle with the vertical.

Energy of destruction was determined by the formula (2.1). For plastic  $E = 3 \cdot 10^4 \text{ kg/cm}^2$ ,  $\nu = 0.4$  was taken. Steel, since it was glued to plastic, could be considered absolutely hard.

On Fig. 6 are given typical results for change of distances  $l_1$  and  $l_2$  (cm) from ends of crack to place of application of force and corresponding values of

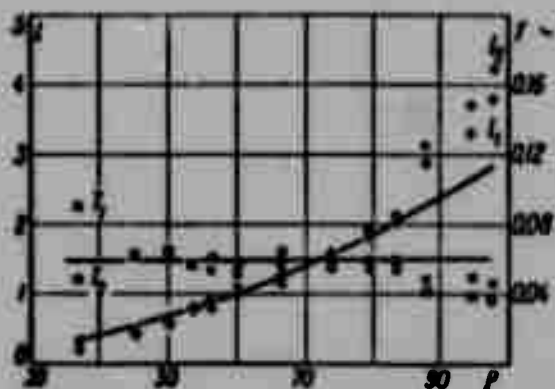


Fig. 6.

energies of destruction  $T_1$ ,  $T_2$  (kg/cm) depending upon magnitude of force  $P$  (kg) (sample — "plastic steel," glue — 10 g ED-6, 0.8 g polyethylene polyamine, 1 g acetone; time of hardening ~5 twenty-four-hour periods). From these results it is clear that there exists a certain intermediate section of constancy of breaking energy in interval of values of tensile stress  $P$  from 45 to 85 kg. Energy of destruction on this

section is close to 0.06 kg/cm. For this value of energy of destruction on Fig. 6 is given a graph of change of length  $l_1 = l_2$  depending upon force  $P$ , calculated by the formula (2.1). Scattering when loads are small is connected with random character of beginning of process and nonelastic behavior of material near points of application of force. For large loads there occurs an apparent fall of energy of destruction. This is explained by disregarding influence of boundaries when calculating energy of destruction. As can be seen from the given example, for the used plates it is necessary to consider influence of boundaries when lengths of cracks are of order  $(l_1 + l_2) \sim 4-6 \text{ cm}$ .

Several tests, conducted for a slanting break, showed that when angle between

force and crack is fixed energy of destruction remains approximately constant, but unequal for both ends. Energy of destruction is less, and crack correspondingly longer than the side where the angle between force applied to plastic and crack is sharp. From this side tangential stresses promote breakaway more than from the opposite. When the angle is  $60^\circ$  ratio of energies of destruction was one and a half, and for an angle of  $30^\circ$  it composed 7-8.

3°. Tests of beams. Beams were prepared of steel and plastic and had the following dimensions of cross section: width  $b = 0.5, 0.6, 0.8$  cm, height  $h = 1.0, 1.2, 1.5$  cm. Beams with identical width were glued in pairs. During tests a breakaway of beams from plastic was always carried out. For determination of energy of destruction the unbending force, displacement of end of beam, and length of crack were measured.

Measurement of unbending force requires application of a sufficiently rigid (little yielding), but very sensitive dynamometer, able without noticeable displacement to react to small changes of forces. Otherwise process of test is

complicated, since crack can become unstable.

Thus, for instance, during test by means of suspension of load starting process of propagation of crack will go to full destruction, inasmuch as force, as can be seen from formulas (2.4), necessary for stable propagation of crack, should drop with increase of its length, and force created by the suspended load remains constant.

As dynamometer was used a thin steel plate with a strain gauge glued to it.

This plate was fastened toward the end of the beam of plastic, whereas the other beam (from plastic or steel) was rigidly clamped all along its length. Force was created by means of gradual displacement of plate in a direction perpendicular to line of bonding.

On Fig. 7 are given typical results for change of force  $P$  (kg), length of crack  $l$  (cm) and energy of destruction  $T$  (kg/cm) depending upon bend  $w$  ( $b = 6$  mm,

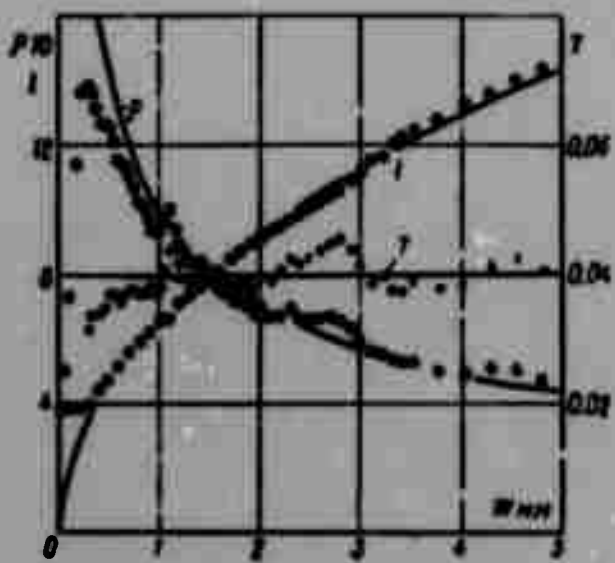


Fig. 7.

$h = 10$  mm, glue - 10 g ED-6, 1 g polyethylene polyamine, 1 g dibutylphthalate, breakaway from plastic, time of hardening  $\sim 5$  twenty-four-hour periods). Energy of destruction, as can be seen from graphs, fluctuates in very narrow limits near 0.04 kg/cm. For this value of energy are given graphs of the dependencies of  $P$  and  $l$  on  $w$ , calculated from relationships (2.4). Considerable deviations of experimental points from these curves are on the initial section, where there occurred a linear growth of force while crack stopped, and near  $w = 1$  mm,  $w = 2.75$  mm, where stopping and delay of development of crack were observed, connected apparently with heterogeneity of bonding.

4°. Tests of plates glued flatwise. Plates of circular form 110 mm in diameter were cut from sheets of plastic 3 and 5 mm thick and were glued to a steel plate, in which a hole was drilled. Force causing breakaway of plate was transmitted through a steel rod inserted in this hole. Tests were conducted on 5-ton Shopper machine. Feed was manual. Force was measured by dynamometer, bend - by indicator, diameter of crack - by ruler. With a good uniform bonding a sufficiently round crack was obtained. This can be seen from photograph shown in Fig. 2c of traces in the form of concentric circumferences left by the crack on the surface of the separated plate. Observing the crack, it was possible to reject samples with nonuniform bonding by deviations of its form from circular.

On Fig. 8 are given typical graphs of change of detaching force  $P$  and radius  $a$  of crack depending upon bend  $w$  for two plates 3 and 5 mm thick, glued and hardened

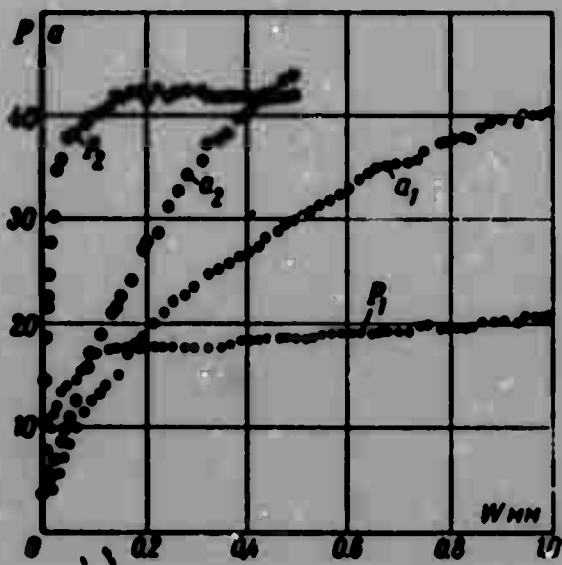


Fig. 8.

in identical conditions (glue - 10 g ED-6, 0.8 g polyethylene polyamine; time of hardening  $\sim 5$  twenty-four-hour periods). From these graphs it is clear that on a certain intermediate section development of crack occurred when detaching force was almost constant (smaller force corresponds to thinner plate). From the first formula of (2.6) it is clear that energy of destruction remained constant. For both plates approximately identical values of energy of destruction,  $\sim 0.017$  kg/cm, are obtained.

Deviations of force  $P$  from constancy in the beginning, and also sometimes for relatively large bends, at the end of process, are connected with inapplicability on these stages of the approximate theory of thin plates, used to derive formulas (2.6). This theory is applicable under the conditions that  $a > h > w$ , of which the first is not executed on the initial, and the second — on the final stages of the load process. With an unsuccessful selection of parameters there can not be a region where both inequalities simultaneously are executed, and then an intermediate section of constancy of force will not be obtained.

Comparison with more exact theories [17] shows that deviations of force  $P$  from constancy on initial and final sections of load process have to be in a direction observable by experiment.

The given typical examples characterize movement of curves obtained in many tests. These tests showed that on corresponding intermediate sections of load process where formulas used for calculation of energy of destruction are accurate the last one remained approximately constant, and this constancy was observed also in tests of plates glued end to end in the case of slanting breakaway.

It is necessary to note that for energy of destruction calculated by various formulas both in the case of a beam setup and also a setup with disk-like crack, somewhat differing values were obtained, which is connected with the not fully elastic behavior of plastic.

Let us note also that all considered experimental setups are based on use of stably developed cracks. To guarantee stability of development of cracks in all three setups it is necessary that the dynamometer and other elements of the system of load be rigid, i.e., store negligible potential energy. This is especially necessary in a beam setup, where to the great length of a stable crack corresponds a smaller unbending force, delay in change of which can lead to rapid dynamic development of crack. Fewer precautions in this relationship are required by a setup with disk-like crack propagating basically under an almost constant force, and even fewer in a setup of breakaway of plates glued end to end, characterized by growth of force necessary for advance of crack. But even in this last setup, experiments showed, there can be instability, if system of load is too yielding.

For determination of energy of destruction during normal breakaway the most convenient is a setup with disk-like crack. In this setup for determination of

energy of destruction it is sufficient to advance crack until force ceases to change, and to measure this value of force. Such method of measurement of energy of destruction is suitable both for the case when at least one of the glued materials is transparent, and also for the case of opaque materials where if the crack leaves traces similar to those depicted on Fig. 8, then by these traces it is possible to check disk-likeness and by deviations from it to judge degree of homogeneity of bonding. In general, one should note that for determination of energy of destruction without measurement of length of crack in the case of opaque materials a beam setup is useful in which it is sufficient to determine  $P$  and  $w$  (see last formula (2.4)), and also the setup of breakaway of plates glued end to end under the condition that besides force  $P$ , relative displacement of any two points of surface of plates will be measured.

Measurements showed that in the case of normal breakaway in all three setups for many samples, glued and hardened in approximately the same conditions, like values of energy of destruction were obtained. However the percent of cases when this was not observed was even greater. This is connected with the fact that small changes of such technological conditions as dosage, method of application of glue and state of surfaces, temperature during gluing and hardening, pressure, etc., strongly affected energy of destruction and could not be removed by the usual rather rough methods of control applied in the considered experiments. High sensitivity of energy of destruction to changes of parameters of process of gluing can be used for strict control of quality of bonding.

Influence of different factors determining behavior of glue and its interaction with glued surfaces can be investigated theoretically on the basis of acceptance of those or other specific models. However for application of the theory of cracks to appraisal of strength of fragile and quasifragile glue bondings this is not obligatory. Considered methods of experimental determination of energy of destruction and its dependence on ratio of normal stresses to tangent stresses in an undestroyed bonding near the end of a crack permit finding the unique characteristic of strength of fragile and quasifragile glue bondings necessary for application of theory of cracks.

The authors are thankful G. I. Barenblatt for constant attention to the work and discussions significantly influencing its content.

Institute of Mechanics of  
Moscow State University

Submitted  
28 August 1964

### Literature

1. B. V. Deryagin and N. A. Krotova. Adhesion. Publishing House of Academy of Sciences of USSR, 1949.
2. S. S. Voyutskiy. Autohesion and adhesion of high polymers. State Technical Press, 1960.
3. Adhesion (glues, cements, solders). Collection trans. Publishing House of Foreign Lit., 1954.
4. G. Epshteyn. Gluing of metals, Oborongiz, 1956.
5. Glues and technology of gluing. Collection of articles. Oborongiz, 1960.
6. G. A. Perri. Gluing reinforced plastic. Sudpromgiz, 1962.
7. K. I. Chernyak. Epoxy compounds and their application. Sudpromgiz, 1963.
8. D. A. Kardashov.. Synthetic glues. Edition of "Chemistry," 1964.
9. S. B. Aynbinder and E. F. Klokova. Determination of magnitude of forces of adhesion between solid bodies. Reports of Academy of Sciences of USSR, 1962, Vol. 146, No. 5.
10. N. A. Krotova, L. P. Morozova and G. A. Sokolina. Mechanical characteristics of adhesion of polymers. Reports of Academy of Sciences of USSR, 1959, Vol. 127, No. 2.
11. G. I. Barenblatt. Mathematical theory of stable cracks formed on brittle rupture. PMTF, 1961, No. 4.
12. G. I. Barenblatt. Certain general representations of the mathematical theory of brittle rupture. PMM, 1964, Vol. 28, Issue 4.
13. R. L. Salganik. Brittle rupture of glued bodies. PMM, 1963, Vol. 27, Issue 3.
14. G. P. Cherepanov. State of strain in a nonuniform plate with cuts. News AS USSR, OTN, Mechanics and machine building, 1962, No. 1.
15. I. V. Obreimov. The splitting strength of mica. Proc. Roy Soc., 1930, A 127, pp.290-297.
16. Adhesion and Cohesion, Elseveir Publ. Co., Amsterdam, 1962.
17. S. P. Timoshenko and S. Voynovskiy-Kriger. Plates and shells. Fizmatgiz, 1963.

THE THEORY OF THE AXIALLY SYMMETRIC STATE  
OF AN IDEAL PLASTIC MATERIAL

G. I. Bykovtsev, D. D. Ivlev  
and T. N. Martynova

(Voronezh)

Properties of equations of the axially symmetric state under the condition of plasticity of Tresca were considered in [1-3].

In [4] are considered equations of the axially symmetric problem of an ideal plastic material when the stressed and deformed state corresponds to the edge of an arbitrary piecewise-linear surface of fluidity, interpreting the condition of plasticity in the space of main stresses.

In this work are considered equations of the axially symmetric problem of an isotropic ideal plastic material when the stressed and deformed state corresponds to the edge of an arbitrary piecewise-linear surface of fluidity. It is shown that in this case the initial system of equations always has real characteristics, coinciding with trajectories of main stresses (isostatic curves). It is shown that there cannot exist a line of discontinuity of rates of displacements.

Let us note that if in the case of conformity of the stressed and deformed state to edge of surface of fluidity the problem is statically definable [4], then for the edge of the surface of fluidity there is always kinematic definability. The last for the condition of plasticity of Tresca was noted in [1, 3]. The work considers also self-simulating solutions, corresponding to conical and spherical flows of ideal plastic material.

Considerations are made that the stressed and deformed state, corresponding to an edge of a prism of fluidity, cannot correspond to basic types of axially symmetric flows of ideal plastic material.

1. Let us consider the space of main stresses  $\sigma_1, \sigma_2, \sigma_3$ . Equation of edge of surface of fluidity in this space has the form

$$a\sigma_1 + b\sigma_2 + c\sigma_3 = 1 \quad (1.1)$$

Let us assume that the condition of plasticity (1.1) does not depend on first invariant of tensor of stresses, then

$$a + b + c = 0 \quad (1.2)$$

Let us consider the axially symmetric state of a body under the condition of plasticity (1.1) in cylindrical coordinates  $\rho, z, \theta$ . Direction of  $\theta$  by condition is principal; subsequently we will take  $\sigma_\theta = \sigma_3, \sigma_1 \geq \sigma_2, \varepsilon_\theta = \varepsilon_3$ .

Considering the condition of plasticity (1.1) as plastic potential, we write the associated law of plastic flow

$$\varepsilon_1 = \lambda a, \quad \varepsilon_2 = \lambda b, \quad \varepsilon_3 = \lambda c, \quad \lambda \geq 0 \quad (1.3)$$

Whence

$$\varepsilon_1 + \varepsilon_2 + \varepsilon_3 = 0, \quad b\varepsilon_1 - a\varepsilon_2 = 0 \quad (1.4)$$

There occur the relationships

$$\begin{aligned} \varepsilon_1 &= \varepsilon_\rho \cos^2 \psi + \varepsilon_z \sin^2 \psi + 2\varepsilon_{\rho z} \sin \psi \cos \psi \\ \varepsilon_2 &= \varepsilon_\rho \sin^2 \psi + \varepsilon_z \cos^2 \psi - 2\varepsilon_{\rho z} \sin \psi \cos \psi \\ \varepsilon_3 &= \varepsilon_\theta, \quad (\varepsilon_\rho - \varepsilon_z) \sin 2\psi - 2\varepsilon_{\rho z} \cos 2\psi = 0 \end{aligned} \quad (1.5)$$

$$\varepsilon_\rho = \frac{\partial u}{\partial \rho}, \quad \varepsilon_z = \frac{\partial w}{\partial z}, \quad \varepsilon_{\rho z} = \frac{1}{2} \left( \frac{\partial u}{\partial z} + \frac{\partial w}{\partial \rho} \right)$$

Here  $u, w$  — components of speed of displacement along axes  $\rho, z$ ;  $\psi$  — angle between first principal direction and axis  $\rho$ .

From (1.4) and (1.5) we will obtain

$$\varepsilon_\rho + \varepsilon_z + \varepsilon_\theta = 0, \quad (\varepsilon_\rho - \varepsilon_z)^2 + 4\varepsilon_{\rho z}^2 = \left( \frac{a-b}{c} \right)^2 \varepsilon_\theta^2 \quad (1.6)$$

Equations (1.6) we rewrite in components of speed of displacement

$$\frac{\partial u}{\partial \rho} + \frac{\partial w}{\partial z} + \frac{u}{\rho} = 0, \quad \left( \frac{\partial u}{\partial \rho} - \frac{\partial w}{\partial z} \right)^2 + \left( \frac{\partial u}{\partial z} + \frac{\partial w}{\partial \rho} \right)^2 = \left( \frac{a-b}{c} \right)^2 \frac{u^2}{\rho^2} \quad (1.7)$$

The system of two equations (1.7) relative two unknowns  $u, w$  is closed, and, consequently, the considered axially symmetric state always is "kinematically definable" (strictly speaking, a "kinematically definable" problem will exist only with corresponding assignment of boundary conditions).

The first of equations (1.7) will be satisfied, considering

$$u = \frac{1}{\rho} \frac{\partial \Phi}{\partial z}, \quad w = -\frac{1}{\rho} \frac{\partial \Phi}{\partial \rho}$$

the second equation (1.7) will take the form

$$\left( \frac{2}{\rho} \frac{\partial^2 \Phi}{\partial \rho \partial z} - \frac{1}{\rho^2} \frac{\partial^2 \Phi}{\partial \rho^2} \right)^2 + \left( \frac{1}{\rho} \frac{\partial^2 \Phi}{\partial z^2} - \frac{1}{\rho} \frac{\partial^2 \Phi}{\partial \rho^2} + \frac{1}{\rho^2} \frac{\partial \Phi}{\partial \rho} \right)^2 = \left( \frac{a-b}{c\rho} \right)^2 \left( \frac{\partial \Phi}{\partial z} \right)^2 \quad (1.8)$$

The type of nonlinear equation (1.8) can be investigated, following [5, 6]. It is easy to show that equation (1.8) belongs to the hyperbolic type, but its characteristics have the form

$$\frac{dz}{d\rho} = \operatorname{tg} \psi \quad (\alpha\text{-lines}) \quad \frac{dz}{d\rho} = -\operatorname{ctg} \psi \quad (\beta\text{-lines}), \quad (1.9)$$

From (1.9) it follows that characteristics coincide with trajectories of main stresses (isostatic curves).

Let us write relationships along characteristics. Passing in relationships (1.5) to differentiation along characteristics (1.9), from (1.4) we will obtain after certain transformations

$$\frac{\partial u}{\partial s_\alpha} \cos \psi + \frac{\partial w}{\partial s_\alpha} \sin \psi - \frac{a}{c} \frac{u}{\rho} = 0, \quad \frac{\partial u}{\partial s_\beta} \sin \psi - \frac{\partial w}{\partial s_\beta} \cos \psi + \frac{b}{c} \frac{u}{\rho} = 0 \quad (1.10)$$

where  $ds_\alpha$ ,  $ds_\beta$  - correspondingly length of arcs of characteristics  $\alpha$ ,  $\beta$ .

In the case of condition of plasticity of Tresca ( $a = 0$  or  $b = 0$ ) relationships (1.10) signify, as follows from (1.4), that the corresponding element of characteristics  $\alpha$  or  $\beta$  is not extended.

The condition of absence of shift along characteristics has the form

$$\left( \frac{\partial u}{\partial s_\beta} + \frac{\partial w}{\partial s_\alpha} \right) \cos \psi - \left( \frac{\partial u}{\partial s_\alpha} - \frac{\partial w}{\partial s_\beta} \right) \sin \psi = 0 \quad (1.11)$$

Let us consider the Cauchy problem for determination of components of speeds of displacements. Let us assume that on arc AB of curve L in plane  $\rho z$ , shown on Fig. 1, are given the values  $u$ ,  $w$ . First of all we show that the given values  $u$ ,  $w$  determine on L the angle  $\psi$ .

Let us assume that normal  $n$  to contour L will form with axis  $\rho$  angle  $\chi$ . From relationships (1.5) and (1.4), passing to differentiation along contour L, we will

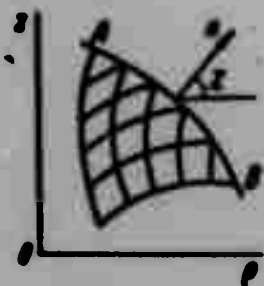


Fig. 1.

obtain

$$\cos 2(\psi + \chi) = \frac{c}{a-b} \left[ \frac{2p}{u} \left( \frac{du}{ds} \sin \chi + \frac{dw}{ds} \cos \chi \right) - 1 \right] \quad (1.12)$$

where  $ds$  — element of arc of contour  $L$ .

Relationship (1.12) determines angle  $\psi$  along  $L$ .

The Cauchy problem is set up for relationships (1.9)-(1.11).

The initial system of relationships (1.9)-(1.11) can be solved by the method of finite differences. It is essentially that the Cauchy problem cannot be posed for arbitrary values of  $u$ ,  $w$  on  $L$ . Really, from (1.12) it follows that there should occur the inequality

$$\left| \frac{c}{a-b} \left[ \frac{2p}{u} \left( \frac{du}{ds} \sin \chi - \frac{dw}{ds} \cos \chi \right) - 1 \right] \right| < 1 \quad (1.13)$$

When the left part of expression (1.13) is equal to one,  $\psi = -\chi$  and contour  $L$  coincides with characteristic.

Let us note that Cauchy problem for corresponding equations under the condition of Tresca, was investigated in [8], in which the Cauchy problem is posed for variables,  $u$ ,  $\psi$ ,  $\omega = \frac{1}{2}(\partial w / \partial p - \partial u / \partial z)$ ; the author did not derive a limitation of type (1.13).

Degenerated cases take place when  $a = b$  and when  $c = 0$  ( $a = -b$ ). The case of  $a = b$  corresponds to edges  $A_1F_1$ ,  $C_1D_1$  of the condition of maximum given stress [7]

(Fig. 2). System (1.7) will take the form

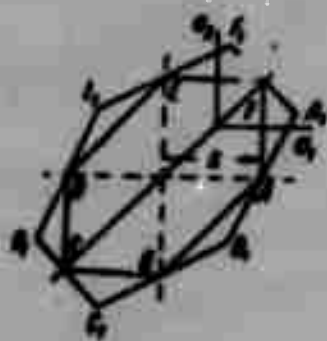


Fig. 2.

$$\frac{\partial u}{\partial p} + \frac{\partial w}{\partial z} + \frac{u}{p} = 0, \quad \frac{\partial u}{\partial p} - \frac{\partial w}{\partial z} = 0, \quad \frac{\partial u}{\partial z} + \frac{\partial w}{\partial p} = 0 \quad (1.14)$$

It is easy to verify that the solution of system of equations (1.14) corresponds to displacement of material as a rigid whole.

The case  $a = -b$  corresponds to edges  $AB$ ,  $DE$  of the condition of plasticity of Tresca (Fig. 2). This case, investigated in [1], leads to a trivial field of speeds of displacements

$$u = 0, \quad w = w(p) \quad (1.15)$$

2. Let us consider the field of stresses. Using formulas

$$\begin{aligned}\sigma_1 &= \frac{1}{2}(\sigma_p + \sigma_z) + \frac{1}{2}[(\sigma_p - \sigma_z)^2 + 4\tau_{pz}^2]^{\frac{1}{2}} \\ \sigma_2 &= \frac{1}{2}(\sigma_p + \sigma_z) - \frac{1}{2}[(\sigma_p - \sigma_z)^2 + 4\tau_{pz}^2]^{\frac{1}{2}} \\ \sigma_3 &= \sigma_0\end{aligned}\quad (2.1)$$

we rewrite the condition of plasticity (1.1) in the form

$$[2c\sigma_0 + (a+b)(\sigma_p + \sigma_z) - 2]^2 - (a-b)^2[(\sigma_p - \sigma_z)^2 + 4\tau_{pz}^2] = 0 \quad (2.2)$$

Considering condition (2.2) as plastic potential, we rewrite the relationship of the associated law of plastic flow

$$\frac{e_p - e_z}{\sigma_p - \sigma_z} = \frac{-(e_p + e_z)(a-b)^2}{(a+b)[2c\sigma_0 + (a+b)(\sigma_p + \sigma_z) - 2]} = \frac{e_{pz}}{\tau_{pz}} = \lambda \quad (2.3)$$

For components of stresses there exist the relationships

$$\begin{aligned}\sigma_p &= p + q \cos 2\psi, \quad \sigma_z = p - q \cos 2\psi, \quad \tau_{pz} = q \sin 2\psi \\ p &= \frac{1}{2}(\sigma_1 + \sigma_2), \quad q = \frac{1}{2}(\sigma_1 - \sigma_2)\end{aligned}\quad (2.4)$$

Putting relationship (2.4) in equations of equilibrium

$$\frac{\partial \sigma_p}{\partial p} + \frac{\partial \tau_{pz}}{\partial z} + \frac{\tau_{pz} - \tau_{pz}}{p} = 0, \quad \frac{\partial \tau_{pz}}{\partial p} + \frac{\partial \sigma_z}{\partial z} + \frac{\tau_{pz}}{p} = 0 \quad (2.5)$$

we will obtain a system of two equations relative to two unknowns  $p$  and  $q$

$$\begin{aligned}\frac{\partial p}{\partial p} + \frac{\partial q}{\partial p} \cos 2\psi + \frac{\partial q}{\partial z} \sin 2\psi &= \frac{\sigma_p - \sigma_z}{p} + 2q \sin 2\psi \frac{\partial \psi}{\partial p} - 2q \cos 2\psi \frac{\partial \psi}{\partial z} \\ \frac{\partial p}{\partial z} + \frac{\partial q}{\partial p} \sin 2\psi - \frac{\partial q}{\partial z} \cos 2\psi &= -\frac{\tau_{pz}}{p} - 2q \cos 2\psi \frac{\partial \psi}{\partial p} - 2q \sin 2\psi \frac{\partial \psi}{\partial z}\end{aligned}\quad (2.6)$$

Function  $\psi$  in equations (2.6) is considered known from solution of the problem for components of speed of displacement. System (2.6) belongs to the hyperbolic type, equations of characteristic are determined from (1.9).

Thus, equations for determination of components of speed of displacements and stresses have coinciding characteristics.

3. Let us show that under the condition of conformity of the stressed and deformed state of the edge of a prism of fluidity in a plastic field lines of discontinuity of speeds of displacements cannot appear. From the associated law (2.3) it follows that in orthogonal system of coordinates  $xy$

$$\frac{e_x - e_y}{\sigma_x - \sigma_y} = \frac{-(e_x + e_y)(a-b)^2}{(a+b)[2c\sigma_0 + (a+b)(\sigma_x + \sigma_y) - 2]} = \frac{e_{xy}}{\tau_{xy}} = \lambda, \quad a+b \neq 0 \quad (3.1)$$

Let us assume that line  $x$  coincides with line of discontinuity of tangent speeds of displacements (discontinuities of normal speeds lead to disturbance of continuity of medium and are not considered here). Then  $e_{xy} \rightarrow \infty$ , and from (3.1) it follows that on the line of discontinuity

$$\sigma_x = \sigma_y, \quad 2c\sigma_2 + (a+b)(\sigma_1 + \sigma_2) = 2 \quad (3.2)$$

Considering condition (1.1) we rewrite the second relationship in the form

$$c\sigma_2 + b\sigma_1 + a\sigma_2 = 1 \quad (3.3)$$

From conditions (3.3) and (1.1) it follows that

$$\sigma_1 - \sigma_2 = 0 \quad \text{when } a-b \neq 0 \quad (3.4)$$

The state determined by (1.1), (3.4) corresponds to edges F, C of the prism on Fig. 2. Condition  $\sigma_1 - \sigma_2 = 0$  corresponds to the particular case at which tangential stress in plane  $\rho z$  is identically equal to zero. Degenerated case  $a = b$  is considered above.

Thus, if tangential stress in plane  $\rho z$  is identically not equal to zero, then field of speeds of displacements, corresponding to edge of prism of fluidity, cannot have lines of discontinuity.

In the case of conformity of stressed and deformed state to edge of prism of fluidity from the associated law of flow it follows [4] that

$$\frac{\sigma_x - \sigma_y}{\sigma_x + \sigma_y} = \frac{e_{xy}}{\tau_{xy}} \quad (3.5)$$

Hence when  $e_{xy} \rightarrow \infty$  there exists  $\sigma_x - \sigma_y \rightarrow 0$ . From condition of plasticity  $(\sigma_x - \sigma_y)^2 + 4\tau_{xy}^2 = 4k^2$  it follows that  $\tau_{xy} \rightarrow k$ . Lines of discontinuity of speeds of displacements always coincide with slip lines, where slip line are characteristics.

4. Equations (1.8) allow a class of self-simulating solutions of form [2]

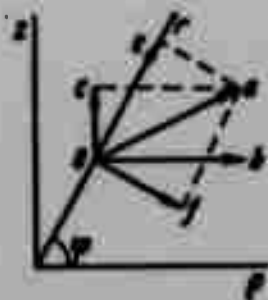
$$u = \rho^n u_1(\xi), \quad w = \rho^n w_1(\xi), \quad \xi = z/\rho \quad (4.1)$$

In this case equations (1.7) take the form

$$\begin{aligned} \xi u_1' - (n+1)u_1 - w_1' &= 0 \\ (\xi u_1' - nu_1 + w_1')^2 + (u_1' + nw_1 - \xi w_1')^2 &= \left(\frac{a-b}{c}\right)^2 u_1^2 \end{aligned} \quad (4.2)$$

where the prime signifies derivative with respect to  $\xi$ .

Let us turn to components of speeds in spherical system of coordinates  $r\varphi\theta$ . On Fig. 3 vector  $oa$  has component  $ob = u$ ,  $oc = w$  in cylindrical system of coordinates and  $oe = U$ ,  $of = W$  in spherical system of coordinates.



Obviously

$$U = u \cos \varphi + w \sin \varphi, \quad W = -u \sin \varphi + w \cos \varphi \quad (4.3)$$

Considering  $U = \rho^n U_1(\xi)$ ,  $W = \rho^n W_1(\xi)$  and considering that

Fig. 3.

$$\cos \varphi = (1 + \xi^2)^{-1/2}, \quad \sin \varphi = \xi(1 + \xi^2)^{-1/2}$$

it is easy to convert system of equations (4.2) to components  $U_1(\xi)$ ,  $W_1(\xi)$ .

Solution of system of equations will be considered for two cases:  $U_1 = 0$ ,  $W_1 = 0$  (conical flows),  $U_1 = 0$ ,  $W_1 \neq 0$  (spherical flows). For conical flows equations will take the form

$$\begin{aligned} (n+2)U_1 &= 0 \\ [U_1'(1+\xi^2) + 2U_1\xi]^2 - \kappa_1 U_1^2 &= 0 \\ \kappa_1 &= \left(\frac{a-b}{c}\right)^2 - 9 \end{aligned} \quad (4.4)$$

System of equations (4.4) has a solution at  $n = -2$ ,  $\kappa_1 \geq 0$ . Here the second equation of (4.4) will take the form

$$[U_1'(1+\xi^2) + U_1(2\xi + \kappa)] [U_1'(1+\xi^2) + U_1(2\xi - \kappa)] = 0 \quad (\kappa^2 = \kappa_1) \quad (4.5)$$

From solution of equation (4.5) we will obtain

$$U = \rho^{-2} U_1 = C r^{-2} e^{\pm \kappa \varphi}, \quad W = 0, \quad C = \text{const}, \quad \rho = r \cos \varphi, \quad \lg \varphi = \xi \quad (4.6)$$

Constant  $C$  characterizes quantity of material flowing through fixed section  $r = \text{const}$ . In the considered case of quasistatic flow constant  $C$  does not affect values of components of stresses, since radial speed  $U$  is directed to center ( $U < 0$ ); we will put  $C = -1$ . Components of speed of deformation in spherical system of coordinates, corresponding to (4.6), have the form

$$\begin{aligned} \epsilon_r &= \frac{\partial U}{\partial r} = 2r^{-3} e^{\pm \kappa \varphi}, \quad \epsilon_{\varphi} = \mp \kappa r^{-3} e^{\pm \kappa \varphi} \\ \epsilon_{\theta} &= \epsilon_{\psi} = \frac{U}{r} = -r^{-3} e^{\pm \kappa \varphi} \end{aligned} \quad (4.7)$$

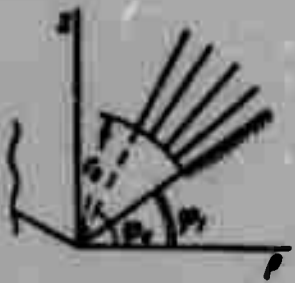


Fig. 4.

Every value of  $\kappa$  corresponds to a fully defined edge of prism of plasticity. From (4.6), (4.7) it follows that to every defined edge of a prism of plasticity corresponds a conical flow with its own value of speed of deformation of shift  $\epsilon_{r\varphi}$ . According to the associated law of flow (2.3), there exists  $\epsilon_{r\varphi} = \lambda \tau_{r\varphi}$ .

If on conical matrix (Fig. 4) is assigned defined tangential stress  $\tau_{r\varphi} \neq 0$ , then  $\epsilon_{r\varphi} \neq 0$  and a solution can be built only for a certain defined value  $\kappa$ . For smooth matrix  $\tau_{r\varphi} = 0$  when  $\varphi = \varphi_1 \neq 0$ ; there exists  $\kappa = 0$ . Then from (4.4) we will obtain

$$a:b:c = 2:-1:-1 \quad \text{or} \quad a:b:c = 1:-2:1 \quad (4.8)$$

Relationships (4.8) correspond to edges  $A_1P_1$ ,  $E_1D_1$  and  $B_1C_1$ ,  $E_1F_1$  of condition of plasticity of maximum given stress [8] (Fig. 2).

Thus, if one were to assume that the stressed and deformed state of an ideal plastic material during conical flow corresponds to a certain edge of a prism of plasticity, then for a smooth matrix with aperture angle  $\varphi_1 \neq 0$  a solution can be constructed only for the condition of plasticity of maximum given stress.

Relationships (4.6), (4.7) have the form

$$U = -r^2, \quad W = 0, \quad \epsilon_r = 2r^{-2}, \quad \epsilon_\varphi = \epsilon_\theta = -r^{-2}, \quad \epsilon_{r\varphi} = 0, \quad \kappa = 0 \quad (4.9)$$

From (4.9) it follows that direction  $r$ ,  $\varphi$  will be principal. Consequently, stresses  $\sigma_r$ ,  $\sigma_\varphi$  will be the main stresses. According to (4.9),

$$\epsilon_r:\epsilon_\varphi:\epsilon_\theta = 2:-1:-1 \quad (4.10)$$

Equation of edge of condition of plasticity of maximum given stress, corresponding to law of flow (4.10), has the form

$$2\sigma_r - \sigma_\varphi - \sigma_\theta = k \quad (4.11)$$

From the condition of positivity of power of dissipation of mechanical energy  $D = \sigma_r \epsilon_r + \sigma_\varphi \epsilon_\varphi + \sigma_\theta \epsilon_\theta > 0$  we will find that  $k > 0$ . Thus, conical flow (4.9) corresponds to edge  $A_1B_1$  (Fig. 2). Components of stresses are changed only in

defined limits

$$\frac{1}{2}k \leq \sigma_r - \sigma_\theta \leq \frac{3}{2}k, \quad -\frac{1}{2}k \leq \sigma_\varphi - \sigma_\theta \leq \frac{1}{2}k \quad (4.12)$$

Equations of equilibrium have the form

$$\frac{\partial \sigma_r}{\partial r} + \frac{1}{r}(2\sigma_r - \sigma_\theta - \sigma_\varphi) = 0, \quad \frac{\partial \sigma_\varphi}{\partial \varphi} + (\sigma_\varphi - \sigma_\theta) \lg \varphi = 0 \quad (4.13)$$

Using relationship (4.11), from the first equation of (4.13) we will find

$$\sigma_r = -k \ln r + f(\varphi) \quad (4.14)$$

Assuming that during pressing of material in conical matrix (Fig. 4) surface  $r = r_0$  is free from stresses ( $\sigma_r = 0$  when  $r = r_0$ ), we will find

$$\sigma_r = -k \ln (r/r_0), \quad r \geq r_0 \quad (4.15)$$

From (4.13), (4.15), (4.11) we will obtain

$$\sigma_\theta = \sigma_r + g(r) \cos^2 \varphi - \frac{1}{2}k, \quad \sigma_\varphi = \sigma_r - g(r) \cos^2 \varphi - \frac{1}{2}k \quad (4.16)$$

In the case of a solid body, composing an integral equation of equilibrium of plastic between sections  $r = r_0$ ,  $r = R$  and matrix ( $\varphi = \varphi_1$ ), we will obtain  $g(r) = 0$ . Expressions (4.16) take the form

$$\sigma_\theta = \sigma_\varphi = \sigma_r - \frac{1}{2}k \quad (4.17)$$

Thus, the state of strain of a material filling the whole cavity of a smooth conical matrix during conical flow, corresponds to one straight line (4.17) condition of plasticity (point A on Fig. 2).

In the case of a body with cavity (Fig. 4) from (4.12) and (4.16) we will obtain

$$-\frac{1}{2}k \leq 2g(r) \cos^2 \varphi \leq \frac{1}{2}k \quad (4.18)$$

Conditions (4.18) cannot be satisfied, if on the internal boundary of body ( $\varphi = \varphi_0$ ) stresses are absent ( $\sigma_\varphi = 0$ ). For satisfaction of inequality (4.18) it is necessary to apply pressure  $\sigma_\varphi = -kp(r)$  on internal boundary of material when  $\varphi = \varphi_0$ , within the limits

$$\ln \frac{r}{r_0} + \frac{1}{2} + \frac{1}{6} \frac{\cos^2 \varphi_0}{\cos^2 \varphi_1} > p(r) > \ln \frac{r}{r_0} + \frac{1}{2} - \frac{1}{6} \frac{\cos^2 \varphi_0}{\cos^2 \varphi_1} \quad (4.19)$$

where  $\varphi_1$  - aperture angle of matrix (Fig. 4). The sufficient condition for change of values of magnitude of pressure can be written in the form

$$\frac{1}{2} + \frac{1}{6} \frac{\cos^2 \varphi_0}{\cos^2 \varphi_1} > p > \ln \frac{R}{r_0} + \frac{1}{2} - \frac{1}{6} \frac{\cos^2 \varphi_0}{\cos^2 \varphi_1} \quad (4.20)$$

Let us note that conical flows cannot correspond to edge of prism of Tresca. Really, edges AB, DE (Fig. 2) correspond to trivial solutions of [1], and for edges AF, BC, CD, EF always  $n_1 = -8$ , and from (4.4) it follows that  $U = 0$ . For the case of spherical flows ( $U_1 = 0$ ,  $W_1 \neq 0$ ) initial equations will take the form

$$W_1'(1 + \xi^2) - (n + 1)\xi W_1 = 0, \quad \xi^2 \left[ 1 - \left( \frac{a-b}{a+b} \right)^2 \right] + (1-n)^2 = 0 \quad (4.21)$$

From the second equation of (4.21) it follows that

$$\left( \frac{a-b}{a+b} \right)^2 - 1 = 0, \quad n - 1 = 0 \quad (4.22)$$

From (4.22) we will obtain  $ab = 0$ . Condition of equality to zero of  $a$  and  $b$  means that the state of strain can correspond only to edges of prism of Tresca AF, BC, CD, EF (Fig. 2). From (4.21) it follows that

$$U = 0, \quad W = rB \sec \varphi, \quad B = \text{const} \quad (4.23)$$

5. Spherical flow, corresponding to field of speeds (4.23), is investigated in detail in [7]. This flow is the only possible one: to no edge of arbitrary piecewise-linear conditions of fluidity (besides edge of prism of Tresca) can correspond spherical flows. Moreover, flow (4.23) can be realized only in the absence of friction on spherical matrix. In case of a rough spherical matrix the state of strain during spherical flow cannot correspond to edges of prism of Tresca and any other piecewise-linear conditions of fluidity.

In [7] Lippman expresses consideration about the fact that among all possible stressed and deformed states of an axially symmetric problem, corresponding to condition of plasticity of Tresca, a basic role must be played by states corresponding to edge of prism of Tresca. With similar affirmations it is difficult to agree. A

great class of problems about the impression of stamps, extraction of axially symmetric procurements, etc., is impossible to solve within the bounds solid plastic analysis without introduction of lines of discontinuity of rates of displacements, whereas equations corresponding to the edge of any prism of the condition of plasticity, do not allow possibility of discontinuity of rates of displacements. While on axis  $z(\rho = 0)$  the condition of full plasticity always exists.

At the same time Lippman does not note that the Cauchy problem for states corresponding to the edge of a prism may be posed only under limitations (1.13) on rate of displacement.

Analysis of flows, considered in this work and [7], reveals their very particular character.

Submitted  
28 March 1964

#### Literature

1. R. Shild. Plastic flow of metals in conditions of axial symmetry. Collection of translations. "Mechanics," No. 1, Publishing House of Foreign Literature, 1957.
2. D. D. Ivlev. The theory of axially symmetric state of strain under the condition of plasticity of Tresca. Publishing House AS USSR, OTN, 1959, No. 6.
3. A. Cox, G. Eason and H. Hopkins. Philos. Trans., 1961, A 254, 1.
4. D. D. Ivlev and T. N. Martynova. The condition of full plasticity for the axially symmetric state, PMTF, 1963, No. 3.
5. I. G. Petrovskiy. Lectures about partial differential equations. Gostekhizdat, M., 1953.
6. R. Kurant and D. Gil'bert. Methods of mathematical physics, Vol. 2. State Technical Press, 1945.
7. G. Lippman. Theory of principal trajectories during axially symmetric plastic deformation. Collection of translations. "Mechanics," No. 3, Publishing House of Foreign Literature, 1963.
8. A. Yu. Ishlinskiy. Axially symmetric problem of the theory of plasticity and the Brinell test. PMM; 1944, Vol. 8, Issue 3.

**BLANK PAGE**

THEORY OF VISCOELASTIC MULTILAYERS OF SHELLS  
WITH RIGID FILLERS WITH THE EXISTENCE  
OF FINITE BENDING

E. I. Grigolyuk and P. P. Chulkov

(Novosibirsk)

Theory is constructed for finite bending of multilayer shells from a linearly-viscoelastic material for every layer. As a basis are assumed equations of sloping shells [1, 2] are set up and a hypothesis about linear change of displacements with respect to height of pack [1], and also a hypothesis about incompressibility of layers in the transverse direction. In distinction from the theory of three-layered shells [3-5], arbitrary alternating of fillers and carrier layers is assumed while the number of them not is established. By a filler, which, as also the carrier layer, receives turning and bending moments, and also force in its middle surface, is implied a layer transmitting deformation of a transverse shift. As a result is obtained a system of three differential equations with respect to function of displacements  $\chi$ , force function  $F$  and certain potential function  $\phi$ . Hence different particular cases can be obtained: system of equations for a shell with light filler, system of equations of three-layered shells, etc. It is shown that during solution of practical problems equations containing  $\phi$  need not be considered and consequently, the solution may be based on a system of nonlinear differential equations containing  $F$  and  $\chi$ .

A series of linear problems was discussed earlier [6-9].

In [6] is given the derivation of equations of a three-layered plate with nonsymmetric structure during small, harmonic displacements on the assumption that carrier layers are elastic diaphragms, fastened by middle surfaces to external surfaces of a viscoelastic filler, and perceiving only transverse shift. For the one-dimensional case follows the expression of [7], in which results of calculation are compared with experiment.

In [8] equations of [3] are extended to the case of small harmonic oscillations of a viscoelastic three-layered orthotropic cylindrical circular shell with hard filler; complex moduli are introduced, describing elastic and damping properties of material; the case of normal harmonic pressure on a circular panel is considered, for which on every edge normal force, sag, bending moment, displacement along edge and angle of inclination are equal to zero.

Work [9] minutely examines the case of small deformations of a three-layered beam symmetric in height with a viscoelastic momentless carrier layer and elastic filler, transmitting transverse shift and transverse compression under transverse pressure which changes with constant speed in time, or remains constant. A thin sloping shell is investigated, whose wall consists of an arbitrary number of layers rigidly connected with respect to surfaces of contact and made of different material, possessing properties of linear viscoelasticity. If there are layers made of a material considerably more weakly resisting shift, as compared to materials of other layers, use of the hypotheses Kirkhoff-Love for the pack as a whole becomes impossible, since phenomena connected with shift of these layers would not be considered. Subsequently we will use a more general system of kinematic hypotheses in which for every layer, first, material is considered incompressible in the transverse direction and, second a line segment perpendicular to surface of shell in the process of deformation turns, not becoming distorted, but, in distinction from the hypothesis of Kirkhoff-Love about a straight normal, it does not remain perpendicular to the bent initial surface of the shell. This more general system of hypotheses [3, 4] permits constructing a rational approach, considering shifts occurring in layers. Transition to an approach corresponding to the hypotheses of Kirkhoff-Love is feasible if one directs to infinity the shear modulus of the corresponding layer.

§ 1. Formulation of problem. Let us consider a shell consisting of  $s$  layers, and as the initial surface we will take the internal surface referred to Cartesian coordinates  $x_1$  ( $i = 1, 2$ ), lines of which coincide with lines of main curvatures of shell. Let us assume that:  $z$  - coordinate measured with respect to external normal,  $h$  - total thickness of shell,  $h_k$  - thickness of  $k$ -th layer,  $\delta_k$  - distance from initial surface to top of  $k$ -th layer,  $k_{11}$  - curvature of 1-th coordinate line;  $u_1, w$  - tangential and normal displacements of point of initial surface;  $\alpha_1^k$  - angles of rotation of normal within limits of  $k$ -th layer.

Equation of compatibility. Bending of shell is constant in thickness  $w = w(x_1, x_2)$ , since material of layers is not compressed in the transverse direction. According to kinematic hypothesis, tangential displacements of points of  $k$ -th layer are determined by the formula

$$u_i' = u_i + \sum_{r=1}^{k-1} \alpha_i^r h_r + \alpha_i^k (z - \delta_{k-1}) \quad (\delta_{k-1} < z < \delta_k)$$

Deformations of arbitrary surface of  $k$ -th layer equal

$$e_{ij}^k = e_{ij} + \sum_{r=1}^{k-1} \alpha_{ij}^r h_r + \alpha_{ij}^k (z - \delta_{k-1}), \quad \epsilon_{ij}^k = \alpha_i^k + w_{,i} \quad (\delta_{k-1} < z < \delta_k) \quad (1.1)$$

Here

$$e_{ij} = \frac{1}{2}(u_{i,j} + u_{j,i}) + k_{ij}w + \frac{1}{2}w_{,i}w_{,j}$$

$$\alpha_{ij}^k = \frac{1}{2}(\alpha_{i,j}^k + \alpha_{j,i}^k), \quad k_{12} = 0$$

As usual, the subscript, set after the comma, signifies differentiation with respect to corresponding coordinate.

For flat state of strain the connection between stresses and deformations in the case of viscoelastic model of body can be brought to the form

$$(R + 2\Omega)R\sigma_{ij} = \frac{E}{1-2\nu}\Omega[(R + 2\Omega)\epsilon_{ij} + \delta_{ij}(R - \Omega)\epsilon_{rr} - 3R\omega\Delta T\delta_{ij}]$$

$$R = \frac{1+\nu}{1-2\nu}\left(1 + a_1\frac{\partial}{\partial t} + \dots + a_m\frac{\partial^m}{\partial t^m}\right)$$

$$\Omega = \left(1 + b_1\frac{\partial}{\partial t} + \dots + b_n\frac{\partial^n}{\partial t^n}\right)$$

$$\epsilon_{rr} = \epsilon_{11} + \epsilon_{22} \quad (\delta_{ii} = 1, \delta_{ij} = 0 \text{ when } i \neq j)$$

Here  $E$  - elastic modulus of the first kind,  $\nu$  - Poisson's ratio,  $\omega$  - coefficient of temperature expansion,  $\Delta T$  - increase of temperature,  $t$  - time. If

$$\frac{\Omega}{R} = \mu\lambda, \quad \mu = \frac{1-2\nu}{1-\nu^2}, \quad 3\omega\Delta T = \tau$$

we have

$$(1 + 2\mu\lambda)\sigma_{ij} = \frac{E}{1-\nu^2}\lambda[(1 + 2\mu\lambda)\epsilon_{ij} + \delta_{ij}(1 - \mu\lambda)\epsilon_{rr} - \tau\delta_{ij}] \quad (1.2)$$

Operator  $\lambda$  has the form

$$\lambda = (1 - \nu) \frac{1 + b_1\frac{\partial}{\partial t} + \dots + b_n\frac{\partial^n}{\partial t^n}}{1 + a_1\frac{\partial}{\partial t} + \dots + a_m\frac{\partial^m}{\partial t^m}}$$

For incompressible material ( $\nu = 1/2, \mu = 0$ ) formula (1.2) is simplified

$$\sigma_{ij} = \frac{1}{3}E\lambda(\epsilon_{ij} + \delta_{ij}\epsilon_{rr} - \tau\delta_{ij})$$

Stresses for  $k$ -th layer are determined by the formula

$$(1 + 2\mu_k\lambda_k)\sigma_{ij}^k = \frac{E_k}{1-\nu_k^2}\lambda_k[(1 + 2\mu_k\lambda_k)\epsilon_{ij}^k + \delta_{ij}(1 - \mu_k\lambda_k)\epsilon_{rr}^k - \tau_k\delta_{ij}] \quad (1.3)$$

$$\sigma_{i3}^k = G_k g_k(a_i^k + w_{,i}) \quad (1.4)$$

Here  $G_k$  - shear modulus for planes  $x_1z$  and  $x_2z$  of material of  $k$ -th layer,  $g_k$  - operator of form

$$g_k = \frac{1 + \epsilon_1^k \theta(\dots)/\theta t \dots}{1 + d_1^k \theta(\dots)/\theta t} \quad \left( G_k = \frac{E_k}{2(1 + \nu_k)}, \quad g_k = \frac{1}{1 - \nu_k} \lambda_k \right)$$

(here in parentheses given for an isotropic material). Let us rewrite relationships (1.3), (1.4) in the following form:

$$\Lambda \sigma_{ij}^k = \frac{E_k \lambda_k}{1 - \nu_k} [\Lambda \epsilon_{ij}^k + \delta_{ij} \Lambda \epsilon_{rr}^k - \frac{\Lambda}{1 + 2\mu_k \lambda_k} \tau_k \delta_{ij}] \quad (1.5)$$

$$\Lambda \sigma_{ij}^k = G_k g_k \Lambda (\epsilon_{ij}^k + w, i), \quad \Lambda = \prod_{k=1}^n (1 + 2\mu_k \lambda_k), \quad \Lambda_k = \Lambda \frac{1 - \mu_k \lambda_k}{1 + 2\mu_k \lambda_k}$$

We determine specific tangential forces, transverse force, and specific moments of k-th layer by the formulas

$$N_{ij}^k = \int_{z_{k-1}}^{z_k} \sigma_{ij}^k dz, \quad Q_i^k = \int_{z_{k-1}}^{z_k} \sigma_{iz}^k dz, \quad M_{ij}^k = \int_{z_{k-1}}^{z_k} \sigma_{ij}^k (z - z_{k-1}) dz \quad (1.6)$$

Equations of equilibrium in forces have the form

$$\sum_{k=1}^n (N_{11,1}^k + N_{22,2}^k) = 0 \quad (1.7)$$

$$h_k \sum_{m=k}^{n-1} (N_{11,1}^{m+1} + N_{22,2}^{m+1}) + M_{11,1}^k + M_{22,2}^k = Q_i^k \quad (1.8)$$

$$\sum_{k=1}^n (Q_{1,1}^k + Q_{2,2}^k) - \sum_{k=1}^n (k_{11} N_{11}^k + k_{22} N_{22}^k) + \sum_{i,j} w, i \left( \sum_{k=1}^n N_{ij}^k \right) + q = 0 \quad (1.9)$$

In order to use these equations, it is necessary to produce above them operation A. Let us consider the first two equations of (1.7). According to formulas (1.6), (1.5) and (1.1)

$$\Lambda N_{ij}^k = \frac{E_k \lambda_k}{1 - \nu_k} \lambda_k \left[ \Lambda \left( \epsilon_{ij}^k + \sum_{q=1}^{k-1} \alpha_{ij}^k h_q \right) + \delta_{ij} \Lambda \left( \epsilon_{rr}^k + \sum_{q=1}^{k-1} h_q \alpha_{rr}^q \right) + \right. \\ \left. + \frac{h_k}{2} \Lambda \epsilon_{ij}^k + \delta_{ij} \Lambda \frac{h_k}{2} \alpha_{rr}^k \right] - \frac{\Lambda \lambda_k}{1 + 2\mu_k \lambda_k} \delta_{ij} N_k, \quad N_k = \int_{z_{k-1}}^{z_k} \frac{E_k \tau_k}{1 - \nu_k} dz$$

Let us find further

$$\Lambda N_{ij} = \Lambda \sum_{k=1}^n N_{ij}^k$$

Let us assume that

$$\frac{Eh}{1-\nu^2} = \sum_{k=1}^n \frac{E_k h_k}{1-\nu_k^2}, \quad \gamma_k = \frac{E_k h_k (1-\nu_k^2)}{(1-\nu_k^2) E h}, \quad \epsilon_k = \frac{h_k}{h}$$

For definitiveness we will designate  $\nu = \nu_1 \gamma_1 + \dots + \nu_n \gamma_n$

Subsequently  $E$  and  $\nu$  we will call accordingly the given elastic modulus and Poisson's ratio. Furthermore, we will introduce

$$h_k a_1^k = h a_{,1}^k + h \varphi_{,2}^k, \quad h_k a_2^k = h a_{,2}^k - h \varphi_{,1}^k$$

Then

$$h_k a_{11}^k = h a_{,11}^k + h \varphi_{,12}^k, \quad h_k a_{22}^k = h a_{,22}^k - h \varphi_{,12}^k \\ h_k a_{12}^k = h a_{,12}^k + \frac{1}{2} h (\varphi_{,22}^k - \varphi_{,11}^k)$$

Functions  $a^k$  and  $\varphi^k$  are accordingly scalar and vector potentials of vector  $(a_1^k, a_2^k)$ . Then

$$\Delta N_{11} = \frac{Eh}{1-\nu^2} [e_{11} + p e_{22}] + \frac{Eh^3}{1-\nu^2} \sum_{r=1}^n (I_r' a_{,11}^r + P_r' a_{,22}^r) + \\ + \frac{Eh^3}{1-\nu^2} \sum_{r=1}^n (I_r' - P_r') \varphi_{,12}^r - \Delta N \\ \Delta N_{22} = \frac{Eh}{1-\nu^2} [e_{22} + p e_{11}] + \frac{Eh^3}{1-\nu^2} \sum_{r=1}^n (I_r' a_{,22}^r + P_r' a_{,11}^r) - \\ - \frac{Eh^3}{1-\nu^2} \sum_{r=1}^n (I_r' - P_r') \varphi_{,12}^r - \Delta N \\ \Delta N_{12} = \frac{Eh}{1-\nu^2} (1-p) e_{12} + \frac{Eh^3}{1-\nu^2} \sum_{r=1}^n (I_r' - P_r') a_{,12}^r + \\ + \frac{Eh^3}{2(1-\nu^2)} \sum_{r=1}^n (I_r' - P_r') (\varphi_{,22}^r - \varphi_{,11}^r)$$

Here

$$1 = \sum_{k=1}^n \gamma_k \lambda_k (\Lambda + \Lambda_k), \quad P = \sum_{k=1}^n \gamma_k \lambda_k' \Lambda_k, \quad N = \sum_{k=1}^n \frac{\lambda_k}{1 + 2\mu_k \lambda_k} N_k \quad (1.10) \\ I_r' = \sum_{k=r}^n \gamma_k \lambda_k (\Lambda + \Lambda_k) - \frac{1}{2} \gamma_r \lambda_r (\Lambda + \Lambda_r), \quad P_r' = \sum_{k=r}^n \gamma_k \lambda_k \Lambda_k - \frac{1}{2} \gamma_r \lambda_r \Lambda_r$$

Let us assume that

$$u_1 = u_1^0 + h v_{,1} + h \varphi_{,2}, \quad u_2 = u_2^0 + h v_{,2} - h \varphi_{,1}$$

Let us require fulfillment of equalities

$$\begin{aligned} l e_{11,1}^{\circ} + P e_{22,1}^{\circ} + (I - P) e_{12,2}^{\circ} - \frac{1 - \nu^2}{Eh} \Lambda N_{,1} &= 0 \\ l e_{22,2}^{\circ} + P e_{11,2}^{\circ} + (I - P) e_{12,1}^{\circ} - \frac{1 - \nu^2}{Eh} \Lambda N_{,2} &= 0 \end{aligned} \quad (1.11)$$

where

$$e_{ij}^{\circ} = \frac{1}{2} (u_{i,j}^{\circ} + u_{j,i}^{\circ}) + k_{ij} w + \frac{1}{2} w_{,i} w_{,j} \quad (1.12)$$

Equations of (1.11) are identically satisfied when

$$\begin{aligned} e_{11}^{\circ} &= \frac{1}{Eh} (l F_{,22} - P F_{,11}) + \frac{1 - \nu^2}{Eh} \Lambda (I + P)^{-1} N \\ e_{22}^{\circ} &= \frac{1}{Eh} (l F_{,11} - P F_{,22}) + \frac{1 - \nu^2}{Eh} \Lambda (I + P)^{-1} N \\ e_{12}^{\circ} &= - \frac{1}{Eh} (I + P) F_{,12} \end{aligned} \quad (1.13)$$

Using the condition of compatibility of deformations (1.12), we will obtain an equation for force function  $F$

$$\begin{aligned} IV^2 \nabla^2 F + \Lambda (I + P)^{-1} (1 - \nu^2) \nabla^2 N &= \\ = Eh (k_{22} w_{,11} + k_{11} w_{,22} + w_{,12}^2 - w_{,11} w_{,22}) \end{aligned} \quad (1.14)$$

Furthermore, from equations (1.7) we obtain equalities

$$l \psi + \sum_{r=1}^{\infty} l_r' \psi^r = 0, \quad l \psi + \sum_{r=1}^{\infty} l_r' \psi^r = 0 \quad (1.15)$$

§ 2. Equation of equilibrium. Let us express specific moments

$$\Lambda H_{ij}^k = \Lambda M_{ij}^k + \Lambda h_k \sum_{m=k+1}^{\infty} N_{ij}^m$$

through scalar  $a^k$  and vector potentials  $\varphi^k$

$$\begin{aligned} \Lambda H_{11}^k &= \frac{Eh^3}{1 - \nu^2} l_2 \left( l_1^k e_{11} + P_1^k e_{22} + h l_1^k \sum_{m=1}^k a_{,11}^m + h P_1^k \sum_{m=1}^k a_{,22}^m + \right. \\ &+ h \sum_{m=k+1}^{\infty} \left( l_1^m a_{,11} + P_1^m a_{,22} \right) - \frac{h}{6} \lambda_k \gamma_k (\Lambda + \Lambda_k) a_{,11}^k - \frac{h}{6} \lambda_k \gamma_k \Lambda_k a_{,22}^k + \\ &+ h (l_1^k - P_1^k) \sum_{m=1}^k \varphi_{,12}^m + h \sum_{m=k+1}^{\infty} (l_1^m - P_1^m) \varphi_{,12}^m - \frac{h}{6} \lambda_k \gamma_k \Lambda \varphi_{,12}^k - \Lambda H_k \end{aligned}$$

$$\begin{aligned} \Lambda H_{22}^k = & \frac{E_k \lambda^2}{1-\nu^2} t_k [I_k^k e_{22} + P_k^k e_{11} + h I_k^k \sum_{m=1}^k a_{,22}^m + \\ & + \Lambda P_k^k \sum_{m=1}^k a_{,11}^m + h \sum_{m=k+1}^{\infty} I_k^m a_{,22}^m + h \sum_{m=k+1}^{\infty} P_k^m a_{,11}^m - \\ & - h(I_k^k - P_k^k) \sum_{m=1}^k \varphi_{,22}^m - h \sum_{m=k+1}^{\infty} (I_k^m - P_k^m) \varphi_{,22}^m - \\ & - \frac{h}{6} \lambda_k \gamma_k (\Lambda + \Lambda_k) a_{,22}^k - \frac{h}{6} \lambda_k \gamma_k \Lambda_k a_{,11}^k + \frac{h}{6} \lambda_k \gamma_k \Lambda \varphi_{,12}^k] - \Lambda H_k \end{aligned}$$

$$\begin{aligned} \Lambda H_{12}^k = & \frac{E_k \lambda^2}{1-\nu^2} t_k [(I_k^k - P_k^k) e_{12} + h(I_k^k - P_k^k) \sum_{m=1}^k a_{,12}^m + \\ & + h \sum_{m=k+1}^{\infty} (I_k^m - P_k^m) a_{,12}^m - \frac{h}{6} \lambda_k \gamma_k \Lambda a_{,12}^k + \frac{h}{2} (I_k^k - P_k^k) \sum_{m=1}^k (\varphi_{,22}^m - \varphi_{,11}^m) + \\ & + \frac{h}{2} \sum_{m=k+1}^{\infty} (I_k^m - P_k^m) (\varphi_{,22}^m - \varphi_{,11}^m) - \frac{h}{12} \lambda_k \gamma_k \Lambda (\varphi_{,22}^k - \varphi_{,11}^k) \end{aligned}$$

where

$$\Lambda H_k = \Lambda h_k \sum_{m=k+1}^{\infty} \frac{\lambda_m}{1 + 2\mu_m \lambda_m} N + \Lambda \frac{\lambda_k}{1 + 2\mu_k \lambda_k} \int_{\delta_{k-1}}^{\delta_k} \frac{E_k \tau_k (z - \delta_{k-1})}{1 - \nu_k^2} dz$$

Transverse forces  $\Lambda Q_i^k$ , according to (1.6), are equal to

$$\Lambda Q_1^k = \Lambda G_k g_k h (a_{,1}^k + w_{,1} t_k + \varphi_{,2}^k), \quad \Lambda Q_2^k = \Lambda G_k g_k h (a_{,2}^k + w_{,2} t_k - \varphi_{,1}^k)$$

Equations (1.8) are broken up into independent systems

$$\begin{aligned} & \frac{1}{E_k \lambda^2} (I P_k^k - I_k^k P) \nabla^2 \nabla^2 F + I_k^k \nabla^2 \nabla^2 v + \\ & + I_k^k \nabla^2 \nabla^2 \sum_{m=1}^k a^m + \nabla^2 \nabla^2 \sum_{m=k+1}^{\infty} I_k^m a^m - \frac{1}{6} \lambda_k \gamma_k (\Lambda + \Lambda_k) \nabla^2 \nabla^2 a^k - \\ & - \frac{1-\nu^2}{E_k \lambda^2} \Lambda \nabla^2 [H_k - (I + P)^{-1} (I_k^k + P_k^k) h N] = \nabla^2 \Lambda g_k h^{-2} \beta_k (a^k + w t_k) \end{aligned} \quad (2.1)$$

$$\begin{aligned} & (I_k^k - P_k^k) \nabla^2 \nabla^2 \psi + (I_k^k - P_k^k) \sum_{m=1}^k \nabla^2 \nabla^2 \varphi^m + \sum_{m=k+1}^{\infty} (I_k^m - P_k^m) \nabla^2 \nabla^2 \varphi^m - \\ & - \frac{1}{6} \lambda_k \gamma_k \Lambda \nabla^2 \nabla^2 \varphi^k = \nabla^2 \Lambda g_k h^{-2} \beta_k \varphi^k \quad (k=1, \dots, s), \beta_k = \frac{G_k (1-\nu^2)}{E_k \lambda^2} \end{aligned} \quad (2.2)$$

From system (2.1) function  $v$  can be excluded with the help of first equality (1.15), and function  $\psi$  from system (2.2) - with the help of second equality (1.15). Multiplying equation (2.1) by operator  $I$  and using first equality (1.15), we will find

$$\begin{aligned} & \frac{1}{Eh^3} I (IP_i^k - I_i^k P) \nabla^2 \nabla^2 F + II_i^k \nabla^2 \nabla^2 \sum_{m=1}^k a^m - \\ & - \nabla^2 \nabla^2 I_i^k \sum_{r=1}^k I_r^k a^r + \nabla^2 \nabla^2 I \sum_{m=k+1}^{\infty} I_m^k a^m - \frac{1}{6} I \lambda_k \gamma_k (\Lambda + \Lambda_k) \nabla^2 \nabla^2 a^k - \\ & - \nabla^2 \frac{1-\nu^2}{Eh^3} I \Lambda [H_k - (I + P)^{-1} (I_i^k + P_i^k) hN] = \nabla^2 I \Lambda g_k h^{-2} \beta_k (a^k + w t_k) \end{aligned}$$

or, in matrix form

$$h^2 \nabla^2 \nabla^2 \Lambda a + \frac{1}{E} \nabla^2 \nabla^2 F = \nabla^2 (Ba + bw + p) \quad (2.3)$$

Here  $a, b, f, p$  - vectors-columns with elements

$$\begin{aligned} a &= \{a^1, \dots, a^k\}, \quad b = \{I \Lambda g_1 \beta_1 t_1, \dots, I \Lambda g_k \beta_k t_k\} \\ f &= \{I (IP_i^1 - I_i^1 P), \dots, I (IP_i^k - I_i^k P)\} \\ p &= \frac{1-\nu^2}{Eh^3} \{I \Lambda [H_1 + (P + I)^{-1} (I_i^1 + P_i^1) hN], \dots, \\ & \dots, I \Lambda [H_k + (P + I)^{-1} (I_i^k + P_i^k) hN]\} \end{aligned}$$

and  $A$  and  $B$  - matrix with elements

$$A_{ij} = \begin{cases} II_i^j - I_i^j I_j^i - \frac{1}{6} \delta_{ij} I \lambda_i \gamma_i (\Lambda + \Lambda_i) & (i > j) \\ II_j^i - I_j^i I_i^j & (i < j) \end{cases} \quad (2.4)$$

$$B_{ij} = I \Lambda g_i \beta_i \delta_{ij} \quad (2.5)$$

As follows from (2.4) and (2.5), matrix  $A$  is symmetric, and matrix  $B$  is diagonal.

Equation (2.3) is obtained during calculation of shift for all layers, however most frequently this is necessary only for the group of layers possessing small, compared with others, rigidity on shift. Otherwise there is obtained an unjustified increase of the order of equations, since this is equivalent to calculation of terms of form  $k_{11}^2 a^2$  ( $a$  - characteristic dimension of shell in plan), therefore for hard (carrier) layers one should consider  $a^i = -w t_i$  ( $\beta_i = \infty$ ). Taking into account this remark equation (2.3) will be rewritten in the form

$$h^2 \nabla^2 \nabla^2 A_1 a_1 - h^2 \nabla^2 \nabla^2 w + \frac{1}{E} \nabla^2 \nabla^2 F = \nabla^2 (B_1 a_1 + b_1 w + p_1) \quad (2.6)$$

Matrices  $A_1$  and  $B_1$  are obtained correspondingly from matrices  $A, B$  by canceling lines and columns, on the intersection of which were elements  $a^k$ , belonging to

carrier layers; by the same means are found vectors  $a_1, f_1, b_1, p_1$ , from vectors  $a, f, b, p$  correspondingly. Vector  $c$  will be obtained if in lines of matrix  $A$ , belonging to fillers, elements corresponding to carrier layers are selected and summed by lines, preliminarily multiplying by thickness  $t_l$  of the corresponding carrier layer.

Let us satisfy identically equation (2.6) under the conditions  $F = 0$  and  $p_1 = 0$ , considering

$$w = \left[ \sum_{n=0}^p (h^2 \nabla^2)^n w_n \right] \chi, \quad a_1 = \left[ \sum_{n=0}^p (h^2 \nabla^2)^n \eta_n \right] \chi \quad (2.7)$$

Here  $w_n$  - scalar time operator,  $\eta_n$  - vector time operator,  $p$  - number of fillers. Putting (2.7) in equation (2.6) and equating to zero coefficients at powers of operator  $h^2 \nabla^2$ , we will obtain the recursion formula for determination of vectors  $\eta_k$

$$\eta_k = B_1^{-1} A_1 \eta_{k-1} - B_1^{-1} c w_{k-1} - B_1^{-1} b w_k$$

equations will be identically satisfied if as scalars  $w_0, w_1, w_2, \dots, w_n$  corresponding coefficients of the characteristic polynomial of matrix  $B_1^{-1} A_1$  are taken.

For full satisfaction of equations (2.6) it is necessary to add to vector  $a_1$ , determined by formula (2.7), vector  $a_1^0$ , satisfying linear equation

$$h^2 \nabla^2 \nabla^2 A_1 a_1^0 + \frac{f_1}{B} \nabla^2 \nabla^2 F = \nabla^2 (B_1 a_1^0 + p_1) \quad (2.8)$$

in which  $\nabla^2 \nabla^2 F$  can be replaced by function  $\chi$  with the help of equation (1.14) or is rejected from smallness of elements of vector  $f_1$ . In the last case the problem is simplified, since it will be sufficient to find any particular solution of this equation. Thus, vector

$$a_1 = \left[ \sum_{n=0}^p (h^2 \nabla^2)^n \eta_n \right] \chi + a_1^0 \quad (2.9)$$

Let us consider equation (1.9). When  $\phi_k = 0$  column vector  $H_{1j}$ , elements of which are moments  $H_{1j}^k$ , has the form

$$H_{1j} = \frac{E h^3}{1 - \nu^2} T \left[ \frac{1}{E h} F_{,ij} + A a_{,ij} \right] - \Lambda H, \quad T = \begin{pmatrix} i_{11} & 0 & \dots & 0 \\ 0 & i_{22} & \dots & 0 \\ 0 & 0 & \dots & i_{33} \end{pmatrix} \quad (2.10)$$

and from equation (1.9) follows equality

$$\Lambda \sum_{k=1}^i (H_{11,11}^k + 2H_{12,12}^k + H_{22,22}^k) - \Lambda(k_{11}N_{11} + k_{22}N_{22}) + \Lambda \sum_{i,j} w_{ij} N_{ij} + \Lambda q = 0 \quad (2.11)$$

Therefore, introducing unit row vector  $e = (1, 1, \dots, 1)$  order  $s$  will be written (2.11) in the form

$$\frac{E\lambda^3}{1-\nu^2} \nabla^2 \nabla^2 e \left( \frac{1}{E\lambda} T(F) + T(A) a \right) - \nabla^2 \Lambda e H - \Lambda(k_{11}N_{11} + k_{22}N_{22}) + \Lambda \sum_{i,j} w_{ij} N_{ij} + \Lambda q = 0$$

but, according to (2.9), vector  $a$  can be represented in the form

$$a = \left[ \sum_{n=0}^p (k^2 \nabla^2)^n \zeta_n \right] \chi + a^0$$

Here  $\zeta_n$  - vector has the following structure: elements corresponding to  $l$ -th carrier layer equal  $-t_l w_l$ , and elements corresponding to fillers coincide with corresponding elements of vectors  $\eta_n$ . Elements of vector  $a^0$  corresponding to fillers, coincide with elements of vector  $a_1^0$ , remaining elements are equal to zero. Furthermore, by (1.34),

$$\Lambda N_{ij} \approx \frac{1-P}{1-\nu^2} \left( \delta_{ij} \nabla^2 - \frac{\partial^2}{\partial x_i \partial x_j} \right) F - \Lambda N \delta_{ij} \quad (2.12)$$

but, according to (1.30)

$$1-P = \Lambda \sum_{k=1}^i \gamma_k \lambda_k$$

Therefore formula (2.12) can be rewritten in the form

$$N_{ij} = K \left( \delta_{ij} \nabla^2 - \frac{\partial^2}{\partial x_i \partial x_j} \right) F - N_{ij} \delta_{ij} \quad (K = \frac{1+P}{1-\nu^2} \sum_{k=1}^i \gamma_k \lambda_k)$$

The equation of equilibrium (2.13) of forces in the direction of the normal to the initial surface finally will be recorded so:

$$\frac{Eh^3}{1-\nu^2} e(T A \nabla^2 \nabla^2 a) \Lambda (k_{11} K F_{,22} + k_{22} K F_{,11}) + \\ + \Lambda (w_{,11} K F_{,22}) - 2 \Lambda (w_{,12} K F_{,12}) + \Lambda (w_{,22} K F_{,11}) + \\ + \Lambda q - \nabla^2 \Lambda e H + \Lambda (k_{11} + k_{22}) N - \Lambda (\nabla^2 w N) = 0$$

In deriving formula (2.10) it was assumed that  $\varphi_k = 0$ . It is easy to see that without this assumption equation (2.13) will not contain the shown functions. As in the case of a purely elastic material, influence of function  $\varphi_k$  insignificant; it determines the distinction in setting boundary conditions along the edge of the shell, and therefore in the absence of external torques it is possible not to consider them. Thus, we arrive at two resolving equations of equilibrium (1.14) and (2.13), formulated with respect to functions  $F$  and  $\chi$ , and one auxiliary equation (2.8). Here in formulas (2.8) and (2.13) small terms containing function  $F$  were disregarded, and during calculation of tangential forces  $N_{ij}$  - small terms containing function  $\chi$  (it is considered that these terms reflect the influence of a certain part of tangential forces perceivable by fillers on bend of shell).

Equations (1.14), (2.13), (2.8) permit investigating finite bending of multilayer thin shells from linear viscoelastic material with an arbitrary number of layers and arbitrary alternating of carrier layers and fillers. During investigation of oscillations of such shells instead of  $q$  it is necessary to introduce the quantity

$$q = q_0 + \left( \sum_{k=1}^n \rho_k h_k \right) \frac{\partial^2 w}{\partial t^2}$$

where  $\rho_k$  - specific density of material of  $k$ -th layer.

§ 4. Boundary conditions. We will base ourselves on system (1.14), (2.13) with respect to force function  $F$  and function of displacements  $\chi$ . Let us write out the basic boundary conditions.

1. Edge  $x_1 = x_1^0$  is freely supported:  $w = H_{11}^1 = \dots = H_{11}^{p+1} = 0$ , or

$$\chi = 0, \nabla^2 \chi = 0, \nabla^2 \nabla^2 \chi = 0, \underbrace{\nabla^2 \nabla^2 \dots \nabla^2}_{p+1} \chi = 0$$

2. Edge  $x_1 = x_1^0$  is pinched:  $w = w_{,1} = a^1 = \dots = a^p = 0$ , or

$$\left[ \sum_{n=0}^p (h^n \nabla^n) w_n \right] \chi = 0, \chi_{,1} = (\nabla^2 \chi)_{,1} = (\nabla^2 \nabla^2 \chi)_{,1} \dots = \underbrace{(\nabla^2 \nabla^2 \dots \nabla^2 \chi)_{,1}}_p = 0$$

3. Edge is free from bonds:  $H_{11}^1, \dots, H_{11}^{p+1} = 0, \sum_{k=1}^p Q_k^1 = 0$  or

$$\left(\frac{\partial^2}{\partial x_1^2} + \nu \frac{\partial^2}{\partial x_2^2}\right) \chi = 0, \quad \left(\frac{\partial^2}{\partial x_1^2} + \nu \frac{\partial^2}{\partial x_2^2}\right) \frac{(\nabla^2 \dots \nabla^2) \chi}{p} = 0$$

$$\left(\frac{\partial^2}{\partial x_1^2} + \nu \frac{\partial^2}{\partial x_2^2}\right) \nabla^2 \chi = 0, \quad \left[\frac{\partial^2}{\partial x_1^2} + (2 - \nu_0) \frac{\partial^2}{\partial x_1 \partial x_2}\right] \left[\sum_{n=0}^p \eta_{1n} (\nabla^2 h^n) \chi\right] = 0$$

coefficients  $\nu_0$  and  $\eta_{1n}$  have to be calculated for every specific type of shell on the basis of formulas (2.2).

Boundary conditions for force function  $F$  do not differ from corresponding boundary conditions of uniform elastic shells. Thus, for instance, if on edge  $x_1 = x_1^0$  tangential forces  $N_{11}$  and deformation  $\epsilon_{22}$  are absent, boundary conditions for  $F$  will be  $F = 0, \nabla^2 F = 0$ .

Other cases of boundary conditions are analogously formulated.

Submitted  
18 April 1964

#### Literature

1. A. Föppl. Vorlesungen über technische Mechanik. München Oldenburg Verlag, 1907, Bd. 5, S. 132.
2. K. Marguerre. Zur Theorie gekrümmten Platte grosser Formänderung. Jahrbuch 1939 der deutschen Akademie der Luftfahrtforschung I, 413-418. Proceedings of the fifth International congress of Applied Mechanics. Cambridge, Massachusetts, September 12-16, 1938. John Wiley and Sons, inc, New York, London: Chapman and Hall, Ltd. 93-101, 1939.
3. E. I. Grigolyuk. Finite bending of three-layered shells with hard filler. News AS USSR, OTN, 1963, No. 1, p. 26.
4. E. I. Grigolyuk and P. P. Chulkov. The general theory of three-layered shells of large bending. Reports of Academy of Sciences of USSR, 1963, Vol. 150, No. 5, p. 1012.
5. E. I. Grigolyuk and P. P. Chulkov. General theory of elastic three-layered shells of large bending. Collection. "Questions of dynamics and strength," Academy of Sciences LatvSSR, Riga, Issue 10, 1963, p. 95.
6. A. Yildiz. On the damping of a multilayer plate. J. Acoust. Soc. America, 1962, Vol. 34, No. 3, p. 353.
7. E. M. Kerwin Jr. Damping of flexural waves by constrained viscoelastic layer. J. Acoust. Soc. America, 1959, Vol. 31, No. 7, p. 952.
8. M. P. Bieniek and A. M. Freudenthal. Forced vibration of cylindrical sandwich shells. J. Aerospace Sci. 1962, Vol. 29, No. 2, p. 180.
9. A. A. Nikishin and A. L. Rabinovich. Certain problems of cylindrical

bend of three-layered plates taking into account high-elastic deformation of sheathing from glass plastics. Reports of Academy of Sciences of USSR, 1963, Vol. 151, No. 3, p. 528.

# DEPENDENCE OF DIMENSIONS OF CRATER ON HARDNESS OF TARGET

Yu. I. Fadeyenko

(Novosibirsk)

Literature on high-speed impact abounds in attempts to connect dimensions of crater in a half-plastic target with mechanical parameters of target and striker. Strength of material of target usually is characterized by hardness  $H$ , measured in static conditions according to method of Brinell. Thus, Eykhel'berger and Gering [1] proposed for determination of volume of crater  $V$  the formula

$$V = \frac{E \cos \alpha}{2.62H} \quad (1)$$

Here  $E$  - kinetic energy of striker,  $\alpha$  - angle of incidence of striker on target.

Fuks [2], based on simplified ideas about mechanism of flow after impact, derived a formula for depth of crater  $h$ . When the striker is a sphere of radius  $r$  with density  $\rho_0$ , it takes the form

$$h = 4r \left( \frac{\rho_0}{\rho} \right) \left[ \ln \left( 1 + v \sqrt{\frac{\rho}{3H}} \right) - \frac{v}{v + \sqrt{3H/\rho}} \right] \quad (2)$$

Here  $v$  - speed of striker,  $\rho$  - density of target. One more variant of logarithmic formula was offered by German and Jones, who made the most full treatment of accumulated experimental data by high-speed impact. The formula of German-Jones for a spherical striker takes the form

**BLANK PAGE**

$$\lambda = 1.2 \left( \frac{\rho_0}{\rho} \right)^{1/2} r \ln \left[ 1 + \frac{\rho_0^{1/2} p^{1/2} r^2}{4H} \right] \quad (3)$$

Results of German and Jones, as the most reliable available, were used by Whipple in his last attempt [3] at reconsideration of appraisals of meteoric danger.

Table

	$\frac{kg}{mm^2}$	p. $\mu$	d. $\mu$		$\frac{kg}{mm^2}$	p. $\mu$	d. $\mu$
st. 3	107	228	474	U 10	261	201	413
	127	228	463		268	193	415
38 K-A	167	224	425		284	194	408
	168	211	438		288	186	397
	211	199	418		292	182	400
	407	176	384		381	173	401
	425	197	396		635	159	391
st. 45	200	208	426	AD 1	21	625	654
	316	162	392	AD 3	43	555	558
	333	159	370	D 16	68	539	548
	414	181	388		76	504	541
	456	178	375		81	520	539
	480	156	381		82	526	558
	483	171	362		84	529	514
	564	165	394		100	525	526
U 8	117	214	434		108	501	515
	387	171	383		116	491	502
	428	155	382		130	479	484
	530	170	385				
	617	154	400				

Time of forming the crater is usually several orders less than time of Brinell test of material on hardness, therefore groundless use of static magnitude H for characteristic of dynamic properties of material can lead to essential errors.

Authors of given formulas as a foundation refer to results of experiments, affirming that "calculations are well correlated with experiment." It was interesting to check these affirmations and to estimate reliability probability of corresponding calculations. This work considered this target along with direct determination of influence of H on dimensions of crater.

A series of experiments was conducted in each of which a certain quantity of Nichrome balls  $160 \pm 5 \mu$  in diameter were accelerated by products of explosion to a speed of  $4050 \pm 180$  m/sec and arrived at the target from the investigated material. Experiments were conducted in vacuum, in order to avoid deceleration of particles by air. Dimensions of targets made it possible to consider them infinitely large. Conditions of acceleration were kept constant, so that speed

and dimensions of particles did not change from experiment to experiment. On every target a section containing 20-25 craters was chosen for measurements; depth  $h$  and diameter  $d$  of craters were measured with respect to level of initial surface, values of  $h$  and  $d$  then were averaged for a given sample. Presence in crater of fragments of striker could be disregarded since, according to [4], in the crater remains 3-8% material of striker, which changes volume of crater not more than 1.5%.

Several aluminum alloys and steel were investigated. Change of hardness in wide limits was attained by heat treatment (hardening with subsequent tempering).

Results of experiments for different materials of target are given in the table and are depicted on Figs. 1, 2.

On Fig. 1 are plotted depth  $h$  (light points) and diameters  $d$  (dark points) of craters in steel targets; on Fig. 2 is plotted depth of craters in targets from aluminum alloys.

Calculations by the formulas (2), (3) gave evidently oversized values of depths. It turned out, however, that if values of depths calculated by (2) are multiplied by correction factor  $2/3$ , and those calculated by (3) are multiplied by  $3/4$ , fair agreement with experiment is obtained. Calculated graphics corrected thus are plotted on Figs. 1, 2 with designations 2 (Fuks) and 3 (German-Jones).

For comparison of obtained data with (1) it was assumed that volume of crater is

$$V = \frac{1}{6}\pi d^2 h$$

Further, from experiment was determined

$$z = E/VH$$

which, according to [1], for normal impact should be constant and equal 2.62.

On Fig. 3 are depicted experimental dependencies  $x(H)$  for steel (dark points) and

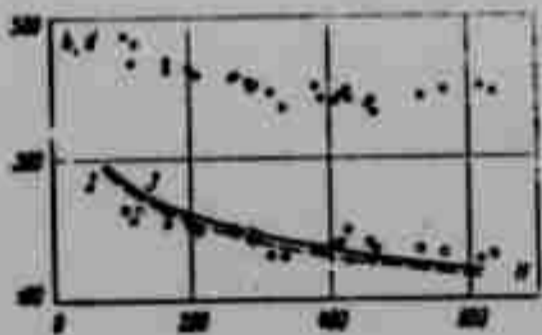


Fig. 1.



Fig. 2.

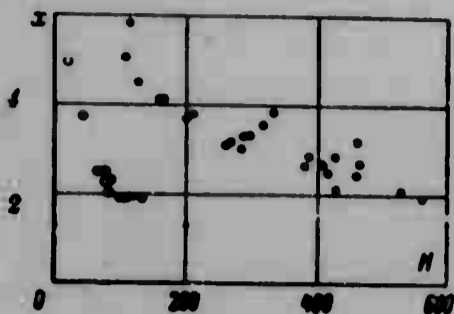


Fig. 3.

aluminum alloys (light points).

Causes of divergence of obtained data with that calculated by (2) and (3) are vague. Here could show, for instance, a scale effect (distinction in dimensions of particles by 1-2 orders) and possible decrease of mass of particles during acceleration.

Submitted  
13 May 1964

#### Literature

1. Eykhel'berger and Gering. Influence of collisions with meteoric bodies on spacecraft. Rocket technology, 1962, No. 10.
2. Fuks. Phenomena under impact. Rocket technology and cosmonautics, 1963, Vol. 1, No. 9.
3. F. L. Whipple. On Meteoroids and Penetration. J. O. Astronaut. Sci., 1963, Vol. 10, No. 3.
4. R. F. Rolsten and R. A. Schmitt. Hypervelocity Impact of Radioactive Projectiles into Stainless Steel and Aluminum. J. Appl. Phys., 1963, Vol. 34, No. 10.

# SIMILARITY OF SURFACE WAVES DURING EXPLOSIONS IN THE GROUND

S. S. Grigoryan

(Moscow)

In [1] are discussed results of experimental study of surface waves formed near the epicenter of shallow sunken explosion in clay ground, and an attempt is made to give with the help of analysis of experimental data generalized empirical relationships, founded on considerations of theory of dimension and similarity. The initial section of surface wave (environment of first entry of seismogram) is subjected to detailed consideration.

The basic qualitative result is that near the epicenter of the explosion maximum velocities of particles of the surface of the ground for a shown section of the seismogram are attained during intervals of time an order smaller than corresponding intervals of time for maximum displacements: a rapidly spreading compressional wave generates an initial field of speeds without noticeable displacements and essentially disturbs the bond between particles of ground; after that particle will accomplish motion, determined basically by action of gravity, which leads to comparatively slow further development of motion. The circumstance that does not influence gravity initial field of speeds is confirmed by the presence of geometric similarity in distribution of maximum speeds along surface of ground, i.e., existence of an empirical relationship

$$u = u_0 \left( \frac{r}{r_0} \right) = u_0 \left( \frac{r}{C^2 t} \right) = K \left( \frac{C^2 t}{r} \right)^2 \quad (1)$$

where  $u_0$  - constant of dimension of speed,  $r_0$  - characteristic dimension of charge,  $C$  - its weight,  $K$  - measured constant,  $n$  - dimensionless constant (see (1), Fig. 4).

However, further conclusions from revealed fact, analysis, and form of presentation of results with respect to maximum displacements  $a$  and intervals of time  $\tau_2$ , during which these displacements are attained are made in [1] incorrectly.

The purpose of this piece is removal of these inaccuracies.

Since gravity does not influence creation of initial field of speeds, on the basis of considerations of dimensional analysis it is possible to write the following expression for distribution of maximum velocities of particles along surface of ground:

$$u = \sqrt{\rho_0 / \rho_0} f(r/r_0, \sigma_0 / p_0, h/r_0) \quad (2)$$

Here  $\rho_0$  - initial density of ground,  $\sigma_0$  - constant of dimension of stress, characterizing elastic and strength properties of ground,  $p_0$  - initial pressure of products of explosion,  $r_0$  - characteristic dimension of charge of VV (explosive),  $h$  - depth of laying of charge. Form of function  $f$  depends on the ground in which explosion occurs and from what VV the charge is made. For the case considered in [1], this function has form (1). Inasmuch as in experiments medium and VV almost did not change, and during change  $C$  of depth of laying changed so that ratio  $h/C^{1/3}$  or which is the same,  $h/r_0$  remained constant; in formula (2) first is a unique variable argument of the function, and the formula can be written in form (1).

After passage of shock waves along ground and appearance of field of speeds

$$v_0 = \sqrt{\rho_0 / \rho_0} V(z/r_0, r/r_0) = v_0 V(z/r_0, r/r_0) \quad (3)$$

slower motion of medium begins. For particles located near surface of ground ( $z/r_0 \sim 0$ ) near the epicenter this motion basically is determined by action of gravity, whereas for more remote regions gravity does not render essential influence on subsequent motion. System of determining parameters for this second stage of motion, obviously, will be

$$v_0 = \sqrt{\rho_0 / \rho_0} r_0 g, \sigma_0, \rho_0, z, r, t \quad (4)$$

Therefore for distribution, for instance of maximum displacements of points of surface  $a$  and times of achievement of these displacements  $\tau_2$  it is possible to

write, using considerations of dimensional analysis, the relationships

$$a = \frac{v_0^2}{g} F_a \left( \frac{r}{r_0}, \frac{v_0^2}{r_0 g}, \frac{v_0^2}{g} \right), \quad \tau_2 = \frac{v_0}{g} F_\tau \left( \frac{r}{r_0}, \frac{v_0^2}{r_0 g}, \frac{v_0^2}{g} \right) \quad (5)$$

In virtue of determination  $v_0$  the last argument in (5) during change of dimensions of phenomenon ( $r_0$ ) does not change, therefore formulas (5) have the form

$$a = \frac{v_0^2}{g} F_a \left( \frac{r}{r_0}, \frac{r_0^3}{r_0 g} \right), \quad \tau_2 = \frac{v_0}{g} F_\tau \left( \frac{r}{r_0}, \frac{r_0^3}{r_0 g} \right) \quad (6)$$

Acceptance of the assumption that in the near zone strength and elasticity properties are immaterial means that particles move, almost not interacting, and

from this it follows that in formulas of (6)  $r_0$  should enter only in combination  $r/r_0$ , i.e., that character of dependence of  $a$  and  $\tau_2$  on  $r$  and  $r_0$  is the same as in (1)-(3). This means that in formulas (6) the second argument is immaterial, i.e., that they have the form

$$a = \frac{v_0^2}{g} f_a \left( \frac{r}{r_0} \right), \quad \tau_2 = \frac{v_0}{g} f_\tau \left( \frac{r}{r_0} \right) \quad (7)$$

If one were to now cross in these formulas from  $r_0$  to  $C^{1/3}$ , then they will have the form

$$a = \frac{v_0^2}{g} \varphi_a \left( \frac{r}{C^{1/3}} \right), \quad \tau_2 = \frac{v_0}{g} \varphi_\tau \left( \frac{r}{C^{1/3}} \right) \quad (8)$$

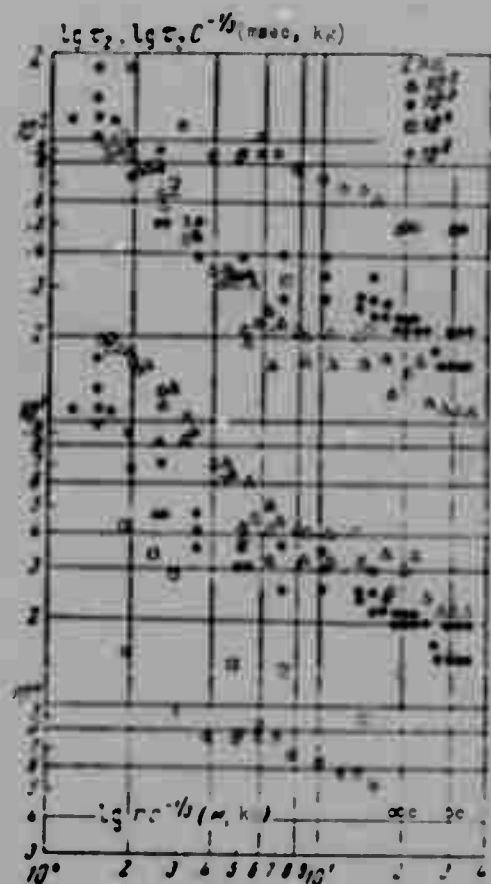


Fig. 1.

On page 98 of [1] are presented formulas

for  $a$  for two cases — during "modeling according to Froude"

$$\frac{a}{C^{1/3}} = K \left( \frac{C^{1/3}}{r} \right)^{2.5}, \quad K = \text{const} \quad (9)$$

and during "geometric modeling"

$$\frac{a}{C^{1/3}} = K \left( \frac{C^{1/3}}{r} \right)^{2.5}, \quad K = \text{const} \quad (10)$$

On page 97 of [1] is Fig. 6, on which is depicted the dependence of  $\tau_2$  on  $r$  (experimental data), built in variables  $\lg(\tau_2 C^{-1/3})$ ,  $\lg(r C^{-1/3})$  for the case of "modeling according to Froude" and in variables  $\lg(\tau_2 C^{-1/3})$ ,  $\lg(r C^{-1/3})$  for "geometric modeling," i.e., graph of relationships for  $\tau_2$ , taken in the form

$$\tau_2 C^{-1/3} = f_1(r C^{-1/3}), \quad \tau_2 C^{-1/3} = f_2(r C^{-1/3}) \quad (11)$$

for two cases correspondingly. It is clear that formulas (9)-(11) differ from formulas (8).

Despite the fact that the basic force affecting the considered motion will be gravity, formulas for treatment and representation of results of experiments cannot have form (9) for  $a$  and the first of (11) for  $\tau_2$ .

Correct formulas have form (8).

In order to reconstruct the graph on Fig. 6 from [1], corresponding to second formula of (11) in correct variables, i.e., to cross from variables

$$y = \lg(\tau_2 C^{-1/3}), \quad z = \lg(r C^{-1/3})$$

to variables,

$$y_1 = \lg \tau_2, \quad z_1 = \lg(r C^{-1/3}) = z$$

corresponding to formula (8), it is necessary, keeping the abscissa of all points of the graph constant, to add to ordinates quantities  $1/3 \lg C$ , since

$$y_1 = y + 1/3 \lg C$$

On the graph of Fig. 6 in [1] are presented points for the values  $C = 10^2$ ,  $10^3$ ,  $10^4$ ,  $10^6$ . Therefore to ordinates it is necessary to add the numbers  $2/3$ ,  $1$ ,  $4/3$ ,  $2$ .

We cite the result of such re-formation on Fig. 1 (upper points) together with data of Fig. 6b from [1], with respect to which this re-formation is carried out.

In [1] on p. 95 (Fig. 5) are also data for the dependence of  $a$  on  $r$  in variables  $y = \lg a$ ,  $x = \lg r$ .

In accordance with the first of formulas (8) these data should be plotted on the graph in variables

$$y_1 = \lg a = y, \quad z_1 = \lg(r C^{-1/3}) = z - 1/3 \lg C$$

i.e., from abscissas of points for values  $C = 10^2, 10^3, 10^4, 10^6$  to add the numbers  $2/3, 1, 4/2, 2$ . Results of such re-formation of Fig. 5 from [1] are shown on Fig. 2 and, for comparison, on Fig. 3 we reproduce Fig. 5 from [1].



Fig. 2.

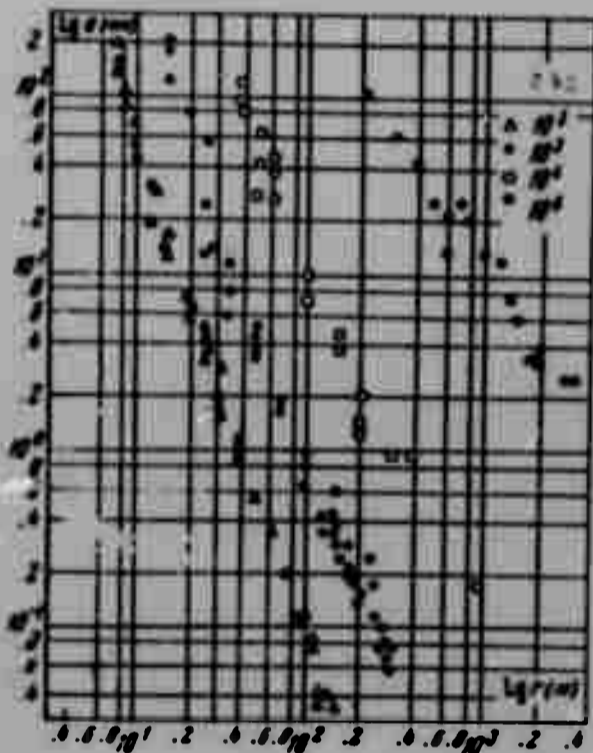


Fig. 3.

From Figs. 1 and 2 it is clear that, indeed, at close distances from epicenter experimental data for various values  $C$  are well described by a single relationship of form (8). As on Fig. 1, so also on Fig. 2 from the general graph for all values  $C$  graph fall points corresponding to the value  $C = 10^6$ . On Fig. 4 from [1] for dependence (1) points for  $C = 10^6$  also fall from the general graph, while on the same side as on Figs. 1 and 2 of the given note. All this indicates that, apparently, the conditions of carrying out the experiment for  $C = 10^6$  differed from conditions for other values of  $C$  — either there were essentially different ground conditions, or the value of  $h/r_0$  for  $C = 10^6$  differed from the corresponding value required by conditions of geometric similarity.

It is possible still to note that the numbers along the axis of abscissas on Fig. 5 from [1], apparently are placed incorrectly, since during recalculation of them to Fig. 2 the same values as on the axis of abscissas of Figs. 4, 6 from [1] must be obtained, which does not occur, there is a difference of one order. For this reason we cite Fig. 5 from [1] and the result of its re-formation with the axis of abscissas displaced one order to the left (see Figs. 3 and 2).

In conclusion one should note that reasoning and conclusions given at the end of [1] with respect to influence at large distances of viscous forces do not follow from experimental data given in [1], since these data, as can be seen from Figs. 1 and 2, are well described by the diagram in which the initial phase of motion is determined by the action of only elastic and strength forces in the medium, and the subsequent — by the action of only gravity. Therefore these conclusions are impossible to consider substantiated.

Submitted  
19 June 1964

#### Literature

1. B. G. Rulev. Similarity of compressional waves during explosions in the ground. PMTF, 1963, No. 3.

## APPROXIMATE EQUATION OF STATE OF SOLID BODIES

V. P. Koryavov

(Moscow)

In the given article assuming accuracy for a solid body of the equation of Mie-Grüneisen with the use of known shock adiabats, a simple approximate construction is conducted of functions entering in the equation of Mie-Grüneisen, useful in particular, for description of the state of a substance compressed in strong shock waves.

For many solid bodies shock adiabats experimentally were obtained [1-10]. The most striking fact following from all measurements is that between speed of shock wave  $D$  and speed of substance after front  $u$ , which in many cases are directly measured linear dependence of form is rather well observed

$$D = D_0 + su \quad (1)$$

Here  $D_0$  and  $s$  — constants.

If such relationship was observed for any compression of a substance, including when  $u \rightarrow 0$ , then  $D_0$  would be the so-called Bridgeman speed of sound  $C_B$ , which is calculated with respect to compressibility  $\kappa$

$$\kappa = -\frac{1}{V} \left( \frac{\partial V}{\partial p} \right)_s, \quad C_B^2 = \frac{1}{\rho \kappa}$$

For the future it is convenient to use dimensionless values: density  $\sigma$ , in reference to initial density  $\rho_0$ , pressure  $p$ , in reference to  $\rho_0 D_0^2$ , energy  $E$ , in

reference to  $D_0^2$ , speeds  $D$  and  $u$ , in reference to  $D_0$ . From relationship (1) and conditions of preservation on front of shock wave it is easy to obtain

$$\Delta P_n = \frac{\sigma(\sigma-1)}{[\sigma - (\sigma-1)\sigma]^2} \quad (2)$$

$$\Delta E_n = \frac{1}{2} \left[ \frac{s-1}{s-(s-1)s} \right]^2 \left( 1 + \frac{2p_0}{\Delta p_n} \right) \quad (3)$$

Here  $p_0$  - pressure before front,  $\Delta p_H$  and  $\Delta E$  - changes of pressure and energy on front of shock wave. It is obvious that, if relationship (1) is executed up to very large pressures, compression of substance tends to limit  $\sigma_s = s / (s - 1)$ . Experimental measurements (for instance, [9]) show that for different substances  $s$  does not strongly deviate from 1.5, and  $D_0$  is close to  $C_B$ , measured by Bridgeman (or according to other data). The less  $s$  differs from 1.5, and  $D_0$  from  $C_B$ , the better all measurements lie on the dependence

$$D = 1 + 1.5u \quad (4)$$

On Fig. 1 are given experimental points for different substances, taken from [1-10] (different designations on Fig. 1 are used only when a group of points

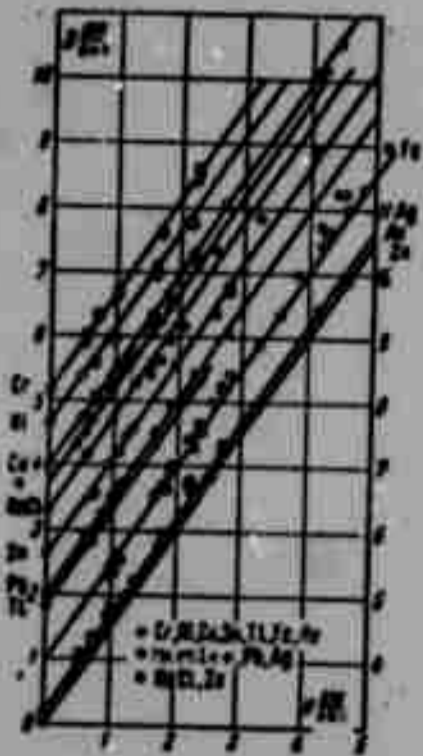


Fig. 1.

belonging to different substances is insufficiently clearly divided). It is clear that for many substances dependence (4) rather well describes experimental points. It is the most probable (at least, in certain range of pressures) also for substances for which we still have no data, although the last measurements at pressures near 9 megabar show that apparently, for certain substances, with increase of pressures deviations from dependence (4) will be increased.

Use of a linear D-u-dependence (1) leads to the simple dependence  $\Delta p_n = u(1 + su)$ . It is clear that when  $\Delta s = s - s_0 \leq s_0 + 1/u$  it is possible to disregard the dependence of  $\Delta p_n$  on  $s$ . This gives an explanation and establishes a boundary of applicability of the "universal" dependence of  $\Delta p_n$  on  $u$ , which

was indicated in [12]. For the connection of  $\Delta p_n$  with  $\sigma$  from D - u-dependence

formula (2) is obtained, which, in distinction from exponential formulas utilized in [12], leads to limiting compression which is necessary with respect to physical considerations.

Knowledge of shock adiabat of substance, for instance, in the form of (1) or (4), under certain additional assumptions permits composing full thermodynamic description of behavior of substance during hydrostatic stress. It is fully natural for solid bodies, during whose compression an essential role is played by rigidity of crystal lattice, to divide energy and pressure into a thermal part and a so-called cold part ( $E_x$ ,  $p_x$ ), connected with deformation of crystal lattice and identical at any temperature, including absolute zero. An equation of form (see [1, 7, 8, 11])

$$\frac{P - P_x}{E - E_x} = \gamma \quad (5)$$

establishing a connection between thermal parts of pressure and energy, is known as an Mie-Grüneisen or Debye equation. The coefficient of Grüneisen  $\gamma$  is sometimes considered constant, and sometimes a function of only density, sometimes depending still on temperature [5]. Since  $p_x$  and  $E_x$  are taken on an isotherm of absolute zero, between them exists the connection

$$dE_x + p_x dV = 0 \quad (V = 1/\sigma) \quad (6)$$

Knowledge of function  $\gamma(\sigma)$  and the relationship  $p$ ,  $\sigma$  and  $E$  along certain curve, for instance, shock adiabat, permits finding functions  $p_x$  and  $E_x$ , as is done in [1-4, 7-9].

Using equation (5), which should hold also along Hugoniot adiabat, equation (6) and equation (2) and (3), in which it is possible to disregard initial pressure and initial internal energy of undisturbed substance (see, for instance, [11], pp. 505 and 508), we arrive at system

$$\frac{P_n - P_x}{E_n - E_x} = \gamma, \quad p_x = \sigma^2 \frac{dE_x}{d\sigma}, \quad P_n = \frac{\sigma(\sigma - 1)}{[s - (s - 1)\sigma]^2}, \quad E_n = \frac{1}{2} \left[ \frac{\sigma - 1}{s - (s - 1)\sigma} \right]^2 \quad (7)$$

The first two equations of the system give the linear equation

$$\frac{dE_x}{d\sigma} - \frac{\gamma}{\sigma} E_x = \frac{P_n}{\sigma^2} - \frac{\gamma}{\sigma} E_n \quad (8)$$

Its solution has the form

$$E_x = \exp\left(\int \frac{\gamma}{\sigma} d\sigma\right) \int \left(\frac{P_n}{\sigma^3} - \frac{\gamma}{\sigma} E_n\right) \exp\left(-\int \frac{\gamma}{\sigma} d\sigma\right) d\sigma \quad (9)$$

For constant  $\gamma$  we obtain

$$E_x = \sigma^\gamma \int \frac{(\sigma-1) [1 - 1/2 \gamma (\sigma-1)]}{\sigma^{\gamma+1} [s - (s-1) \sigma]^2} d\sigma \quad (10)$$

This integral is easily taken when  $s = 1.5$  and  $\gamma$  equals 1 ( $E_{x1}$ ) or 2 ( $E_{x2}$ )

$$E_{x1} = \frac{4}{27} \sigma^3 \left[ \ln \frac{2\sigma}{3-\sigma} - \frac{2}{3-\sigma} + \frac{3}{\sigma^2} - \frac{5}{\sigma} + 3 \right] \quad (11)$$

$$E_{x2} = \frac{4}{9} \sigma \left[ \ln \frac{2\sigma}{3-\sigma} + \frac{3}{2\sigma} - \frac{3}{2} \right] \quad (12)$$

On Fig. 2 are shown dependencies (11) and (12). For comparison in the same place is given  $E_n$ . Behavior of (11) and (12) near  $\sigma = 1$  is determined by expansions along  $\delta = \sigma - 1$ :

$$E_{x1} = \frac{1}{2} \delta^2 + \frac{1}{16} \delta^4 + \dots, \quad E_{x2} = \frac{1}{2} \delta^2 - \frac{1}{16} \delta^4 + \dots$$

With increase of  $\sigma$  the quantity  $E_{x1}$  monotonically increases to  $+\infty$  (when  $\sigma = 3$ ), and  $E_{x2}$ , attaining maximum, tends to  $-\infty$  (when  $\sigma = 3$ ). Such behavior of  $E_x$  near  $\sigma_*$  is connected with a feature of the right side of equation (8) in this point. By



Fig. 2.

the form of this feature  $(2/\gamma + 1 - \sigma)/(\sigma_* - \sigma)^2$  it may be concluded that in the framework of accepted assumptions (linearity D-u-diagram and accuracy of equation of Mie-Grüneisen) no constant  $\gamma$  can ensure finiteness of  $E_x$  during limiting  $\sigma$ , although for constant  $\gamma$  of the order of infinity  $E_x$  is always lower than  $E_n$ . It would be easy to select function  $\gamma(\sigma)$ , ensuring boundedness of  $E_x$  for any finite  $\sigma$ .

Such a function will be dealt with somewhat after other considerations.

It is known [5, 10, 11] that  $\gamma$  is not constant, although it does not change strongly. If one were to assume fulfillment of (1) and (5) up to very large pressures, then limiting  $\gamma$  can be found. During compression in strong shock waves and subsequent adiabatic expansion, starting from certain compressions, thermal

parts of pressure and energy strongly exceed  $p_x$  and  $E_x$ . Therefore

$$\gamma_0 = \frac{p_n - p_x}{\sigma(E_n - E_x)} \approx \frac{p_n}{\sigma_0 E_n} = \frac{2}{\sigma_0 - 1}$$

Above it was found that  $\sigma_0 = s / (s - 1)$ , hence

$$\gamma_0 = 2(s - 1) \quad (13)$$

(for comparison let us remember that for initial  $\gamma$  when  $\sigma = 1$  from the relationship of Dugdal-MacDonald we obtain  $\gamma_D = 2s - 1$ ). From the above follows the fact that for phenomena in shock waves it is sufficient to determine functions  $p_x$  and  $E_x$  as accurately as possible only up to average compressions, since for large compressions their role in equation (5) is immaterial.

Equation (8) is easily integrated assuming smallness  $\delta = \sigma - 1$ . Here  $\gamma$  is presented in the form of a series in  $\delta$ . Integration gives

$$E_x = \frac{\delta^2}{2} + \left(\frac{3-a}{a-1}\right) \frac{\delta^3}{3} + \left[\frac{3}{(a-1)^2} - \frac{3-a}{a-1} \left(1 + \frac{\gamma_0}{6}\right) - \frac{\gamma_0}{2}\right] \frac{\delta^4}{4} + \dots \quad (14)$$

Here  $a = s / (s - 1)$ . For comparison we will give the expansion  $E_n$

$$E_n = \frac{\delta^2}{2} + \frac{\delta^3}{a-1} + \frac{3\delta^4}{2(a-1)^2} + \dots$$

When  $s = 1.5$  ( $a = 3$ ) (14) has the form

$$E_x = \frac{1}{2}\delta^2 + \left(\frac{2}{3} - \frac{1}{2}\gamma_0\right) \frac{1}{4}\delta^4 + \dots \quad (15)$$

It is possible to note immediately that constant  $\gamma_0$  from expansion of  $\gamma$  in  $\delta$  entered only in coefficient when  $\delta^4$ , i.e.,  $\gamma$  starts to play role in the expression for  $E_x$  only when  $\delta$  is sufficiently close to 1 ( $\sigma = 2$ ). If we wanted to replace  $\gamma$  (in the expression for elastic energy) by a certain constant, then the most suitable constant obviously would be  $\gamma$  in the region where influence  $\gamma$  (on shown expression) will be the biggest. In connection with the above the role of  $\gamma$  in the expression for elastic energy is essential for average compressions (during large compressions, as already was noted, the actual elastic component is immaterial). For a number of substances  $\gamma$  changes approximately between 2 and 1, and the average magnitude therefore is 1.5. If also  $s = 1.5$  (or close to 1.5), then, as can be seen from

(15),  $E_x$  is very well (accurate to small quantities of the fifth order) approximated in the following way:

$$E_x = \gamma \delta^2 = \frac{1}{2} (\sigma - 1)^2 \quad (16)$$

This expression can be taken as a basis for approximate constructions of the equation of state of substances with  $s$  close to 1.5. Dependence (16) is depicted on Fig. 2. In the table are given values of coefficients in expansion (14) for certain values of  $s$  and  $\gamma$ .

$s$	$a_1$	$a_2$	$a_3$		
			$\gamma_0 = 1.4$	$\gamma_0 = 1.5$	$\gamma_0 = 1.6$
1.4	0.5	-0.067	0.009	-0.005	-0.015
1.5	0.5	0	0.012	0	-0.012
1.6	0.5	0.067	0.033	0.02	0.007

With the help (6) and (14) we find

$$p_x = \delta + \frac{\alpha + 1}{\alpha - 1} \delta^2 + \left[ \frac{3}{(\alpha - 1)^2} + \frac{3 - \alpha}{(\alpha - 1)} \left( 1 - \frac{\gamma_0}{6} \right) - \frac{\gamma_0}{2} + 1 \right] \delta^3 + \dots \quad (17)$$

Let us give here the expansion for  $p_n$

$$p_n = \delta + \frac{\alpha + 1}{\alpha - 1} \delta^2 + \left[ \frac{3}{(\alpha - 1)^2} + \frac{2}{\alpha - 1} \right] \delta^3 + \dots$$

For  $s = 1.5$  ( $\alpha = 3$ )

$$p_x = \delta + 2\delta^2 + \frac{1}{6}(7 - 2\gamma_0) \delta^3 + \dots, \quad p_n = \delta + 2\delta^2 + \frac{7}{6} \delta^3 + \dots \quad (18)$$

In approximation (16) for  $p_x$  we obtain

$$p_x^2 = \sigma^2 (\sigma - 1) \quad (19)$$

In that same approximation for  $\gamma$  we obtain the following expression, which we find from exact satisfaction of (7) with the help (16)

$$\gamma = 2(4 - \sigma)/(5 - \sigma) \quad (20)$$

On Fig. 2 is represented this dependence. It is clear that for small and average compressions this is almost constant, close to 1.5, and for limiting

compressions it tends to limiting  $\gamma$ . Thus uncontradictorily and with good approximation are constructed all functions entering in equation (5). (The written formulas permit calculating  $\gamma(\sigma)$  also for  $s \neq 1.5$ .)

It is especially necessary to say something on the region of rarefaction. Unfortunately, for the region of rarefaction we do not have an experimental dependence similar to the shock adiabat. It is possible to propose the following approximate representation (interpolation) functions of cold compression. Let us assume that for small extensions elastic energy has the same form as compression and then tends to energy of sublimation. The assuming (16) it is possible to consider for  $\sigma < 1$

$$E_x = \frac{1}{2}(\sigma - 1)^2 + (U - \frac{1}{2})(\sigma - 1)^4 \quad (21)$$

where  $U$  - energy of sublimation (belonging to  $D_0^2$ ). The fourth power in the second term is used only as a first approximation for satisfaction of above conditions. Under some additional conditions the power can be different (for instance, higher). For  $\gamma$  in region  $\sigma < 1$  an interpolation formula also can be written (for instance, polynomial), which in first approximation should satisfy when  $\sigma = 1$  continuities  $\gamma$  and  $d\gamma/d\sigma$  (in order not to change slope of isoentropy when  $\sigma = 1$ ) and transition into ideal gas when  $\sigma \rightarrow 0$ . Such dependence is depicted on Fig. 2 and is noted by Fig. 2, and Fig. 1 designates continuation of dependence (20).

The author thanks S. S. Grigoryan and Yu. P. Rayzer for useful discussion of the article.

Submitted  
23 April 1964

#### Literature

1. L. V. Al'tshuler, K. K. Krupnikov, B. N. Lednev, V. I. Zhuchikhin and M. I. Brazhnik. Dynamic compressibility and equation of state of iron at high pressures. Jour. experim. and theor. physics, 1958, Vol. 34, No. 4, p. 874.
2. L. V. Al'tshuler, K. K. Krupnikov and M. I. Brazhnik. Dynamic compressibility of metals at pressures from 400 thousand to 4 million atmospheres. Jour. experim. and theor. physics, 1958, Vol. 34, No. 4, p. 886.
3. L. V. Al'tshuler, S. B. Kormer, A. A. Bakanova and R. F. Trunin. Equations of state of aluminum, copper, and lead for the region of high pressures. Jour. experim. and theor. physics, 1960, Vol. 38, No. 3, p. 790.
4. L. V. Al'tshuler, L. V. Kuleshova and M. N. Pavlovskiy. Dynamic compressibility, equation of state, and electrical conductivity of NaCl at high

pressures. Jour. experim. and theor. physics, 1960, Vol. 39, No. 1(7), p. 16.

5. L. V. Al'tshuler, M. N. Pavlovskiy, L. V. Kuleshova and G. V. Simakov. Investigation of halides of alkali metals at high pressures and temperatures of shock compression. FTT, 1963, Vol. 5, No. 1.

6. A. N. Dremin and G. A. Adadurov. Shock adiabat of marble. Reports of Academy of Sciences of USSR, 1959, Vol. 128, No. 2, p. 261.

7. J. M. Walsh, M. H. Rice, R. G. McQueen and E. L. Garger. Shock-wave compressions of 27 metals. Equations of State of Metals. Phys. Rev., 1957, Vol. 108, No. 2.

8. M. H. Rice, R. G. McQueen and J. M. Walsh. Compression of Solids by strong Shock waves, Solid State Physics, 1958, Vol 6, p. 1.

9. R. G. McQueen and S. P. Marsh. Equation of State for 19 Metallic Elements from shock-wave measurements to two megabars. J. Appl. Phys., 1960, Vol. 31, No. 7.

10. Solids under Pressure, edited by W. Paul, D. M. Warschauer McGraw-Hill, N. Y. 1963.

11. Ya. B. Zel'dovich and Yu. P. Rayzer. Physics of shock waves and high-temperature hydrodynamic phenomena. Fizmatgiz, M., 1963.

12. V. M. Gogolev, V. G. Myrkin and G. I. Yablokova. Approximate equation of state of solid bodies. PMTF, 1963, No. 5, p. 93.

EXPERIMENTAL INVESTIGATION OF FLOW AROUND BLUNTED BODIES  
BY A FLAT FLOW OF A PLASTIC MEDIUM

I. G. Bulina, V. P. Myasnikov  
and V. G. Savin

(Moscow)

For the first time the problem about flow around blunted bodies by a flat flow of viscoplastic medium was experimentally investigated in [1]. It was revealed that ahead of the blunted body in this case, in distinction from viscous liquid, will be formed a stagnant region, moving as a solid whole together with it.

Theoretical research of the above problem was given in [2, 3].

Qualitatively streamline flow of a body, obtained both on the basis of theoretical representations and also on the basis of experimental data coincided well.

Results obtained in [1-3], made it possible to indicate certain qualitative peculiarities sharply distinguishing flow around blunted bodies by a flow of viscous-plastic medium from flow around these bodies by a viscous liquid. It was, for instance, shown that in certain conditions magnitude of the resisting force acting on the streamlined body will not depend on geometric peculiarities of the structure of its frontal part.

Experimental investigations conducted earlier carried a qualitative character. Therefore it was very interesting to conduct a more detailed experimental investigation and to obtain such data which would allow a more thorough comparison of theory with experiment and confirmation of the above qualitative effects on the

basis of measurements.

§ 1. Let us assume that the body moves in an infinite viscous-plastic medium with constant speed, and flow of medium is flat.

Streamline flow of body of viscous-plastic liquid when speeds are small and under the condition that  $S_l \gg 1$ , will be very close to streamline flow of a body of ideally plastic medium. Influence of viscosity will show only in film near surface of body [2]. In this case for magnitude of tangential stress on surface of streamlined body we will have

$$\tau = \tau_0 + \eta \left( \frac{\partial u}{\partial y} \right)_{y=0} + O\left(\frac{1}{S_l}\right), \quad S_l = \frac{\tau_0 l}{\mu v} \quad (1.1)$$

Here  $\tau_0$  - yield point of medium,  $\eta$  - coefficient of viscosity,  $u$  - speed of particles of medium in boundary layer,  $S_l$  - parameter of Sen-Venan,  $v$  - speed of model,  $y$  - transverse coordinate in layer and  $l$  - length of body.

Passing to dimensionless variables, we will obtain

$$\tau = \tau_0 \left[ 1 + \frac{1}{\sqrt{S_l}} \left( \frac{\partial U}{\partial Y} \right)_{Y=0} \right] \quad \left( Y = \frac{y}{\delta}, \quad U = \frac{u}{v} \right) \quad (1.2)$$

( $\delta$  - thickness of boundary layer)

Resisting force acting on streamlined body (Fig. 1) can now be presented in the following way:

$$\Delta F = 2\Delta h \left[ \int_L P(x) \sin \alpha(x) dx + \int_L \eta \left( \frac{\partial u}{\partial y} \right)_{y=0} \cos \alpha(x) dx \right] \quad (1.3)$$

( $\Delta F = F_k - F_l, \quad \Delta h = h_k - h_l$ )

Here  $F_k$  - resisting force at depth of submersion of body  $h_k$ ,  $P_k$  - pressure of medium on surface of streamlined body,  $x$  - longitudinal coordinate in boundary layer. Integration is conducted over contour  $L$ , consisting of contour of streamlined body and stagnant region.

Putting now (1.2) in (1.3), we will obtain

$$C_x = 2 \frac{\tau_0 l}{\rho v^2} \left[ \lambda + \int_0^L P(\xi) \sin \alpha(\xi) d\xi + \frac{1}{\sqrt{S_l}} \int_0^L \left( \frac{\partial U}{\partial Y} \right)_{Y=0} \cos \alpha(\xi) d\xi \right] \quad (1.4)$$

( $\lambda = \frac{l+d}{l}, \quad x = l\xi, \quad C_x = \frac{\Delta E}{\rho v^2 l \Delta h}$ )

Here  $d$  — length of stagnant region,  $\alpha$  — angle between tangent to  $L$  and axis of symmetry of body,  $\rho$  — density of medium.

It is necessary to note that when integration is conducted over boundary of stagnant zone, it is necessary to assume [2, 3]

$$\frac{\partial U}{\partial Y} = 0 \quad \text{when } Y = 0 \quad (1.5)$$

Let us designate

$$\begin{aligned} K_1 &= 2 \left[ \lambda + \int_0^L P(\xi) \sin \alpha(\xi) d\xi \right] \\ K_2 &= 2 \int_0^L \left( \frac{\partial U}{\partial Y} \right)_{Y=0} \cos \alpha(\xi) d\xi \end{aligned} \quad (1.6)$$

Then from (1.4) follows

$$C_x = \frac{1}{R_e} (K_1 S_l + K_2 \sqrt{S_l}) \quad (1.7)$$

Coefficients  $K_1$  and  $K_2$  in (1.7) are certain functionals whose values are determined by peculiarities of geometric structure of body and conditions of flow in external ideally plastic flow. Independence of  $K_1$  and  $K_2$  from Reynolds number  $R_e = \rho v a / \mu$  is evident, inasmuch as in system of equations of motion of medium in external flow it enters the coefficient of viscosity, but there is independence of them from  $S_l$  in virtue of static definability of problem about flat flow of ideally plastic material and possibility of independent assignment of boundary conditions for speeds and stresses.

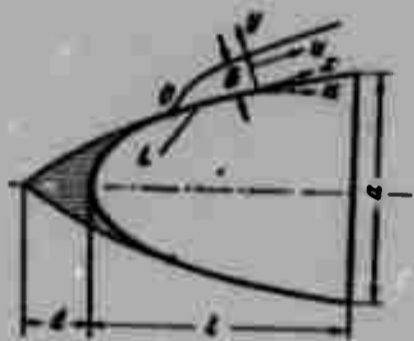


Fig. 1. Diagram of flow.

§ 2. Experiments in determination of resistance were carried out with the help of a special dynamometer on an improved installation, similar to that described earlier [1].

The installation consists of a tray with dimensions  $50 \times 25 \times 50$  cm (Fig. 2), above which at a height of 30 cm a cart moves along rails. In the center of the frame of the cart on a Spitzen scale is fixed a dynamometer, to which the tested models are rigidly fastened. The cart is put in motion by a dc electric motor

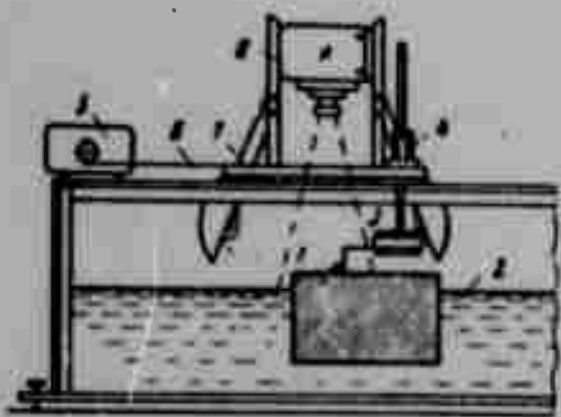


Fig. 2. Diagram of installation:  
1 - tested model, 2 - clay suspension, 3 - dynamometer, 4 - Spitzen scale, 5 - electric motor with reductor, 6 - rope, 7 - cart, 8 - movie camera, 9 - illuminating equipment.

through a reductor, on pulley of which is wound a cable secured at one end on the frame of the cart. Change of speed of cart is attained by replacement of pulleys by a reducing gear and change of number of turns of motor.

The installation permits drawing the models from 0.5 to 70 cm/sec, where sufficient uniformity of motion in the whole shown speed range is ensured. On cart are fastened also movie and photographing equipment, and illuminating instruments (tubes).

The dynamometer is fastened between two mobile frames. The first frame - support - is rigidly fastened to the Spitzen scale. The second frame - measuring - with the help of a bearing system with a great base easily shifts along the support frame only in a strictly horizontal direction. To the measuring frame is fastened the extended model. On the mobile end of the dynamometer spring is fixed the movable arm of the linear wire potentiometer, switched into the network of the self-recording instrument of type H-370-AM.

Speed of models was measured by a special electro-stop watch, which was switched on and turned off by travel micro-switches when the cart passed over a fixed range. Range was 150 cm.

Two series of experiments were conducted. In the first series influence of form of bodies on magnitude and form of stagnant zone was investigated and measurements of resisting force were conducted. Flow round cylinders, a wedge, and parallelepipeds was investigated. For all modes photography and comparison of dimensions and form of stagnant regions at identical speed was carried out, and resisting forces at different depths of submersion of models in a speed range from 5 to 50 cm/sec were also measured. Furthermore, was conducted investigation of flow around model whose frontal part had the form of the stagnant region formed on a wedge when it is drawn in a tray with the blunt section forward.

In the second series of experiments conformity of conditions of flow around models on installation to conditions of flat flow around was checked more thoroughly.

GRAPHIC NOT  
REPRODUCIBLE

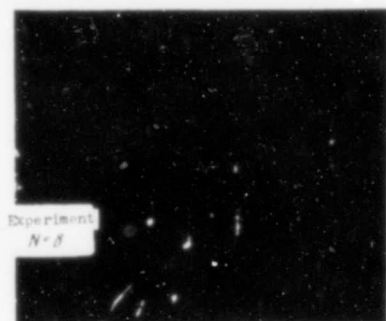


Fig. 3. Characteristic form of chalky lines on surface of suspension during motion of model in tray.

For this were used models having the form of right angle parallelepipeds, which were drawn along in the whole speed range shown above for five different depths of submersion. Influence of lateral walls of tray in both series of experiments was determined by means of drawing models similar in plan and photographing deformation of suspension surface with chalky lines perpendicular to walls of tray (Fig. 3) preliminarily drawn on it.

Form and dimensions of models are shown in the table. Investigations were conducted on

suspensions of gray clay. Density of suspension  $\rho$  changed from 1.39 to 1.64 g/cm<sup>3</sup>. For every value of density was constructed a rheological curve according to measurements on rotary viscosimeter PB-8, and standard method were determined corresponding values of coefficient of viscosity and limiting stress of shift. Method of treatment of experimental data was chosen on the basis of the following considerations.

In the general case of motion of a model in a tray its drag coefficient will depend on parameters

$$C_a = \Phi_1 \left( R_a, S_t, \frac{l}{a}, \frac{h}{a}, \frac{D}{a}, \frac{L}{a}, \frac{H}{a} \right) \quad (2.1)$$

where  $a$  — the biggest thickness of model,  $D$  — width of tray,  $L$  — its length and  $H$  — thickness of layer of suspension in tray.

Comparison of (2.1) with (1.7) shows that for possibility of comparison of theoretical and experimental results experiments could be conducted so that influence of the last four parameters in (2.1) was removed.

Independence of experimental data from  $D/a$  and  $L/a$  was controlled by results of drawing models geometrically similar in plan (table) in the tray.

In accordance with general ideas of flow around bodies of a viscoplastic medium, region of flow has bounding dimensions. Location of walls, limiting volume of viscoplastic medium, inside which is included the region of flow, does not influence magnitude of resistance of body, inasmuch as medium outside region of flow is in the hard state [2]. Therefore, to control independence of  $C_a$  from  $D/a$  and

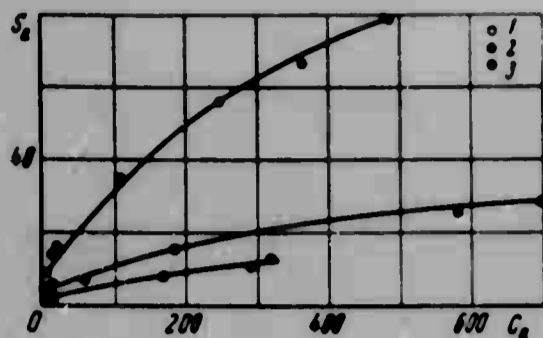


Fig. 4. Dependence of  $C_d$  on  $S_f$  for parallelepipeds:  
1 -  $l = 30.6$  cm; 2 -  $l = 11.0$  cm; 3 -  $l = 4.8$  cm.

L/a it is sufficient to photograph surface of suspension in tray and to establish that during motion of body chalky lines of grid near walls of tray remain practically undeformed (Fig. 3).

To remove the dependence of  $C_d$  on bottom and skin effect tests of every model were conducted at several different depths of submersion.

Difference in magnitudes of resisting forces, measured at two different depths of submersion of model and the same speed of its motion, for calculation of drag coefficient was divided by the product of dynamic pressure and increase of site of frontal section during change of depth of submersion. Thereby, dependence of results of experiments on depth of submersion of model was removed.

Graphs of the dependence of  $C_d$  on  $S_a$  (Figs. 4-7) were constructed by results of treatment of measurements. With respect to conditions of experiments, for every model in the process of experiments the product

$$R_a S_l = \frac{\rho v_0^2}{\eta} = \gamma \quad (2.2)$$

remained constant, so that relationship (2.1) could be represented in two equivalent forms

$$C_d = \frac{1}{\gamma} [K_1 S_l^2 + K_2 S_l^{1/2}] = \frac{\gamma^2}{R_a^2} [K_1 + K_2 \sqrt{\frac{R_a}{\gamma}}]$$

Solid lines on Figs. 4-7 are plotted on the basis of experimental data according to the method of least squares. The basic analytic dependence is chosen as in relationships (2.3). Empirical values of  $K_1$  and  $K_2$ , obtained on the basis of these calculations, are cited in the table.

Estimates of errors during measurements were conducted by standard method [4] and showed that maximum error in experiments did not exceed 25%.

§ 3. For the case of flow around parallelepipeds, by a viscoplastic medium it is possible from theoretical considerations to determine the dependence of  $K_1$  on determining parameters of the problem. Actually, in accordance with [2], on

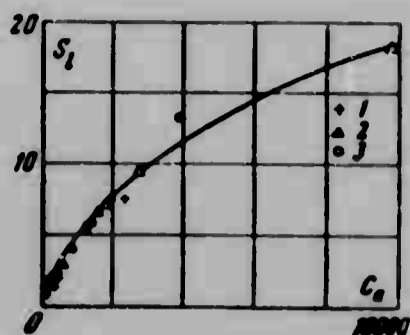


Fig. 5. Dependence of  $C_a$  on  $S_l$  for cylinders:  
1 -  $d = 2.0$  cm; 2 -  $d = 3.5$  cm; 3 -  $d = 5.0$  cm.

boundary of stagnant zone, which is for external flow a slip line, pressure is constant, since the boundary is rectilinear. But then, considering  $P(\xi) = P_0$  from (1.6) we will obtain

$$K_1 = 2 + \frac{a}{l} (1 + P_0) \quad (3.1)$$

Using values of  $K_1$  found as a result of treatment of experiments (table), we will determine corresponding values of  $P_0$ . For all three parallelepipeds this value turns out to be identical and equal to  $P_0 = 11.2$  when maximum relative deviation of values of  $P_0$  for every model is not more than 7%. The dependence of  $C_a$  on  $S_l$  for parallelepipeds of various length is represented on Fig. 4. It is easy to see that with increase of length of parallelepipeds rate of growth of  $C_a$  depending upon  $S_l$  is delayed, which corresponds to character of the earlier shown dependence (3.1). Order of growth of  $C_a$  is determined by  $K_1/\gamma$ , and the latter with growth of  $l$  for constant  $a$  rapidly decreases.

Form of models	Dimensions, cm	$ K_1 $	$K_2$
Parallelepipeds	$l = 30.5 \quad a = 2.3$	2.90	12.60
	$l = 11.0 \quad a = 2.3$	4.76	3.67
	$l = 4.8 \quad a = 2.3$	7.50	18.0
Parallelepipeds, square in plan	$a = 2.3$	13.73	1.25
	$a = 3.5$		
Round cylinders	$a = 5.0$	24.75	0
	$a = 3.4$		
	$a = 2.0$		
Wedge	$a = 2.0$	80.20	19.18
	$l = 5.9$		
Body with frontal part in the form of a stagnant region	$a = 2.0$	69.30	6.32
	$l = 8.9$		

We turn now to analysis of results of flow around round cylinders and parallelepipeds with a square base. From (1.7) it follows that the dependence of  $C_a$  on  $L/a$  and  $D/a$  can take place only through coefficients  $K_1$  and  $K_2$ . If there is no such dependence, for geometrically similar bodies  $C_a$  can be represented in the form

$$C_a = \frac{1}{\gamma} / (K_1, K_2, S_l) \quad (3.2)$$

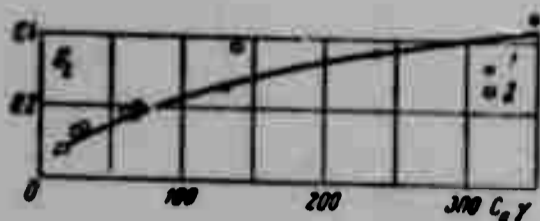


Fig. 6. Dependence of  $C_a \gamma$  on  $S_l$  for squares: 1 -  $a = 3.5$  cm; 2 -  $a = 2.3$  cm.



Fig. 7. Dependence of  $O_a \gamma$  on  $S_l$ : 1 - for wedge and 2 - for body with head in the form of a stagnant region.

Here  $f$  is a function universal for given bodies, and  $\gamma$  is determined in accordance with (2.2) and will change from model to model.

The dependencies of  $\gamma C_a$  on  $S_l$ , represented on Figs. 5 and 6, show that all experimental points lie well on single curves, allowing the conclusion that in experiments conditions of a flat flow around bodies by a flow of viscoplastic medium indeed were realized. These results confirm the above observations of the behavior of chalky lines near walls of tray during motion of models in it. For all models at all speeds these lines remained perpendicular to walls of tray (Fig. 3).

Conditions of flow around the frontal part of parallelepipeds with square base are absolutely analogous to conditions of flow around frontal parts of prolonged parallelepipeds. Formula (3.1) is also applicable in this case. The corresponding value of  $P_0$  well agrees with the value shown earlier and is equal to 10.7.

On the other hand, during flow around parallelepipeds with a square base the extent of the boundary layer on its lateral walls is close to the extent of the boundary layer on round cylinders. Therefore  $K_2$  for these models must have close values, which indeed is confirmed by results of experiments (table). Results of treatment of experimental data on flow around a wedge and a body with frontal part in the form of a stagnant region on the wedge during forward motion of the end are represented on Fig. 7.

First of all let us note that resistance of shown models does not depend on orientation of them in the direction of motion. Upon reversal of direction of motion of these models resistance of motion (within limits of accuracy of present experiments) was not changed.

Such does not occur during flow around analogous bodies by a viscous liquid and is a characteristic peculiarity of flow around a model by a viscoplastic medium.

A distinction of conditions of flow around a body with a special form of nose cone from flow around a corresponding wedge is the increase of length of boundary layer. The quantity  $\gamma$  for a body with a head, considering change of general length of model, changes. This leads to corresponding change of  $C_a$  depending upon  $S_l$ , analogous to what took place for parallelepipeds.

Thus, obtained results of experimental investigations satisfactorily confirm qualitative theoretical conclusions about character of dependence of drag coefficient of body on determining parameters of problem. For geometrically similar bodies the product  $\gamma C_a$  is a universal function of  $S_l$ , which can be experimentally determined on one model and used for calculation of flow around bodies with other geometric dimensions. Basic geometric characteristics of a streamlined body are the parameters  $a$  and  $l$ . The dependence of  $C_a$  on other geometric peculiarities of their structure is essentially weaker. It is experimentally shown that resistance of wedge-shaped bodies during their motion in a viscoplastic medium does not depend on how the wedge moves in the medium — whether the end or the front moves forward. This essentially distinguishes the flow around bodies by a viscoplastic medium from flow around them under the same conditions by a viscous liquid.

The authors thank G. I. Barenblatt for leadership in the work and S. S. Grigoryan for valuable discussions.

Submitted  
16 May 1964

#### Literature

1. I. G. Bulina and V. G. Savin. Formation of frontal stagnant zone during flow around blunted bodies by a viscoplastic liquid. Reports of Academy of Sciences of USSR, 1962, Vol. 145, No. 1.
2. V. P. Myasnikov. Formulation of the problem of flow around bodies by a viscoplastic liquid. PMTF, 1962, No. 4.
3. V. P. Myasnikov. Certain questions of the theory of viscoplastic flows. Cand. dis., Moscow State University, 1962.
4. K. P. Yakovlev. Mathematical treatment of results of measurements. State Technical Press, M., 1953.

**BLANK PAGE**

CALCULATION OF FLOW AROUND A PLATE BY A LIQUID-DROP  
LIQUID WITH VARIABLE VISCOSITY

V. P. Kashkarov and A. T. Luk'yanov (Alma Ata)

We consider the solution of the system of equations of the boundary layer of a liquid with variable viscosity with the help of a static electrointegrator for flow around a plate by a uniform flow.<sup>1</sup>

The number of works dedicated to study of nonisothermal flows of a liquid-drop viscous liquid is comparatively small. Let us note that problems about laminar flows are solved sufficiently simply (see, for instance, [1]). Regarding flow in boundary layer, then the authors know of only two works in which it was possible to find analytic solutions. In the first of them [2] is the approximate solution of a simplified system of equations of a boundary layer. In [3] is used the method of Karman-Pol'gauzen, giving, as is known, a basically qualitative picture of the flow.

Integration of system of equations of boundary layer taking into account dependence of viscosity on temperature must be conducted by numerical methods. Initial differential equations are replaced by a system of nonlinear finite-difference equations, solution of which is connected with a great deal of calculating work and a whole series of specific difficulties. In this case application of static electrointegrators turned out to be very effective [4], considerably simplifying and accelerating the calculations. Below is described one of the variants of the

---

<sup>1</sup>Contents of report made at the II All-Union conference on theoretical and applied mechanics, January 29-February 6, 1964, Moscow.

static electrointegrator for direct integration of a system of equations of nonisothermal plane-parallel boundary layer, appearing for a plate around which flows a uniform flow.

The considered problem is brought in dimensionless variables to system of equations

$$u \frac{\partial u}{\partial x} + v \frac{\partial u}{\partial y} = \frac{\partial}{\partial y} \left[ \nu \frac{\partial u}{\partial y} \right], \quad \frac{\partial u}{\partial x} + \frac{\partial v}{\partial y} = 0, \quad u \frac{\partial \theta}{\partial x} + v \frac{\partial \theta}{\partial y} = \frac{1}{P} \frac{\partial^2 \theta}{\partial y^2} \quad (1)$$

(P - Prandtl number)

with boundary conditions

$$u = 0, \quad v = 0, \quad \theta = 0 \quad \text{when } y = 0; \quad u = 1, \quad \theta = 1 \quad \text{when } y = \infty \quad (2)$$

$$\left( u = \frac{U}{U_\infty}, \quad v = \frac{V}{U_\infty}, \quad \theta = \frac{T - T_\infty}{T_w - T_\infty}, \quad x = \frac{X}{L}, \quad y = \frac{Y}{L}, \quad L = \frac{\nu_\infty}{v_\infty}, \quad v = \frac{\nu_\infty}{U_\infty}, \quad P = \frac{\nu_\infty}{\nu} \right)$$

Equation (1) in finite differences, solved relative to the desired functions, has the form

$$u_{n,h+1} = \frac{\Delta x}{(\Delta y)^2} \frac{1}{U_{nh}} \frac{1}{b} \sum_{i=1}^b \nu_i (u_{n+1,h} - u_{nh}) -$$

$$- \frac{\Delta x}{(\Delta y)^2} \frac{1}{U_{nh}} \frac{1}{b} \sum_{i=1}^b \nu_i (u_{nh} - u_{n-1,h}) + u_{nh} - \frac{\Delta x}{\Delta y} \frac{\nu_{nh}}{U_{nh}} (u_{n+1,h} - u_{nh})$$

$$\left( a = \frac{u_{n+1,h} - u_{nh}}{N}, \quad b = \frac{u_{nh} - u_{n-1,h}}{N} \right) \quad (3)$$

$$\theta_{n,h+1} = \frac{\Delta x}{(\Delta y)^2} \frac{1}{U_{nh}} \frac{1}{P} (\theta_{n+1,h} - 2\theta_{nh} + \theta_{n-1,h}) + \theta_{nh} - \frac{\Delta x}{\Delta y} \frac{\nu_{nh}}{U_{nh}} (\theta_{n+1,h} - \theta_{nh}) \quad (4)$$

$$v_{n,h+1} = v_{n,h} + u_{nh} - u_{n,h+1} \quad (5)$$

Here  $N = 0.001$  is the least change of function at which is considered change of coefficients;  $\nu_1$  - value of coefficient of viscosity, taken with step  $N = 0.001$   $U_\infty$  ( $U_\infty$  is usually taken equal to one). Expression

$$\frac{1}{b} \sum_{i=1}^b \nu_i \quad (i = 1, 2, \dots)$$

corresponds to average magnitude in interval  $u_{n+1,h} - u_{nh}$ . If, for instance,  $u_{n+1,h} = 0.235 u_{nh}$ ,  $u_{nh} = 0.232 u_{nh}$ , then

$$a = \frac{0.003}{0.001} = 3, \quad \frac{1}{a} \sum_{i=1}^a v_i = \frac{v_{0.222} + v_{0.224} + v_{0.226}}{3}$$

The static integrator consists of three discrete potentiometers of high resolving power. Yields from potentiometers are removed on a general switching panel with three-pronged sockets (Fig. 1).

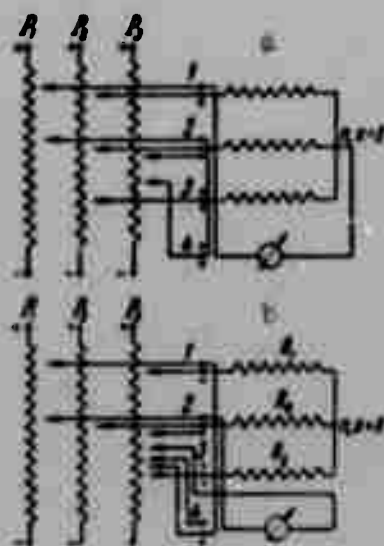


Fig. 1.

Potentiometers  $P_1$  and  $P_2$  are functional and serve for programming the change of coefficients of the equation; potentiometer  $P_3$  is discrete; resistors  $R_1$ ,  $R_0$ ,  $R_2$  compose the calculating element. The solution is carried out by means of displacement of calculating element with respect to points of grid region, represented in the integrator by potentials.

Before beginning the solution on potentiometers  $P_1$  and  $P_2$  are established functional dependencies (between number of discharges and stress) of form

$$F_1 = f(\Delta x / \Delta y, v/u) \text{ and } F_2 = f(v/u). \text{ After that, with the}$$

help of plugs with cords on ends of function generator stresses proportional to the values of function in selected points of grid region are given. On Fig. 1a, is shown a connection diagram in the integrator during solution of differential equation (3). For the integrator it is possible to write the equality

$$V_{n,k+1} = \frac{1}{2 + R/R_0} \frac{1}{V_{nk}} \frac{1}{a} \sum_{i=1}^a v_i' (V_{n-1,k} - V_{nk}) - \frac{1}{2 + R/R_0} \frac{1}{V_{nk}} \frac{1}{\beta} \sum_{i=1}^{\beta} v_i' (V_{nk} - V_{n-1,k}) + V_{nk} - A(V_{n+1,k} - V_{nk}) \quad \left( \alpha = \frac{V_{n-1,k} - V_{nk}}{N}, \beta = \frac{V_{nk} - V_{n-1,k}}{N} \right) \quad (6)$$

Here  $\alpha$  and  $\beta$  are the numbers of least fractions of division of the functional potentiometer which are contained in the intervals  $V_{n-1,k} - V_{nk}$  or  $V_{nk} - V_{n-1,k}$ ,  $v' \sim v$ ,  $\alpha = a$ ,  $\beta = b$ . Comparing equations (3) and (6), we will find conditions of modeling

$$\frac{\Delta x}{(\Delta y)^2} = \frac{1}{2 + R/R_0}, \quad \frac{1}{V_{nk}} \frac{1}{a} \sum_{i=1}^a v_i' = \frac{1}{u_{nk}} \frac{1}{a} \sum_{i=1}^a v_i \quad (7)$$

$$\frac{\Delta x}{\Delta y} \frac{v_{nk}}{u_{nk}} = A, \quad \frac{1}{V_{nk}} \frac{1}{\beta} \sum_{i=1}^{\beta} v_i' = \frac{1}{u_{nk}} \frac{1}{b} \sum_{i=1}^b v_i$$

During the solution of equation (4) separate units of the integrator are connected according to the diagram of Fig. 1b. For the integrator the following equality is accurate:

$$V_{n,k+1} = \frac{1}{2 + R/R_0} \frac{1}{V_{nk}} (V_{n+1,k} - 2V_{nk} + V_{n-1,k}) + V_{nk} - A(V_{n-1,k} - V_{nk}) \quad (8)$$

Comparing equations (4) and (8), we will find conditions of modeling

$$\frac{\Delta x}{(\Delta y)^2} \frac{1}{P} = \frac{1}{2 + R/R_0}, \quad \frac{\Delta x}{\Delta y} \frac{v_{nk}}{u_{nk}} = A \quad (9)$$

For stability of calculation it is necessary to have fulfillment of inequalities [5]

$$\frac{\Delta x}{(\Delta y)^2} \frac{1}{P} \leq \frac{1}{2}, \quad \frac{\Delta x}{(\Delta y)^2} \frac{v}{u} \leq \frac{1}{2}$$

During calculations the region is divided on two grids - motionless ( $\Delta x = 0.005$  and  $\Delta y = 0.1$ ) and mobile ( $\Delta x = \Delta y = 0.1$ ).

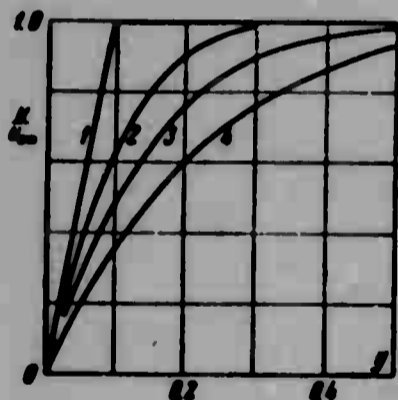


Fig. 2.

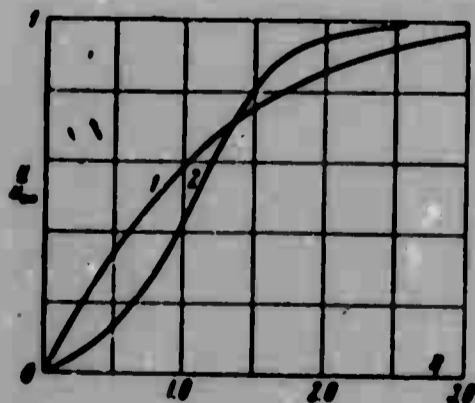


Fig. 3.

Results of solution, obtained with the help of static integrator by the means described above, are represented on Figs. 2-4.

Curves on Fig. 2 show development of velocity profile in boundary layer along plate; for initial distribution of speed when  $x = 0$  a curve of form 1 is accepted; curves 2, 3, 4 correspond to values  $x = 3\Delta x, 7\Delta x, 15\Delta x$ ; curve 4 corresponds to a self-simulating profile. On Fig. 3 are depicted self-simulating profiles of speed in a boundary layer formed during flow-around by a uniform flow of water of hot ( $T_0 = 80^\circ \text{C}, T_\infty = 20^\circ \text{C}$  - curve 1) and cold ( $T_0 = 20^\circ \text{C}, T_\infty = 80^\circ \text{C}$  - curve 2) plates. A characteristic peculiarity of these profiles (which qualitatively coincide with those in [2]) is the presence on curve 2 of a point of inflection (for lubricating oil deformation of profile of speed on a cold plate would be expressed more

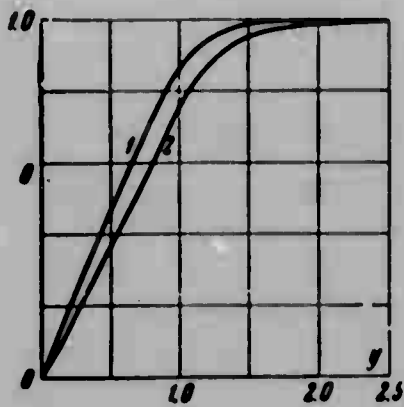


Fig. 4.

sharply); for the same values of  $T_w$  and  $T_\infty$  of plate and flow on Fig. 4 are given profiles of temperature in boundary layer. Comparison of the constructed curves for profiles of speed with those given in [2] shows their qualitative proximity.

Results of calculation permit finding relationship of stresses of friction and heat flow on a cold and a hot plate

$$\begin{aligned} \frac{\tau_{w20}}{\tau_{w30}} &= \left( \frac{v_{20}}{v_{30}} \right)^{1/2} \frac{\partial u}{\partial \eta} \Big|_{w20} / \frac{\partial u}{\partial \eta} \Big|_{w30} & \left( \frac{\tau_{w20}}{\tau_{w30}} = 1.20 \right) \\ \frac{q_{w20}}{q_{w30}} &= - \left( \frac{v_{20}}{v_{30}} \right)^{1/2} \frac{\partial \theta}{\partial \eta} \Big|_{w20} / \frac{\partial \theta}{\partial \eta} \Big|_{w30} & \left( \frac{q_{w20}}{q_{w30}} = 1.30 \right) \end{aligned} \quad (10)$$

In parentheses are shown values for water.

Accuracy of results is determined by magnitudes of steps of grid, taken from calculation plan, and thoroughness of manufacture of separate units of the integrator.

Submitted  
1 April 1964

#### Literature

1. S. A. Regirer. Certain thermohydrodynamic problems about established one-dimensional flow of viscous liquid-drop liquid. PMM, 1957, Vol. 21, Issue 3.
2. S. M. Targ. Basic problems of the theory of laminar flows. State Technical Press, Moscow-Leningrad, 1951.
3. O. T. Hanna and J. E. Myers. Amer. I. Chem. Engng J., 1961, Vol. 7, No. 3.
4. L. A. Vulis and A. T. Luk'yanov. Static analog devices. Collection: "Questions of calculating mathematics and computer technology." Mashgiz, M., 1963.
5. D. Yu. Panov. Reference book on numerical solution of partial differential equations. State Technical Press, Moscow-Leningrad, 1954.

**BLANK PAGE**

# THE THEORY OF NONSTATIONARY SURFACE WAVES

Yu. A. Berezin and V. I. Karpman

(Novosibirsk)

A nonsteady-state solution is found for the Korteweg-de Vries equation [1], describing profile of surface wave of finite but small amplitude at large distances from initial perturbation.

In [1] Korteweg and de Vries obtained an equation describing propagation of waves of finite but small amplitude on the surface of a heavy liquid which is in a canal of finite depth which has the form

$$\frac{\partial \eta}{\partial t} + u_0 \frac{\partial \eta}{\partial x} + \frac{3}{2} \frac{u_0}{h} \eta \frac{\partial \eta}{\partial x} - \frac{1}{2} u_0 \delta^2 \frac{\partial^2 \eta}{\partial x^2} = 0 \quad \left( u_0 = \sqrt{g h}, \quad \delta^2 = \frac{\alpha}{\rho g} - \frac{h^3}{3} \right) \quad (1)$$

Here  $\eta(x, t)$  - elevation of free surface of liquid,  $h$  - depth of canal,  $\rho$  - density of liquid,  $\alpha$  - coefficient of surface tension. As is noted in [1], this equation describes waves moving only in one direction, i.e., describes one of two systems of waves moving in opposite directions, which will be the result of a certain perturbation, after their full separation occurs.

Linearization of equation (1) gives the dispersion equation

$$\omega/k = u_0 (1 + \frac{1}{2} \delta^2 k^2) \quad (2)$$

which follows also from the known dispersion equation for capillary gravity waves [2]

$$\omega^2 = kg \left( 1 + \frac{g}{\rho g} k^2 \right) \tanh kh \quad (3)$$

in the limit of long waves ( $kh \ll 1$ ). Thus, during derivation of equation (1) the ratio  $h/\lambda$  — depth of channel to wavelength is a small parameter.

From equation (2) it follows that depending upon depth of channel phase speed of small oscillations either increases with increase of  $k$  (when  $h < \sqrt{3a/\rho g}$ ,  $\delta^2 > 0$ ), or decreases with growth of  $k$  (when  $h > \sqrt{3a/\rho g}$ ,  $\delta^2 < 0$ ). We say that in the first case there is a positive dispersion, and in the second a negative dispersion.

Steady-state solutions of equation (1), obtained in [1], gives secluded and periodic waves of finite amplitude. For secluded waves we have

$$\eta(x, t) = \pm |\max \eta| \operatorname{sech}^2 \left[ \left( \frac{|\max \eta|}{h|\delta|} \right)^{1/2} \frac{x}{2} \right] \left( \frac{z = x - ut}{u = u_0 \left( 1 + \frac{1}{2} \max \eta/h \right)} \right) \quad (4)$$

Here  $u$  — speed of secluded wave. It follows from this that length of secluded wave is determined by its amplitude and magnitude  $|\delta|$ , which we will call the length of dispersion. In the case of positive dispersion there exist nonlinear stationary waves of type of cavities (minus sign in (4)), and in the case of negative dispersion — wave of type of elevations (plus sign in (4)).

As was noted in [3, 4], propagation of waves on the surface of a heavy liquid in a channel of finite depth reveals an analogy with propagation of waves of finite amplitude in rarefied plasma, where propagation of secluded and periodic waves, which were considered, for instance, in [5-7] also turns out to be possible. In [8] was obtained an equation for nonstationary waves of finite but small amplitude, propagating in plasma both across magnetic field and also under a small angle to it, which has a form similar to equation (1). In the same place was found the nonstationary solution of the obtained equation, self-simulating with respect to certain variables. As will be shown below, an analogous nonstationary solution can be obtained also for equation (1).

We cross in (1) to new variables

$$\eta = \mp \frac{1}{2} z^2 h / \mu, \quad \xi = z^2 |\mu|^{-1/2} \frac{x - ut}{h}, \quad \tau = \mp |\mu|^{-1/2} \frac{ut}{h} \left( \mu - \frac{\delta^2}{h^2} \right) \quad (5)$$

Here the upper sign corresponds to the case of positive dispersion ( $\delta^2 > 0$ ),

and the lower to the case of negative dispersion ( $\delta^2 < 0$ ). As a result we will obtain the equation

$$\frac{\partial f}{\partial \tau} + f \frac{\partial f}{\partial \xi} + \frac{\partial^2 f}{\partial \xi^2} = 0 \quad (6)$$

Equation (6) is invariant with respect to transformation

$$\tau \rightarrow \gamma \tau, \quad \xi \rightarrow \gamma^{1/2} \xi, \quad f \rightarrow \gamma^{-1/2} f \quad (7)$$

Therefore we consider

$$f(\xi, \tau) = -\tau^{-1/2} \psi(z), \quad z = -\tau^{-1/2} \xi \quad (8)$$

and after substitution of (8) in (6) we obtain the equation

$$3\psi''' + 3\psi\psi' + z\psi' + 2\psi = 0 \quad (9)$$

Such an equation was investigated by the authors in [8], where it was shown that the family of solutions of equation (9), fading when  $z \rightarrow -\infty$ , has when  $z \rightarrow -\infty$  asymptotic behavior

$$\psi(z) = \frac{1}{2} C (3^{-1/2} |z|)^{1/2} \exp \left[ -2 \left( \frac{|z|}{3} \right)^{3/2} \right] \quad (10)$$

Here  $C$  is a certain arbitrary constant. Equation (9) was solved numerically on an [EVM] (ЭВМ) (computer) with the use of asymptotic behavior of (10) for determination of values  $\psi(z)$ ,  $\psi'(z)$ ,  $\psi''(z)$  for certain large negative  $z$ . Results of solution are shown in Fig. 1. Curves 1, 2, 3, 4 correspond to values  $C = 1.0, 1.6, 1.8, 5.0$ . When  $C \leq 1.6$  function  $\psi(z)$  has oscillatory character (curves 1, 2); when  $C \geq 1.8$  solutions are curves of type 3, 4 and do not have physical meaning. As was shown in [8], solution  $\psi(z)$  for sufficiently small  $C$  (according to numerical solution when  $C \leq 1.6$ ) has when  $z \rightarrow +\infty$  asymptotic behavior

$$\psi(z) = z^{1/2} [C_1 \cos [2(1/2z)^{3/2}] + C_2 \sin [2(1/2z)^{3/2}]] \quad (11)$$

Here  $C_1, C_2$  are certain arbitrary constants. For sufficiently large  $C$  (according to numerical solution, when  $C \geq 1.8$ ) solution  $\psi(z)$  has in certain points depending on the value of  $C$ , a pole of the second order. Actually, if constant  $C$

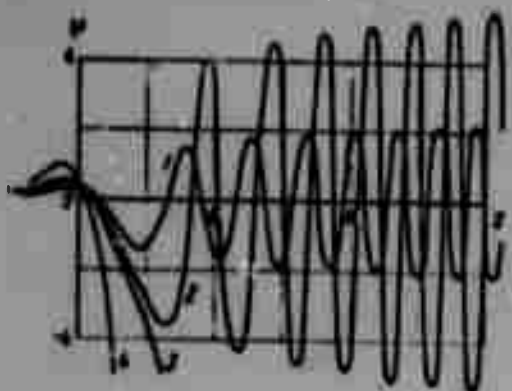


Fig. 1.

in (10) is sufficiently great, then in region of small  $z$  in equation (9) it is possible to disregard the last two terms, and when  $\psi(\psi < 0)$  is large with respect to absolute value, we will have

$$\psi(z) = -12(z - \beta)^{-2} \quad (12)$$

where  $\beta$  - arbitrary constant. Thus, for sufficiently large  $C$  solutions of equation (9) diverge as  $(z - \beta)^{-2}$ , while  $\beta$  decreases with increase of  $C$ .

Using formulas (5) and (8), we write elevation of free surface of liquid

$$\eta(x, t) = -\frac{1}{3} 2^{1/2} h \mu^{1/2} \left(\frac{h}{u_0 t}\right)^{1/2} \psi\left\{\left(\frac{2h}{\mu u_0 t}\right)^{1/2} \frac{x - u_0 t}{h}\right\} \quad (13)$$

In the case of positive dispersion ( $h < \sqrt{3a/\rho g}$ ) for sufficiently large  $x$  and  $t$  we have

when  $u_0 t < x$

$$\eta(x, t) = -\frac{1}{3} 2^{1/2} h \mu^{1/2} \left(\frac{h}{u_0 t}\right)^{1/2} \left(\frac{x - u_0 t}{h}\right)^{1/2} \left\{ C_1 \cos\left[\left(\frac{2}{3}\right)^{1/2} \left(\frac{h}{\mu u_0 t}\right)^{1/2} \left(\frac{x - u_0 t}{h}\right)^{1/2}\right] + C_2 \sin\left[\left(\frac{2}{3}\right)^{1/2} \left(\frac{h}{\mu u_0 t}\right)^{1/2} \left(\frac{x - u_0 t}{h}\right)^{1/2}\right] \right\} \quad (14)$$

when  $u_0 t > x$

$$\eta(x, t) = -\frac{h}{3} C \left(\frac{\mu}{2\sqrt{3}}\right)^{1/2} \left(\frac{h}{u_0 t}\right)^{1/2} \left(\frac{u_0 t - x}{h}\right)^{1/2} \exp\left\{-\left(\frac{2}{3}\right)^{1/2} \left(\frac{h}{\mu u_0 t}\right)^{1/2} \left(\frac{u_0 t - x}{h}\right)^{1/2}\right\} \quad (15)$$

In the case of negative dispersion ( $h > \sqrt{3a/\rho g}$ ) for sufficiently large  $x$  and  $t$  we have

when  $u_0 t < x$

$$\eta(x, t) = -\frac{h}{3} C \left(\frac{|\mu|}{2\sqrt{3}}\right)^{1/2} \left(\frac{h}{u_0 t}\right)^{1/2} \left(\frac{x - u_0 t}{h}\right)^{1/2} \exp\left\{-\left(\frac{2}{3}\right)^{1/2} \left(\frac{h}{|\mu| u_0 t}\right)^{1/2} \left(\frac{x - u_0 t}{h}\right)^{1/2}\right\} \quad (16)$$

when  $u_0 t > x$

$$\eta(x, t) = -\frac{1}{3} 2^{1/2} h |\mu|^{1/2} \left(\frac{h}{u_0 t}\right)^{1/2} \left(\frac{u_0 t - x}{h}\right)^{1/2} \left\{ C_1 \cos\left[\left(\frac{2}{3}\right)^{1/2} \left(\frac{h}{|\mu| u_0 t}\right)^{1/2} \left(\frac{u_0 t - x}{h}\right)^{1/2}\right] + C_2 \sin\left[\left(\frac{2}{3}\right)^{1/2} \left(\frac{h}{|\mu| u_0 t}\right)^{1/2} \left(\frac{u_0 t - x}{h}\right)^{1/2}\right] \right\} \quad (17)$$

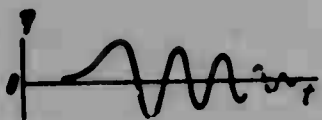


Fig. 2.

Form of surface of liquid in certain point  $x$ , described by formulas (14)-(17), qualitatively (without observance of scale), is depicted on Figs. 2 and 3, from which Fig. 2 corresponds to elevation of surface of liquid in the case of negative dispersion, and Fig. 3 corresponds to elevation of surface of liquid in the case of positive dispersion. By analogy with [8], we conclude that these solutions describe asymptotic form of free surface of liquid

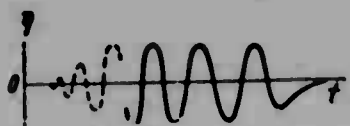


Fig. 3.

after a certain initial perturbation, concentrated near point  $x = 0$ , for a sufficiently large  $x$  and  $t$  not too far from front of wave  $x = u_0 t$  (by front of wave here is understood front of perturbation propagating with speed  $u_0 = \sqrt{gh}$ ). Parts of profile shown on Figs. 2 and 3 by dotted line correspond to regions far from the front, which are not described by formulas (14)-(17).

In conclusion the authors thank R. Z. Sagdeyev for constant attention to the work and valuable discussions.

Submitted  
11 May 1964

#### Literature

1. D. J. Korteweg and G. de. Vries. On the change of form of long waves advancing in a rectangular canal and on a new type of long stationary waves. Philos. Mag., 1895, Vol. 39, Ser. 5.
2. L. D. Landau and Ye. M. Lifshits. Mechanics of solid media. State Technical Press, Moscow, 1954
3. R. Z. Sagdeyev. One analogy between waves on surface of heavy liquid and nonlinear oscillations of plasma. Report on Riga conference on magnetohydrodynamics, 1960.
4. C. S. Gardner and G. K. Morikawa. Similarity in the asymptotic behavior of collision-free hydromagnetic waves. Preprint, New York. University, 1960.
5. A. A. Vedenov, Ye. P. Velikhov and R. Z. Sagdeyev. Nonlinear oscillations of rarefied plasma. Nuclear fusion, 1961, Vol 1, No. 1.
6. V. I. Karpman. Structure of front of shock wave propagating at an angle to a magnetic field in rarefied plasma. Jour. tech. physics, 1963, Vol. 33, No. 8.
7. A. P. Kazantsev. Established flow of plasma in magnetic field. Jour. experim. and theor. physics, 1963, Vol. 44, No. 4.
8. Yu. A. Berezin and V. I. Karpman. The theory of nonstationary waves of finite amplitude in rarefied plasma. Jour. experim. and theor. physics, 1964, Vol. 45, No. 5.

**BLANK PAGE**

## THE STRUCTURE OF FLOW IN ELECTRODISCHARGE SHOCK TUBES

M. I. Vorotnikova and R. I. Soloukhin

(Novosibirsk)

Terminal velocity of shock waves, obtained in usual or, as they are sometimes called, diaphragm shock tubes, corresponds to Mach numbers of order 10-30 (temperature of "worker" gas  $T \sim 6000^{\circ}\text{K}$ ). Therefore interest toward methods of obtaining shock waves with  $M_1 \sim 5 \cdot 10^2$ , founded on electrodynamic acceleration of conducting gas masses during fast discharge is fully understandable. To this question is dedicated extensive literature (see for instance, [1] and surveys [2, 3]), where in a number of investigations an attempt is made to study structure of jump and different unbalanced processes after front of shock waves obtained in such a way. Immediately let us note that one should observe known caution during application of methods which are wide-spread during work on usual shock tubes, in conditions of experiments with electrodischarge tubes. In this relation data of experiment of M. Cloupeau [4], in which was shown a practical coincidence of front of glow of gas which is in the channel of a shock tube, with front of glow of near-electrode plasma of discharge. From experiments of M. Cloupeau it follows that in waves with  $M_1 \sim 10^2$  plasma of discharge ("piston") and thermal plasma ("plug" of investigated gas) mutually penetrate and shift.

In this connection it is necessary also to mention the investigation of Chang [5], where along with the non one-dimensional structure of flow in a shock tube with coaxial accelerator by recordings of pressure it is possible to note also

deflections from one-dimensional laws of preservation on front of shock wave during its reflection from closed end of tube. Below is compared an optical picture of the process with measurements of pressure by piezotransducer and with other methods of "sounding" the state of the medium after the shock wave — for more detailed information about degree of deflections from one-dimensionality. Corresponding oscillograms and developments are shown in Figs. 1-5.

# 1. Combination of picture of glow with recording of pressure in wall of tube.

For simultaneous registration of front of pressure and front of glow of shock waves

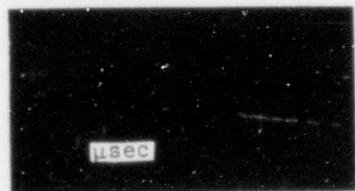


Fig. 1. Simultaneous recording of luminescence (PM) and pressure (p);  $D \sim 1.5$  cm/μsec.

a tube from plastic with a right angle cross section  $15 \times 50$  mm, and length 160 cm, with discharge section of the type: axial elongated electrode-wall,  $C = 600-750$  microfarad,  $V = 5-5.8$  kv. Discharge was produced in air at initial pressure  $p_0 = 0.2$  mm Hg. Speed of shock wave could be determined accurate to 1-2% both by scannings made by photoregister

and also with the help of a [FEU] (ФЭУ) (photomultiplier, PM) and two transverse slots. Pressure was measured by pulse piezoelectric transducer [6] with diameter of

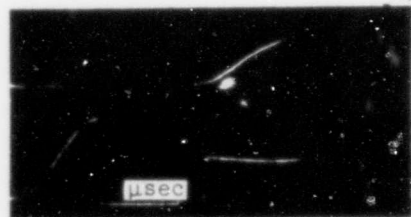


Fig. 2. Combined in time frame of glow, taken through a transverse slot  $46 \times 0.5$  mm<sup>2</sup>, and oscillogram of pressure, recorded by a piezotransducer embedded in lateral wall of tube strictly opposite slot. Narrow luminescent band on frame is obtained during passage of perturbation through auxiliary slot  $4 \times 0.5$  mm<sup>2</sup>, located 23 mm ahead of basic slot. A light signal, passing the auxiliary slot simultaneously is recorded by the PM.

sensing device 1 mm. Calibration by sensitivity and check of accuracy of reproduction of form of signal by transducer were conducted on a diaphragm shock tube. Error in determination of absolute value of pressure was not more than  $\pm 8.5\%$ . The transducer was embedded in the lateral wall of the tube strictly opposite slot of recording channel of PM, dimensions of which were  $1 \times 0.3$  mm.

Comparison of oscillograms of pressure and glow (Fig. 1) indicates combination in time of maxima of measured magnitudes accurate to  $\sim 0.1$  μsec. However beginning of growth of glow, as a rule, noticeably leads beginning of rise of pressure. Difference in time constant of buildup

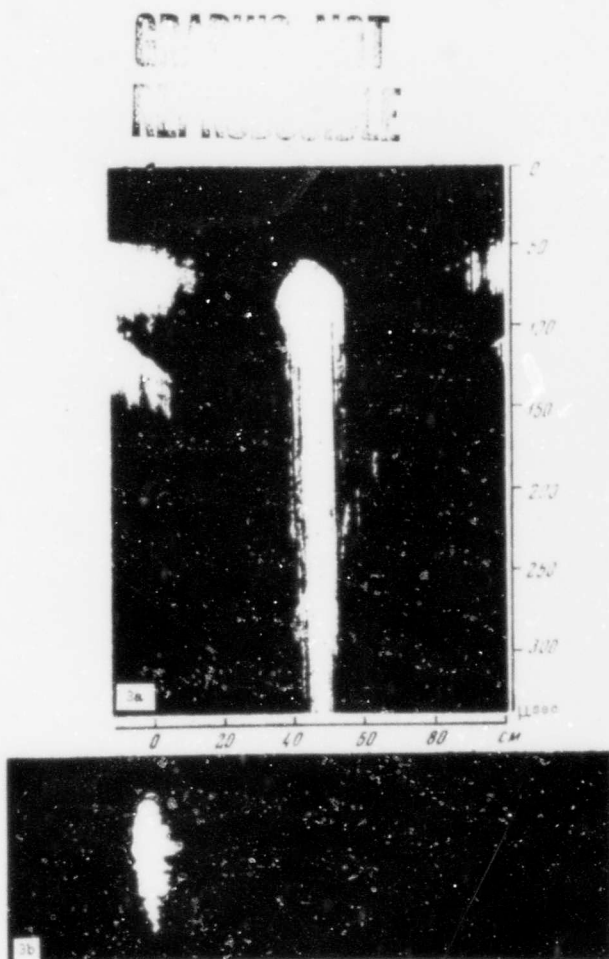


Fig. 3. (a) Phototracing of process of collision of two waves of identical intensity;  $D \sim 3 \text{ cm}/\mu\text{sec}$ . (b) Frame of luminescence of propagating perturbation.

there is a characteristic absence of a clear and smooth line of the front — in undisturbed gas it is as though clusters of plasma are "introduced," forming their own kind of "semipermeable piston." Considering difference in internal energy of plasma of discharge and gas compressed by shock wave due to mixing, as a whole it is possible to expect deflections of mean values of temperature, density, and pressure of medium after the front from those calculated from one-dimensional laws of preservation for plane wave.

2. Pressure after front of shock wave. On Fig. 6 are given absolute values of measured pressures after the front of a wave. From comparison of them with given one-dimensional calculation it is possible to see that there is a divergence of approximately twice in understating data of experiment. Let us note that a decrease of pressure can be shown also in measurements of [4] (after a reflected wave), where the author relates this to errors of experiment. It is necessary

of signals for waves with a speed  $\sim 1.5 \text{ cm}/\text{msec}$  was near  $0.3 \mu\text{sec}$  or (in space solution) near  $0.5 \text{ cm}$ . The most graphic explanation of this fact can be found in comparison of recording of pressure with simultaneous registration of form of contour of luminescent front of shock wave. For this purpose the gas luminescence was photographed through a transverse slot by the method of partial (to 0.9) compensation of motion of wave (image on film in photoregister moves with a speed close to speed of wave in that same direction, see [6]). On Fig. 2 are given typical photographs of contour of luminescent front with recordings of pressure in corresponding section superimposed on them. On photographs

to note also that small values of measured pressures are directly connected with appraisals of deviations from calculation in temperature and density, given in [2], where it is shown that the ratio of experimental values of temperature to theoretical values have an order of 2, and the ratios of experimental values of density to theoretical values equal  $\sim 1/3$ .

3. Speed of reflected and refracted shock waves. Comparison of measured speeds of reflected and refracted shock waves with calculated speeds can also serve as a method of appraisal of deflections from one-dimensionality (registered deflections from equilibrium in this case are difficult to expect due to large values of temperature of medium). Experiments on collision and reflection of shock waves were conducted in a round tube with internal diameter 27 mm and with coaxial discharge device. As also in tube with right angle cross section, front of glow of wave at 60 cm from discharge turns out to be irregular (most frequently - convex, see Fig. 3b). Typical scannings of collision of waves of equal intensity are shown on Fig. 3a. Scannings of reflection of wave from closed end of tube in virtue of symmetry of phenomenon are fully analogous to each of the halves of a scanning of type (Fig. 3a).

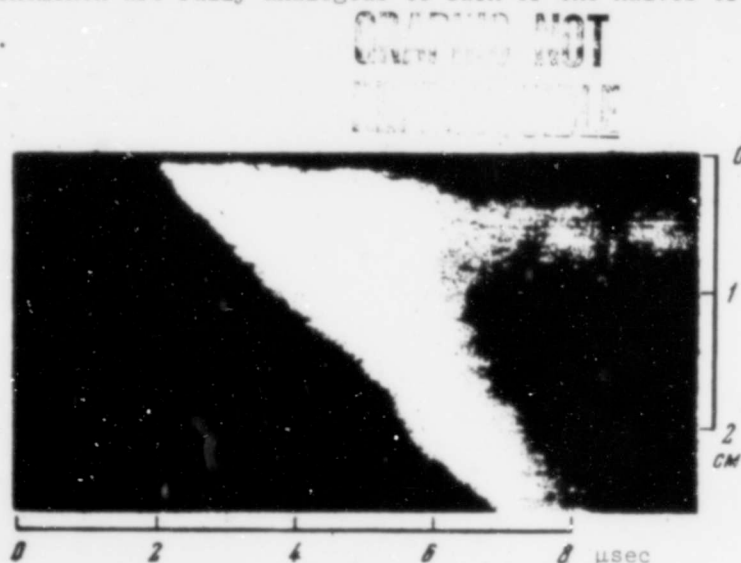


Fig. 4. Phototracing of reflection of wave from end of tube.

Scannings with resolution in time and space essentially larger than on Fig. 3a ( $\sim 50$  times) were processed (Fig. 4). On Fig. 7 values of speed of reflected waves, desired at  $\sim 1$  cm near reflecting wall, are compared with one-dimensional

equilibrium calculation (solid curve). From this comparison it is simple to verify that speed of reflected (refracted) waves is 1.3-1.5 times higher than the calculated value. If one were to consider that speed of reflected wave  $D'$  is connected with compression in this wave  $\beta$  and flow rate  $u$  is a simple relationship.  $D' = u/(\beta - 1)$ , obtained data will correspond not to computed value of compression  $\beta_2 \sim 7$  for a wave in air ( $D = 2 \text{ cm}/\mu\text{sec}$ ), but to compression  $\beta_2' \sim 5$ . This result does not contradict observations by mutual penetration and mixing of electrodischarge and thermal plasma in an incident wave, if one considers that discharge plasma has higher temperature than thermal plasma. Thus, if it is considered that change of noted above is connected only with increase of temperature (speed of sound) after an incident wave with corresponding change of Mach number of reflected wave  $M' \sim 0.6M$ , then the necessary increase of temperature should compose  $T_1' \sim 1.5T_1$ , i.e., somewhat lower than in [2], where  $T_1' \sim 2T_1$ . However if one were to take obtained value for  $T'$  and, according to [2], to consider  $\rho_1' \sim 1/3\rho_1$ , then we obtain  $p_1'/p_1 \sim 1/2$ , which more nearly corresponds above obtained data on measurement of pressure than estimates of expected decrease of pressure according to [2].

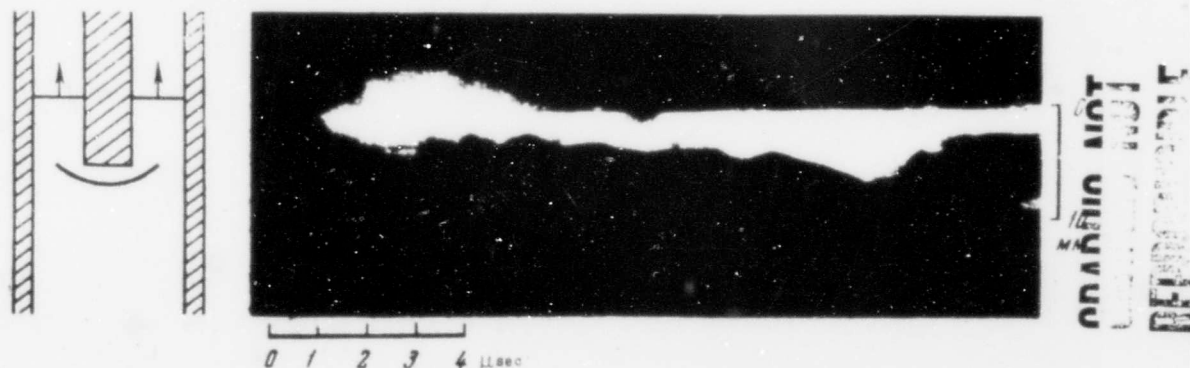


Fig. 5. Diagram of experiment and time scanning of flow around by a wave of a cylinder 5 mm in diameter with axis coinciding with axis of tube.

4. Shock wave during flow around an obstacle. For the diagram of the experience shown on Fig. 8, the scanning is given on Fig. 5. With respect to position of shock wave forming for braking surface of obstacle (end of cylinder of area S), it is possible to watch state of flow after incident shock wave, in particular it is possible to estimate Mach number of flow of medium incident on the body. In accordance with data of [7, 8], ratio of distance between forward shock



Fig. 6. Comparison of measured absolute values of pressure with calculation by one-dimensional set up in the case of equilibrium state after a front.

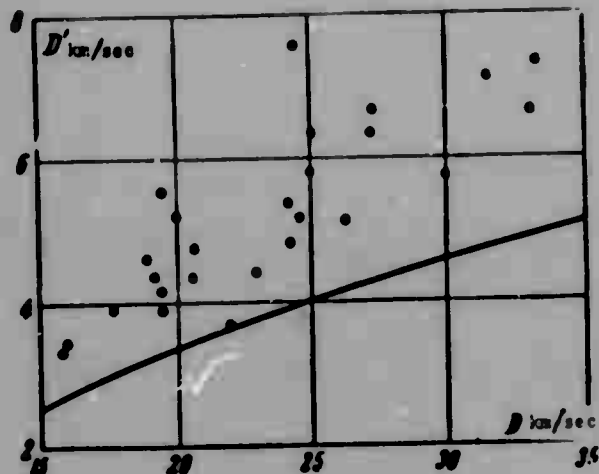


Fig. 7. Dependence of speed of cut shock wave  $D'$  km/sec on speed of incident shock wave  $D$  km/sec. The points plot experimental data, the curve - calculated dependence with respect to one-dimensional laws of preservation in the case of equilibrium.

and end of cylinder  $S$  to diameter of cylinder  $d$  decreases in proportion to ratio of density before and after jump. We compare now with this estimate Fig. 5. On

the given scanning  $S/d \sim 0.33$ , i.e., closely corresponds to  $M \approx 2.5$  when  $\gamma = 9/7$  - namely to the case of higher ( $T_1' \sim 1.5T_1$ ) temperature - and not to the parameter of purely thermal plasma, where  $M \sim 3.5$  and expected value  $S/d \sim 0.2$ . Thus, here is obtained one more independent proof of accuracy of basic moment - absence of delimitation between thermal and discharge plasma and their mixing in electromagnetic tubes initial pressures less than 1 mm Hg.

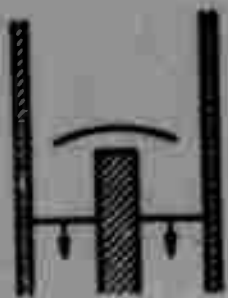


Fig. 8. Diagram of experiment.

In conclusion the authors thank B. V. Boshenyatov for

help during experiments.

Submitted  
2 July 1964

#### Literature

1. S. R. Kholev and D. S. Poltavchenko. Acceleration of plasma of discharge and obtaining strong shock waves in chamber with coaxial electrodes. Reports of Academy of Sciences of USSR, 1960, Vol. 131, No. 5, p. 1060.

2. E. McLean, C. Faneuff, A. Kolb and H. Griem. Spectroscopic Study of Helium Plasmas Produced by Magnetically Driven Shock Wave. Phys. Fluids, 1960, Vol. 3, No. 6, 843.

3. A. Kolb and H. Griem. High Temperature Shock Waves. "Atomic and Molecular Processes," ed. by D. Bates, Shterscience, N. Y., 1962, p. 141 (Russ. Trans: Uspekhi Fiz. nauk, 1964, Vol 82, No. 1, p. 83); see also: Kolb A. Proc. IV Int. Confer. Ionisation Phenomena in Gases. Amsterdam, 1960.

4. M. Cloupeau. Interpretation of Luminous Phenomena Observed in Electromagnetic Shock Tubes. Phys. Fluids, 1963, Vol. 6, No. 5, p. 679.

5. C. Chang. Shock Wave Phenomena in Coaxial Plasma Guns. Phys. Fluids, 1961, Vol. 4, No. 9, p. 1085.

6. R. I. Soloukhin. Shock waves and detonation in gases. Fizmatgiz, 1963.

7. H. W. Liepman and A. Roshko. Element of Gasdynamics. N. Y., 1957, p. 105.

8. W. C. Griffith. Vibrational Relaxation Times. Fundamental Data obtained from Shock Tube Exp. Perg. Pr., 1961.

**BLANK PAGE**

THE STRUCTURE OF SHOCK WAVES IN THE CASE OF PHASE  
TRANSITIONS OF THE FIRST KIND

N. M. Kuznetsov

(Moscow)

Structure of a shock wave in gas with reversible chemical reactions was investigated by Ya. B. Zel'dovich [1]. In [1] it is shown that in the structural relation one should distinguish weak and strong waves, while in weak and also in strong waves pressure  $p$  and density  $\rho$  in the relaxing zone increase with approach to state of thermodynamic equilibrium. Such a movement of  $p$  and  $\rho$  is obtained during fulfillment of condition  $\delta p > 0$ , where  $\delta p$  — difference of pressures on "frozen" and equilibrium branches of shock adiabat at the same value of density and in the absence of breaks of shock adiabat. During reversible chemical reactions both these conditions are executed.<sup>1</sup>

However during phase transition of kind I, occurring slower than establishment of thermodynamic equilibrium in each of the phases, reverse location of considered branches of shock adiabat is also possible, i.e.,  $\delta p < 0$  [3, 4]. Furthermore,

---

<sup>1</sup>S. P. D'yakov [2] indicated possibility of  $\delta p < 0$  in case of dissociation of diatomic or polyatomic gas, resulting because branches of shock adiabat, corresponding to undissociated and dissociated gases in the state of thermodynamic equilibrium in all degrees of freedom, besides dissociation, during sufficiently great intensity of shock wave have a point of intersection. However it is possible to show that at the point of intersection and above it, i.e., where  $\delta p < 0$ , energy of vibrational degree of freedom attains a magnitude of the order of energy of dissociation of a molecule. Rate of dissociation of course will not be small as compared to relaxation rate molecular oscillations, and actual consideration of the shown branches of adiabat is deprived of a physical content.

shock adiabat  $p(V)$ , where  $V = 1/\rho$ , in the presence of phase transition has breaks, where in the case of sufficiently strong intermittent decrease  $(\partial p/\partial V)$  with growth of  $p$  on equilibrium shock adiabat is possible the formation of diwave configuration [5]. (Let us note that in any case  $\delta p > 0$ .) Dependence of the sign of  $\delta p$  on thermodynamic properties of a substance undergoing phase transitions of kind I is considered in [4]. Not returning again to this question, we will consider the qualitative character of structure of shock wave when  $\delta p < 0$ .

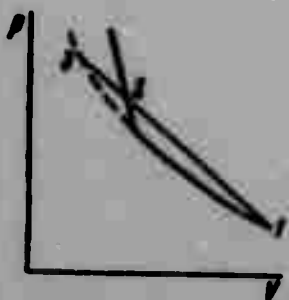


Fig. 1.

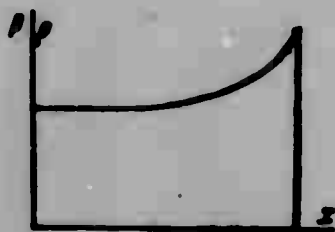


Fig. 2.

1. When  $\delta p < 0$  one should consider only a strong shock wave. (In a weak wave  $\delta p$  is always positive [6], and phase transitions here give nothing qualitatively new [4]. Conclusions of Ya. B. Zel'dovich about structure of weak shock wave are accurate not only during reversible chemical reactions, but also in the general case of slow establishment of equilibrium with one relaxation time.) Location of shock adiabats of "frozen" and equilibrium state when  $\delta p < 0$  is depicted on Fig. 1. With approach of substance to state of full thermodynamic equilibrium, the point describing state of substance on plane  $pV$  (Fig. 1), shifts along chord 3-2 from position 3 to position 2. Density and pressure decrease. Qualitative character of dependence of  $p$  and  $\rho$  on distance  $x$  to shock wave is depicted on the figure.

2. When  $\delta p > 0$  there is diwave configuration (see Fig. 3) during fulfillment of condition

$$\frac{p_2 - p_1}{V_2 - V_1} > \frac{p_3 - p_1}{V_3 - V_1} \quad (1)$$

Location of "frozen" and equilibrium shock adiabats in the case of diwave configuration is depicted on Fig. 3 (the small dotted line depicts Poisson adiabat



Fig. 3.



Fig. 4.

of the metastable phase). The second wave, shifting the substance from state 2 to state 3, in structure [1] is always weak. Actually, the second wave would be strong if

$$\frac{p_3 - p_2}{V_3 - V_2} < \left( \frac{\partial p}{\partial V} \right)_2. \quad (2)$$

Here in the right part is an isentropic derivative of pressure with respect to volume of initial phase at point 2. But from requirement of gas-dynamic stability of shock wave in the absence of phase transition follows

$$\left( \frac{\partial p}{\partial V} \right)_2 < \frac{p_3 - p_2}{V_3 - V_2}$$

which together with (2) contradicts condition of realization of diwave configuration (1).

Qualitative dependence of  $p$  and  $\rho$  on  $x$  for diwave configuration is depicted on Fig. 4. Both waves can be stationary, but rates of their propagation, in general, are different. With increase of pressure  $p_3$  inequality (1) is disturbed, and in steady state operation, as follows from the above and directly from the drawing (Fig. 3), the waves merge into one earlier than the second of them becomes strong. The monowave configuration which forms is, in the structural relation, the strong wave considered by Ya. B. Zel'dovich.

Submitted  
27 December 1963

#### Literature

1. Ya. B. Zel'dovich. About propagation of shock waves in gas with reversible chemical reactions. Jour. experim. and theor. physics, 1946, Vol. 16, p. 365.

2. S. P. D'yakov. Shock waves in relaxing medium. Jour. experim. and theor. physics, 1954, Vol. 27, p. 728.
3. V. D. Urlin and A. A. Ivanov. Fusion during compression by shock wave. Reports of Academy of Sciences of USSR, 1963, Vol. 149, No. 6, p. 1303.
4. N. M. Kuznetsov. Break of shock adiabat during first order phase transition. Reports of Academy of Sciences of USSR, 1964, Vol. 155, No. 1, p. 156.
5. D. Bancroft, E. Peterson and S. Minshall. Polymorphism of Iron at High Pressure. J. Appl. Phys., 1956, Vol. 27, No. 3, p. 291.
6. L. D. Landau and Ye. M. Lifshits. The Mechanics of continuous media. State Technical Press, 1953, pp. 375-381.

# FLOW AROUND A ROUND PLATE IN CONDITIONS OF MOLECULAR BOUNDARY LAYER

V. A. Perepukhov

(Moscow)

During investigation of a round plate located at zero angle of incidence to a flow of strongly rarefied gas, there occur different types of flows, realization of which depends on the relationship between Mach number  $M_\infty$  and Knudsen number  $K_\infty$  in the incident flow.

In [1] is given analysis of different types of flows which are observed during flow around bodies in the framework of the theory of first intermolecular collisions; in the same place for the first time possibility of existence of molecular boundary layer was shown.

In [2] this problem was investigated under the condition that Knudsen number and Mach number  $K_\infty \gg M_\infty \gg 1$ . Below is proposed a solution of an analogous problem under the condition that  $K_\infty^2 \gg M_\infty \gg K_\infty \gg 1$ ; numerical calculation is conducted for  $M_\infty = 30$ ,  $K_\infty = 12$ .

We assume macroscopic flow rate  $U$  much larger than thermal velocity of molecules in incident flow and much higher than speed of reflected molecules.

Reflection of molecules from surface consider diffuse with Maxwellian distribution of speeds

$$f_0 = n_0 \left( \frac{h_0}{\pi} \right)^{3/2} e^{-h_0 v^2}$$

and coefficient of accommodation  $\alpha \sim 1$ .

We simulate the molecules by hard balls of diameter  $\sigma$ . In order to estimate probability of collision of different types of molecules (reflected and incident) with each other, we introduce average lengths of molecular mean free paths (index 1 will designate molecule of incident flow, index 2 - molecule of reflected flow):

mean free path of incident molecules during collision with each other

$$\lambda_{11} \sim M_{\infty} \lambda_0 \quad \left( \lambda_0 = \frac{1}{\sqrt{2} \pi \sigma^2 n_{\infty}}, M_{\infty} = \frac{U}{\sqrt{2KT_{\infty}}} \right)$$

mean free path of reflected molecules during collision of them with molecules of incident flow  $\lambda_{21} \sim \lambda_0 / M_{\infty}$ ;

mean free path of incident molecules during their collision with reflected molecules  $\lambda_{12} \sim \lambda_0$ ;

mean free path of reflected molecules during their collision with reflected molecules  $\lambda_{22} \sim \lambda_0$ .

Of these four lengths the least is  $\lambda_{21}$ ; this permits reflected molecules to be almost completely dispersed into molecules of incident flow at small distance from surface of plate. At the time of collision of reflected molecule with incident molecule one may assume that the reflected molecule is at rest; after the collision part of the molecules will arrive back on the plate, part will fly away in the flow, but molecules undergoing collision, will no longer possess thermal velocity, but on the average, speed of order  $U$ . Consequently, now on the plate arrives almost the same quantity of molecules without collisions and part of the molecules undergoing collision; this permits the quantity of molecules getting on the plate and reflected from it to be increased as long as flow of molecules from infinity not undergoing collisions, is equal to the part of the flow of reflected molecules flowing out through ends of plate.

Here it is possible to show that mean free path of molecules undergoing collision on molecules of another sort and, conversely, molecules of any sort on molecules undergoing collisions, will be large or of order  $\lambda_0$ .

This means that the given problem can be solved in the framework of the theory of first collisions. Strictly speaking, this process is accurate during the following relationships between  $M_{\infty}$  and  $K_{\infty}$ :

$$K_{\infty}^2 > M_{\infty} > K_{\infty} > 1. \quad (K_{\infty} = 1/2 \lambda_0 / \sigma = (2^{1/2} \pi \sigma^2 n_{\infty})^{-1})$$

But this condition may be weakened, requiring

$$K_{\infty}^2 > M_{\infty} > K_{\infty} > 1$$

Below is an example of calculation of such flows when  $M_{\infty} = 30$ ,  $K_{\infty} = 12$ .

As a result of the collision of a molecule possessing speed  $U$  with a motionless reflected molecule (if direction of line of centers at the time of collision is bound by solid angle  $d\Omega$ ), speed of molecules after collision will lie in intervals

$$V_{11}, \quad V_1 + dV_{11}, \quad V_2, \quad V_2 + dV_2$$

where accordingly indices 1 and 2 designate speed of incident and reflected molecules after collision.

The Boltzmann equation we record in the form

$$(\partial / \partial t) V dV = 2n_{\infty} n(r) \sigma^2 U \cos \theta d\Omega \quad (1)$$

Here  $\theta$  — angle between direction of line of centers and direction of speed  $U$  at the time of collision,  $n(r)$  — density of reflected molecules,  $n_{\infty}$  — density of incident flow,  $f$  — distribution function of molecules undergoing collision in gas,  $V$  — speed of molecules after collision in direction 1.

Now it is necessary to find the connection between magnitude of scattering of speeds  $dV_{12}$  and solid angle  $d\Omega$ . Let us assume that molecules collide so that line of centers is in the solid angle with  $d\Omega$ .

Then from simple geometric considerations we find that

$$dV_{12} = U^2 \sin \theta \cos \theta d\theta d\chi \quad (2)$$

Let us write the law of preservation of number of particles  $N$  for arbitrary element of plate  $dS_1$ .

$$n_{\infty} \left( \frac{RT_{\infty}}{2\pi} \right)^{1/2} + N_1 = n_{\infty} \left( \frac{RT_w}{2\pi} \right)^{1/2} \quad (3)$$

Here  $T_{\infty}$  and  $T_w$  — temperature of flow on infinity and temperature of wall correspondingly, and as before it is assumed that reflection occurs with Maxwellian function of distribution by the speeds

$$f_0 = n_0 \left( \frac{h_0}{\pi} \right)^{3/2} e^{-h_0 v^2}, \quad N_1 = \iiint_V f_1 dV \quad (4)$$

So that in the decision process of integral equation (3) it was possible to calculate multiple integral  $N_1$  by the Monte Carlo method, it is necessary to cross to a system of coordinates in which the integrand would satisfy Lipschitz conditions. In connection with this the following variables were introduced  $R_1, \varphi$  (see Fig. 1).

Integral (4) in new variables will take the form

Fig. 1.

$$N_1 = 2 \left( \frac{\pi}{2\pi} \right)^{1/2} a_{\infty} \sigma^2 U \int_0^\infty dL \int_0^{1/2\pi} d\theta \int_{-1/2\pi}^{1/2\pi} d\chi \int_0^{2\pi} d\Phi \int_0^R dR_1 \int_0^\infty A^{-1/2} \sin^2 \theta \cos^2 \theta \cos \chi L V^2 R_1 n_{01}(R, \Phi) \times$$

$$\times \exp(-1/4 \pi V^2) \exp\left(-\frac{R_{\infty} V \bar{A}}{2 V^2 \bar{V}}\right) dV \quad (5)$$

Here  $a$  - radius of plate

Let us introduce designations

we introduce the new variable

Then the integral in new designations will be written so:

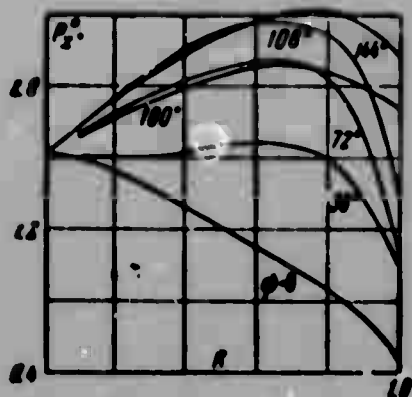


Fig. 2.

In solving the integral equation for density of reflected molecules (3) on surface  $n_{01}(R, \psi)$  the method of successive approximations was used, where for zero approximation was selected

$$n_{01} = N_{\text{Reco}} n_{\infty} = \frac{M_{\infty}}{K_{\infty}} n_{\infty} = 2.5 n_{\infty}.$$

Taking into account collisions expressions for x and y axes and energy flow will take the form

$$\begin{aligned} P_x &= P_{x\infty} + P_{x+}, & P_y &= P_{y\infty} + P_{y+}, \\ P_{x+} &= 2m(h_0/\pi)^{1/2} n_{\infty} \sigma^2 U^2 I[n_0(r, \varphi) \cos^2 \theta \sin^2 \theta \cos^2 \chi] \\ P_{y+} &= 2m(h_0/\pi)^{1/2} n_{\infty} \sigma^2 U^2 I[n_0(r, \varphi) \cos^2 \theta \sin^2 \theta \sin^2 \chi] \\ E &= E_{\infty} + E_+, & E_+ &= 1/2 U P_{x+} \end{aligned}$$

where the index  $\infty$  designates corresponding flows of molecular features occurring during free molecular flow around, and the index + designates corresponding flows of molecular features caused by collisions, I - integral, analogous to (6), in which instead of  $n_0(r, \varphi) \sin^2 \theta \cos^2 \theta \cos \chi$  stands the expression shown in brackets. Results of calculations (with error of 10%) of distribution of pressure with respect to plate and incident energies are shown in Figs. 2, 3, where

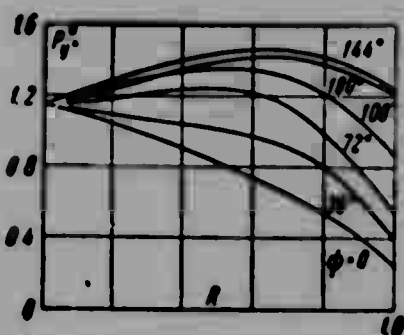


Fig. 3.

$$P_{x+}^* = \frac{P_{x+}}{0.00291} = \frac{2E_+}{0.00291}, \quad P_{y+}^* = \frac{P_{y+}}{0.00291}$$

For aerodynamic coefficients  $C_x$  and  $C_y$  the following formulas with an error of 4% are obtained:

$$\begin{aligned} C_x &= \frac{2}{\sqrt{2\pi\pi} M_{\infty}} + 0.145 \frac{1}{K_{\infty}}, & \frac{C_x}{C_x^*} &= 1.537 \\ C_y &= \frac{2}{2\pi\pi M_{\infty}} + 0.0912 \frac{1}{K_{\infty}}, & \frac{C_y}{C_y^*} &= 31.1 \end{aligned}$$

Here quantities with asterisks are equal to corresponding values of aerodynamic coefficients in free molecular flow.

Calculations confirmed the assumption [1], that during flow around a flat plate in conditions of a molecular boundary layer of force acting on it forces acting in free molecular flow can be many times larger.

The author thanks M. N. Kogan for discussion of results and interest in the work.

Submitted  
29 July 1963

Literature

1. M. N. Kogan. Hypersound flows of rarefied gas. PMM, 1962, Vol 26, Issue 3, p. 520.
2. V. A. Perepukhov. Flow around a flat plate located under zero angle of incidence by a flow of strongly rarefied gas. Comp. math. and math. physics, 1963, Vol. 3, No. 3, p. 581.

HYPERSONIC FLOW AROUND THIN DULLED BODIES WITH  
PHYSICOCHEMICAL TRANSFORMATIONS OF GAS  
IN A HIGH-ENTROPY SHELL

V. V. Lunev

(Moscow)

During hypersonic ( $M \gg 1$ ) flow around thin bodies adjoins to their surface a high-entropy shell of gas with high temperature and small density, formed by gas passing through a shock wave of great intensity in the neighborhood of blunting. In this shell, in distinction from external, low-entropy region of flow, where the law of flat sections is valid and longitudinal speed of gas  $u$  is close to approach stream velocity  $U$ , these speeds can be noticeably distinguished.

For imperfect gas there exists a great speed range  $U$  and densities  $\rho$  of flow around ( $U$  for air from 3000 to 1000 m/sec), in which physicochemical transformations of gas flowing in equilibrium or unbalanced state, take place only in a high-entropy shell, whereas outside of it gas may be considered perfect with the same adiabatic index  $\gamma$  as in incident flow. Below is considered such a case.

Different sides of the influence of high entropy layer on flow around thin bodies is considered in [1, 2] and others. In [1] it is shown that calculation of influence of physicochemical transformations of air in a high-entropy shell and longitudinal motion of gas in it, from the point of view of application of explosion analogy, qualitatively is equivalent to change of energy imparted to gas by a blunted nose, i.e., change of drag coefficient  $c_x$  of nose. Analogous ideas in this or that form for particular cases are contained in [3, 5].

In the development of this for flat ( $\nu = 0$ ) and axially symmetric ( $\nu = 1$ ) flow around the law of similarity founded on introduction of effective drag coefficient of nose already is established. Besides distributing of pressure along body, form of shock waves and distribution of parameters outside high-entropy layer have a universal form, which does not depend on processes in high-entropy shell, flowing in balanced or unbalanced form.

Analogous law of similarity exists for explosion in the atmosphere when distinction of gas from perfect is essential only in central part of explosive zone.

1. For description of flow around thin bodies we use for elementary perpendicular to axis of layer, during its passage by the body, integral relationships of energy and momentum in the radial direction, which we bring to the form

$$\frac{1}{2} R^{1+\nu} v_R^2 J_1 + \frac{p_w}{\gamma-1} (R^{1+\nu} - r_w^{1+\nu}) J_2 = \frac{1}{2} c_x^* + 2^\nu \int_0^R p_w r_w^\nu dr + \frac{R^{1+\nu}}{\gamma(\gamma-1)M^2} \quad (1.1)$$

$$2^\nu R^{1+\nu} v_R J_3 = 1 + \int_0^R \left( p_w r_w^\nu - \frac{1}{\gamma M^2} \right) R^\nu dx \quad (1.2)$$

$$J_1 = \frac{1}{v_R} \int_0^R \left( \frac{v}{v_R} \right)^2 \frac{d\psi}{v}, \quad J_2 = 2^\nu (R^{1+\nu} - r_w^{1+\nu})^{-1} \int_0^R \frac{p}{p_w} r^\nu dr$$

$$J_3 = \frac{1}{v_R} \int_0^R \frac{v}{v_R} \frac{d\psi}{v}, \quad J_4 = \int_0^R \frac{p}{p_w} dr, \quad c_x^* = c_x \left( 1 - \frac{2E_1}{c_x} \right)$$

$$v_R = \frac{2}{1+\gamma} R = \left( 1 - \frac{1}{M^2 R^2} \right), \quad \psi_R = R^{1+\nu}$$

Here and below  $xr_0$ ,  $rr_0$  - longitudinal (counted off from place of linkage of nose and lateral surface) and radial coordinate  $r_0R$ ,  $r_0r_w$  - form of shock wave and surface of body,  $2r_0$  - diameter of midship of nose  $p, \rho, U^2, U_x, U_r$  - pressure, density, enthalpy, velocity of gas and component along axis  $r$ ,  $p_w, \rho_w, U_w^2$  - pressure on surface of body,  $\pi r_0^{1+\nu} \rho_w U_w$  - stream function. The quantity  $\pi r_0^{1+\nu} \rho_w U_w$  is equal to momentum in the direction perpendicular to axis  $r$ , obtained by gas (per unit of angle between two close meridian planes when  $\nu = 1$ ) during passage of environment of blunting. The quantity  $c_x^*$  is, as it were, the local, effective drag coefficient of nose.

Function  $E_1$  considers influence of physicochemical processes in high-entropy

shell (first component under integral) and change of energy in considered elementary shell due to longitudinal overflowing of gas through its boundary. This function has the form<sup>1</sup>

$$E_1 = 2 \int_{r_0}^R r \rho \left[ \left( i - \frac{p}{\rho} - \frac{1}{\gamma-1} \frac{p}{\rho} \right) + \frac{(1-u)^2}{2} \right] dr - \\ - 2 \int_{-\infty}^{\infty} \frac{d}{dx} \int_{r_0}^R \left\{ \left[ \frac{(1-u)^2}{2} + \frac{v^2}{2} + i - \frac{p}{\rho} \right] \rho + p \right\} (1-u) r^2 dr = \\ = \int_0^{\psi_R} \left( i - \frac{\gamma}{\gamma-1} \frac{p}{\rho} \right) \frac{d\psi}{u} + \int_0^{\psi_R} \left[ \frac{u(1-u)^2}{2} + \frac{v^2}{2} - (1-u)i \right] \frac{d\psi}{u} \quad (1.3)$$

Using Bernulli equation

$$i = \frac{1}{2}(1-u^2) + 1/(\gamma-1)M^2$$

disregarding terms of order  $M^{-2}$ , and replacing speed  $u$  by the close quantity  $w$ , we will obtain

$$\frac{1}{c_x} E_1 = \int_0^{\psi_1} \left[ \left( i - \frac{\gamma}{\gamma-1} \frac{p}{\rho} \right) - \frac{(1-w)^2}{2} \right] \frac{d\psi}{w} \quad \left( \psi = \frac{\Psi}{c_x} \right) \quad (1.4)$$

Here integration is extended only to the region of high-entropy layer, since outside its integrand expression (1.4), according to assumption, is negligible. Known uncertainty in selection of threshold flow line  $\psi_0$  does not influence, obviously, the quantity  $E_1$ .

For dissociated air the first component  $E_1$  usually much exceeds the second, and function  $E_1$  is positive. For ideal gas when  $\gamma = 1.4$ ,  $E_1$  is negligible.

Integrals  $J_k$  are close to unity, which was used earlier in approximate theories: when  $J_k = 1$  and  $E_1 = 0$  system (1.1)-(1.2) coincides with equations of G. G. Chernyy [6], and when  $J_k = 1$  - with equations of [1]. Here we will assume only that profiles of quantities under these integrals are similar in such degree that  $J_k$  may be considered identical, at least, for bodies with affine form of lateral surface for assigned product  $M\theta$ , where  $\theta$  is relative thickness of body.

In the general case of unbalanced motion of gas in a high-entropy shell variation of its parameters along flow lines under an assigned distribution of

<sup>1</sup>In [1] in a formula analogous to (1.3), in the integrand expression of the second component is omitted small term  $v^2/2$ , and instead of  $i$  due to a misprint stands  $p/\rho$ .

pressure is determined by equations of type

$$\begin{aligned} \omega \frac{da_j}{dz} &= W(p_\infty U^2 p, T, a_1, \dots, a_n) \quad \left( \omega = \frac{U\tau}{r_0}, \quad j = 1, \dots, n \right) \\ \frac{di}{dz} &= \frac{1}{p} \frac{dp}{dz}, \quad i = i(p_\infty U^2, p, T, a_1, \dots, a_n), \quad p = p(p_\infty U^2 p, T, a_1, \dots, a_n) \end{aligned} \quad (1.5)$$

Here  $a_j$  — concentration of components of gas mixture,  $T$  — temperature of gas,  $\tau$  — time characterizing reaction rate. It follows from this that function  $E_1$  for assigned gas and form of nose depends on conditions of flow around and is a functional from distribution of pressure  $p_w$ . In limiting cases of balanced flow ( $\omega \rightarrow \infty$ ) and frozen flow ( $\omega \sim 0$ ) with respect to composition in initial section  $E_1$  depends only on local value of  $p$ .

In these limiting cases  $E_1 \sim p^{\gamma_0 - 1}$ , where  $\gamma_0$  effective adiabatic index in high-entropy shell. Since usually the difference  $\gamma_0 - 1$  is small, especially for stable dissociating air at high temperatures, then  $c_x^*$  in limiting cases  $\omega \sim 0$  and  $\omega \rightarrow \infty$  is changed along the generatrix of the lateral surface very slowly, especially if change of  $p_w$  is small (for instance, dulled cone, wedge). It is possible to expect that this circumstance — slow change of ratio  $c_x^*/c_x$  along lateral surface — occurs also in general moderate values of parameter  $\omega$ ; on a given stage we will take this as assumption and limitation of applicability of results presented below.

2. In the mathematical expression the accepted assumption signifies

$$\frac{dc_x^*}{dz} \sim \epsilon \ll 1 \quad (2.1)$$

where  $\epsilon = (\gamma_0 - 1)/\gamma_0$  for limiting cases  $\omega = 0$  and  $\omega \rightarrow \infty$ .

Let us assume that  $r_0 = \theta r_0^{(0)} + 1$ ,  $r_0^{(0)}(0) = 0$ . From equation (1.1) we have  $pR^{1+\gamma} \sim 1$ , therefore order of the ratio of  $I$  to the other term of the right side of equation (1.2) does not exceed  $IR/x$ . Then at sufficiently large distance from nose, where  $x \gg 1$ ,  $1 \ll R \ll x$ , in system (1.1), (1.2) it is possible to disregard  $I$  and, furthermore, to set  $r_0 = \theta r_0^{(0)}$ ,  $R(0) = 0$ . Let us introduce

$$s_1 = \lambda s, \quad r_1 = \lambda r, \quad R_1 = \lambda R, \quad r_0^{(0)} = \lambda r_0^{(0)}, \quad \lambda = (2/c_x^*)^{1/(1+\gamma)} \quad (2.2)$$

Then accurate to terms of order  $\epsilon$  system (1.1), (1.2) will take the form

$$\begin{aligned}
& \frac{1}{2} R_1^{1+\nu} r_R^2 J_1^{(0)} + \frac{p_w}{\gamma-1} [R_1^{1+\nu} - (\theta r_w^{(0)})^{1+\nu}] J_1^{(0)} = \\
& -1 + 2^\nu \theta \int_0^{x_1} p_w(r_{1w}^{(0)})' (r_{1w}^{(0)})^\nu dx_1 + \frac{R_1^{1+\nu}}{\gamma(\gamma-1)M^2} \\
& 2^\nu R_1^{1+\nu} r_R J_2^{(0)} = \int_0^{x_1} \left[ p(J_1^{(0)})^\nu - \frac{1}{\gamma M^2} \right] R_1^\nu dx_1 \quad (R_1(0) = 0)
\end{aligned} \tag{2.3}$$

where  $J_k^{(0)}$  are equal to  $J_k$ , if in the latter we set  $r_w = \theta r_w^{(0)}$ .

Equations (2.3) in accepted setting do not depend on processes in the high-entropy shell.

It follows from this that in variables (2.2) forms of shock waves  $R_1(x_1)$  and distribution of pressure  $p_w(x_1)$  for assigned  $\gamma$ ,  $M$  and  $\theta$  are identical for all affine bodies with form  $r_w^{(0)}(x_1)$  and coincide with those characteristics for an ideal gas. These characteristics obey particular cases of the law of similarity, known for an ideal gas [6]. Thus, for finite  $\theta$  in variables of similarity

$$R_2 = \theta^{1-\nu} R_1, \quad p_2 = p \theta^{-2}, \quad r_2 = \theta^{1-\nu} r_1, \quad x_2 = \theta^{1-\nu} x_1$$

for identical  $r_{1w}^{(0)}(x_1)$  flow depends only on parameters  $\gamma$  and  $M\theta$ . When  $\theta = 0$  there exists a universal dependence of  $R_1 M^{-2/(1+\nu)}$  and  $p M^2$  on  $\gamma$  and variable  $x_1 M^{-(2+\nu)/(1+\nu)}$ . Thus, the presented law of similarity excludes from criteria of similarity of basic characteristics of the flow around thin dulled bodies the requirement of similarity of equation of state of gas in high-entropy shell.

In the low-entropy region equations of motion in variables of similarity  $(x_1, r_1)$  and relationships on the shock wave do not contain other determining parameters besides  $M$ ,  $\gamma$ . Therefore, since assignment of shock wave completely determines flow in region of its influence, from coincidence of forms of shock waves  $R_1(x_1)$  should follow identical distribution of functions  $v(x_1, r_1)$ ,  $p(x_1, r_1)$  and  $\rho(x_1, r_1)$  in the region near the shock wave filled by flow lines proceeding through similar sections of shock waves. This similarity will be disturbed with approach to high-entropy layer, where distribution of parameters will depend on equation of state and in general will not be similar. In more strict consideration for similarity of flows outside high-entropy layer its boundaries  $r_{1\delta} = r_{1\delta} + \lambda \delta$ , where  $r_{1\delta}$  — thickness of layer. For similarity of flow in high-entropy shell, according to [7], in comparable flows functions  $s(\varphi) = \sin^2 \beta$  must be identical, where  $\beta$  — angle of inclination of shock wave at point of intersection of its

considered flow line, and function  $f(1) = p/\rho$  in equation of state of gas in this shell.

In the case of insignificant change of  $c_x^*$  along lateral surface (blunted cone, wedge under stable or frozen flow) from what has been presented it follows that flow around a dulled body with real properties of gas will be identical (with the exception of flow in a high-entropy shell) to flow around such a body by an ideal gas, but with another nose, having a drag coefficient equal to  $c_x^*$ .

For a stable process under assigned conditions of flow around 1,  $p/\rho$  and  $w$  in a high-entropy shell depend on  $p_w$  and parameter  $s$ . Curves of ratios  $c^0 = c_x^*/c_x$  for flow around a sphere by an ideal gas with  $M = \infty$ ,  $\gamma = 1.4$  (curve 1) and stable dissociating air when  $\rho_\infty = 3 \cdot 10^{-7} \text{ g/cm}^3$  and  $U = 5, 7.5, 10 \text{ km/sec}$  (curves 2, 3, 4) are shown in Fig. 1. In [8] it is shown that for a broad class of bodies functions  $s(\varphi)$  are close (exceptions are bodies of the flat disk or plate type when  $(\gamma - 1)^{1/2} \rightarrow 0$ ). Therefore Fig. 1 may be used for noses of other form.

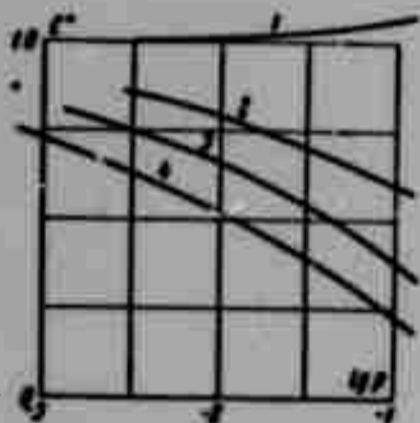


Fig. 1.

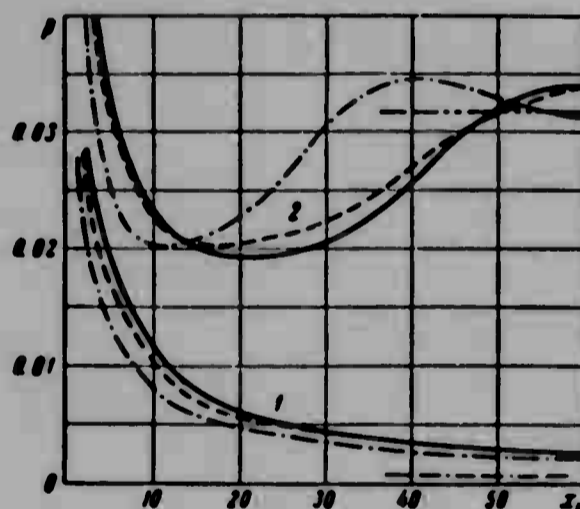


Fig. 2.

On Fig. 2 are plotted curves  $p_w(x)$  for the case of flow around cylinders blunted like a sphere  $\theta_0 = 0$  (curves 1) and cone with half angle  $\theta = 10^\circ$  (curves 2) by an ideal gas with  $\gamma = 1.4$  (solid lines), equilibrium dissociating air when  $\rho_\infty = 3 \cdot 10^{-7} \text{ g/cm}^3$ ,  $U = 10^4 \text{ m/sec}$  (dotted line) when  $M = 30$ . In the same place for comparison by dot-dash line are plotted initial curves for air in the same coordinates as for an ideal gas; the double dotted line with a point shows asymptotic values of magnitudes when  $x_1 \rightarrow \infty$ . As can be seen, in coordinates of similarity curves are close.

When using the law of similarity for recalculation of known distribution of pressure on other conditions of flow-around quantities  $c_x^*$ , given for instance on Fig. 1, depend on the desired distribution of pressure  $p_w(x)$ , and conversely, are beforehand unknown. However due to weak dependence of  $c_x^*$  on  $p_w$  the latter for these purposes need not be known exactly. For instance, for a blunted cone  $c_x^*$  can sufficiently accurately be determined by pressure on a sharp cone. In the extreme case,  $c_x^*$  and  $p_w$  can be found with the help of iterations.

The law of similarity extends to the case of an explosion, if gas differs from ideal only for finite mass  $m_0$  in the center of the explosive zone. Parameters with such an explosion with energy  $E_0$  coincide with parameters during explosion in an ideal gas with the same  $\gamma$ , but with energy

$$E = E_0 - \int_0^{m_0} \left( e' - \frac{p'}{\rho'(\gamma-1)} \right) dm$$

where  $e'$ ,  $p'$ ,  $\rho'$  - measured internal energy, pressure, and density. Determination of  $e$  and  $\rho'$  is the object of special investigation. The author thanks V. G. Pavlova for calculations connected with the work.

Submitted  
20 April 1964

#### Literature

1. V. V. Lunev. Motion in the atmosphere of a blunted body with large supersonic speeds. News AS USSR. Mechanics and machine building, 1959, No. 4.
2. V. V. Sychev. The theory of hypersonic flows of gas with shock waves of exponential form. PMM, 1960, Issue 3.
3. H. K. Cheng and A. L. Chang. On Numerical Comparison Between Inviscid Flow Past Slender Blunt Nosed Bodies. ARSJ, 1961, No. 7.
4. G. R. Inger. Similitude of Hypersonic Flows Over Slender Bodies in Nonequilibrium Dissociated Gases. AIAA, 1963, No. 1.
5. G. G. Chernyy. Analogy with explosion of hypersonic flow around a thin body blunted in front. Reports of Academy of Sciences of USSR, 1963, Vol. 151, No. 2.
6. G. G. Chernyy. Flow of gas with great supersonic speed. Fizmatgiz, Moscow, 1959.
7. V. V. Lunev. Law of similarity for hypersonic flow around thin bodies by viscous gas. AM, 1961, Issue 6.
8. V. V. Lunev. The form of shock wave during hypersonic flow around dull bodies. News AS USSR. OTN. Mechanics and machine building, 1964, No. 6.

**BLANK PAGE**

BREMSSTRAHLUNG OF AN ELECTRON DURING SCATTERING  
BY NEUTRAL ATOMS TAKING INTO ACCOUNT  
COLLISION CORRELATION

Yu. P. Rayzer

(Moscow)

By means of direct consideration of bremsstrahlung of an electron during collisions with neutral atoms taking into account correlation between collisions a formula is derived for emissivity, containing a frequency factor. Earlier this formula was derived only by indirect means through the coefficient of absorption, with the help of the Kirchhoff law.

1. In classical electrodynamics a moving electron radiates in spectral interval from  $\omega$  to  $\omega + d\omega$  energy

$$dE_\omega = -\frac{8\pi e^2}{3c^3} |\dot{w}_\omega|^2 d\omega \quad (1.1)$$

where  $w_\omega$  — Fourier component of acceleration  $w(t)$ . If duration of interaction of electron with atom  $\tau_s$  is much less than period of electromagnetic oscillations, more exactly, if  $\omega\tau_s \ll 1$ , then radiation during one elastic collision does not depend on frequency and is determined [1] only by the full change of velocity vector of the electron<sup>1</sup>

---

<sup>1</sup>Duration of collision  $\tau_s \sim r/a$ , where  $v$  — velocity of an electron,  $a$  — dimensions of atom. Condition  $\omega\tau_s \ll 1$  is executed for all frequencies  $\omega < mv^2/2\hbar$ , radiated by electrons whose energy does not exceed several eV, i.e., for thermal electrons in weakly ionized gas — practically always.

$$dE_{\omega} = \frac{2}{3\pi} \frac{e^2}{c^2} (\Delta v)^2 d\omega \quad (1.2)$$

It is known that formula (1.2) is convenient to obtain from (1.1), considering  $w(t) = \Delta v \delta(t)$ .

When collisions occur relatively rarely and average time between collisions  $\tau$  is such that  $\omega\tau \gg 1$ , separate acts of bremsstrahlung can be considered independent. Spectral radiation of electron per second  $dQ_{\omega}$  erg/sec is calculated simply by means of averaging (1.2) over scattering angles  $\theta$  and multiplication by number of collisions per second  $\nu = 1/\tau$ . During elastic scattering

$$\langle (\Delta v)^2 \rangle = 2v^2(1 - \langle \cos \theta \rangle) \quad (v - \text{velocity of an electron}) \quad (1.3)$$

Therefore

$$dQ_{\omega} = \frac{4}{3\pi} \frac{e^2 v_{\text{eff}}^2}{c^2} d\omega, \quad v_{\text{eff}} = v(1 - \langle \cos \theta \rangle) \quad (1.4)$$

(it is assumed that radiated energy is small as compared to energy of electron, so that velocity during scattering does not change).

If one were to find emissivity of an electron with the help of the Kirchhoff law and the known expression for coefficient of absorption of electromagnetic waves in a weakly ionized gas, where a basic role is played by the collision of electrons with neutral atoms [2], then we obtain formula [3]

$$dQ_{\omega} = \frac{4}{3\pi} \frac{e^2 v_{\text{eff}}^2}{c^2} \frac{\omega^2}{\omega^2 + v_{\text{eff}}^2} d\omega \quad (1.5)$$

which differs from (1.4) by the presence of frequency factor  $\omega^2/(\omega^2 + v_{\text{eff}}^2)$ .

As Ya. B. Zel'dovich noted, during radiation of frequencies  $\omega$ , comparable with frequency of collision  $\nu_{\text{eff}}$ , there exists a correlation between the individual collisions.

For the best understanding of origin and physical meaning of frequency factor in (1.5) not by indirect means through coefficient of absorption, but directly, by means of direct calculation of bremsstrahlung of an electron undergoing a large number of collisions  $N \rightarrow \infty$ . This will be done below.

2. Let us present, in accordance with condition  $\omega r_e \ll 1$ , acceleration of electron in the form

$$w(t) = \sum_{k=1}^N \Delta v_k \delta(t_k) \quad (2.1)$$

where  $t_k$  - moment of k-th collision,  $\Delta v_k$  - corresponding change of speed.

Radiation of an electron is determined by averaging over all collisions by square modulus of Fourier-component of acceleration

$$\langle |w_\omega|^2 \rangle = \left\langle \frac{1}{4\pi^2} \sum_{j=1}^N \sum_{k=1}^N (\Delta v_j \Delta v_k) e^{i\omega(t_j - t_k)} \right\rangle \quad (2.2)$$

Let us separate from the double sum terms with identical indices  $j = k$  and combine terms with identical pairs of indices.

$$\langle |w_\omega|^2 \rangle = \left\langle \frac{1}{4\pi^2} \sum_{j=1}^N \left\{ (\Delta v_j)^2 + 2 \sum_{k=j+1}^N (\Delta v_k \Delta v_j) \cos \omega(t_k - t_j) \right\} \right\rangle$$

On the average, not one of the collisions releases anything among the others, therefore in averaging the sum over  $j$  will be turned into  $N$  identical components, and in the sum over  $k$  the  $j$ -th collision can be taken for the initial, "zero," collision, and it is possible to conduct a time reading from it ( $j \rightarrow 0$ ,  $\Delta v_j \rightarrow \Delta v_0$ ,  $t_j \rightarrow t_0 \rightarrow 0$ ). As a result we will obtain

$$\langle |w_\omega|^2 \rangle = \frac{1}{4\pi^2} N \left\{ \langle (\Delta v_0)^2 \rangle + 2 \sum_{k=1}^N \langle (\Delta v_k \Delta v_0) \cos \omega t_k \rangle \right\} \quad (2.3)$$

Here the first factors in the components of the sum are averaged with respect to directions of speeds, and the second - by the times of collisions. To absence of correlation corresponds conversion of sum into zero.

Mean values of velocity of an electron after  $i$ -th collision  $v_{i+1}$  and change of speed  $\Delta v_i = v_{i+1} - v_i$  for a fixed direction of speed prior to collision  $v_i$  are equal to

$$\langle v_{i+1} \rangle = \mu v_i, \quad \langle \Delta v_i \rangle = -(1 - \mu) v_i \quad (\mu = \langle \cos \theta \rangle)$$

We will consecutively "contract" expression  $(\Delta v_k \cdot \Delta v_0)$ , averaging with respect to directions  $v_{k+1}$  for fixed  $v_k$ ,  $v_{k-1}$ , ...,  $v_0$ , then with respect to  $v_k$  for fixed

$v_{k-1}, v_{k-2}, \dots, v_0$ , etc. As a result we will obtain

$$\langle (\Delta v_k \Delta v_0) \rangle = - (1 - \mu)^2 \mu^{k-1} v^2 \quad (k = 1, 2, \dots) \quad (2.4)$$

(when  $k \rightarrow \infty$  this expression tends to zero: correlation between collisions distant in time, naturally, disappears).

Let us now average with respect to time

$$\langle \cos \omega t_k \rangle = \int_0^\infty P_k(t) \cos \omega t dt \quad (2.5)$$

where  $P_k(t) dt$  - probability that  $k$ -th collision will occur in the interval of time from  $t$  to  $t + dt$ . Obviously

$$P_k(t) dt = \int_0^t P_{k-1}(t') dt' P_1(t - t') dt$$

where probability of first collision after given  $P_1(t) dt = \nu e^{-\nu t} dt$ . This gives the formula<sup>1</sup>

$$P_k(t) dt = \frac{(\nu t)^{k-1}}{(k-1)!} e^{-\nu t} \nu dt \quad (2.6)$$

We will not calculate integral (2.5) and will place (2.4)-(2.6) in (2.3). The sum over  $k$  when  $N \rightarrow \infty$  is simply the expansion in a series of the exponential  $(\mu \nu t)$ . The integral obtained as a result of summation is equal to

$$\int_0^\infty e^{-(1-\mu)\nu t} \cos \omega t \nu dt = \frac{(1-\mu) \nu^2}{\omega^2 + (1-\mu)^2 \nu^2}$$

Considering that  $(1 - \mu)\nu = \nu_{\text{eff}}$ , we will find

$$\langle |E_\omega|^2 \rangle = \frac{1}{4\pi^2} N \left\{ 2r^2 (1 - \mu) - 2r^2 (1 - \mu) \frac{\nu_{\text{eff}}^2}{\omega^2 + \nu_{\text{eff}}^2} \right\}$$

Putting this expression in (1.1) and dividing  $dE_\omega$  by the time of process  $N/\nu$ , we will obtain for radiation in one second formula (1.5).

Thus, the interference of partial waves radiated during different collisions, on the average leads to decrease of intensity of total wave. This, as we saw, is

<sup>1</sup>Probability that in the interval from  $t$  to  $t + dt$  any collision will occur will occur, is equal.

$$\sum_k P_k(t) dt = \nu dt = \frac{dt}{\tau}$$

connected with the fact that the amplitudes of any two partial waves, which are determined by corresponding values  $\Delta v$ , on the average always are directed to opposite sides.

At high frequencies, when  $\omega^2 \gg v_{th}^2$  interference, on the average, naturally tends to zero and formula (1.5) is turned into (1.4).

The author sincerely acknowledged Ya. B. Zel'dovich for turning his attention to the effect of correlation.

Submitted  
22 April 1964

#### Literature

1. L. D. Landau and Ye. M. Lifshits. Field theory. Fizmatgiz, 1960.
2. V. L. Ginzburg. Propagation of electromagnetic waves in plasma. Fizmatgiz, 1960.
3. G. Bekefi, I. L. Hirshfield and S. C. Brown. The Kirchhoff law for plasma with non Maxwellian distribution. Phys. Fluids, 1961, Vol. 4, No. 2, p. 173.

**BLANK PAGE**

# MEASUREMENT OF FLOW RATE OF LIQUID IN A ROUND PIPE BY THE MAGNETOHYDRODYNAMIC METHOD

A. Ye. Yakubenko

(MOSCOW)

A connection is found between flow rate of liquid in a round pipe and potential difference on electrodes which are arcs of circumference, during a flow of conducting liquid with assigned profile of speed in transverse magnetic field.

Let us consider the flow of a conducting liquid in a round pipe of radius  $R_0$  with assigned profile of speed, depending only on  $r$

$$\mathbf{v} = V(r)\mathbf{e}_r, \quad V(R_0) = 0$$

Here  $z$  - coordinate along axis of pipe, but  $r$  and  $\theta$  - polar coordinates in a certain plane perpendicular to the axis of the pipe.

Subsequently we will assume that all magnitudes from coordinate  $z$  do not depend.

Let us assume that electrical current induced under action of uniform magnetic field

$$H = H_{\text{eff}}$$

is taken from arcs of the contour (electrodes) into an external circuit, as was shown on Fig. 1.

The problem consists of determination of the connection between potential difference on external

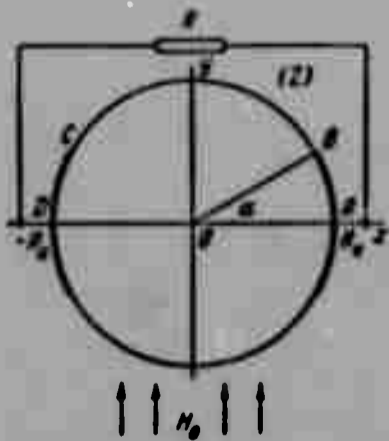


Fig. 1.

load R with flow rate of liquid in round pipe.

For solution of problem we write Ohm's law in polar coordinates

$$\begin{aligned} i_r &= s \left( -\frac{\partial \varphi}{\partial r} - \frac{V(r) H_0}{c} \cos \theta \right) \\ i_\theta &= s \left( -\frac{1}{r} \frac{\partial \varphi}{\partial \theta} + \frac{V(r) H_0}{c} \sin \theta \right) \end{aligned} \quad (1)$$

Here  $\varphi$  — potential of electrical field.

For determination of  $\varphi$  from continuity equation for density of electrical current we obtain

$$\Delta \varphi = -\frac{H_0 V'(r)}{c} \cos \theta \quad (2)$$

This equation is solved under the following boundary conditions:

$$\begin{aligned} \varphi &= -\varphi_0 \quad \text{when } r = R_0, \quad -\alpha < \theta < \alpha \\ \varphi &= \varphi_0 \quad \text{when } r = R_0, \quad \pi - \alpha < \theta < \pi + \alpha \\ \frac{\partial \varphi}{\partial r} &= 0 \quad \text{when } r = R_0, \quad \alpha < \theta < \pi - \alpha, \quad \pi + \alpha < \theta < 2\pi - \alpha \\ 2\varphi_0 &= RJ, \quad J = \int_{-\alpha}^{\alpha} i_r(R_0, \theta) R_0 d\theta \end{aligned} \quad (3)$$

Solution of equation (2) is sought in the form

$$\varphi = \Phi(r, \theta) + \frac{H_0}{c} \left[ \frac{r}{R_0^2} \int_0^{R_0} r V(r) dr - \frac{1}{r} \int_0^r r V(r) dr \right] \cos \theta \quad (4)$$

Here as is simple to check, function  $\Phi(r, \theta)$  will be harmonic.

Let us convert Ohm's law with the help of relationship (4)

$$\begin{aligned} i_r &= s \left[ -\frac{\partial \Phi}{\partial r} - \frac{H_0}{c} \left( \frac{1}{R_0^2} \int_0^{R_0} r V(r) dr + \frac{1}{r^2} \int_0^r r V(r) dr \right) \cos \theta \right] \\ i_\theta &= s \left[ -\frac{1}{r} \frac{\partial \Phi}{\partial \theta} + \frac{H_0}{c} \left( V(r) + \frac{1}{R_0^2} \int_0^{R_0} r V(r) dr - \frac{1}{r^2} \int_0^r r V(r) dr \right) \sin \theta \right] \end{aligned} \quad (5)$$

Let us consider analytic function

$$w(z) = u + iv = r \frac{\partial \Phi}{\partial r} - i \frac{\partial \Phi}{\partial \theta} \quad (z = r + iy)$$

To determine  $w(z)$  we obtain the following boundary value problem, which in

virtue of symmetry we solve for upper semicircle,

$$\begin{aligned} w &= 0 \quad \text{when } \theta = 0, \pi, \text{ and when } z = R_0 e^{i\theta} \text{ for } 0 < \theta < \alpha, \pi - \alpha < \theta < \pi \\ u &= -\frac{QH_0}{c\pi R_0} \cos \theta \quad \text{when } z = R_0 e^{i\theta} \text{ for } \alpha < \theta < \pi - \alpha \\ w(0, 0) &= 0 \quad \left( Q = 2\pi \int_0^{R_0} r V(r) dr \right) \end{aligned} \quad (6)$$

Here  $Q$  - flow rate of liquid in pipe.

Besides enumerated conditions of (6), functions  $u$  and  $v$  have to satisfy the condition

$$2\varphi_e = RJ \quad (7)$$

For  $2\varphi_e$  and  $J$  we have

$$2\varphi_e = \int_{-\pi}^{\pi} \frac{\partial \varphi(R_0, \theta)}{\partial \theta} d\theta = - \int_{-\pi}^{\pi} v(R_0, \theta) d\theta \quad (8)$$

$$J = 2R_0 \int_{-\pi}^{\pi} j_r(R_0, \theta) d\theta = -2\pi \left[ \int_{-\pi}^{\pi} u(R_0, \theta) d\theta - \frac{H_0 Q}{c\pi R_0} \sin \alpha \right] \quad (9)$$

Considering (8) and (9), from relationship (7) we obtain

$$\int_{-\pi}^{\pi} v(R_0, \theta) d\theta = 2\pi R \left[ \int_{-\pi}^{\pi} u(R_0, \theta) d\theta - \frac{QH_0}{c\pi R_0} \sin \alpha \right] \quad (10)$$

Thus, besides conditions (6), function  $w(z)$  should still satisfy condition (10).

For solution of problem (6), (10) we will depict semicircle of plane  $z$  on upper half-plane  $\zeta$  so that origin of coordinates passed into a point at infinity with the help of conformal mapping

$$\zeta = \xi + i\eta = -\frac{(z - R_0)^2}{4zR_0} \quad (11)$$

Points  $A, B, C, D, O$  of contour of semicircle of plane  $z$  will cross moreover into points lying on real axis of plane  $\zeta$  with coordinates  $A_1(0, 0), B_1(\xi_1 = -(\sin^2 \frac{1}{2}\alpha), 0), C_1(\xi_2 = (\cos^2 \frac{1}{2}\alpha), 0), D_1(1, 0), O_1(\infty, 0)$ . Using (11), we will obtain formulas connecting new variables with old on segment  $A_1D_1$

$$\xi = (\sin \frac{1}{2} \theta)^2, \quad \cos \theta = 1 - 2\xi$$

On plane  $\zeta$  we have a boundary value problem. To find in upper half-plane an analytic function satisfying the following boundary conditions on axis  $\xi$

$$\begin{aligned} v(\xi, 0) &= 0 & \text{when } \xi < \xi_1 \text{ or } \xi > \xi_2 \\ u(\xi, 0) &= \frac{QH_0}{c\pi R_0} (2\xi - 1) & \text{when } \xi_1 < \xi < \xi_2 \quad u(\infty) = 0 \end{aligned} \quad (12)$$

$$\int_{\xi_1}^{\xi_2} \frac{u(\xi, 0) d\xi}{\sqrt{\xi(1-\xi)}} = 2\pi R \left[ \int_{\xi_1}^{\xi_2} \frac{u(\xi, 0) d\xi}{\sqrt{\xi(1-\xi)}} - \frac{QH_0}{c\pi R_0} \sin \alpha \right] \quad (13)$$

Solution of the boundary value problem is obtained with the help of the formula of Keldysh-Sedov [1].

$$u(\zeta) = \frac{QH_0}{c\pi R_0} [2\zeta - 1 - 2\sqrt{(\zeta - \xi_1)(\zeta - \xi_2)}] + \frac{\gamma}{\sqrt{(\zeta - \xi_1)(\zeta - \xi_2)}} \quad (14)$$

Here by  $\sqrt{(\zeta - \xi_1)(\zeta - \xi_2)}$  is understood that branch of the function which when  $\eta = 0$  and  $\xi > \xi_2$  is taken with a plus sign.

Constant  $\gamma$  in (14) is determined from condition (13). As a result of simple computations we obtain

$$\gamma = \frac{1}{2} \frac{QH_0}{c\pi R_0} \frac{\sigma R [E(\sin \alpha) - \cos^2 \alpha K(\sin \alpha)] - E(\cos \alpha) + \sin^2 \alpha K(\cos \alpha)}{K(\cos \alpha) + \sigma R K(\sin \alpha)} \quad (15)$$

Here  $E(k)$  - full elliptic integral of the 2nd kind, and  $K(k)$  - full elliptic integral of the 1st kind.

By determination of  $\gamma$  solution of problem is finished. Let us find now with the help of the obtained solution electrical magnitudes in the external circuit.

For potential difference and full current by the formulas (8) and (7) we will find

$$2\varphi_0 = \frac{QH_0}{cR_0} \frac{\sigma R}{K(\cos \alpha) + \sigma R K(\sin \alpha)}, \quad J = \frac{QH_0 \sigma}{cR_0} \frac{1}{K(\cos \alpha) + \sigma R K(\sin \alpha)} \quad (16)$$

Formulas (16) give the desired connection between flow rate of liquid in pipe  $Q$  and electrical characteristics in external circuit.

We investigate the obtained formulas. When  $R \rightarrow \infty$ , which corresponds to the

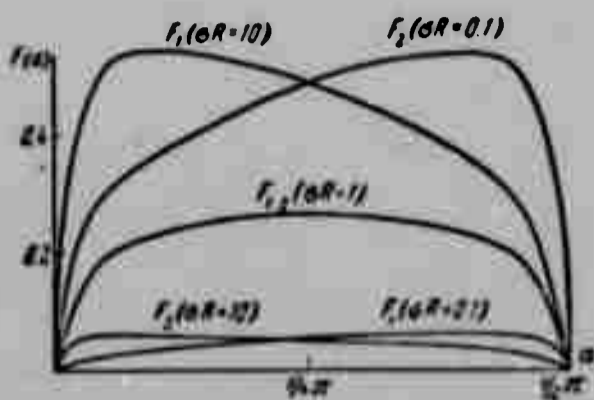


Fig. 2.

i.e., in the case of point electrodes. When  $\alpha = 0$

case of an open external circuit or inclusion in circuit of voltmeter with large resistance, we will obtain

$$2\varphi_e = \varepsilon = \frac{QH_0}{cR_0K(\sin \alpha)} \quad (17)$$

From formula (16) it is clear that maximum value of  $\varepsilon$  is attained when  $\alpha = 0$ ,

$$2\varphi_e = \frac{2QH_0}{c\pi R_0} \quad (18)$$

When  $\alpha = 1/2\pi$  the quantity  $\varepsilon$  attains a minimum which is equal to zero. Under finite final external load

$$2\varphi_e = 0 \text{ when } \alpha = 0 \text{ and } \alpha = 1/2\pi$$

Thus, for certain  $\alpha = \alpha(\sigma R)$  function  $2\varphi_e$  attains a maximum value.

Thus,  $\sigma R = 1$ , for instance, maximum value is attained when  $\alpha = 1/4\pi$ . On Fig. 2 are given graphs of functions

$$F_1(\alpha) = \frac{\sigma R}{K(\cos \alpha) + \sigma R K(\sin \alpha)}, \quad F_2(\alpha) = \frac{1}{K(\cos \alpha) + \sigma R K(\sin \alpha)}$$

for  $\sigma R = 0.1, 1$  and  $10$ .

It is simple to show that when  $\sigma R < 1$  the maximum of  $F_1(\alpha)$  will lie on segment  $(1/4\pi, 1/2\pi)$ , and when  $\sigma R > 1$  on segment  $(0, 1/4\pi)$ .

For finite angle  $\alpha$  the potential difference will increase from 0 when  $\sigma R = 0$  to  $\varepsilon$  when  $\sigma R \rightarrow \infty$ .

Full current will change from value

$$J = \frac{QH_0}{cR_0K(\cos \alpha)}$$

corresponding to short circuit, when  $\sigma R = 0$ , to zero when  $R \rightarrow \infty$ , when external circuit is opened.

Submitted  
26 March 1964

#### Literature

1. M. A. Lavrent'yev and B. V. Shabat. Methods of theory of functions of a complex variable. State Technical Press, 1958.

CERTAIN METHODS OF INVESTIGATION OF NONSTATIONARY  
PHENOMENA IN SHOCK TUBES

M. K. Berezkina, A. N. Semenov  
and M. P. Syshchikova

(Leningrad)

A shock tube can be used for study of a series of nonstationary problems of gas dynamics. One such problem is appearance and development of flow near a model, when flow is created by a passing shock wave. Process of forming of flow, consisting of reflection and diffraction of shock waves, formation of forward shock before body, appearance and development of boundary layer, forming of flow in trail after body, presents interest for the theory of nonstationary gas dynamic processes, and also has large practical value. Inasmuch as duration of processes is very small, special recording equipment is necessary. This article describes a simple shock tube, its equipment and methods used for investigation of such processes.

1. Construction and equipment of shock tube. A schematic diagram of an experimental installation is given on Fig. 1. The pipe has a right-angle cross section of  $150 \times 50$  mm. Length of channel is 5 m, length of chamber is 2 m. Channel of pipe is finished by a tank separated from the channel by a thin diaphragm.

Channel of pipe is rigidly fixed on a base. Chamber of high pressure and tank can shift along it. This displacement and simultaneously crowding of diaphragms (between tank and channel, between channel and chamber) are carried

out by two load screws with supports on end walls of tank and chamber.

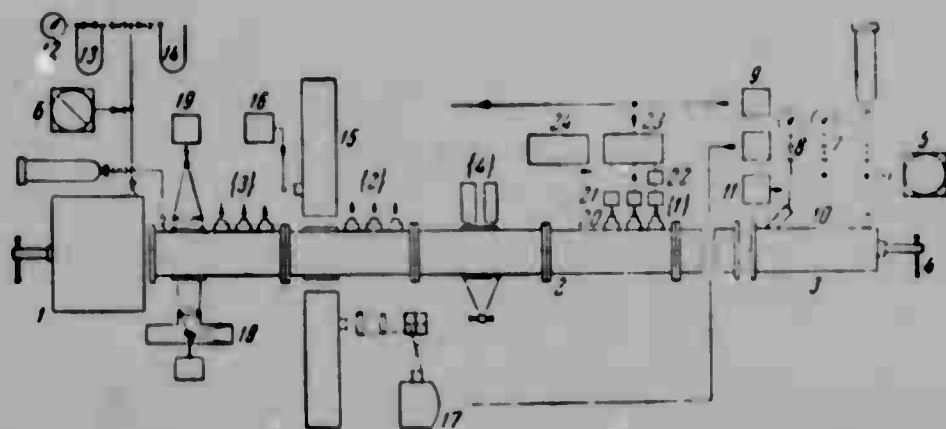


Fig. 1. Block diagram of experimental installation:  
 1 - tank; 2 - channel; 3 - chambers; 4 - cargo screw;  
 5, 6 - pumps; 7 - vacuum gage; 8 - manometer; 9 - feed  
 of camera relay; 10 - needle; 11 - needle feed;  
 12 - thermocouple vacuum gage; 13, 14 - butyric and  
 mercury manometers; 15 - shadow instrument IAB-451;  
 17 - high speed photorecorder ZhFR-1; 18 - installation  
 for high speed spark survey; 19 - piezotransducers;  
 21 - cathode follower; 22 - amplifier; 23 - oscillo-  
 graph OK-17M; 24 - generator of standard signals  
 GSS-6; {1}, {2}, {3} - piezoelectric station;  
 {4} - photoelectric stations.

Channel and chamber of pipe before being filled by their working gases are pumped out by fore pumps of type [VN-1M] (BH-1M) and [VN-2] (BH-2) to a pressure  $1 \cdot 10^{-2}$  mm Hg. Pump VN-1M is supplied by a gas ballast device, making it possible to evacuate gases with water vapor. Initial pressure of gas in pipe channel is recorded by thermocouple vacuum gage [VT-2] (BT-2) (range of measured pressures from  $1 \cdot 10^{-2}$  to 1 mm Hg), butyric manometer (from 1 to 50 mm Hg) and mercury manometer at pressures over 50 mm Hg.

Break of diaphragm between channel and chamber of pipe is made by a needle set into motion by an electromagnet. The presence of a needle makes it possible to reproduce initial conditions in chamber of shock tube with good accuracy.

Channel of pipe consists of a series of replaceable sections 1 m long each. Sections are equipped by stations to measure speed of front of shock wave.

To produce shadow pictures of the flow there are applied simple shadow photographs, a spark high speed survey, and a special setup for obtaining countdown profiles, using shadow instrument [IAB-451] (IAB-451) and driven photorecorder [ZhFR-1] (ЖФР-1).

2. Measurement of speed of front of shock wave. At the majority of stations speed of propagation of shock wave in channel of pipe is determined by the time during which a wave passes the distance between two piezo pressure transducers.

Every station consists of three piezotransducers.

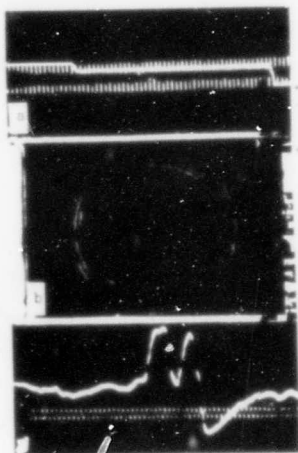


Fig. 1. Oscillograms for measurement of speed of front of shock wave: a - by piezotransducers; b - by photomultipliers; c - form of signal on PM.

Intensive signal of first piezotransducer starts the scan of oscillograph OK-17M. Preliminary starting of OK-17M permits considering fronts of pressure pulses on one beam of the oscillograph. Steepness of pulse edge of pressure is determined by dimensions of plate of barium titanate and speed of the shock wave proceeding past the piezoelement. The second beam of oscillograph OK-17M serves for registration of "oscillogram time marks" from generator of standard signals [GSS-6] (PCC-6). Accuracy of determination of interval of time is of order 1%. A typical oscillogram of signals from piezotransducers is shown on Fig. 2a.

The method of determination of speed of shock waves in shock tubes with the help of light screens is widely known [1]. Every light screen constitutes a small streak system consisting of a source of light, two objectives and a blade. Not less exact, but a simpler method of measurement of speed is the photoelectric method, the basis of which is the simple shadow method of registration of shock waves.

The setup contains two basic elements: point source of light and two photomultipliers. The point source of light is mercury quartz tube of super high pressure [DRSh-100] (ДРШ-100) with dimension of arc  $0.3 \times 0.3$  mm, working in steady state conditions. The light receivers are photomultipliers [PM-19] (ФЭУ-19) or [PM-33] (ФЭУ-33). Photomultiplier together with cathode follower is enclosed in a metallic light tight housing, face of which has adjustable slot [UF-1] (УФ-1). Selection of PM operating conditions is carried out by variation of supply voltage (stabilized rectifier [VS-16] (BC-16)), by width and height of slot. Conditions are controlled in magnitude of current on PM load. To lower natural noises of photomultiplier minimum supply voltage of PM is chosen (600-700 v). Width of slot is several

hundredth fractions of a millimeter, height of order 5 mm.

To measure interval of time between pulses from two photomultipliers chronograph [IV-22] (MB-22) was applied, in circuit of which are introduced certain changes. Positive pulse from first PM, passing first channel of broad band amplifier, is fed at "start" of chronograph and a spiral scanning starts. Positive pulse from second PM; passing through second channel of amplifier, enters circuit of extinguishing thyatron. Negative pulse from output of thyatron circuit is fed through high voltage separating capacity directly to modulator of tube [23L051] (23A051) of chronograph and extinguishes the scanning. Circuit of extinguishing thyatron completely repeat circuit of starting thyatron of chronograph. On Fig. 2b is given the oscillogram on which at the end of spiral is seen the break corresponding to pulse of extinguishing thyatron.

Form of pulse which appears on photomultiplier during motion of shadow image of front of shock wave along slot of PM, is shown on Fig. 2c. Pulse is registered on oscillograph OK-17M, frequency of oscillogram time marks  $f = 5$  Mc, speed of shock wave  $U = 1100$  m/sec, initial pressure of nitrogen  $p_0 = 200$  mm Hg.

In case of divergent beam of light the basis of measurement of speed is  $l$ , which is determined by formula

$$ml = (L_1 + L_2) + \frac{h}{d} (L_1 - L_2) \quad \left(m = \frac{a+b}{a}\right)$$

Here  $a$  — distance from source of light to axis of pipe,  $b$  — distance from axis of pipe to plane of slots of photomultipliers,  $h$  — half width of channel of pipe,  $(L_1 + L_2)$  — distance between PM slots. In case of symmetric location of slots ( $L_1 = L_2$ ) the base is determined by expression  $l = (L_1 + L_2)/m$ .

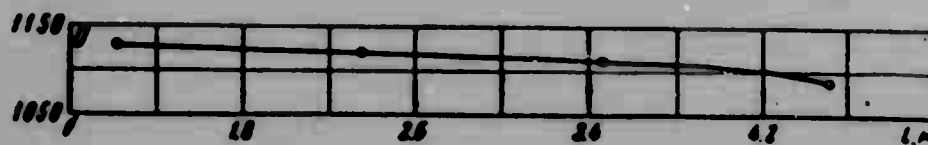


Fig. 3. Speed of front of shock wave with respect to length of pipe.

Figure 3 shows results of measurement of speed of front of shock wave on four stations along pipe. Every point of graph gives mean arithmetical value of speed

for twenty experiments at a constant value of initial parameters in the chamber and channel of pipe:  $p_4 = 15$  atm, hydrogen;  $p_0 = 200$  mm Hg, nitrogen. Mean deviation of measured values from average magnitudes depicted on Fig. 3 does not exceed 1%.

3. Methods of survey of flow of gas near model. To study flow of process in time simple shadow photography and a setup for synchronization of spark source of light were used, making it possible to obtain flow fields of model in exactly defined moments of time. A series of shadow photography were obtained in a number of experiments, maintaining constant initial conditions in chamber and channel of shock tube. Accuracy of process is very great.

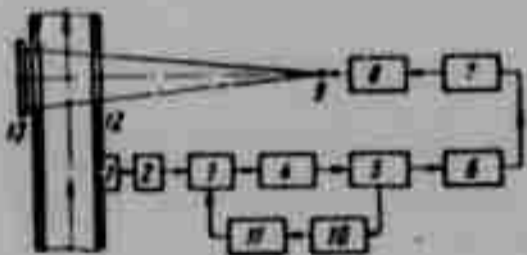


Fig. 4. Diagram of obtaining simple shadow photography:  
1 - piezotransducer; 2 - phase reversing cascade; 3 - amplifier; 4 - phantastron; 5 - cathode follower; 6 - differentiating circuit; 7 - block of forming and amplification; 8 - output cascade on thyatron; 9 - discharge interval; 10 - phase reversing amplification; 11 - block of single operation of circuit; 12 - shock tube; 13 - photographic plate.

Diagram for obtaining simple shadow photography is given on Fig. 4. It consists of photographic plate, point source of light, and block of synchronization. A spark discharge of around 1 microsecond occurs during discharge of 0.01-0.02 microfarad through spark gap and thyatron [TGI-1] (TFM-1) 325/16. A resistor of 150 ohm is connected in parallel to the spark gap. The capacitor is charged to a voltage of 16 kv.

Synchronization of spark source of light with studied process is carried out with the help of piezotransducer through phantastron delay circuit. Signal from piezotransducer, passing phase reversing cascade and amplifier, enters block of adjustable delay (phantastron, cathode follower, differentiating circuit). Delay time can be changed from 20 to 1500 microsecond on four ranges. After the block of forming and amplification the pulse is fed to the output thyatron; the pulse from the latter is used for ignition of high voltage thyatron, through which occurs discharge of basic illuminating spark. Phase reversing amplifier and block of single operation of circuit protect photographic plate of repeated exposing.

Calibration of phantastron circuit showed that dependence of time of delay on resistance is linear. Magnitude of delay is reproduced accurate to  $\pm 1\%$ . Graduation of phantastron periodically is checked using any meter of time.

GRAPHING NOT  
REPRODUCIBLE

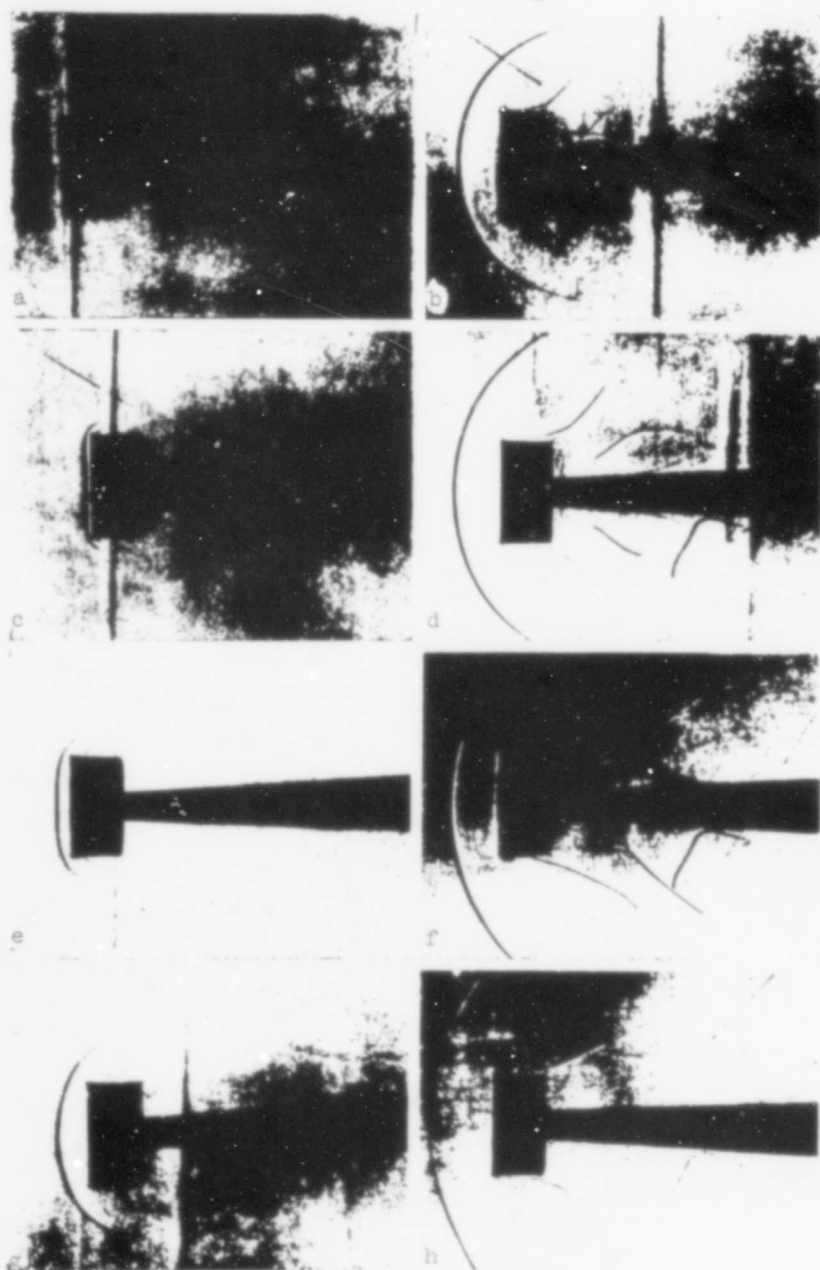


Fig. 5. Interaction of shock wave with cylinder in shock tube. Simple spark survey.

As an illustration on Fig. 5 are represented several photographings showing development of flow near cylinder in nitrogen at  $M_1 = 3.67$  for the shock wave.

Figure 6 shows time response of position of forward shock appearing before cylinder,

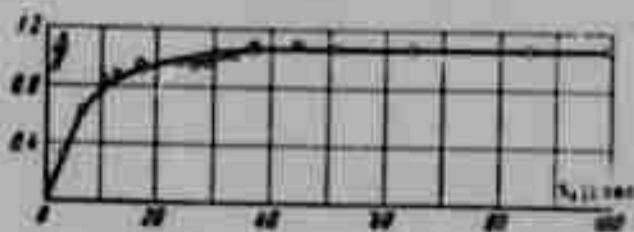


Fig. 6. Change of departure of forward shock in time. Method of simple spark survey.

obtained as a result of treatment of such a series of photography (Mach number of companion flow  $M_2 = 1.51$ ). By these photographings can be obtained data about change in time of form of shock wave, appearance and development of boundary layer, and many other characteristics of process.

More expedient is the creation of a spark installation with the help of which a certain number of consecutive snapshots of one and the same phenomenon can be obtained. In literature are described similar setups [2, 3]. When consecutive

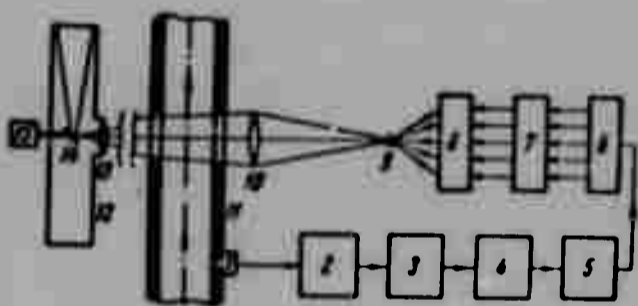


Fig. 7. Diagram of high speed spark survey: 1 - piezotransducer; 2 - entrance thyatron; 3 - trigger; 4 - master multivibrator; 5 - blocking generator; 6 - block of scaler; 7 - multichannel amplifier; 8 - spark device; 9 - source of light; 10 - objective; 11 - shock tube; 12 - photographic chamber; 13 - entrance objective of chamber; 14 - revolving mirror; 15 - motor.

flashes of spark occur in a single discharger the optical circuit of a photorecorder is the simplest. Therefore the diagram depicted on Fig. 7 was used.

Light from spark source (dimension 0.3 mm) is collected by objective 10.

Investigated object is in convergent cone of beams near the surface of this objective. Objective of chamber 6 (Industar-51) and revolving mirror give image of surveyed object on film. Film is motionless and is placed on internal side of cylindrical chamber at 187 mm from axis of rotation of mirror. Images of object are divided

by revolving mirror, plane of which forms  $45^\circ$  with optical axis of system. During the time of one turn of mirror image of object on film turns  $360^\circ$ . Mirror is set into rotation by a 0.1 kw electric motor with maximum number of turns  $1 \cdot 10^4 \text{ min}^{-1}$ . Using the reductor, a speed of rotation of mirror up to  $6 \cdot 10^4 \text{ min}^{-1}$  can be obtained, and linear speed of displacement of image on film will compose 1200 m/sec. Feed of electric motor of chamber and registration of speed of rotation were carried

# GRAPHIC NOT REPRODUCIBLE

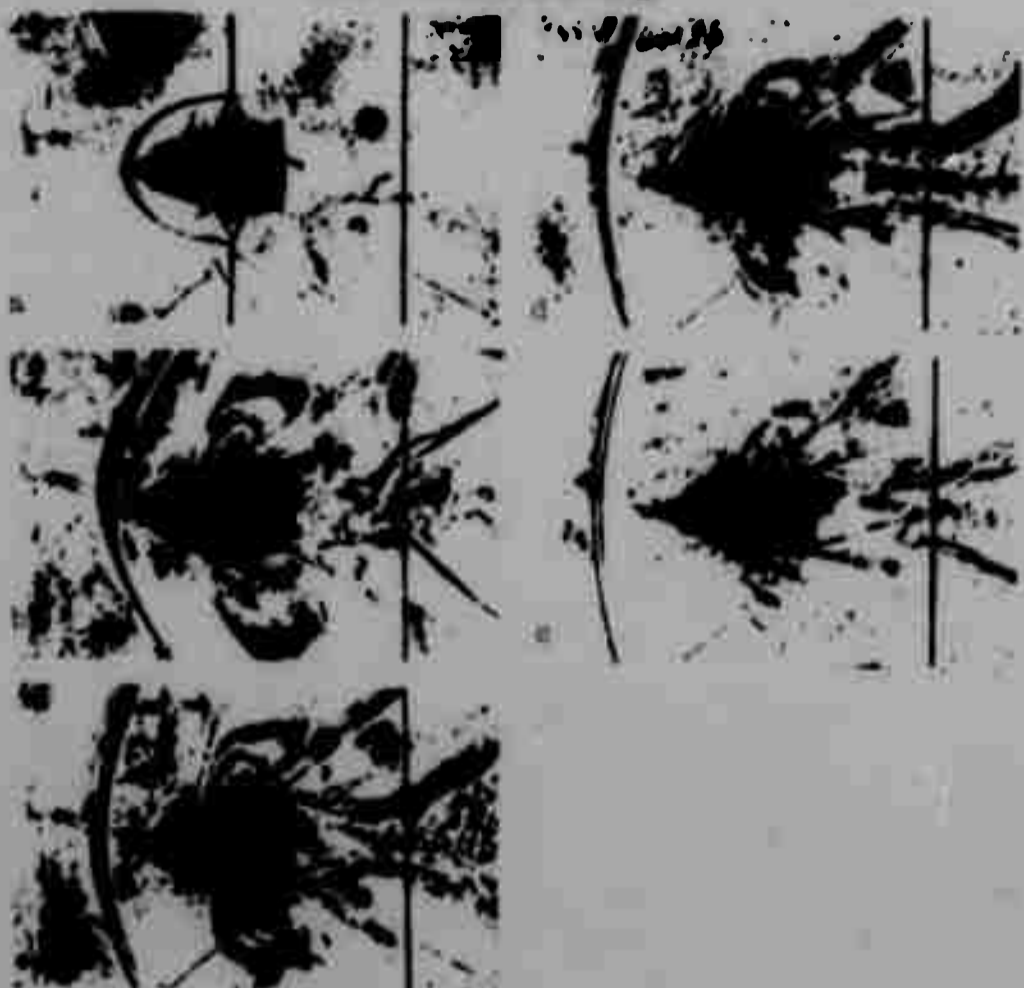


Fig. 8. Interaction of shock wave with two dimensional body in shock tube. High speed spark survey.

out with the help of panel of instrument [SFR-2M] (COP-2M).

The basis of the block of driving pulses, supplying frequency of high voltage pulses of spark illuminating device, is the circuit of the multichannel electron synchronizer proposed in [4]. Here is used an open scaler with a series of auxiliary devices. Frame frequency is exactly established from  $5 \cdot 10^3$  to  $4 \cdot 10^4$  frames per second with volume number of frames equal to 5. Number of frames can be increased at will.

Starting signal is fed to entrance thyatron of block. From load of thyatron is taken signal for starting of trigger, which locks the tube controlling the multivibrator. After that the master multivibrator begins to work, while the frequency generated by it can be easily changed in required limits. Pulses obtained on output of master multivibrator are formed and are strengthened according to the circuit of the blocking generator.

These pulses with steep fronts and amplitude of order from 150 to 200 v enter block of scaler where they divide.

Divided pulses are strengthened each in its own channel and are fed to spark arrangement.

Spark photographings, obtained on above described installation for high speed photographing, are shown in Fig. 8. Flow fields of two dimensional model in nitrogen are taken  $M_2 = 1.5$ . Frame frequency is 20,000 frames/sec, coefficient of increase is 0.25, diameter of image of field on film is 23 mm.

Survey of processes in shock tube requires driven recording equipment. This is because shock wave and flow in pipe are excited due to break of diaphragm, time of opening of which can be changed in relatively wide limits, whereas duration of processes is small and requires synchronization. Therefore it is practically difficult to use photorecorder SFR for high speed survey of processes in pipe. Instrument ZhFR-1 does not require synchronization of beginning of phenomenon with position of revolving mirror. Speed of registration can be modified from 1500 to 4000 m/sec at a speed of rotation of the mirror dodecahedron from 3000 to 80,000  $\text{min}^{-1}$ .

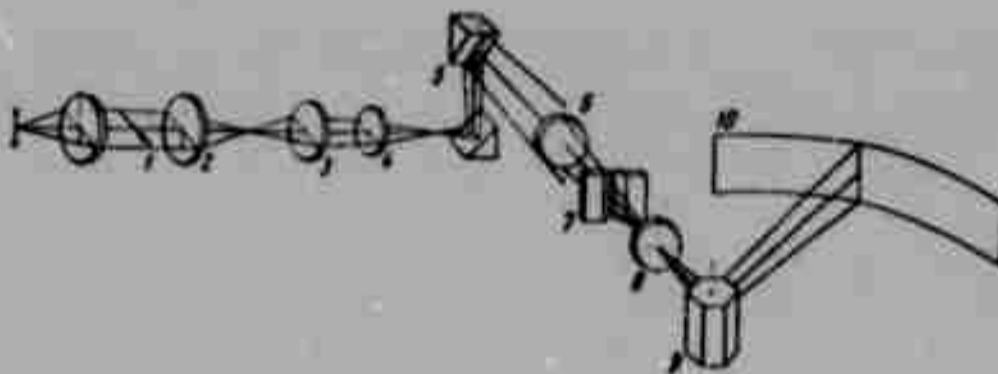


Fig. 9. Optical diagram of continuous scanning: 1 - model; 2 - objective IAB-451; 3-4 - objectives of transition optical system; 5 - turning mirrors; 6 - entrance objective ZhFR-1; 7 - slot ZhFR; 8 - internal objective ZhFR; 9 - mirror dodecahedron; 10 - photographic film.

Method of optical connection of shadow instrument IAB-451 and photorecorder ZhFR-1 is presented in [5]. However there is calculated an additional system specifying full use of field of instrument IAB-451 at coefficient of increase 0.1. For registration of process of formation of forward shock, when position of shock wave is changed within limits of several millimeters, the diagram given on Fig. 9 was used.

Image of model is constructed by objective 2 of shadow installation and objective 3 (Industar-51) of additional system near front focal plane of objective 4 [R02-2] (P02-2). Two flat mirrors 5 turn image of object  $90^\circ$  from horizontal plane in the vertical. Entrance objective ZhFR-1 gives image of object into a plane, vertical adjustable slot, which will cut from this image a narrow line up to 0.01 mm in width. Objective 8 with the help of revolving mirror 9 constructs an image of this line on the focal surface, where the disposed photographic film 10 is. During construction of transition system it is necessary to anticipate possibility of exact displacement of objective 4, since focusing of image on film is most conveniently produced by displacement of this objective. As source of light were used pulse tubes [IFK-20] (ИФК-20) and [IFK-50] (ИФК-50), working in rated conditions. At assigned parameters of optical system in frame ZhFR-1 is obtained image of small part of field IAB-451, but coefficient of increase is  $\sim 1$ .



Fig. 10. Change of departure of forward shock in time. Method  $(x, t)$ -scanning.

On Fig. 10 is given  $(x, t)$ -scanning, showing the change in time of the position of the forward shock before the sphere 10 mm in diameter in carbon dioxide with  $M_1 = 6.4$ .

By  $(x, t)$ -scannings can be obtained a whole series of data about flow in pipe and about forming of flow near model. One can determine speed of incident shock wave, flow rate in hot and cold zones, speed of contact surface, duration of flow of gas between shock wave and contact surface, mach number of flow with respect to magnitude of departure of forward shock in uniform zones of flow. It is possible to determine also time during which forward shock attains stationary position, and dependence of this time on parameters of shock wave creating motion of gas near model.

In conclusion we consider it necessary to note that development of separate units of shock tube and high speed camera was carried out by Ya. P. Andreyev and electronic equipment was developed by I. G. Pariyskiy, whom the authors thank.

Submitted  
14 March 1964

#### Literature

1. B. Khenshell. Certain aspects of the use of shock tubes in aerodynamic research. Collection. "Shock tubes," Publishing house of foreign literature, Moscow, 1962.
2. G. D. Salamandra, and others. Certain methods of investigation of fast flowing processes and their application to the study of the formation of a detonational wave. Publishing House of Academy of Sciences of USSR, Moscow, 1960.
3. A. A. Sakharov. High speed filming. Goskinoizdat, Moscow, 1950.
4. Yu. A. Dunayev and G. I. Mishin. Ballistic pipe for measurement of drag coefficients of bodies in free flight. News AS USSR, OTN, mechanics and machine building, 1959, No. 2.
5. A. S. Dubovik and N. M. Sitsinskaya. Application of high speed cameras jointly with shadow installations. Instruments of tech. experiment, 1962, No. 5.

**BLANK PAGE**

EXPERIMENTAL DETERMINATION OF SPEED OF PROPAGATION  
OF SOUND WAVES IN SATURATED WATER  
VAPOR AT HIGH PRESSURES

V. I. Avdonin, I. I. Novikov  
and Ye. P. Sheludyakov

(Novosibirsk)

In [1] were given results of measurements of speed of sound in saturated water vapor in the interval of temperatures 50-250°C. Recently it was possible to bring measurement up to 350°C. For these purposes the experimental installation described in [1, 2] was reconstructed, and a new experimental installation developed, also based on the method of standing waves.

In the reconstructed installation a new acoustic resonator was used, prepared together with a ridge from stainless steel of length 803.75 mm, internal diameter 65 mm, and thickness of wall 10 mm. In the ridge and wall of pipe of resonator adjacent to it were drilled holes 1.5 mm in diameter with a step of 10 mm for filling the resonator with saturated vapor.

A new autoclave designed for work with high temperatures and large pressures, was prepared in the form of a cylinder from stainless steel [IKh18N9T] (IX18H9T) of length 124.0 cm, internal diameter 12.0 cm, and thickness of wall 1.5 cm.

The container of the autoclave on one end has a hole closed by a cover with flanged joints, and on the second end it is hermetically sealed. Both flanges of the container are surveying. The first flange is fastened to the container on a screw thread, and the second flange serves as a cover and is fastened to the first by twelve bolts 20 mm in diameter from steel of increased strength.

Constant temperature in thermostat was ensured by two heating elements — basic and auxiliary (prior to reconstruction there was one heater). The basic heater is fed by stabilized voltage power of which varies from 0 to 6 kw depending upon the assigned temperature level in thermostat.

The second automatically regulated heater is established on a power from 0 to 0.5 kw. Adjustable power of second heater composes not more than 10% of the power of the basic heater. This permits using a low-inertia relay for adjustment of thermostat. Transducer of adjustment of temperature regulating liquid is a mercury contact thermometer, located near second heating element. Depending upon magnitude of temperature level one of set of contact thermometers was used with different limits of adjustment.

Regulating liquid in thermostat was intensely mixed by four mixers of propeller type, set into rotation by four electric motors located on cover of thermostat.

A simple and reliable control system of the thermostat made it possible to maintain a temperature in it with an accuracy of  $0.02^{\circ}\text{C}$ . Reliability of adjustment of thermostat is confirmed also by the fact that 4 copper constantan thermocouples, located in autoclave for measurement of gradient of temperature in it along length and radius, did not give a difference in readings of temperature with an accuracy of  $0.02^{\circ}\text{C}$ .

Measurement of temperature in autoclave was made by a 100-ohm platinum resistance thermometer and four copper constantan thermocouples on potentiometers [PMS-48] (PMC-48) and [PPTN-1] (ППТН-1) with an accuracy of  $0.02^{\circ}\text{C}$ .

During measurements below room temperature a water ice thermostat was used. From room temperature to  $120^{\circ}\text{C}$  the regulating liquid was mineral oil with small viscosity, and from  $120^{\circ}\text{C}$  and above — the oil "Vanor T."

Measurements of speed of sound in saturated steam at pressures higher than 1.5 atm (abs) included also measurements of pressure in autoclave by a loadpiston manometer [MP-60] (МП-60) or MP-600 of accuracy class 0.05 — depending upon magnitude of pressure. Obtained values of pressure with accuracy of instruments used for measurement of pressure coincided with tabular data [3] on curve of saturation corresponding to the measured temperatures.

The separating arrangement between autoclave and loadpiston manometer during measurement of pressure in autoclave was differential manometer [DM-6] (ДМ-6).

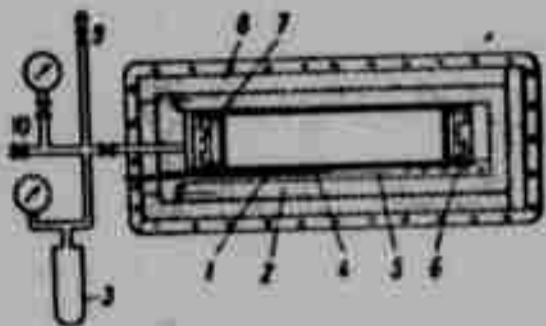


Fig. 1.

For measurement of difference of pressure, not compensated by loadpiston manometer, was applied electron differential transformer instrument [EPID-09] (ЭПИД-09) of accuracy class 2, with limits of measurement 45-180 mm Hg.

Measurement of frequency of generator is considerably improved by a scaling device with established standing wave in resonator. Measurements were conducted on new stabler audio-frequency oscillator [LIU-150] (ЛНУ-150).

Difficulties occurring during former measurements and caused mainly by disturbance of electrical contact in coils of dynamic loudspeaker and microphone after reconstruction, were considerably removed. The use of heavy gage cast wire in the glass insulation made it possible to increase period of work of dynamic loudspeaker and microphone by a few times. A new form with motionless coils, used in this work, especially increased period of duty of transducers at high temperatures and large pressures.

The new experimental installation is schematically shown on Fig. 1.

The resonator is pipe 1 from stainless steel of brand IKh18N9T with internal diameter 34, length 566 and thickness of wall 2.5 mm. Resonator was placed in horizontally located autoclave 2 of internal diameter 50 and length 650 mm. Autoclave was flooded by 0.5-1.2 liter distilled water. With heating of autoclave level of water dropped. To increase level water was added to vessel 3. Before filling the autoclave was thoroughly pumped out and airtightness was checked. After filling the autoclave was heated to 80-90°C, and at this temperature for degasification of the water evacuation of steam volume of autoclave was carried out. Cleanness of vapor was controlled by coincidence of pressure of saturation with tabular. Pressure was measured in various ranges by standard manometers on 25, 160 and 250 kg/cm<sup>2</sup> of accuracy class 0.35. Temperature was measured by platinum-rhodium - platinum thermocouple 4 with potentiometer PMS-4C and galvanometer M17/4. Thermocouple was placed in case 5. Sound waves in resonator were created by telephone 6. Fixation of standing wave in resonator was carried out with power of microphone 7. Wires from telephone and microphone were brought through special

lead-ins in cover of autoclave. Telephone and microphone are arranged in the following way. In body from stainless steel was a strengthened electromagnet, consisting of a permanent magnet with pole pieces and coils set on them. With small gap above pole pieces of core was disposed diaphragm from permendur with diameter 35.5 and thickness 0.35 mm.

On the permanent magnet, tips, and diaphragm by galvanic means was deposited a film of chromium. For coil of telephone was used Nichrome wire of diameter 0.8 mm, isolated by tape from teflon-4. Resistance of coil was 6 ohm, number of turns - 20.

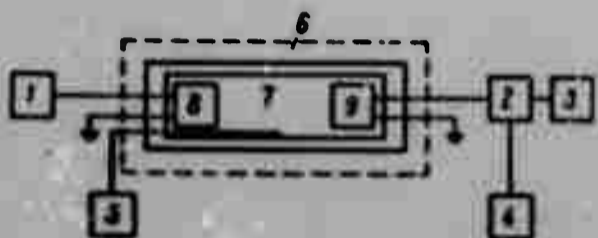


Fig. 2.

Coil of microphone was wound by Nichrome wire 0.15 mm in diameter, also isolated by tape from teflon-4. Resistance of coil was 80 ohm, number of turns - 70. For thermodynamic equilibrium before measurement temperature of autoclave was held for 30

minutes accurate to  $0.1^{\circ}\text{C}$ . Autoclave was placed in thermostat 8, constituting a copper block with internal diameter 100, external 150, length 770 mm, bounded from the ends by copper covers. Heating of thermostat was produced with the help of three electrical heaters (two -- from ends and one -- along length of thermostat). Control of temperature in copper block was carried out by a series of Chromel-Alumel thermocouples. Adjustment of temperature was carried out by means of change of current in heaters with the help of autotransformers. General block diagram of installation is shown in Fig. 2, where 1 - audio-frequency oscillator; 2 - amplifier; 3 - oscillograph; 4 - feed unit of amplifier; 5 - potentiometer; 6 - autoclave; 7 - interferometer; 8 - telephone; 9 - microphone.

Measurements on installation were produced in the following way. Changing frequency of sound generator, and feed oscillation on telephone, 8-9 maxima were observed on oscillograph. Each of these maxima corresponded to standing sound wave in resonator; first maximum corresponded to half wave length, second - whole wave, etc. Speed of sound was determined by the formula

$$c = 2L / n$$

where  $c$  - speed of sound in [m/sec],  $L$  - distance between telephone and microphone in [m],  $f$  - frequency of sound waves in [cps],  $n$  - number of half waves in resonator.

Four series of measurements were conducted under different conditions.

In the first series of experiments volume of resonator of the part of telephone and microphone was bounded by diaphragms with holes 4 mm in diameter for acoustic connection of telephone and microphone. Distance was measured between diaphragms for 20°C and was  $L = 540.0$  mm.

In the second series of experiments diaphragms were absent. Distance between telephone and microphone was determined by earlier obtained data on speed of sound in saturated water vapor at 200°C and was  $L = 559.0$  mm.

In the third and fourth series of experiments diaphragms also were absent, and distance was measured directly between diaphragms at 20°C and turned out to be  $L = 553.0$  mm.

Results of measurements of all four series of experiments were plotted on one curve. Maximum spread of points was 0.4%.

Table 1.

$t, ^\circ\text{C}$	$c$	$t, ^\circ\text{C}$	$c$	$t, ^\circ\text{C}$	$c$	$t, ^\circ\text{C}$	$c$	$t, ^\circ\text{C}$	$c$	$t, ^\circ\text{C}$	$c$
0.03	408	30.20	430	77.68	459	141.48	489	204.31	505	263.41	497
0.85	411	32.10	431	82.11	461	145.29	490	209.86	506	267.58	496
3.16	411	35.14	433	87.25	464	148.34	492	215.17	506	272.32	494
4.37	412	37.99	434	93.02	467	153.56	493	220.23	505	276.77	493
5.62	413	43.22	438	98.27	469	157.64	495	221.50	505	281.43	490
8.07	415	46.06	440	101.40	471	162.33	496	226.59	505	285.90	489
10.05	416	48.70	441	105.78	474	166.15	497	229.71	505	289.51	486
12.54	417	52.39	444	110.45	475	171.46	499	234.92	504	292.00	485
14.28	419	56.05	446	114.73	478	174.19	499	240.13	503	293.89	483
17.04	421	59.47	448	118.91	480	179.61	500	240.84	503	297.08	482
19.83	423	63.94	451	123.96	482	185.80	502	246.35	502	300.21	479
20.65	423	68.12	453	126.03	483	189.97	503	250.49	501	302.67	478
23.16	425	71.09	455	131.87	486	194.75	504	256.76	500	306.82	474
26.01	427	74.52	457	137.26	487	200.24	505	260.30	498	310.55	470

Results of measurements of speed of sound in saturated water vapor depending upon temperatures are given in Tables 1 and 2 and graphically on Fig. 3, where curve is constructed according to the empirical formula

$$c = \sqrt{1.25gP_s v''}$$

where  $P_s$  - pressure of saturated vapor [ $\text{kg}/\text{m}^2$ ],  $v''$  - specific volume of saturated vapor [ $\text{m}^3/\text{kg}$ ]; light points are obtained by measurements on new installation, and dark - on the reconstructed installation. Table 1 contains results of measurement on the reconstructed, and Table 2 - on the new installation.

Table 2.

t, °C	c	t, °C	c	t, °C	c
150	487	220	507	290	487
160	491	230	508	300	481
170	495	240	505	310	472
180	500	250	503	320	461
190	503	260	501	330	448
200	505	270	497	340	433
210	506	280	493	350	415

On Fig. 3 it is clear that experimental points in interval of temperatures from 150 to 350°C lie well on empirical curve [1] shown in (1).

At temperatures up to 320°C experimental data will well agree with the theoretical formula obtained by I. I. Novikov [4], for rate of propagation of sound in a two-phase system, which verifies the small jump of the speed of sound on the saturation curve at these temperatures.

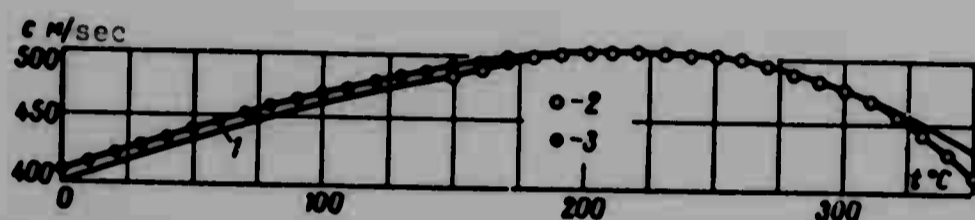


Fig. 3.

At large temperatures magnitude of jump of speed becomes so considerable that to disregard it is impossible, and therefore to the speed of sound, calculated by the shown formula, it is necessary to add magnitude of jump of speed of sound during transition through curve of saturation. Analysis of accuracy of measurements, and also control experiments with air show that error of measurement of speed of sound in the whole range of temperatures does not exceed 1%.

Comparison of results of measurements on both installations, and also with those obtained earlier [1] shows a good coincidence of measured values of speed of sound

Submitted  
4 May 1964

#### Literature

1. V. I. Avdonin and I. I. Novikov. Speed of sound on curve of vapor liquid phase equilibrium. PMTF, 1960, No. 1, p. 58.
2. A. V. Avdonin. Measurement of speed of propagation of sound waves in saturated water vapor. Jour. tech. physics, 1960, Vol. 30, No. 10, p. 1245.
3. M. P. Vukalovich. Thermodynamic properties of water and steam, 6th edition, Mashgiz, Moscow-Berlin, 1958.
4. I. I. Novikov. Adiabatic index of saturated steam. Reports Academy. Academy of Sciences of USSR, 1948, Vol. 9, No. 8, p. 1425.

# NONSTATIONARY RADIANT-CONVECTION HEAT EXCHANGE ON RECTANGLE

A. L. Burka

(Novosibirsk)

We consider the boundary value problem for a right angle region  $[0 \leq x \leq L; 0 \leq y \leq l]$  with mixed boundary conditions, including convection and radiant fluxes. (Ambient temperature is assumed equal to zero.)

In linear approximation analytic solution is obtained for dimensionless radiant fluxes of heat. Mathematical formulation of problem is recorded in the following way:

$$\frac{\partial T}{\partial \tau} = a \left( \frac{\partial^2 T}{\partial x^2} + \frac{\partial^2 T}{\partial y^2} \right) \quad (0 < x < L, \quad 0 < y < l, \quad 0 < \tau < \infty) \quad (1)$$

$$\left( \frac{\partial T}{\partial x} - hT \right)_{x=0} = 0, \quad \left( \frac{\partial T}{\partial x} + hT \right)_{x=L} = 0 \quad (2)$$

$$\left( \frac{\partial T}{\partial y} \right)_{y=0} = E_1(x, 0, \tau) = H [T_1^4(x, 0, \tau) - T^4(x, 0, \tau)] \quad (3)$$

$$\left( \frac{\partial T}{\partial y} \right)_{y=l} = E_2(x, l, \tau) = H [T_2^4 - T^4(x, l, \tau)] \quad \left( H = \frac{\sigma_0}{\lambda_0} \right) \quad (4)$$

$$T(x, y, 0) = T_0$$

Here  $E_1, E_2$  - ratio of resultant radiation fluxes to coefficient of thermal conduction,  $a$  - coefficient of temperature transfer,  $T_0$  - initial temperature of region,  $T_1, T_2$  - temperatures of sources of radiation,  $h$  - relative coefficient of

heat radiation,  $\sigma_0$  - radiation factor of ideal black body,  $\lambda_0$  - coefficient of thermal conduction. Below is considered the approximate solution of a system from two nonlinear integral equations relative to resultant radiation densities on sides of rectangle.

Applying Laplace transform to (1)-(4), we obtain general solution of problem in representations

$$\begin{aligned}
 u(x, y, p) &= \sum_{n=1}^{\infty} \left[ \frac{f_n}{\gamma_n^2} + \frac{1}{N} \frac{\operatorname{ch} \gamma_n y}{\gamma_n \operatorname{sh} \gamma_n l} \int_0^L E_2^*(\xi, l, p) X_n(\xi) d\xi - \right. \\
 &\quad \left. - \frac{1}{N} \frac{\operatorname{ch} \gamma_n (y-l)}{\gamma_n \operatorname{sh} \gamma_n l} \int_0^L E_1^*(\xi, 0, p) X_n(\xi) d\xi \right] X_n(x) \\
 u(x, y, p) &= \int_0^{\infty} T(x, y, \tau) e^{-p\tau} d\tau, \quad \gamma_n = \left( \lambda_n^2 + \frac{p}{a} \right)^{1/2} \\
 E_1^*(x, 0, p) &= \int_0^{\infty} E_1(x, 0, \tau) e^{-p\tau} d\tau, \quad E_2^*(x, l, p) = \int_0^{\infty} E_2(x, l, \tau) e^{-p\tau} d\tau
 \end{aligned} \tag{5}$$

Here  $f_n$  - coefficient of decomposition  $T_0/a$  according to eigenfunctions  $X_n(x)$  corresponding to uniform problem,  $X_n(x)$  constitute nontrivial solutions of equation  $X''(x) + \lambda^2 X(x) = 0$ , satisfying boundary conditions

$$X'(0) - hX(0) = 0, \quad X'(L) + hX(L) = 0$$

These solutions exist for all values  $\lambda_n$  - roots of equation  $\operatorname{ctg} \lambda L = 1/2(\lambda/h - h/\lambda)$ , and have form

$$X_n(x) = \sin \left( \lambda_n x + \operatorname{arc} \operatorname{tg} \frac{\lambda_n}{h} \right) \quad (n = 1, 2, 3, \dots)$$

"Operational" temperatures on sides  $y = 0$  and  $y = l$  are determined

$$\begin{aligned}
 u(x, 0, p) &= \sum_{n=1}^{\infty} \left[ \frac{f_n}{\gamma_n^2} + \frac{1}{N} \frac{1}{\gamma_n \operatorname{sh} \gamma_n l} \int_0^L E_2^*(\xi, l, p) X_n(\xi) d\xi - \right. \\
 &\quad \left. - \frac{1}{N} \frac{\operatorname{ch} \gamma_n l}{\gamma_n \operatorname{sh} \gamma_n l} \int_0^L E_2^*(\xi, 0, p) X_n(\xi) d\xi \right] X_n(x)
 \end{aligned} \tag{6}$$

$$\begin{aligned}
 u(x, l, p) &= \sum_{n=1}^{\infty} \left[ \frac{f_n}{\gamma_n^2} + \frac{1}{N} \frac{\operatorname{ch} \gamma_n l}{\gamma_n \operatorname{sh} \gamma_n l} \int_0^L E_2^*(\xi, l, p) X_n(\xi) d\xi - \right. \\
 &\quad \left. - \frac{1}{N} \frac{1}{\gamma_n \operatorname{sh} \gamma_n l} \int_0^L E_1^*(\xi, 0, p) X_n(\xi) d\xi \right] X_n(x), \quad N = \int_0^L X_n^2(x) dx
 \end{aligned} \tag{7}$$

Applying to (6) and (7) inverse Laplace transformation we find true temperatures on sides of rectangle and express them through resultant flows

$$\left(T_1 + \frac{E_1}{H}\right)^{1/4} = \frac{1}{2\pi i} \int_{\epsilon-i\infty}^{\epsilon+i\infty} u(x, 0, p) e^{pt} dp, \quad \left(T_2 - \frac{E_2}{H}\right)^{1/4} = \frac{1}{2\pi i} \int_{\epsilon-i\infty}^{\epsilon+i\infty} u(x, l, p) e^{pt} dp \quad (8)$$

Expressions (8) represent a system from two nonlinear integral equations relative to resultant flows  $E_1, E_2$ . Its solution in closed form is impossible.

As parameters, with respect to which linearization of system (8) is carried out, ratios resultant radiation fluxes to incident  $E_1/HT_1^4$  and  $E_2/HT_2^4$  is taken. Below is considered the case when these ratios in any moment of time are essentially less than unity. Taking this into account, we expand left parts (8) in series and will be limited to the first two terms of the expansion. Passing to "operational" radiation fluxes and assuming legality of change of order of summation and integration in (8), we obtain

$$\begin{aligned} \varphi_1^*(x, 0, p) &= -\frac{T_1}{pT_0} + 2h \sum_{n=1}^{\infty} \frac{X_n(x)}{\gamma_n^2 \omega_n} + \\ &+ \alpha \int_0^L \sum_{n=1}^{\infty} \frac{X_n(x) X_n(\xi)}{N \gamma_n \operatorname{sh} \gamma_n l} \varphi_2^*(\xi, l, p) d\xi - \beta \int_0^L \sum_{n=1}^{\infty} \frac{X_n(x) X_n(\xi)}{N \gamma_n \operatorname{th} \gamma_n l} \varphi_1^*(\xi, 0, p) d\xi \\ \varphi_2^*(x, l, p) &= \frac{T_2}{pT_0} - 2h \sum_{n=1}^{\infty} \frac{X_n(x)}{\gamma_n^2 \omega_n} - \alpha \int_0^L \sum_{n=1}^{\infty} \frac{X_n(x) X_n(\xi)}{N \gamma_n \operatorname{th} \gamma_n l} \varphi_2^*(\xi, l, p) d\xi + \\ &+ \beta \int_0^L \sum_{n=1}^{\infty} \frac{X_n(x) X_n(\xi)}{N \gamma_n \operatorname{sh} \gamma_n l} \varphi_1^*(\xi, 0, p) d\xi \end{aligned} \quad (9)$$

Here

$$\varphi_1^*(x, 0, p) = \frac{E_1^*}{4HT_0 T_1^3}, \quad \varphi_2^*(x, l, p) = \frac{E_2^*}{4HT_0 T_2^3}, \quad \alpha = \frac{4HT_1^3}{4HT_0 T_2^3}, \quad \omega_n = \lambda_n N \sqrt{\lambda_n^2 + h^2}$$

Expressions (9) constitute a system from two line integral equations of Fredholm type of the second kind with symmetric nuclei. To such a system is applicable the theorem of Gilbert-Schmidt for equations with symmetric nuclei [1], and the actual solution can be obtained in analytic form.

Multiplying (9) by  $X_n(x) dx$  and integrating both equations by  $x$  in the interval  $(0, L)$ , we bring system (9) in force of orthonogality of eigenfunctions  $X_n(x)$  on interval  $(0, L)$  to algebraic system

$$\begin{aligned} \left(1 + \frac{\beta}{\gamma_n \operatorname{th} \gamma_n l}\right) A_1 - \frac{\alpha}{\gamma_n \operatorname{sh} \gamma_n l} A_2 &= \frac{2hN}{\omega_n} \left(\frac{1}{\alpha \gamma_n^2} - \frac{T_1}{pT_0}\right) \\ \frac{\beta}{\gamma_n \operatorname{sh} \gamma_n l} A_1 - \left(1 + \frac{\alpha}{\gamma_n \operatorname{th} \gamma_n l}\right) A_2 &= \frac{2hN}{\omega_n} \left(\frac{1}{\alpha \gamma_n^2} - \frac{T_2}{pT_0}\right), \quad A_k = \int_0^L \varphi_k^*(\xi, p) X_n(\xi) d\xi \end{aligned} \quad (10)$$

Here  $A_k$  — unknown Fourier coefficients of expansion of function  $\varphi_k^0(x, p)$  by eigenfunctions  $X_n(x)$ , and  $k = 1, 2$ . Determining  $A_1$  and  $A_2$  from (10) and substituting in (9), we obtain the solution for "operational" flows in closed form

$$\varphi_1^*(x, 0, p) = -\frac{T_1}{pT_0} + \frac{2h}{\alpha} \sum_{n=1}^{\infty} \frac{X_n(x)}{\gamma_n^2 \omega_n} + \frac{2h}{\alpha T_0} \sum_{n=1}^{\infty} \frac{F_1(\gamma_n) X_n(x)}{\omega_n} \quad (11)$$

$$\varphi_2^*(x, l, p) = \frac{T_2}{pT_0} - \frac{2h}{\alpha} \sum_{n=1}^{\infty} \frac{X_n(x)}{\gamma_n^2 \omega_n} - \frac{2h}{\alpha T_0} \sum_{n=1}^{\infty} \frac{F_2(\gamma_n) X_n(x)}{\omega_n} \quad (12)$$

$$F_1(\gamma_n) = \frac{\alpha(\delta \gamma_n^2 + \lambda_n^2 T_0) \operatorname{sh} \gamma_n l + \alpha(\delta \gamma_n^2 + \lambda_n^2 T_0) \gamma_n + \beta(\delta \gamma_n^2 + \lambda_n^2 T_0) \gamma_n \operatorname{ch} \gamma_n l}{\gamma_n^2 (\gamma_n^2 - \lambda_n^2) (\gamma_n^2 \operatorname{sh} \gamma_n l + \alpha \operatorname{sh} \gamma_n l + q \gamma_n \operatorname{ch} \gamma_n l)} \quad (13)$$

$$F_2(\gamma_n) = \frac{\alpha(\delta \gamma_n^2 + \lambda_n^2 T_0) \operatorname{sh} \gamma_n l + \beta(\delta \gamma_n^2 + \lambda_n^2 T_0) \gamma_n + \alpha(\delta \gamma_n^2 + \lambda_n^2 T_0) \gamma_n \operatorname{ch} \gamma_n l}{\gamma_n^2 (\gamma_n^2 - \lambda_n^2) (\gamma_n^2 \operatorname{sh} \gamma_n l + \alpha \operatorname{sh} \gamma_n l + q \gamma_n \operatorname{ch} \gamma_n l)} \quad (14)$$

( $\delta = T_1 - T_0$      $\delta = T_2 - T_0$      $\alpha = \alpha\beta$      $q = \alpha + \beta$ )

During inverse Laplace transformation finding the originals of the first two terms of expressions (11) and (12) does not cause difficulties

$$\frac{T_1}{pT_0} + \frac{T_2}{pT_0} \cdot \frac{T_2}{pT_0} + \frac{T_2}{T_0} \cdot \frac{2h}{\alpha} \sum_{n=1}^{\infty} \frac{X(x)}{\gamma_n^2 \omega_n} + 2h \sum_{n=1}^{\infty} \frac{X_n(x)}{\omega_n} e^{-\alpha \lambda_n \tau} \quad (15)$$

Original  $F_k(\gamma_n)$  ( $k = 1, 2$ ) is determined by the formula

$$f_k(\tau) = \frac{e^{-\alpha \lambda_n \tau}}{2\pi i} \int_{-\infty}^{+\infty} F_k(\gamma_n) e^{s \gamma_n \tau} d(\alpha \gamma_n^2) \quad (16)$$

After change of variables  $s = \alpha \gamma_n^2$  expression (16) takes the form

$$f_k(\tau) = \frac{e^{-\alpha \lambda_n \tau}}{2\pi i} \int_{-\infty}^{+\infty} F_k(s) e^{s \tau} ds \quad (k = 1, 2) \quad (17)$$

Here

$$F_1(s) = G^{-1}[\alpha(0\sigma^2 + \lambda_n^2 T_0) \operatorname{sh} \sigma l + \alpha(0\sigma^2 + \lambda_n^2 T_0) \sigma + \beta(0\sigma^2 + \lambda_n^2 T_0) \sigma \operatorname{ch} \sigma l]$$

$$G = \sigma^3 (\sigma^2 - \lambda_n^2) (\sigma^2 \operatorname{sh} \sigma l + \alpha \operatorname{sh} \sigma l + q \sigma \operatorname{ch} \sigma l), \quad \sigma = s / a^{1/2}.$$

Integrands in (17) are ambiguous with respect to  $s$  in origin of coordinates. For calculation of these integrals we will consider the contour composed of segment  $(a - ib; a + ib)$ , arcs  $C_R', C_R''$  circumference  $|s| = R$ , two-edged cut (1), (2) and circumference  $C_\rho: |s| = \rho$  (Fig. 1). Inside this contour  $F_k(s)$  are simple and have an infinite number of poles; these functions satisfy on arcs  $C_R'$  and  $C_R''$  Jordan lemma [2], i.e.,

$$\lim_{R \rightarrow \infty} \int_{C_R'} F_k(s) e^{s\tau} ds = 0, \quad \lim_{R \rightarrow \infty} \int_{C_R''} F_k(s) e^{s\tau} ds = 0 \quad (18)$$

Then by the Cauchy theorem

$$\frac{1}{2\pi i} \left[ \int_{-\infty}^{+\infty} F_k(s) e^{s\tau} ds + \int_{(1)} F_k(s) e^{s\tau} ds + \int_{(2)} F_k(s) e^{s\tau} ds + \int_{C_\rho} F_k(s) e^{s\tau} ds \right] =$$

$$= \operatorname{res} F_k(s \lambda_n^2) + \sum_{m=1}^{\infty} \operatorname{res} F_k(\mu_m) \quad (19)$$

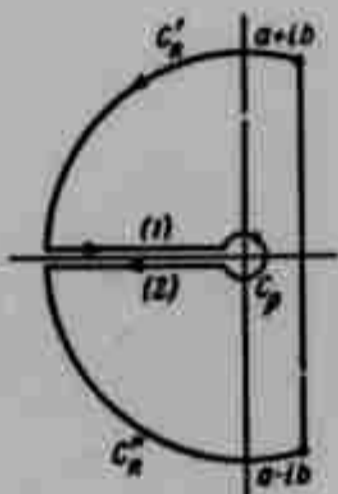


Fig. 1.

Here  $a\lambda_n^2$ ,  $\mu_m$  - singular points (poles).

On edges (1) and (2) we have correspondingly

$$s = ze^{i\alpha}, \quad s = ze^{-i\alpha} \quad \text{when} \quad \sqrt{s} = i\sqrt{z}, \quad \sqrt{s} = -i\sqrt{z}$$

It is easy to note that  $F_k(s)$  are even relative to  $i\sqrt{z}$  function, and due to this on the two-edged cut

$$\int_{(1)} F_k(s) e^{s\tau} ds + \int_{(2)} F_k(s) e^{s\tau} ds = 0 \quad (20)$$

In this case expression (19) has the form

$$\frac{1}{2\pi i} \int_{-\infty}^{+\infty} F_k(s) e^{s\tau} ds = -\frac{1}{2\pi i} \lim_{\rho \rightarrow 0} \int_{C_\rho} F_k(s) e^{s\tau} ds + \operatorname{res} F_k(\lambda_n^2 a) + \sum_{m=1}^{\infty} \operatorname{res} F_k(\mu_m) \quad (21)$$

Considering  $s = \rho e^{i\varphi}$ ,  $-\pi < \varphi < +\pi$ , for the first integral in the right part we will obtain

$$\frac{1}{2\pi} \lim_{\rho \rightarrow 0} \int_{-\pi}^{+\pi} F_k(\rho e^{i\varphi}) \exp(i\varphi + \rho e^{i\varphi} \tau) \rho d\varphi = -sT_0 \quad (22)$$

In expression (21) residues of functions  $F_k(s)$  in points  $\lambda_n^2$ ,  $\mu_m$  equal

$$\begin{aligned} \operatorname{res} F_1(s\lambda_n^2) &= sT_0 \Psi_1(\lambda_n) \exp \lambda_n^2 s\tau \\ \sum_{m=1}^{\infty} \operatorname{res} F_1(\mu_m) &= 2sT_0 \sum_{m=1}^{\infty} \Phi_1(\lambda_n, \mu_m) \exp\left(-\frac{s\mu_m^2 \tau}{l^2}\right) \end{aligned} \quad (23)$$

$$\begin{aligned} \operatorname{res} F_2(s\lambda_n^2) &= sT_0 \Psi_2(\lambda_n) \exp \lambda_n^2 s\tau \\ \sum_{m=1}^{\infty} F_2(\mu_m) &= 2sT_0 \sum_{m=1}^{\infty} \Phi_2(\lambda_n, \mu_m) \exp\left(-\frac{s\mu_m^2 \tau}{l^2}\right) \end{aligned} \quad (24)$$

Here

$$\begin{aligned} \Psi_1(\lambda_n) &= \frac{1}{g} \left( \alpha \frac{T_1}{T_0} \operatorname{sh} \lambda_n l + \alpha \frac{T_2}{T_0} \lambda_n + \beta \frac{T_1}{T_0} \lambda_n \operatorname{ch} \lambda_n l \right) \\ \Psi_2(\lambda_n) &= \frac{1}{g} \left( \alpha \frac{T_1}{T_0} \operatorname{sh} \lambda_n l + \beta \frac{T_1}{T_0} \lambda_n + \alpha \frac{T_2}{T_0} \lambda_n \operatorname{ch} \lambda_n l \right) \\ g &= \lambda_n^2 \operatorname{sh} \lambda_n l + \alpha \operatorname{sh} \lambda_n l + q \lambda_n \operatorname{ch} \lambda_n l \end{aligned}$$

$$\begin{aligned} \Phi_1(\lambda_n, \mu_m) &= \frac{1}{Q} \left[ \alpha \left( \frac{\delta}{T_0} \frac{\mu_m^2}{l^2} - \lambda_n^2 \right) \sin \mu_m + \alpha \frac{\mu_m}{l} \left( \frac{\delta}{T_0} \frac{\mu_m^2}{l^2} - \lambda_n^2 \right) + \right. \\ &\quad \left. + \beta \frac{\mu_m}{l} \left( \frac{\delta}{T_0} \frac{\mu_m^2}{l^2} - \lambda_n^2 \right) \cos \mu_m \right] \\ \Phi_2(\lambda_n, \mu_m) &= \frac{1}{Q} \left[ \alpha \left( \frac{\delta}{T_0} \frac{\mu_m^2}{l^2} - \lambda_n^2 \right) \sin \mu_m + \beta \frac{\mu_m}{l} \left( \frac{\delta}{T_0} \frac{\mu_m^2}{l^2} - \lambda_n^2 \right) + \right. \\ &\quad \left. + \alpha \frac{\mu_m}{l} \left( \frac{\delta}{T_0} \frac{\mu_m^2}{l^2} - \lambda_n^2 \right) \cos \mu_m \right] \\ Q &= \frac{\mu_m^2}{l^2} \left( \frac{\mu_m^2}{l^2} + \lambda_n^2 \right) \left[ (2 + ql) \sin \mu_m - \left( \frac{\alpha l^2}{\mu_m} + \frac{ql}{\mu_m} - \mu_m \right) \cos \mu_m \right] \end{aligned}$$

and  $\mu_m$  — constitute roots of the following transcendental equation:

$$\operatorname{ctg} \mu = \frac{l}{q\mu} \left( \frac{\mu^2}{l^2} - \alpha \right)$$

Considering (15), (17), (22), (23), (24), finally we obtain for dimensionless flows

$$\begin{aligned} \varphi_1(x, 0, \tau) &= -\frac{T_1}{T_0} + 2\lambda \sum_{n=1}^{\infty} \frac{\Psi_1(\lambda_n) X_n(x)}{\omega_n} - \\ &= -4\lambda \sum_{n=1}^{\infty} \sum_{m=1}^{\infty} \frac{\Phi_1(\lambda_n, \mu_m) X_n(x)}{\omega_n} \times \\ &\quad \times \exp \left[ -s \left( \lambda_n^2 + \frac{\mu_m^2}{l^2} \right) \tau \right] \end{aligned} \quad (25)$$

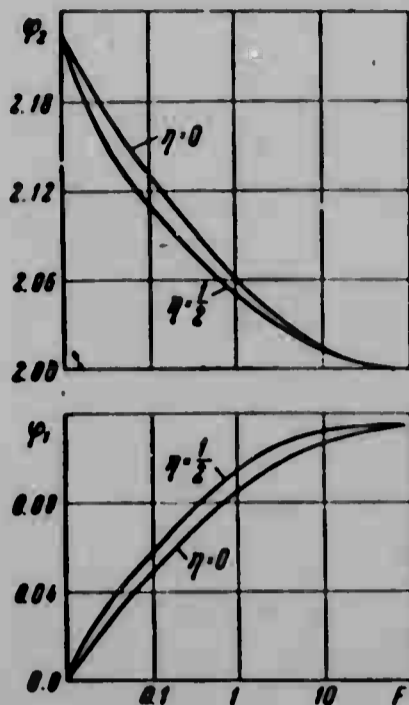


Fig. 2.

$$\begin{aligned} \varphi_2(x, l, \tau) = & \frac{T_2}{T_0} - 2h \sum_{n=1}^{\infty} \frac{\psi_2(\lambda_n) X_n(x)}{\omega_n} + \\ & + 4h \sum_{n=1}^{\infty} \sum_{m=1}^{\infty} \frac{\Phi_1(\lambda_n, \mu_m) X_n(x)}{\omega_n} \times \\ & \times \exp \left[ -a \left( \lambda_n^2 + \frac{\mu_m^2}{l^2} \right) \tau \right] \end{aligned} \quad (26)$$

Series in (25) and (26) rapidly converge; the first sum converges approximately as  $\lambda_n^{-3}$ , and the second converges approximately as  $\mu_m^{-2} \exp[-(\lambda_n^2 + \mu_m^2)l^2]$ . This makes it possible to be limited in calculations to the first terms of the series. In particular, if  $L, l \sim 0.1$  m,  $a \sim 10^{-3}$  m<sup>2</sup>/hr, then with sufficient

accuracy it is possible to be limited to expressions:

$$\varphi_1(x, 0, \tau) = -\frac{T_1}{T_0} + 2h \frac{\psi_1(\lambda_1) X_1(x)}{\omega_1} - 4h \frac{\Phi_1(\lambda_1, \mu_1) X_1(x)}{\omega_1} \exp \left[ -a \left( \lambda_1^2 + \frac{\mu_1^2}{l^2} \right) \tau \right] \quad (27)$$

$$\varphi_2(x, l, \tau) = \frac{T_2}{T_0} - 2h \frac{\psi_2(\lambda_1) X_1(x)}{\omega_1} + 4h \frac{\Phi_2(\lambda_1, \mu_1) X_1(x)}{\omega_1} \exp \left[ -a \left( \lambda_1^2 + \frac{\mu_1^2}{l^2} \right) \tau \right] \quad (28)$$

On Fig. 2 is represented the dependence of flows  $\varphi_1(F, \eta)$  and  $\varphi_2(F, \eta)$  on Fourier criterion  $F$  for  $\eta = 0$ ,  $\eta = 1/2$ , (here  $\eta = x/L$ ) — by the formulas (27) and (28).

Submitted  
19 October 1963

#### Literature

1. R. Kurant and D. Gil'bert. Methods of mathematical physics, Vol. 1. State Technical Press, 1953.
2. M. A. Lavrent'yev and B. V. Shabat. Methods of theories of functions of complex variable. Fizmatgiz, Moscow-Leningrad, 1958.

NON STEADY-STATE BURNING OF THIN  
PLATES OF POWDER

Yu. A. Gostintsev and  
A. D. Margolin

(Moscow)

In the article, within limits of the theory of Ya. B. Zel'dovich of burning powders [1], is considered the question about non steady-state burning of thin plates of powder. For the solution of equations is used the method of integral relationships [2-4]. The formula for determination of full time of combustion  $\tau_+$  of a plate with initial thickness  $2\delta_0$  is obtained. Curves of change of burning rate  $w$  and temperature in center of plate  $\theta_0$  are built depending upon thickness of plate.

We consider an infinite plane parallel plate of powder burning on two sides. Origin of coordinates is selected in middle of plate. Burning surfaces are perpendicular to axis  $x$  and move along this axis in the direction to origin of coordinates. With approach of burning surfaces to middle of plate occurs warming of its central part, leading to decrease of gradient of temperatures on surface and to increase of burning rate. Temperature  $T_s$  on surface of powder changes little during change of burning rate, therefore in first approximation one may assume that non steady-state burning rate depends only on pressure and temperature gradient, and temperature of surface is constant [1].

To produce the expression of burning rate of powder in the non steady-state case we use temperature dependence of stationary speed on initial temperature of

powder  $T_0$  in the form

$$u = u_1 \frac{P^v}{1 - \beta T_0} \quad (1)$$

Here  $u_1$ ,  $\beta$ ,  $v$  - constants, depending on composition of fuel. For stationary burning the gradient of temperature at the surface depending upon burning rate has the form [1]

$$q = \frac{u}{x} (T_0 - T_0) = \left( \frac{dT(x)}{dx} \right) \Big|_{x=\Delta} \quad (2)$$

( $\Delta$  - half of thickness of plate)

From (1) and (2) we will obtain the expression for non steady-state burning rate

$$u = \frac{u_1}{1 - \beta T_0} P^v - \frac{\beta x}{1 - \beta T_0} \left( \frac{\partial T(x, t)}{\partial x} \right)_{x=\Delta} \quad (3)$$

Let us introduce the dimensionless quantities

$$\tau = t \frac{u_0^2}{x} = \frac{t}{\tau_0}, \quad \xi = x \frac{u_0}{x} = \frac{x}{\Delta_0}, \quad \eta = \frac{1 - \beta T_0}{1 - \beta T_0},$$

$$\theta = \frac{T - T_0}{T_0 - T_0}, \quad \omega = \frac{u}{u_0}, \quad \delta = \frac{\Delta}{\Delta_0}$$

Here  $\tau_0$  and  $\Delta_0$  - characteristic time of heating and thickness of heated zone during steady-state burning,  $\eta$  - parameter characterizing the degree to which powder is heated (the greater  $\eta$ , the less fuel is heated).

In these variables initial system of equations for burning of plate at constant pressure has the form (with respect to symmetry of problem we consider only one half of the plate)

$$\omega = \eta - (\eta - 1) \left( \frac{\partial \theta(\xi, \tau)}{\partial \xi} \right)_{\xi=\delta} \quad (4)$$

$$\frac{\partial \theta(\xi, \tau)}{\partial \tau} = \frac{\partial^2 \theta(\xi, \tau)}{\partial \xi^2} \quad (\tau > 0, 0 \leq \xi \leq \delta(\tau))$$

$$\theta(\xi, \tau) = 1 \text{ when } \xi = \delta(\tau), \quad \frac{\partial \theta(\xi, \tau)}{\partial \xi} = 0 \text{ when } \xi = 0, \quad \theta = \frac{\text{ch } \xi}{\text{ch } \delta} \text{ when } \delta \rightarrow \infty \quad (5)$$

Boundary condition when  $\xi = 0$  signifies zero heat transfer between right and left part of plate; the condition when  $\delta \rightarrow \infty$  is obtained from two symmetric

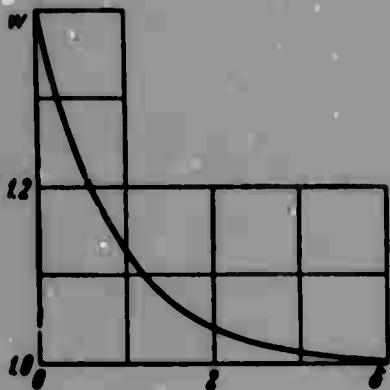


Fig. 1.

distribution curves of temperature when  $\omega = 1$  and  $\delta \rightarrow \infty$ .

The heat conduction equation with boundary conditions of such type is not possible to solve by exact methods. We use the method of integral relationships, first used for solution of differential equations of boundary layer [2] and later used for solution of problems of filtration [3] and thermal conduction [4]. We seek distribution of temperature by thickness of plate in

the form of certain function  $\theta(\xi, \tau)$ , satisfying boundary conditions of problem (4) when  $\xi = \delta$  and  $\xi = 0$ . We select function

$$\theta = \psi(\tau) \frac{\text{ch } \xi}{\text{ch } \delta(\tau)} + 1 - \psi(\tau) \quad (6)$$

where  $\psi(\tau)$  - function of time as yet not determined.

Function (6) when  $\psi = 1$  coincides with exact solution of problem about burning with constant rate of plate of sufficiently great thickness ( $\delta \rightarrow \infty$ ), when the interaction of thermal layers is immaterial. Let us integrate heat conduction equation over coordinate  $\xi$  from 0 to  $\delta(\tau)$

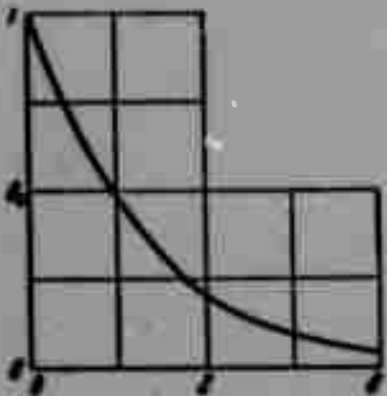


Fig. 2.

$$\frac{d}{d\tau} \int_0^{\delta(\tau)} \theta(\xi, \tau) d\xi = [\theta(\xi, \tau)]_{\xi=\delta(\tau)} \cdot \frac{d\delta(\tau)}{d\tau} + \frac{d\theta(\xi, \tau)}{d\xi} \Big|_{\xi=0}^{\xi=\delta(\tau)} \quad (7)$$

After substitution of (6) in (7) we will obtain considering gradient conditions the ordinary first order differential equation

$$\frac{d}{d\tau} (\psi \text{th } \delta - \psi \delta) = \psi \text{th } \delta \quad (8)$$

Equation for burning rate obtains the form

$$\frac{d\delta}{d\tau} = -\eta + (\eta - 1) \psi \text{th } \delta \quad (9)$$

The obtained system of ordinary differential equations is solved in general form

$$\psi(lh\delta - \delta) - \psi_0(lh\delta_0 - \delta_0) - \frac{\delta - \delta_0}{\eta - 1} = \frac{\eta}{\eta - 1} \tau \quad (10)$$

Hence for time of combustion  $\tau_+$  plate with initial thickness  $2\delta_0$  we find

$$\tau_+ = \frac{\eta - 1}{\eta} \left[ \frac{\delta_0}{\eta - 1} - \psi_0(lh\delta_0 - \delta_0) \right] \quad (11)$$

Initial condition (5) when  $\delta \rightarrow \infty$  means that plate burns with constant rate  $\omega = 1$ , when thickness of plate is infinite and there is no interaction of thermal layers spreading toward each other. For numerical results it is necessary to assign charged condition not on infinity, but on final thickness of plate.

In connection with the fact that heating of plate is small during considerable thicknesses and begins to show only when thicknesses of plate are of the order of the heated layer, it is possible without considerable error to consider that on a certain finite, but sufficiently large as compared to width of heated layer, value  $\delta_0$  burning rate and gradient were not changed from their initial values.

Therefore we will use initial conditions  $d\psi/d\tau = 0$  and  $\delta = \delta_0$  ( $\delta_0 \gg 1$ ) when  $\tau = 0$ .

For  $\delta_0 = 4$  and  $\eta = 1.40$  results of numerical calculation of change of burning rate  $w$  and temperature  $\theta_0$  in center of plate depending upon current value of half of thickness of plate are  $\delta$  represented on Figs. 1 and 2.

It is clear that burning rate tends to its highest possible value  $\max w = \eta$ , equal to burning rate of powder heated to temperature of burning surface  $T_s$ .

Submitted  
7 February 1964

#### Literature

1. Ya. B. Zel'dovich. The theory of burning of powders in explosives. Jour. experim. and theor. physics, 1942, Vol. 12, No. 11-12.
2. K. Pohlhausen. Zur naherungsweise Integration der Differentialgleichungen der laminaren Grenzschicht. Z. angew. Math. und Mech., 1921, H. 1.
3. G. I. Barenblatt. Certain transient motions of liquid in porous medium. PMM, 1952, Vol. 26, Issue 1.
4. T. R. Goodman. The heat-balance integral and its application to problems involving a change of phase. Transaction of the ASME, 1958, No. 2.